
Molecular Effects of Idebenone

Inauguraldissertation

zur
Erlangung der Würde eines Doktors der Philosophie
vorgelegt der
Philosophisch-Naturwissenschaftlichen Fakultät
der Universität Basel

von

Roman Hans Haefeli

aus Wetzikon, ZH

Winterthur, 2012

Genehmigt von der Philosophisch-Naturwissenschaftlichen Fakultät
auf Antrag von

Prof. Dr. Markus Rüegg
PD Dr. Thomas Meier
PD Dr. Dirk Fischer

Basel, den 20. September 2011

Prof. Dr. Martin Spiess
Dekan



Table of Contents

Table of Contents	3
1 Abstract	7
2 Introduction	9
2.1 Mitochondria-Related Diseases	9
2.1.1 Mitochondrial Encephalomyopathy, Lactic Acidosis, and Stroke-Like Syndrome (MELAS)	10
2.1.2 Leber's Hereditary Optic Neuropathy (LHON)	10
2.1.3 Duchenne Muscular Dystrophy	11
2.2 Mitochondria and Energy-Generating Systems	13
2.2.1 Glycolysis Produces ATP Independent of Mitochondria	14
2.2.2 Electron Transport Chain and Oxidative Phosphorylation	15
2.2.3 Other Relevant Electron Transport Systems	18
2.2.4 Janus-faced Mitochondria: The Rise of Reactive Oxygen Species during Respiration	20
2.3 The Importance of the Redox Environment	23
2.3.1 Oxidative Stress	23
2.3.2 Redox Environment and ROS Signaling	25
2.4 Idebenone	26
2.4.1 Quinones	26
2.4.2 Idebenone: An Overview	27
2.4.3 Idebenone: Preclinical Data of the Brain	28
2.4.4 Idebenone: Interaction with the Electron Transport Chain	28
2.4.5 Idebenone: Preclinical Evidence for an Antioxidant Effect	29
2.4.6 Idebenone: Additional Findings	29
2.4.7 Idebenone: Clinical Data	30
2.5 Perspectives	30
3 Results	31
3.1 Confirmation of Duchenne Muscular Dystrophy Model Systems	31
3.2 Influence of Idebenone on Mitochondrial Activity	37
3.3 Idebenone Rescues ATP Levels under Conditions of Dysfunctional Complex I	39
3.4 Investigating the Mode of Quinone-Dependent ATP Rescue	43
3.5 Can Idebenone Ameliorate ATP Levels Via AMPK?	45
3.6 Quinone-Dependent ATP Rescue Is Dependent on NQO1 and Complex III	46
3.7 The Influence of Cell Medium on ATP Rescue Experiments	51
3.8 Idebenone Reduced ATP Levels in Cells Deficient of NQO1	52
3.9 Interactions of Idebenone with Additional Oxidoreductases	54
3.10 Potential Benefits from ATP Rescue in Disorders with Deficient Complex I	59
3.11 Toxicological Analyses of Idebenone and Related Quinones	61
3.12 Idebenone Influences Akt-1 Status	62
3.13 Idebenone Protects Cells from Oxidative Stress-Induced Cell Death	65
3.14 Alteration in Gene Expression as a Mode of Action of Idebenone?	70
3.15 Metabolic Effects of Idebenone <i>in Vivo</i>	74
3.16 Characterization of Idebenone Analogs	79
4 Discussion	86
4.1 Choice of Suitable Model Systems	86
4.2 Influence of Idebenone on Mitochondrial Parameters in Healthy Mitochondria	88
4.3 Idebenone Is an Inhibitor of Complex I	88
4.4 Idebenone Restores ATP Levels under Conditions of Impaired Complex I	91
4.5 ATP Restoration in Presence of Dysfunctional Complex I Is Carried Out by Cytosolic-Mitochondrial Electron Shuttling	92
4.6 Idebenone Is Reduced by Other Oxidoreductases than NQO1 as Well	98
4.7 Idebenone Inhibits Complex I <i>in Vivo</i> and Thereby Changes Metabolism	98
4.8 Idebenone Is a Mild Pro-Oxidant	101
4.9 Idebenone Analogs Exhibit a High Disparity in Biological Function	102
4.10 Idebenone Protects From Oxidative Stress-Induced Cell Death	103
4.11 Implications of this Thesis on Mitochondrial Diseases: DMD, MELAS, and LHON	105
4.11.1 Duchenne Muscular Dystrophy	105
4.11.2 Mitochondrial Encephalomyopathy, Lactic Acidosis, and Stroke-like Syndrome	106
4.11.3 Leber's Hereditary Optic Neuropathy	107
4.12 Conclusions	108
5 Methods	111
5.1 Enzyme Kinetics	111
5.1.1 NQO1 and NQO2 Activity	111

5.2	Cell Culture.....	111
5.2.1	Culturing of Cells.....	111
5.2.2	Thawing and Freezing of Cells.....	112
5.2.3	Passaging of Cells.....	112
5.2.4	Seeding of Cells into Plates.....	112
5.2.5	Treatment of Cells.....	112
5.2.6	Cell Growth Rates.....	112
5.3	Assays.....	112
5.3.1	Determination of ATP Levels.....	112
5.3.2	Determination of Reactive Oxygen Species.....	113
5.3.3	Measurement of Mitochondrial Mass.....	114
5.3.4	Measurement of Mitochondrial ROS Production.....	114
5.3.5	Measurement of Mitochondrial Membrane Potential.....	114
5.3.6	Measurement of Quinone Reduction (WST-1 Assay).....	115
5.3.7	Determination of Extracellular Lactate Levels.....	115
5.3.8	Quantification of Live and Dead Cells.....	115
5.3.9	Protein Determination.....	116
5.3.10	GAPDH Assay.....	116
5.3.11	Creatine Kinase Assay.....	116
5.3.12	Determination of Blood Levels of Ketone Bodies.....	116
5.4	Gene Knock-Down.....	117
5.4.1	Small interfering Ribonucleic Acid-Mediated Gene Knock-Down.....	117
5.4.2	Lentiviral Gene Knock-Down of NQO1.....	117
5.5	Nucleotide Manipulations.....	117
5.5.1	Isolation of Ribonucleic Acid.....	117
5.5.2	Synthesis of Complementary Desoxyribonucleic Acid.....	117
5.5.3	Quantitative Real-Time Polymerase Chain Reaction.....	118
5.6	Proteins Analysis.....	118
5.6.1	Western Blotting.....	118
5.6.2	Histological Staining of Oxidative Stress Markers.....	118
5.7	<i>Ex vivo</i> Experiments.....	118
5.7.1	Isolation of Hepatocytes.....	118
5.7.2	Isolation of Murine Blood and Tissues.....	119
5.8	<i>In vivo</i> Experiments.....	119
5.8.1	Animal Husbandry.....	119
5.8.2	Glucose Tolerance Test.....	119
5.8.3	Genotyping.....	119
5.8.4	Food Intake Experiments.....	120
5.9	Determination of Changes in Gene Expression Using Microarray.....	120
5.9.1	Treatment of Mice.....	120
5.9.2	RNA Isolation and MicroArray.....	120
5.9.3	Statistical Analyses.....	120
6	Materials.....	123
6.1	Animals.....	123
6.1.1	Strains.....	123
6.1.2	Animal Chow.....	123
6.1.3	Animal Facility Material.....	123
6.2	Software.....	123
6.3	Machines.....	123
6.3.1	Pipets.....	124
6.3.2	Miscellaneous.....	124
6.4	Cells and Cell Lines.....	124
6.4.1	Human Primary Cells.....	124
6.4.2	Human Cell Lines.....	125
6.4.3	Rodent Cell Lines.....	126
6.5	Macromolecules.....	126
6.5.1	Recombinant Enzymes.....	126
6.5.2	Oligonucleotides.....	126
6.5.3	siRNAs.....	128
6.5.4	Lentiviral Particles.....	128
6.5.5	Antibodies.....	128
6.6	Media, Cell Cultures Supplements and Buffers.....	128
6.6.1	Cell Culture Media.....	128
6.6.2	Sera.....	129

6.6.3	Cell Culture Chemicals.....	129
6.6.4	Buffers.....	129
6.7	Chemicals.....	129
6.7.1	Chemicals for Formulation.....	129
6.7.2	Chemicals.....	129
6.7.3	Fluorescent Dyes.....	132
6.8	Kits.....	132
6.9	Consumables.....	133
6.9.1	Cell Culture Flasks.....	133
6.9.2	Cell Culture Dishes.....	133
6.9.3	Microplates.....	133
6.9.4	Pipet Tips.....	133
6.9.5	Tubes.....	134
6.9.6	Miscellaneous.....	134
7	Acknowledgements.....	135
8	Abbreviations.....	137
9	Table of Figures.....	143
10	Table of Tables.....	145
11	References.....	147
12	Appendices.....	161
12.1	Appendix I: Tables of Gene Ontology from Micro Array Data.....	161
12.2	Appendix II: Figures of Additional <i>in Vivo</i> Experiments.....	163
12.3	Appendix III: Vitamin Composition of Different Chows Used <i>in Vivo</i>	170
12.4	Appendix IV: Relevant Publications Describing Molecular Effects by Idebenone.....	171

1 Abstract

Idebenone is a synthetic compound which shares analogous structures with coenzyme Q₁₀ (CoQ₁₀). It has been shown to attenuate the pathology of disorders with a mitochondrial phenotype or increased levels of oxidative damage. Not surprisingly, idebenone was primarily associated with antioxidant function and interaction with enzymes of the electron transport chain of mitochondrial respiration. In line with the proposed antioxidant function, idebenone protects cells from hydrogen peroxide-induced cell death. This work also confirms that idebenone inhibits mitochondrial complex I of healthy cells *in vitro* and for the first time, complex I inhibition is described *in vivo*, manifesting in an increased food intake relative to body weight and a transient drop in blood glucose. Furthermore, the reduction of idebenone by the cytosolic enzymes NQO1 and NQO2 are shown for the first time. In cells with a dysfunctional complex I, idebenone is able to promote mitochondrial respiration in an NQO1- and complex III-dependent manner. Hence, a new activity for idebenone is proposed in which idebenone facilitates the electron flow from the cytosol into the mitochondria and thereby restores depleted ATP content in complex I-deficient cells. This new mechanism is one of several justifications for the use of idebenone in mitochondrial disorders such as *mitochondrial encephalomyopathy, lactic acidosis, and stroke-like syndrome* (MELAS) and Leber's hereditary optic neuropathy (LHON). Additionally, over 50 novel idebenone analogs are characterized in different bioassays.

Idebenone ist eine synthetische Verbindung, die analoge Strukturen zu Coenzym Q₁₀ (CoQ₁₀) aufweist. Idebenone, so wurde gezeigt, verringert die pathologischen Symptome von mitochondrialen Krankheiten oder solchen mit erhöhtem oxidativen Stress. Daher ist es nicht überraschend, dass Idebenone hauptsächlich als Antioxidans angesehen wurde und auch in die Regulation der mitochondrialen Elektronentransportkette involviert wurde. In Übereinstimmung mit der vorgeschlagenen antioxidativen Wirkung schützt Idebenone Zellen vor oxidativem Stress. Diese Arbeit bestätigt ebenfalls, dass Idebenone den mitochondrialen Komplex I gesunder Zellen *in vitro* hemmt. Diese inhibitorische Aktivität wurde erstmals *in vivo* beschrieben und manifestiert sich in einer erhöhten Futteraufnahme und in einem kurzzeitigen Abfall des Blutzuckers. Zusätzlich wird zum erstenmal gezeigt, dass Idebenone durch die zytosolischen Enzyme NQO1 und NQO2 reduziert wird. In Zellen mit defektem mitochondrialen Komplex I kann Idebenone die mitochondrielle Atmung abhängig von NQO1 und Komplex III begünstigen. Demzufolge wird ein neuer Wirkmechanismus für Idebenone vorgeschlagen: Idebenone ermöglicht den Elektronenfluss aus dem Zytosol in die Mitochondrien, um dadurch den reduzierten zellulären ATP Gehalt bei defektem Komplex I zu normalisieren. Dieser neue Mechanismus ist eine von mehreren Gründen für den Einsatz von Idebenone bei mitochondrialen Krankheiten wie Leber'sche hereditäre Optikusneuropathie (LHON) oder *mitochondriale Encephalomyopathie, Lactatacidose, und Schlaganfall-ähnliche Episoden* (MELAS). Darüber hinaus werden über fünfzig neuartige Analoge von Idebenone in verschiedenen biologischen Untersuchungen charakterisiert.

2 Introduction

In recent years, more evidence for mitochondrial involvement in a variety of diseases has been reported [Wallace 1999, de Moura *et al.* 2010, and Moreira and Oliveira 2010]. Aside from a growing knowledge on primary mitochondrial disorders—such as *mitochondrial encephalomyopathy, lactic acidosis, and stroke-like syndrome* (MELAS), Leber's hereditary optic neuropathy (LHON), and *myoclonic epilepsy and ragged-red fibers* (MERRF) [Schon 2000]—impaired mitochondrial function has been discussed in diseases generally caused by non-mitochondrial factors as diverse as depression and bipolar disorder [Rezin *et al.* 2008, Jou *et al.* 2009, and Clay *et al.* 2011], several types of cancer [Chatterjee *et al.* 2010, de Moura *et al.* 2010], diabetes [Moreira and Oliveira 2011] and autism [Haas 2010]. In addition, growing evidence of mitochondrial dysfunction emerged in many neurodegenerative diseases like Alzheimer's disease (AD) [Ferreira *et al.* 2010, Tillement *et al.* 2011], Parkinson's disease (PD) [Xie *et al.* 2010], and Huntington's disease (HD) [Mochel and Haller 2011]. In this regard, it is important to note that mitochondrial impairment is also discussed as a cornerstone for normal and accelerated aging [Romano *et al.* 2010].

Given the fundamental role of mitochondria in the cell, i.e. for the generation of energy, it is not astonishing that their impairment leads to a number of disorders. Whereas incidences of primary mitochondrial disorders—with approximately 12 incidences per 100,000—are rather low [Chinnery and Turnbull 2001], neurodegenerative diseases, depression and diabetes affect a large part of human population. Thus, research on mitochondria and, in addition, treatment against mitochondrial dysfunction becomes more and more important. In this context, mitochondrial disorders constitute useful models for developing compounds that can modify mitochondrial function to ameliorate not only their molecular dysfunction, but also the course and pathology of the mentioned prevalent diseases.

2.1 Mitochondria-Related Diseases

Mitochondria are pivotal organelles in most cells and are mainly responsible for the generation of energy. Genetic disorders showing a mitochondrial phenotype can be either caused indirectly as consequence of primary failures of cellular integrity or directly by mutations of genes involved in mitochondrial function. Since mitochondria hold a genome of their own, genes associated with their function can be either encoded by the mitochondrial genome or within the nucleus of the cell. It is important to note that mutations of mitochondrial genes do not follow Mendelian rules of inheritance [Sproule and Kaufmann 2008], since mitochondria are solely maternally derived. Implementation and inheritance of such mutations are further complicated by two concepts of mitochondrial replication: heteroplasmy and segregation. The first one refers to the fact, that one cell can contain up to several thousand copies of mitochondrial DNA (mtDNA) and that these copies may differ in sequence [Sproule and Kaufmann 2008]. Segregation compromises the distribution of mitochondria among daughter cells during mitosis. This partition of the vast number of mitochondria of a cell in two daughter cells occurs randomly. Therefore, accumulation of a given mutation in a specific cell or even tissue happens incidentally and the same mutation may not manifest itself similarly in two carriers thereof [Sproule and Kaufmann 2008]. In a special case of segregation, higher incidence of mutated mtDNA in children than in the mother can be explained by a genetic bottle neck effect; namely if mutated mtDNA is not distributed evenly during generation of female germ cells. These concepts can therefore explain the diverse clinical phenotypes observed in patients with mitochondrial mutations.

Despite the heterogeneity of the course of disease, mutations of mtDNA lead to symptoms that sometimes overlap between the different diseases as patients often show muscle atrophy, blindness, deafness, impaired cognitive functions and diabetes [Schon 2000]. This is not surprising, since these symptoms affect organs with high energy demand such as muscles, eyes, and the brain. Mitochondrial myopathies (MELAS, MERRF), some ophthalmological neuropathies (LHON, macular degeneration, MELAS), and *maternally-inherited diabetes and deafness* (MIDD) fall in this category [Sproule and Kaufmann 2008].

Mutations in nuclear-encoded genes responsible for mitochondrial function can also lead to disorders with a mitochondrial phenotype. Loss of frataxin, which is assumed to participate in iron cluster formation in mitochondria [Mühlenhoff *et al.* 2002], is the underlying cause of Friedreich's ataxia (FRDA). As a result, mitochondrial energy production is impeded in patients possessing a mutation in the according gene [Rötig *et al.* 1997].

Furthermore, dysfunction of mitochondria can be elicited as a consequence of accumulation of toxic compounds unrelated to mitochondria or to exogenous toxins. This is the case in neurodegenerative disorders as the example of AD suggests: high levels of oxidative stress assaults mitochondrial health by accumulation of amyloid- β and this can result in an accelerated decline of neurons [Ferreira *et al.* 2010]. In Duchenne muscular dystrophy (DMD), it is assumed that mitochondrial function is impaired as a result of membrane disruption and disturbed calcium homeostasis (see 2.1.3 for details). Finally, the neurotoxin 1-methyl-4-phenyl-1,2,3,6-tetrahydropyridine (MPTP) blocks an enzyme complex of mitochondrial energy production and, upon administration of this compound, a Parkinson-like phenotype is apparent [Degli Esposti 1998].

Three mitochondria-related diseases will be looked at in more details in the forthcoming sections; namely two diseases with mutations in mtDNA (MELAS and LHON) and a disease wherein mitochondrial impairment results as a consequence of preceding pathological changes (DMD).

2.1.1 Mitochondrial Encephalomyopathy, Lactic Acidosis, and Stroke-Like Syndrome (MELAS)

The pathology of *mitochondrial encephalomyopathy, lactic acidosis, and stroke-like syndrome* (MELAS) is defined by the occurrence of the following criteria: (i) stroke-like episodes in the first four decades, (ii) at least one of the encephalopathic symptoms seizures or dementia, and (iii) at least one of the myopathic symptoms lactic acidosis or red-ragged fibers [Hirano and Pavlakis 1994]. Sproul and Kaufmann [2008] reported that, in addition, a majority of patients suffers from exercise intolerance, headache, hearing loss, and gastrointestinal disturbances. Disease onset is usually stated between the age of 2 and 20 [Pavlakis *et al.* 1984, Hirano and Pavlakis 1994].

Even though MELAS is a polygenetic disorder associated with at least 29 specific point mutations, all mutations causing this phenotype are found in mtDNA [Sproul and Kaufmann 2008]. The most prominent mutation is an A-to-G transition mutation at position 3243 (3243A>G mutation; meaning the adenine is exchanged with a guanine nucleotide) found in approximately 80% of patients [Testai and Gorelick 2010]. Whereas many mutations affect genes encoding for mitochondrial transfer ribonucleic acids (tRNA)—nucleotide 3243 lies within the gene for a lysine tRNA (tRNA^{lys})—some affect genes encoding for subunits of mitochondrial complexes which are also associated with other mitochondrial disorders like LHON, MERRF, or Leigh disease. Thus, two interesting, yet unaccounted incidents for mitochondrial disorders become apparent: they could be both (i) polygenetic disorders, i.e. a mutual set of symptoms is caused by different mutations, and (ii) overlapping, meaning that exactly the same mutation can lead to multiple phenotypes as reported for LHON/MELAS, MELAS/Leigh syndrome, and LHON/MELAS/Leigh syndrome in regard to mitochondrially encoded complex I subunits [Wong 2002].

Since tRNA are required for building new proteins, mutations lead to dysfunctional mitochondrial enzyme complexes. Accordingly, deficiency of energy production by mitochondria has to be counteracted by increased anaerobic glycolysis. As will be explained in a following subchapter (see 2.2.1), this change in energy source results in elevated levels of lactate in the blood. Indeed, lactic acidosis in blood is not only found in all mitochondrial disorders, but also specifically in brain areas affected by stroke in MELAS patients [Kaufmann *et al.* 2004, Davidson *et al.* 2009].

Deficiency in mitochondrial energy production in MELAS patients has been described by several groups. James *et al.* [1996] reported that fibroblasts from a MELAS patient carrying the 3243A>G mutation had decreased complex I and IV activity, but increased complex II activity and normal complex III activity compared to control fibroblasts. They therefore suggested an elevated complex II-III activity in MELAS patients. They also found increased acidification of culture medium and concluded enhanced anaerobic glycolysis in these cells. This is consistent with the lactic acidosis found in blood of MELAS patients. Furthermore, their studies showed decreased mitochondrial membrane potential also adding to the picture of dysfunctional mitochondria.

Other groups reported failures of additional respiratory complexes. Sarnat and María-García [2005] described a patient with an unidentified mutation but showing MELAS symptoms who has decreased activity of mitochondrial complexes I, III, IV, and ATP synthase. Davidson *et al.* [2009] introduced the 3243A>G mutation into an immortalized brain capillary endothelial cells and astrocytes and they found not only reduced complex I activity, but also decreased activity of complex IV and, to a lesser extent, complex II. In a study by Sarasman *et al.* [2008], 3243A>G mutation prevented the assembly of complexes I, IV and ATP synthase in myoblasts by a combination of faulty incorporation of amino acids and shorter half-lives of mitochondrial translation products.

Further evidence for direct involvement of mitochondrial respiration and MELAS comes from several findings of point mutations within subunits of complex I. Kirby *et al.* [2004] reported three unrelated MELAS patients with mutations within subunit ND1 of complex I, namely 3697G>A, 3946G>A, and 3949T>C. In fibroblasts of a MELAS patient harboring the 13528A>G mutation, which affects the ND5 subunit of complex I, decreased mitochondrial membrane potential and increased lactate production was found [McKenzie *et al.* 2007]. The authors showed in the same study that ATP generated by glycolysis was used to support the remaining mitochondrial membrane potential. Malfatti *et al.* [2007] described a MELAS patient harboring the 3481G>A mutation affecting subunit ND1 of complex I who showed markedly reduced complex I activity in muscle biopsy homogenates and fibroblasts, which was countered by increased complex II and ATP synthase activity at least in the latter. Activities of complexes II-V and complexes III and IV in muscle homogenates and fibroblasts, respectively, remained unchanged. A failure in mitochondrial respiration was also affirmed by Sano *et al.* [1995] who found a decreased ratio of oxygen consumption to glucose metabolism in the brain of a 3243A>G point mutation carrier.

Hence, disruption of mitochondrial energy production leads to the described phenotype of MELAS. However, MELAS differs from other mitochondrial diseases which also involve mitochondrial-encoded enzymes of the respiratory chain [Sproule and Kaufmann 2008]. The heterogeneity of symptoms in mitochondrial diseases is still far from understood.

2.1.2 Leber's Hereditary Optic Neuropathy (LHON)

Another devastating disease with underlying mitochondrial dysfunction is Leber's Hereditary Optic Neuropathy (LHON). The clinical symptoms manifest as a sudden loss of vision, mostly experienced in the second or third decade of life, caused by the degeneration of retinal ganglion cells (RGCs) and their axons [Sadun 2010]. Three mutations in the mitochondrial gene for complex I subunits account for 98% of all LHON cases,

namely 11778G>A in subunit ND4, 3460G>A in subunit ND1 and 14484T>C in subunit ND6 [Mackey *et al.* 1996]. Even though mutations affect the same enzyme complex as in MELAS, the phenotypes—i.e. age of onset, affected tissues—significantly differ in these two diseases.

Cells harboring a mutation in conserved components of the mitochondrial electron transport chain, such as cells from LHON patients, are expected to show signs of energy deprivation. Indeed, some groups have demonstrated a clear deficit of mitochondrial membrane potential, ATP synthesis and oxygen consumption rates. This was shown in primary peripheral blood mononuclear cells (PBMCs) of affected LHON patients as well as unaffected carriers [Korsten *et al.* 2010], but was also observed previously in cybrid cells harboring the three common LHON mutations [Baracca *et al.* 2005, Floreani *et al.* 2005] and skin fibroblasts [Bonnet *et al.* 2008].

Surprisingly, no consistent reduction of cellular ATP levels in LHON cybrids and LHON PBMCs compared to control cells could be demonstrated [Beretta *et al.* 2004, Baracca *et al.* 2005, and Pommer *et al.* 2008], which suggest that LHON cells *in vitro*, or in the case of PBMCs *ex vivo*, have activated compensatory mechanisms to ensure energy homeostasis. Whether part of the compensatory mechanism is an up-regulation of complex II activity as suggested by an earlier study using LHON PBMCs [Yen 1996] is still disputed [Brown *et al.* 2000, Korsten *et al.* 2010]. Likewise, the presence of LHON mutations neither seems to affect mitochondrial content [Pommer *et al.* 2008] nor the amount or composition of the complexes of the mitochondrial electron transport chain [Korsten *et al.* 2010]. In three related 3460G>A mutation-carrying LHON patients, markedly reduced ATP levels compared to its degradation products were detected in the brain, assuming impairment of cellular energy production [Lodi 2002].

Although data so far generally demonstrates a connection between the severity of the mutation and the severity of the respiratory defect, they are unable to account for the pathomechanism of LHON. This is also reflected by observations that ATP synthesis defects can be observed in multiple cellular systems of LHON patients, whereas the phenotype of LHON is restricted to the optic nerve and RGCs. One possible explanation could be that mitochondria or complex I in particular function differently in a neuronal context compared to other cell types [Wong *et al.* 2002].

Since mitochondrial dysfunction is often associated with elevated levels of reactive oxygen species (ROS) produced by a dysfunctional respiratory chain, ROS as mediators of cellular impairment were regarded as an attractive hypothesis. ROS are highly aggressive agents that promiscuously and indiscriminately react with whatever molecule in their vicinity and thereby, they cause devastating damage to proteins and membrane lipids [see 2.3.1]. However, normal levels of an antioxidant defense molecule, glutathione (GSH) [see 2.3.1 for further information], in blood samples from LHON patients [Klivenyi *et al.* 2001] and in LHON cybrid cells [Ghelli *et al.* 2008] would ostensibly speak against a major involvement of ROS in the pathology of LHON. On the other hand, support for the hypothesis of excess ROS production stems from elevated levels of 8-hydroxy-2'-deoxyguanosine (8-oxo-dG) that were observed in leucocytes from LHON patients [Yen *et al.* 2004]. Nevertheless, production of ROS in LHON cells might be more complex than anticipated. LHON-NT2 cybrid cells that can be differentiated into a neuronal phenotype were reported to be indistinguishable with regards to ROS levels when comparing the undifferentiated LHON-NT2 cybrid cells with cybrids harboring wild-type (WT) mitochondria [Wong *et al.* 2002]. However, in a differentiated, neuronal-like state, the same LHON cybrid cells showed about 2.5-fold increased ROS levels compared to control cells [Wong *et al.* 2002], which led the authors to suggest a different function of complex I in a neuronal retinal background. Indeed, work by Levin [2007] demonstrated fundamentally different rates of ROS production in brain neurons compared to RGC-5 cells—a rodent cell line with some characteristics of retinal ganglion cells. Finally, ribozyme-mediated down-regulation of mitochondrial superoxide dismutase (SOD2) in mouse eyes was reported to induce a LHON-like phenotype including axonal loss, demyelization of the optic nerve and ganglion cells in the retina [Qi *et al.* 2003].

The atrophy of the optic nerve, characteristic to LHON patients, immediately raises the question whether apoptosis is involved in this process. Apoptosis is an active, orchestrated self-degradation of a cell which is often referred to as suicide; whereas the other form of cell death, necrosis, is a chaotic rupture of the cell membrane leading to inflammation and impairment of neighboring cells. Since cell death in patients is generally painless and only few signs of inflammation could be detected in the optic nerve [Saadati *et al.* 1998], it is likely that apoptosis represents the predominant mode of cell death in LHON. This is also supported by detection of nuclear fragmentation of LHON cybrids in response to the oxidizing agent tBH [Ghelli *et al.* 2008]. In addition, LHON cybrids in glucose-deficient galactose media and thereby forced to rely on the mitochondrial electron chain as their primary energy source, experienced apoptotic death and increased cytochrome *c* release [Ghelli *et al.* 2003]. Thus, despite the general agreement that apoptosis is the most likely mode of cell death in LHON, proof that these *in vitro* model systems recapitulate the mechanism of cell death that occurs *in vivo*, is still lacking.

2.1.3 Duchenne Muscular Dystrophy

Duchenne muscular dystrophy (DMD) is a severe degenerative disease of both skeletal and cardiac muscle. Despite the characterization of one single gene responsible for the disease, its subsequent cellular and molecular pathological mechanisms are still not fully elucidated [McArdle *et al.* 1995, Zhou *et al.* 2006, Deconinck and Dan 2007].

Patients are diagnosed with DMD at the age of four to five years mainly on the basis of gait abnormalities [Boland *et al.* 1996]. Regarding skeletal muscles, the characteristic feature of DMD is a progressive proximal

muscular dystrophy and a pseudohypertrophy of the calves [Reimers *et al.* 1996]. The progression of fibrosis accompanied by muscle degeneration leads to wheelchair dependency at a median age of ten years. Smooth muscle impairments are detected in a portion of patients in the gastrointestinal tract [Barohn *et al.* 1988]. By the age of six, most patients display myocardial symptoms, which become progressively severe over the course of the disease. Eventually, death occurs due to respiratory or cardiac failure in the early twenties. The mutations within the affected gene arise either spontaneous in approximately 30% of the cases or are inherited in an X-linked recessive manner in the remaining cases which is why DMD is predominantly found in males with a prevalence of one in 3,500 births [Emery 1991].

The defective protein dystrophin, causing both DMD and the allelic disease Becker muscular dystrophy (BDM), is encoded by the largest human gene which is located on chromosome Xp21. The 2.4 mega base pair gene contains 79 exons, leading—as a fully transcribed isoform—to a 14 kb mRNA. Several different promoters allow cell- and developmental stage-specific expression of seven different isoforms, which can be further diversified by alternative splicing of pre-messenger ribonucleic acid (mRNA) [Sadoulet-Puccio and Kunkel 1996]. Dystrophin binds to both actin and a membrane-spanning complex called dystrophin-associated glycoprotein complex which in turn is connected to laminin [Suzuki *et al.* 1992, Ehmsen *et al.* 2002]. Thus, full-length dystrophin in muscle cells links the sarcolemmal cytoskeleton to the extracellular matrix. Knowing this central role of dystrophin, it is not surprising that its loss has severe clinical consequences. Although the disorder can be linked to a single gene, the emphasis and chronology of the molecular consequences—such as increased levels of intracellular calcium (Ca^{2+}) and oxidative stress—is controversially debated [McArdle *et al.* 1994, Whitehead *et al.* 2006]. Furthermore, it was reported that cellular deficiency in dystrophin leads to altered expression of about 1,000 genes [Chen *et al.* 2000]. These alterations were not only detectable in the expression of genes closely interacting with dystrophin, but also of genes involved in a variety of processes such as proteolysis, muscular regeneration, and immune response.

To delineate which of those changes are crucially responsible for the pathology observed in patients, research is conducted in an animal model bearing a spontaneous mutation of dystrophin. However, the so-called *mdx* mouse, deficient of functional dystrophin [Bulfield *et al.* 1984], shows a significantly milder phenotype than human patients [Peri *et al.* 1994]. Nevertheless, *mdx* mice show disruption of sarcolemmal integrity and muscle cell necrosis. These findings were affirmed by the detection of high plasma levels of creatine kinase and pyruvate kinase as a consequence of muscle cell death [Bulfield *et al.* 1984] which is associated with intracellular accumulation of serum markers like albumin. This was also used to experimentally detect muscle damage, using cellular uptake of low molecular weight diazo dyes such as Evans blue as a diagnostic tool [Straub *et al.* 1997, McArdle *et al.* 1994]. The specific vulnerability of membrane integrity in dystrophin-deficient muscle cells was assumed to be correlated with the magnitude of mechanical stress applied to the membrane during muscle contraction in the absence of functioning dystrophin protein [Petrof *et al.* 1993, Straub *et al.* 1997]. However, a lack of uptake of another diazo dye, procion orange, in young and pre-necrotic *mdx* animals [McArdle *et al.* 1994] would suggest that membrane fragility is rather a consequence of the advanced pathology and not one of its eliciting features. Nevertheless, loss of membrane integrity could be a catalyst in the progression of the disease, for example by impairing the homeostasis of intracellular calcium (Ca^{2+}) levels. Elevated levels of intracellular Ca^{2+} have been reported in DMD patients and *mdx* mice [Fong *et al.* 1991, Turner *et al.* 1991]. The aberrant Ca^{2+} homeostasis in dystrophic muscle—i.e. the inability to maintain a low intracellular Ca^{2+} level at rest and a prolonged elevation of Ca^{2+} concentration during stimulation—results in activation of proteases, such as calpain, and thus, enhanced protein degradation [Turner *et al.* 1988] and increased production of reactive oxygen species (ROS), which can cause protein and membrane damage [see 2.3.1]. A connection between DMD and oxidative stress was first hypothesized due to the similarities of DMD and muscle pathology provoked by deficiency of the antioxidant vitamin E [Binder *et al.* 1965]. Despite decades of research, the question whether oxidative stress is a necessary precondition for dystrophic cell death or just a parenthetic consequence of the pathology still remains unclear [Tidball and Wehlings-Hendrick 2007]. However, substantial evidence strongly suggests a pivotal role of oxidative damage in DMD: (i) Kar *et al.* [1979] detected byproducts of free radical damage to unsaturated fatty acids, (ii) Hunter and Mohamed [1986] reported elevated products of lipid peroxidation in DMD muscle cells, and (iii) two independent groups found enhanced levels of enzymes engaged in the cellular response to oxidative stress in both pre-necrotic and affected muscle in *mdx* mice [Ragusa *et al.* 1997, Disatnik *et al.* 1998]. For example, levels of the antioxidant enzymes catalase, superoxide dismutase (SOD), and glutathione peroxidase (GPX) [see 2.3.1] are increased in both human DMD patients and *mdx* mice. Furthermore, (iv) Touboul *et al.* [2005] concluded that the sarcolemma might be under oxidative stress based on the observation that the concentrations of the antioxidants vitamin E and coenzyme Q₁₀ (CoQ₁₀) are elevated within the membranes of DMD patients. In addition, Rando *et al.* [1998] discovered a specific susceptibility of dystrophin-deficient cells to exogenously induced oxidative stress *in vitro*; whereas non-oxidant metabolic stressors were equally harmful to both *mdx* and control muscle cells. Whilst the question about the chronological position of oxidative stress in the pathology of DMD still remains unanswered, these experiments all taken together suggest that muscle degeneration and oxidative stress are closely connected.

Among the compartments most vulnerable to ROS-induced damage are mitochondria. Interestingly, mitochondria are also a major source of ROS. Especially under conditions where mitochondrial function is impaired, they generate high levels of ROS which are hazardous by damaging macromolecules and can ultimately lead to necrosis. Additionally, owing to its role as important Ca^{2+} storage organelle, mitochondria are linked to

DMD pathology via Ca^{2+} overload. Dystrophic muscle cells seem to counteract increased intracellular Ca^{2+} concentrations by mitochondrial uptake of Ca^{2+} [Chen *et al.* 2000]. There is evidence that Ca^{2+} imbalance impairs the mitochondrial function, especially its metabolic processes [Brini 2003, Kinnally *et al.* 2011]. Consistent with this hypothesis, Chen *et al.* [2000] reported that approximately one third of all down-regulated genes in muscle biopsies of DMD patients coded for enzymes involved in energy production and mitochondrial activity. One of the first describing impaired oxidative phosphorylation as a feature of DMD was the report by Scholte *et al.* [1985]. Later, using ^{31}P magnetic resonance spectroscopy, increased adenosine diphosphate (ADP) and inorganic phosphate (P_i) levels relative to adenosine triphosphate (ATP) and reduced phosphocreatine levels were found in muscle of DMD patients [Kemp *et al.* 1993]. Sperl *et al.* [1997] also reported decreased oxidation rates in muscle biopsies from DMD patients and some indication of loose coupling of oxidative phosphorylation in mitochondria from those patients. These findings were also supported by Kuznetsov *et al.* [1998] who detected reduced rates of respiration and lower activities of enzymes of the mitochondrial respiratory chain in biopsy samples of a DMD patient. Furthermore, several studies demonstrated decreased mitochondrial activity in dystrophic humans and *mdx* animals [Barbiroli *et al.* 1992, Gannoun-Zaki *et al.* 1995, and Kuznetsov *et al.* 1998]. Analysis of skeletal *mdx* muscle showed a 50% decrease in the activity of all respiratory chain-linked enzymes compared to control animals [Kuznetsov *et al.* 1998]. The authors also reported that isolated mitochondria from *mdx* muscles had only 60% of maximal respiration rates compared to control and attributed this impairment to a Ca^{2+} overload of dystrophin-deficient muscle fibers. Interestingly, this study identified no deficiencies in the cardiac muscle. Contrary to that, Braun *et al.* [2001] reported that irrespective of muscle type, the absence of dystrophin had no effect on the maximal capacity of oxidative phosphorylation, or on coupling between oxidation and phosphorylation. However, in the myocardium and *m. soleus*, the coupling of mitochondrial creatine kinase to adenine nucleotide translocase was attenuated as evidenced by the decreased effect of creatine on the K_m for ADP in the reactions of oxidative phosphorylation.

In conclusion, despite the documented loss of function of one single gene, coherent knowledge of the origin of biochemical and cellular consequences is still not consolidated. Nevertheless, there is certainty that absent or defective dystrophin protein leads to reduced mechanical stability and increased leakiness of the sarcolemma and elevated intracellular Ca^{2+} levels. The pathology also includes increased oxidative damage and impaired mitochondrial function. Therefore, DMD is a good example for a mitochondrial phenotype in a disorder which is not primarily a mitochondrial disease.

2.2 Mitochondria and Energy-Generating Systems

As stated in the previous subchapter [2.1], mitochondrial dysfunction was reported in three diseases with differing underlying causes, showing mitochondrial involvement in a broad range of disorders. In contrast to DMD, wherein impairment of mitochondria occurs indirectly, the affected genes in MELAS and LHON code for proteins directly involved in mitochondrial function. Furthermore, mitochondrial dysfunction has not only been reported in diseases directly associated with mitochondria, but also in a variety of disorders caused by nuclearly encoded genes [Smeitink *et al.* 2000] and in degenerative diseases such as Parkinson's or Alzheimer's disease and even in cancers and ageing [Wallace 1999, Schon 2000, and Moreira and Oliveira 2010].

In the light of the fact that malfunctions of this organelle are a feature in such a broad range of disorders, a closer look on its cellular role seems appropriate. Mitochondria can be found in eukaryotic cells and are the main site of cellular energy production. Current discussion favors an endo-symbiont theory of mitochondrial origin: this theory states that mitochondria evolved from bacterial ancestors which were integrated into eukaryotic cells [Gross 2011]. A mitochondrion is composed of two phospholipid bilayer membranes of which the outer membrane separates the organelle from the cytoplasm. An inner membrane encloses the matrix which contains ribosomes and mitochondrial DNA (mtDNA) [Diaz and Moraes 2007]. Additionally, the matrix and the inner membrane shelter enzymes and enzyme complexes of the mitochondrial energy machinery [Campbell and Reece 2005]. Even though the main function of mitochondria is their role in cellular energy production, two additional prominent functions are necessary to keep in mind. First, mitochondria play a central role in the orchestrated cell death called apoptosis [Brunelle and Letai 2009]. And second, mitochondria are large intracellular repository for calcium ions which are crucial in muscle contraction or function as second messenger [Brini 2003].

In contrast to observations in dead cells or illustrations in textbook pictures, mitochondria of living cells are not static rod-shaped cylinders, but dynamic, steadily transforming compartments. In the last decades, constant remodeling processes in mitochondria have been discovered and suggested to be involved in mitochondrial and cellular health [Diaz and Moraes 2007, Suen *et al.* 2008, and Twig *et al.* 2008]. Mitochondria can either undergo fusion, i.e. the merging of two individual organelles, or fission which describes the separation of one organelle in two successors. Fusion facilitates the exchange of metabolites, whereas malfunctioning parts of the mitochondria can be isolated during fission and degraded by a process called mitophagy [Twig *et al.* 2008]. In case of the orchestrated cell death called apoptosis, alleviation of mitophagy by increased fission was observed and reviewed by Suen *et al.* [2008].

The number or—more precisely—the total mass of mitochondria in a cell is dependent of its metabolic activity. For example, muscle fibers can be divided according to their latency towards fatigue: type I and IIa fibers tire slowly and are used for prolonged activity dependent on endurance. They contain a high quantity of mitochondria and rely on oxidative phosphorylation. In contrast, type IIb and IIc fibers have an intermediate or

low number of mitochondria, respectively, and use glycolysis as their main source of energy. Therefore, they are quicker to perform, but—as a consequence—quicker to fatigue.

However, the following subchapters will outline energy production by non-mitochondrial and mitochondrial means and their implications.

2.2.1 Glycolysis Produces ATP Independent of Mitochondria

From a physical point of view, energy is never destroyed nor created, but converted from one sort into another. From the subjective point of view of a creature, however, energy is constantly used up by its activities. Therefore, mammals need to gain energy from food for (i) fueling the processes needed to maintain pivotal functions and (ii) producing heat. The energy of food molecules, such as glucose or fatty acids, is stored in their chemical bonds and can be released upon breakdown. Cells dispose diverse methods to store the thus gained energy, one being the generation of molecules containing energy-rich bonds. The most prominent thereof is ATP which stores the energy in the covalent bond between its second and third phosphate group. Hydrolysis of this bond yields ADP, P_i and disposable energy which is used by a myriad of enzymes to run energy-consuming reactions.

To sustain cellular functions, the production of this main energy currency, ATP, is fundamental. ATP is primarily produced during breakdown of food molecules such as sugars, amino acids and fats and by oxidative phosphorylation (OXPHOS) which takes place in the mitochondria and is basically one of its main functions [see 2.2.2]. OXPHOS—being an additional step to primary decomposition of food particles—increases the amount of energy gained from nutrition particles. The primary degradation of different types of food molecules is separated into distinct and elaborate pathways. Fatty acids, for example, are disassembled within peroxisomes and mitochondria in a process called β -oxidation [see 2.2.3]. Since glucose and other sugars are the most prominent source of energy in human diet, the breakdown of sugars, called glycolysis, takes an important place in cellular metabolism.

Glycolysis describes the enzyme-driven breakdown of glucose into pyruvate. During this elaborate process involving ten enzymes, two molecules of ATP per glucose molecule are produced [Alberts *et al.* 2000]. In addition, each two molecules of nicotinamide adenine dinucleotide (NADH) and pyruvate result from this cytosolic pathway. Both NADH and pyruvate can be further processed to gain more ATP during OXPHOS [see 2.2.3]. Despite the rather low yield of ATP, glycolysis produces sufficient energy for some human cells to survive. For example, cancer cells—even in the presence of sufficient amount of oxygen—predominantly rely on glycolysis as source of energy, neglecting OXPHOS, a process called Warburg effect or aerobic glycolysis [Mathupala *et al.* 2010]. Thus, glycolytic activity can be seen (i) under hypoxic conditions where mitochondria do not contribute to energy production (anaerobic glycolysis), (ii) under normoxic conditions where only 5% of glycolytically produced pyruvate is conveyed to mitochondria (aerobic glycolysis), or (iii) under normoxic conditions where all pyruvate is degraded in mitochondria (OXPHOS) [Vander Heiden *et al.* 2009 and Figure 1].

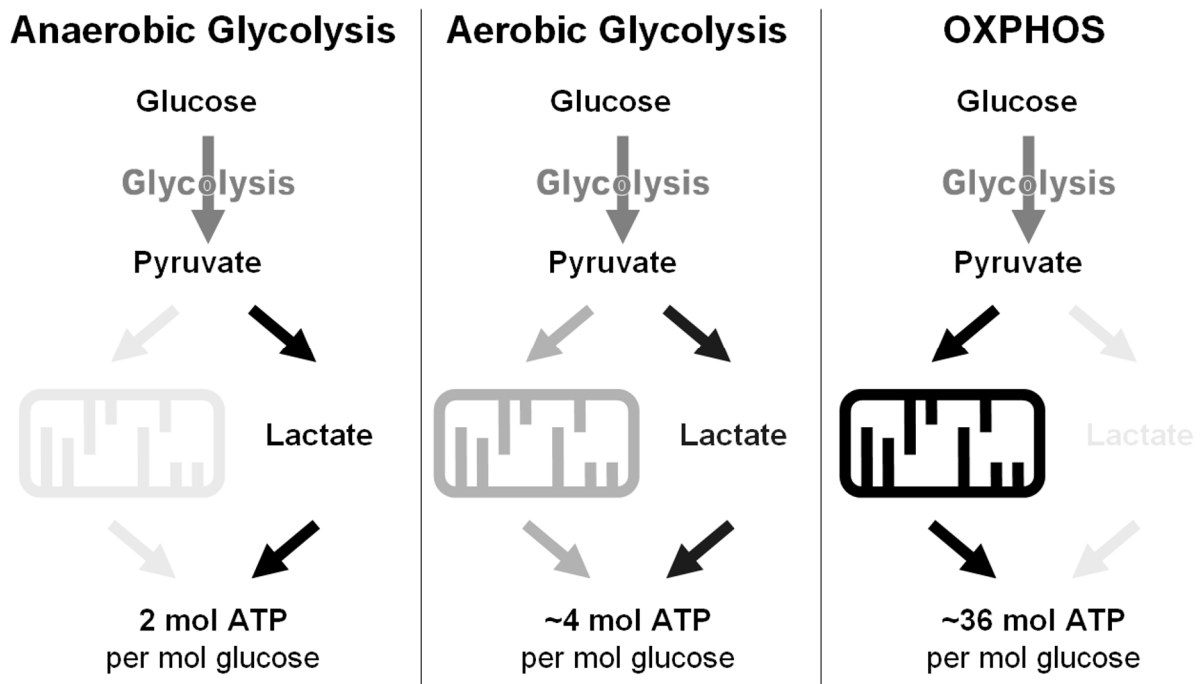


Figure 1: Schematic Representation of ATP Production by Anaerobic and Aerobic Glycolysis and Oxidative Phosphorylation.

The energy stored in glucose can be retrieved to produce ATP. After the production of pyruvate by the break-down of glucose by glycolysis, pyruvate can either enter the electron transport chain (ETC) of the mitochondria or be converted into lactate. This conversion results in the production of NAD^+ which is used to maintain glycolysis. In anaerobic glycolysis, mitochondria are not used and pyruvate is converted into

lactate. Under these conditions, two molecules of ATP are produced per molecule of glucose. In aerobic glycolysis (which is also known as the Warburg effect), mitochondrial energy production is barely active despite normoxic conditions. Instead, the majority of pyruvate is converted to lactate and only a small fraction (~5%) of pyruvate enters the ETC. The marginal usage of mitochondria increases the amount of ATP produced from glucose compared to anaerobic glycolysis (~4 mol ATP/mol glucose). If oxygen is available and pyruvate is entirely transported into the ETC, ATP production relies mainly on oxidative phosphorylation (OXPHOS) with a substantially higher efficacy (36 mol ATP/mol glucose) [ATP yields are denoted according to Vander Heiden *et al.* 2009].

During glycolysis, NAD^+ is reduced to NADH. Under normal conditions, NADH is used to fuel OXPHOS which thereby regenerates the NAD^+ pool [see 2.2.2]. Thus, this cycling does not only link glycolysis and OXPHOS, but also allows constant turnover of glucose by maintaining a sufficient amount of NAD^+ . Under conditions of suppressed OXPHOS—for example in anaerobic cells or cells with defective mitochondria—the recycling of NAD^+ has to be guaranteed differently. Generation of NAD^+ by other means in order to maintain glycolysis and ATP production is all the more important in these cases, since such cells primarily rely on glycolysis as a source of energy. Mainly, this reaction is carried out by a process called lactic acid fermentation in which pyruvate is converted into lactate [Campbell and Reece 2005].

Hence, lactate is a waste product of anaerobic glycolysis. In some physiological processes, for example in glycolytic muscle cells, lactate production is used to support the generation of the required high ATP levels. Glycolytic muscle fibers—i.e. type IIb and IIc fibers—contain few mitochondria and are characterized by fast contractions. These contractions are conducted by a short, massive consumption of energy which is generated by glycolysis. After contraction, the cells require a long recovery time. In this type of muscle cells, lactic fermentation is used to restore NAD^+ levels [Robergs *et al.* 2004]. The thereby generated lactate is released from the muscle and can be recycled to glucose in the liver under the expense of six molecules of ATP. This sumptuous process, called Cori cycle, provides glycolytic muscle cells with new glucose [Waterhouse and Keilson 1969]. Nonetheless, this remedy is only favorable for a limited time when glycolytic muscle cells demand a large quantity of available sugar. Since the net yield of energy is negative for the whole body, it is not propitious for the Cori cycle to be maintained over an extended period of time.

A cell solely relying on glycolysis for ATP production faces further problems. Since the protons generated by hydrolysis of ATP (i.e. the breakdown of ATP to release the energy stored within its phosphoester bond) cannot be buffered by glycolytic cells [Hochachka and Mommsen 1983], the pH within the cell and also the blood decreases. Because this acidosis is accompanied by the release of lactate into the blood—two independent incidents caused by the same process—the clinical symptoms have been subsumed in the term lactic acidosis. It is important to emphasize that lactate, and not lactic acid is produced by fermentation and while the rise of lactate in the blood coincides with, it does not cause acidosis [Robergs *et al.* 2004, Lindinger *et al.* 2005]. However, the simultaneous appearance of lactate and protons in the blood makes lactate a good marker for acidosis provoked by anaerobic glycolysis.

Lactic acidosis is most prominently known to occur during exercise. There, glycolytic muscle cells work under anaerobic, hypoxic conditions and use glycolysis as sole mechanism of ATP production. As a result, blood lactate levels increase, whereas blood pH decreases simultaneously and the examiner experiences muscle soreness. However unpleasant this feeling might be perceived, the effect is reversible. In contrast, in some pathological settings, hypoxic conditions are constantly mimicked by impairment of mitochondrial function and therefore, glycolysis remains the sole source of energy. In MELAS for example, lactic acidosis is such a prominent feature that it even appears in the name of the disease. Although elevated lactate levels in blood and cerebrospinal fluid are a hallmark of most mitochondrial diseases [Sproule and Kaufmann 2008], they have been most extensively described for MELAS patients by many different groups [among others van Hellenberg Hubar *et al.* 1991, Malfatti *et al.* 2007, Fornuskova *et al.* 2008, and Tam *et al.* 2008]. The accumulation of lactate in the ventricles was explained by Davidson *et al.* [2009] as a result of severe energy failure caused by deficient mitochondria and stroke-like episodes-induced hypoxia. Kaufmann *et al.* [2004] reported a correlation between lactate levels in the cerebrospinal fluid with the severity of clinical symptoms. Similar findings have been reported *in vitro* where excess lactate in the supernatant coincided with impaired mitochondrial membrane potential [McKenzie *et al.* 2007].

Hence, mitochondrial dysfunction leads to a switch in energy production, i.e. focusing on glycolysis, which causes cellular and systemic impairments. To better understand the importance of mitochondria in cellular metabolism, it is necessary to look at OXPHOS more closely.

2.2.2 Electron Transport Chain and Oxidative Phosphorylation

In mitochondria, the products of anaerobic glycolysis and other metabolic pathways can be further processed to increase the energetic yield from the organic starting material. In a first step, electrons obtained in the breakdown of organic molecules are donated to a final acceptor, oxygen, in a chemical reaction type called redox reaction. Redox reactions describe the transfer of a single electron from one molecule to another. The reducing agent donates an electron to and thereby reduces the oxidant whilst being oxidized itself [Riedel 2002]. The electron transfer from organic molecule to oxygen, however, is not performed in one single step but separated in many minor redox reactions. The energy released therein is used to transport protons across the inner mitochondrial membrane into the intermembrane space and during this process, an electrochemical gradient is generated. By re-entering the matrix through the F_1F_0 ATP synthase, the protons change the conformation of

this rotor-shaped protein complex, thereby catalyzing the generation of ATP [Campbell and Reece 2005 and Figure 2].

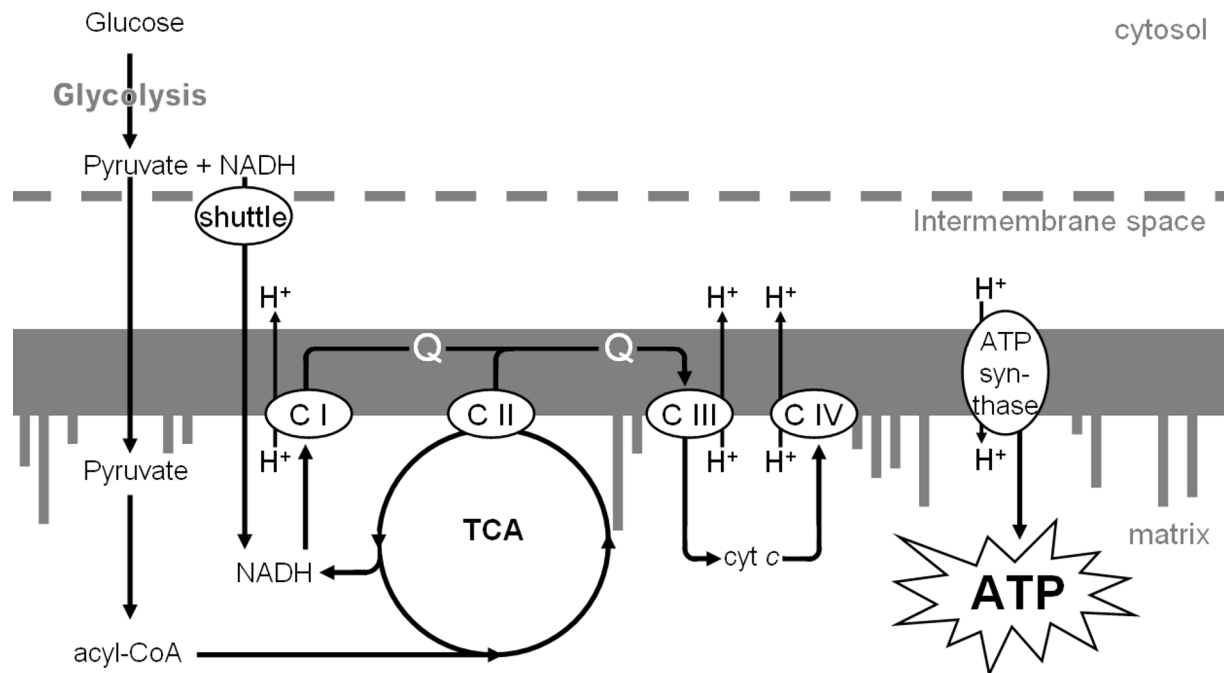


Figure 2: Schematic Representation of Mitochondrial Respiration.

Glucose is degraded in the cytoplasm into pyruvate via glycolysis. Pyruvate is transported into the mitochondria where it is converted into acyl-CoA which then enters the tricarboxylic cycle (TCA) to produce NADH and succinate as intermediates. The latter is oxidized by complex II (C II), a component of the TCA. NADH produced by glycolysis and shuttled into the mitochondria or by TCA is oxidized by complex I (C I), thereby transferring electrons onto the lipophilic carrier CoQ₁₀ (Q). Subsequently, Q donates the electrons to cytochrome *c* (cyt *c*) via complex III (C III). Electrons from reduced cyt *c* are then transferred to molecular oxygen via complex IV (C IV) to form water. During redox reactions of complexes I, III, and IV, protons (H⁺) are transported from the matrix to the intermembrane space. The force of this proton gradient is then used by the ATP to produce adenosine triphosphate (ATP).

The reactions for ATP production mainly take place in the inner membrane and the matrix. The intermembrane space is used as a repository of protons which are pumped in there from the matrix during OXPHOS. The inner membrane is extensively folded to increase the total surface area, since the complex apparatus of the respiratory chain is mainly located in and adjacent to the inner membrane. The matrix finally holds enzymes, substrates and intermediates of the tricarboxylic acid cycle which provides the machinery and fuel for OXPHOS as will be explained in detail below.

OXPHOS consists of two coupled entities: first, the electron transport chain (ETC), where the passage of high-energy electrons to oxygen generates a proton gradient, and the secondary synthesis of ATP, driven by this gradient. To elucidate the system more closely, the fate of the products of glycolysis, pyruvate and NADH, is described in more detail.

Since the inner mitochondrial membrane is impermeable for NADH, cytoplasmic NADH from glycolysis is transported into the mitochondria using special shuttle systems. One of them, the malate-aspartate shuttle employs malate dehydrogenase and aspartate aminotransferase on both sides of the inner membrane, as well as two amino acid antiporters located within the inner membrane. Malate dehydrogenase catalyzes the delivery of the electrons of NADH from the inter membrane space onto oxaloacetate. The thereby generated malonate is then transported into the matrix by an antiporter, where it is oxidized back to oxaloacetate by malate dehydrogenase, giving rise to NADH. The shuttle is completed by an orchestrated interplay of transformations and transports of different amino acids including aspartate, glutamate and α -ketoglutarate [Washizu 2010 and Figure 3A].

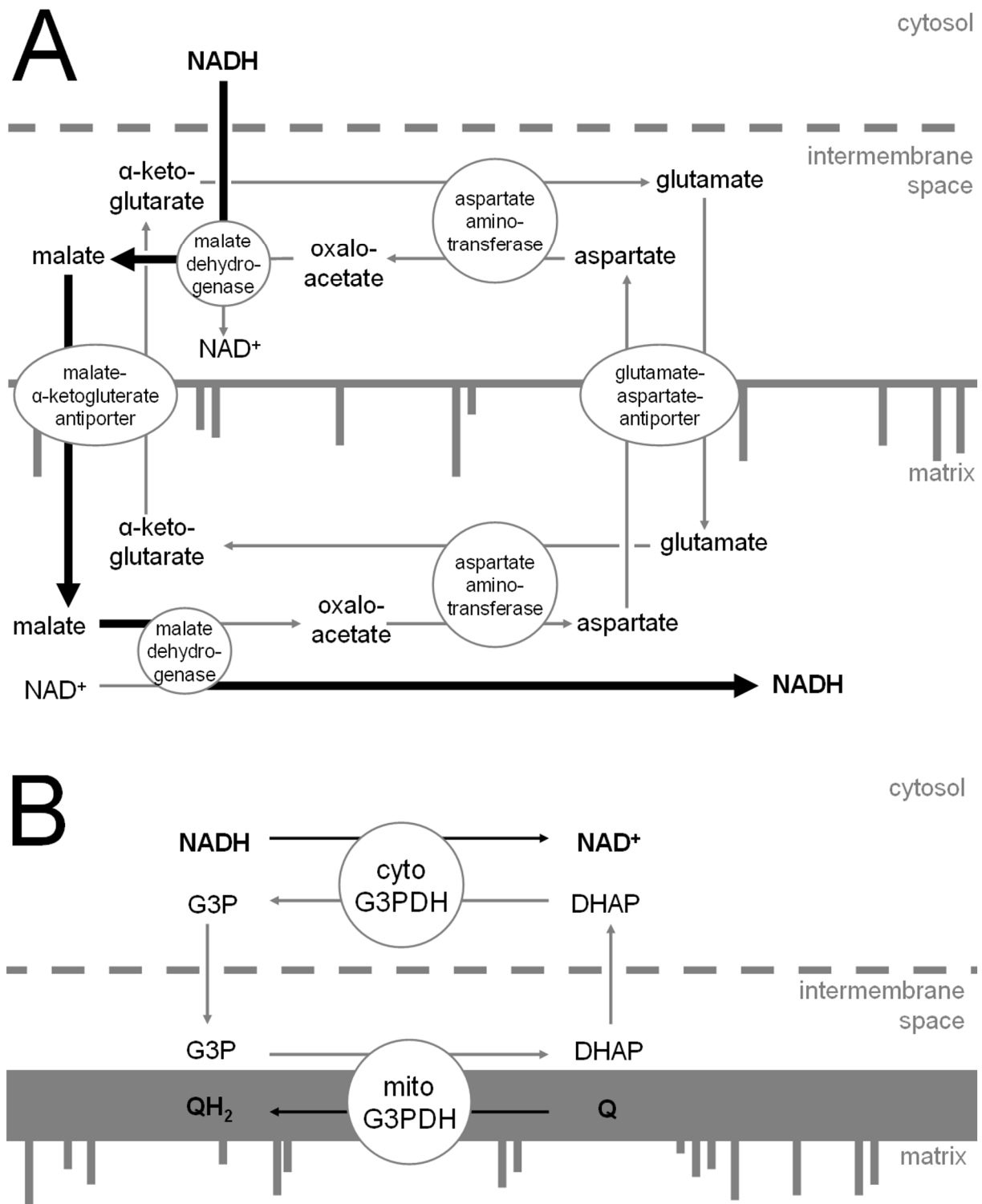


Figure 3: Two Different Shuttle Systems Transport Electron Equivalents from NADH into the Mitochondria.

Since mitochondrial membranes are impermeable for NADH, the energy-rich electron equivalents are transported into the mitochondria via different pathways. (A) The malate-aspartate shuttle employs the NADH-dependent reduction of oxaloacetate by malate dehydrogenase in the intermembrane space. Malate is then transported into the matrix where it is re-oxidized to oxaloacetate, thereby oxidizing matrix-based NAD^+ . An elegant system of an aminotransferase and antiporters keep energy costs for the transport of malate across the inner membrane low. The route of electrons transported from cytosolic to mitochondrial NADH is depicted in bold black arrows. (B) A more direct pathway for transporting electron equivalents into the mitochondria is accomplished by the glycerol-3-phosphate (G3P) shuttle. Cytosolic G3P dehydrogenase (cyto G3PDH) couples the reduction of dihydroxyacetone (DHAP) to the oxidation of NADH. The thereby generated G3P is oxidized back to DHAP by a mitochondrial G3PDH (mito G3PDH) located in the inner membrane. The electrons from G3P are then transferred onto CoQ_{10} via a prosthetic flavin adenine dinucleotide (FAD).

Complex I

When in the matrix, NADH transfers its electrons into the ETC. The entry site for these electrons is located on an impressive enzymatic complex consisting of 46 subunits; called complex I (EC 1.6.5.3). The subunits for complex I are encoded both in the mitochondrial and nuclear genome [for complex I-related mutations of the

mitochondrial DNA see also 2.1.1 and 2.1.2]. Complex I has an L-shape with one arm—containing one flavin mononucleotide (FMN) and eight iron-sulfur (FeS) clusters as pivotal prosthetic groups—inclining into the matrix [Brandt *et al.* 2003]. NADH delivers its electrons to the FMN site from where they are passed via the FeS clusters to the mobile electron carrier CoQ₁₀. During the electron transport throughout complex I, four protons are added to the proton gradient. Ohnishi and Salerno [2005] proposed a mechanism, in which two protons are pumped across the membrane and two more are removed from the matrix by binding to CoQ₁₀. They agree with Brandt *et al.* [2003] which linked the proton pumping to conformational energy transfer and not to a separate, direct proton pump. The two electrons bound to H₂-CoQ₁₀ are passed onto complex III further downstream of the ETC.

Complex III

Complex III (EC 1.10.2.2) is a multi-subunit, membrane-spanning protein complex that catalyzes the transfer of electrons from H₂-CoQ₁₀ to cytochrome *c* and further adds to the proton gradient. Re-oxidation of CoQ₁₀ enables the redox cycle conducted by this mobile electron carrier between complexes I and III. The electrons are passed onto cytochrome *c* which constitutes the second mobile electron carrier of the ETC. During this process, four protons are released into the intermembrane space and two electrons are dislodged from the matrix [Campbell and Reece 2005].

Complex IV

The final step of the ETC occurs in complex IV (EC 1.9.3.1) is a multi-subunit, transmembrane enzyme complex which catalyzes the reduction of molecular oxygen to water. For this reaction, four molecules of reduced cytochrome *c* and four protons from the matrix are used to reduce one molecule of O₂. Thus, complex IV fulfills the redox cycle for cytochrome *c* by re-oxidation and, in addition, pumps four protons from the matrix into the intermembrane space, further enhancing the proton gradient [Campbell and Reece 2005].

F₁F₀ ATP synthase

In the course of the ETC, electrons are passed from molecules with low electronegativity to such with high electronegativity. This transfer is energetically favorable and is coupled to the production of a proton gradient. In a subsequent step of ETC, this gradient is used to drive the synthesis of ATP. Therein, by allowing protons to re-enter the matrix, F₁F₀ ATP synthase (EC 3.6.3.14) undergoes conformational changes that bring ADP and inorganic phosphate closely together, facilitating the production of ATP [Campbell and Reece 2005]. The ATP synthase is sometimes also referred to as complex IV.

Finally, one molecule of NADH oxidized at complex I results in the generation of 2.5 molecules of ATP at the F₁F₀ ATP synthase [Campbell and Reece 2005]. Hence, alone from this source, OXPHOS enhances ATP yield from one molecule of glucose—which is degraded into two molecules of NADH during glycolysis—to seven molecules of ATP instead of only two in anaerobic glycolysis. However, the second product of anaerobic glycolysis, pyruvate, is not included in this calculation.

Complex II

Pyruvate enters the mitochondrial matrix via the pyruvate dehydrogenase complex which transforms pyruvate into acetyl-coenzyme A (CoA) and leaves NADH and carbon dioxide (CO₂) as side products. Acetyl-CoA then enters the tricarboxylic acid cycle (TCA) which is also called citric acid cycle or Krebs cycle. This cycle, consisting of eight enzymes or enzyme complexes and nine intermediates (one being succinate), breaks acetyl-CoA down to two molecules of CO₂ and thereby generating three molecules of NADH and one molecule of guanosine triphosphate (GTP). Thus, out of one molecule of pyruvate, 7.5 molecules of ATP may be generated via the ETC. Furthermore, one enzyme of the TCA is the succinate:CoQ₁₀ dehydrogenase (EC 1.3.5.1), also called complex II, which catalyzes the reduction of CoQ₁₀. As its name suggests, complex II is a part of the ETC and—next to complex I—a source for the entry of electrons. Again, the mobile electron carrier H₂-CoQ₁₀ can then transfer its electrons to complex III and, upon execution of the ETC and the F₁F₀ ATP synthase, 1.5 molecules of ATP are generated per molecule of pyruvate [Alberts 2002].

Hence, under aerobic conditions, the breakdown of one molecule of glucose yields in theoretically 25 molecules ATP and two molecules GTP. Other estimates suggest a production of 30 to 36 molecules of ATP [Vander Heiden *et al.* 2009]. Either way, this amount outshines the two molecules of ATP produced by anaerobic glycolysis many fold and thus, the energy production of mitochondria cannot be underestimated. Considering the excess of ATP produced by mitochondria, it is not surprising that their deficiency leads to major alterations in cellular metabolism as seen in patients with mitochondrial disorders and their overdrawn reliance on glycolysis [see **Figure 1**].

2.2.3 Other Relevant Electron Transport Systems

The classic ETC described in the previous subchapter 2.2.2 consists of complexes I and II as the only entry site for electrons derived from the breakdown of organic molecules. There are, however, other electron transport systems involved in ATP production. NADH derived from glycolysis can enter the ETC directly via another dehydrogenase than complex I. Furthermore, other organic food molecules, for example fatty acids, are degraded to different products than glucose.

In contrast to the malate-aspartate shuttle [see description in 2.2.2], the glycerol-3-phosphate (G3P) shuttle does not reconstitute NADH within the mitochondrial matrix, but delivers electrons directly into a branch of the electron transport chain [**Figure 3B**]. Specifically, cytosolic NADH is oxidized to NAD⁺ by the cytosolic enzyme G3P dehydrogenase (cG3PDH; EC 1.1.1.8), generating G3P by reduction of dihydroxyacetone phosphate

(DHAP) along the way. G₃P can easily enter the intermembrane space and bind to the mitochondrial G₃PDH (EC 1.1.5.3), where its electrons are transferred to CoQ₁₀, thereby generating DHAP and reduced CoQ₁₀ (H₂-CoQ₁₀). DHAP is then shuttled back into the cytosol, thus closing the loop. When bound to H₂-CoQ₁₀, the electrons finally enter the classical ETC at the site of complex III and, in consequence, are able to generate 1.5 molecules of ATP per molecule of NADH [Campbell and Reece 2005].

Fatty acids are an important and abundant source of dietary energy input – at least in modern western countries. Their breakdown within cells is separated in three steps [Figure 4]: first, fatty acids are activated—i.e. they are substituted with CoA—in the cytosol, whereupon they are secondly transported into the mitochondria where they are degraded in a third stage (branched or very long (≥ 20 carbons) fatty acid chains are first broken down into smaller ones in peroxisomes before activation). Cytosolic activation gives rise to acyl-CoA to the expense of one molecule ATP being twice hydrolyzed to adenosine monophosphate (AMP). Acyl-CoA then enters the mitochondrial matrix via the carnitine shuttle: carnitine is added to acyl-CoA to form acyl-carnitine by carnitine palmitoyl transferase I (CPT₁; EC 2.3.1.21) located on the outer membrane. Acyl-carnitine is then transported into the matrix by the antiporter carnitine-acylcarnitine translocase spanning the inner membrane. CPT₂ (EC 2.3.1.21) reverses the reaction of CPT₁, thus giving rise to acyl-CoA in the matrix [Longo *et al.* 2006].

Acyl-CoA is then broken down into acetyl-CoA—the substrate for the TCA [see 2.2.2]—by a process called β -oxidation [Figure 4]. Since fatty acids vary in their chain lengths and degree of saturation, the basic principle of the β -oxidation will be explained by means of a fully saturated fatty acid with an even-numbered chain (special enzymes and additional reactions deal with unsaturated or odd-numbered chain containing fatty acids). In general, four enzymes are responsible for the step-wise decomposition of the acyl chain from the thioester site. In this process, the carbon on the β -position of the chain is oxidized—hence the name—to form a keton which can be attacked by a nucleophile, such as CoA. This β -ketothiolase-mediated reaction (EC 2.3.1.16) results in one acetyl-CoA and one acyl-CoA. The latter is shorter by two carbons than it was before this cycle. This process is repeated until the chain of acyl-CoA consists of only two carbons (which essentially is acetyl-CoA). In addition to one molecule of the TCA substrate, acetyl-CoA, each cycle produces each one molecule of NADH and reduced flavin adenine dinucleotide (FADH₂). Similarly to NADH, FADH₂ can convert the energy gained by its oxidation—re-constituting its more stable, aromatic form—into the generation of a proton gradient via the ETC with a value of 1.5 molecules ATP [Campbell and Reece 2005].

Knowing the entry sites for NADH and acetyl-CoA into the ETC, the question arises where FADH₂ may donate its high-energy electrons. Although FADH₂ is used by complex II as a prosthetic group, free FADH₂ cannot bind to it. In contrast, FADH₂ transfers its electrons to an electron-transferring-flavoprotein (ETF) which is thereupon oxidized by an ETF dehydrogenase (ETFDH; EC 1.5.5.1) [Figure 4]. ETFDH is a FeS cluster-containing flavoprotein located in the inner mitochondrial membrane and acts as junction between fatty acid catabolism and OXPHOS [Frerman 1987]. It catalyzes the reduction of CoQ₁₀ which then can donate the electrons to cytochrome *c* via complex III.

Hence, ETFDH, as well as G₃PDH, belongs to the ETC, even though they are not listed in its classic itemization.

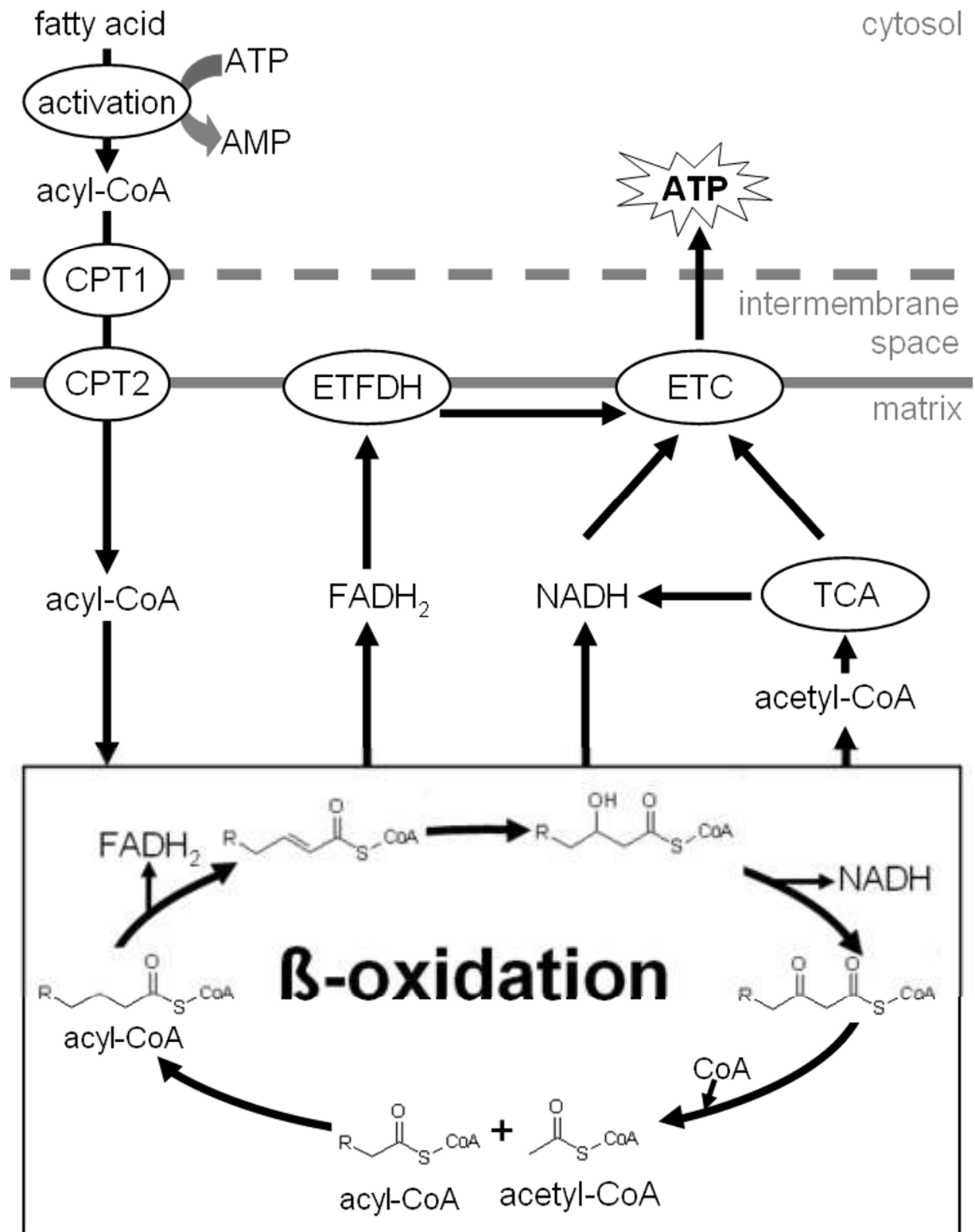


Figure 4: Fatty Acid Metabolism and β -Oxidation.

Fatty acids are activated, i.e. substituted with coenzyme A (CoA) to form acyl-CoA in the cytosol to the expense of ATP being doubly hydrolysed to AMP. Acyl-CoA is then transported into the mitochondrial matrix via carnitine palmitoyl transferase I and II (CPT₁ and CPT₂) where it is degraded by β -oxidation. During this process, the initial molecule of acyl-CoA is shortened by two carbons and enters β -oxidation again. Furthermore, NADH, FADH₂, and acetyl-CoA are generated which are used to produce ATP via mitochondrial respiration. The Acetyl-CoA enters the tricarboxylic acid cycle (TCA), whereas NADH and FADH₂ donate electrons to the electron transport chain (ETC) via complex I or electron-transferring-flavoprotein dehydrogenase (ETF_{DH}), respectively. The insertion shows structures of the intermediates in the β -oxidation.

2.2.4 Janus-faced Mitochondria: The Rise of Reactive Oxygen Species during Respiration

Persuading with an impressive yield of ATP, mitochondria advertise their function in cellular energy metabolism. As always, however, there are two sides to a coin: the very mechanism employed to produce the

highly needed, energy-bearing molecule ATP gives rise to hazardous toxins. Given a chance, electrons leak from their designated route of the ETC to spontaneously react with molecular oxygen and in turn, form reactive oxygen species (ROS).

ROS unite different molecules possessing highly redox-active oxygen such as superoxide ($O_2^{\cdot-}$), hydroxyl radical ($HO^{\cdot-}$), and hydroperoxides (ROOH). Functionally, they are related to reactive nitrogen species (RNS) and other aggressive free radicals. They all possess at least one unpaired electron and therefore, imperatively request another electron. They can do so by purloining an electron from any unspecific, close-by molecule and thereby generating a new free radical in turn. This leads to a chain reaction in which macromolecules—prevalently membrane lipids and proteins—are damaged. To counteract such a process of destruction—generally called oxidative stress—cells utilize a refined apparatus of detoxifying agents and enzymes [see 2.3.1].

The generation of ROS occurs even during healthy, normal respiration [Murphy 2009]. However, due to the negligible amount and effective innate protection mechanisms, their free electrons are quickly captured. Nonetheless, mitochondria are the major source of ROS in cells with oxidoreductases such as complexes I and III responsible for their formation [Murphy 2009]. In contrary, to the save two-electron reductions carried out enzymatically by the complexes of the ETC, molecular oxygen (O_2), a strong electron acceptor, spontaneously accommodates one electron at the time and thereby, it is reduced to superoxide.

Murphy [2009] proposed three modes of mitochondrial ROS production [Figure 5]: Under normal conditions, he admitted the abundance of low levels of mitochondrial ROS but lacked an explanation for their formation [Figure 5A]. As second mode he suggested a combination of an ample ratio of NADH/NAD⁺ and low ATP demand that would lead to superoxide production at the FMN prosthetic group of complex I [Figure 5B]. Finally, a high proton-motive force—i.e. the increased mitochondrial membrane potential ($\Delta\Psi_m$) caused by the proton gradient—and a reduced CoQ₁₀ pool would drive reverse electron transport (RET) and consequently ROS production [Figure 5C]. The previously described forward electron transport [see 2.2.2] transfers electrons from NADH to CoQ₁₀; a process coupled to pumping protons across the inner membrane. A high $\Delta\Psi_m$ can invert this process if a suitable amount of electron donor in form of reduced CoQ₁₀ is available. In that case, RET—driven by the reverse action of the proton pump—shuttles electrons from H₂-CoQ₁₀ back to NAD⁺ until complete reduction of the latter. Whilst this process is not associated with ROS formation, Treberg and Brand [2011] proposed a model for radical production during RET after full reduction of the NADH pool: if the pressure from an elevated $\Delta\Psi_m$ still persists and a sufficient amount of H₂-CoQ₁₀ remains, electrons are transferred from a partially reduced CoQ₁₀ within the binding pocket to O₂. Superoxide generated by this means is believed to be the major source of mitochondrial ROS [Murphy 2009, Treberg and Brand 2011].

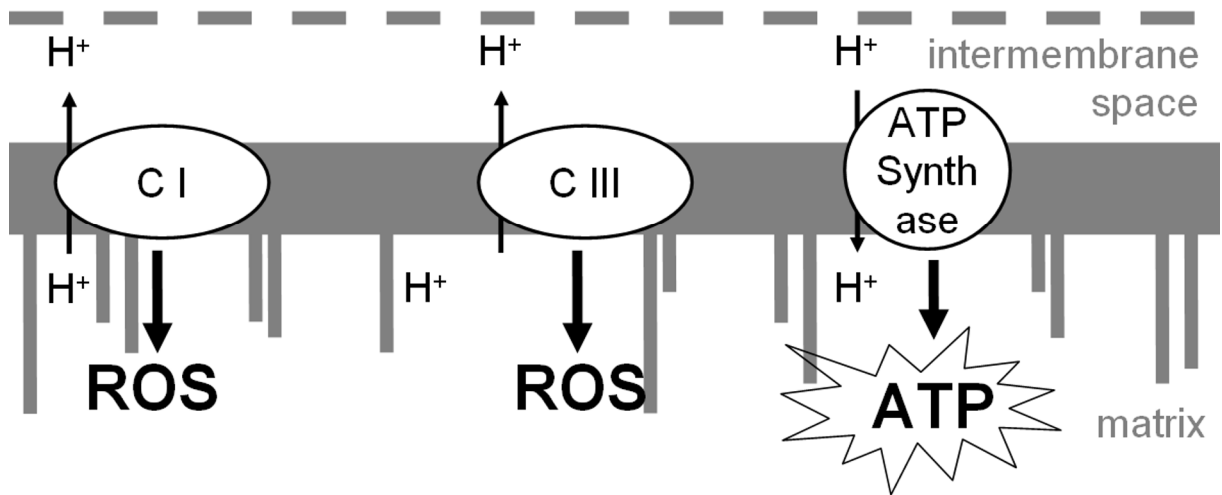
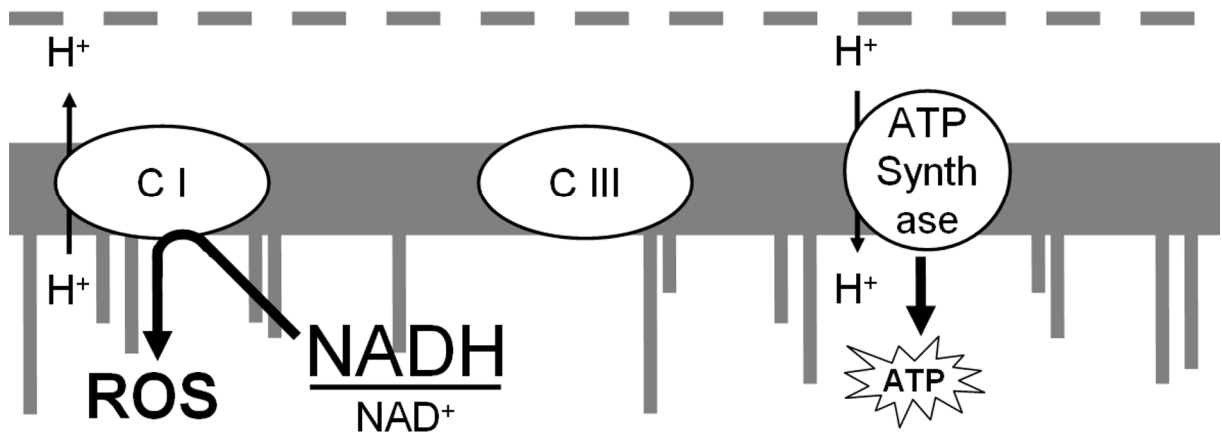
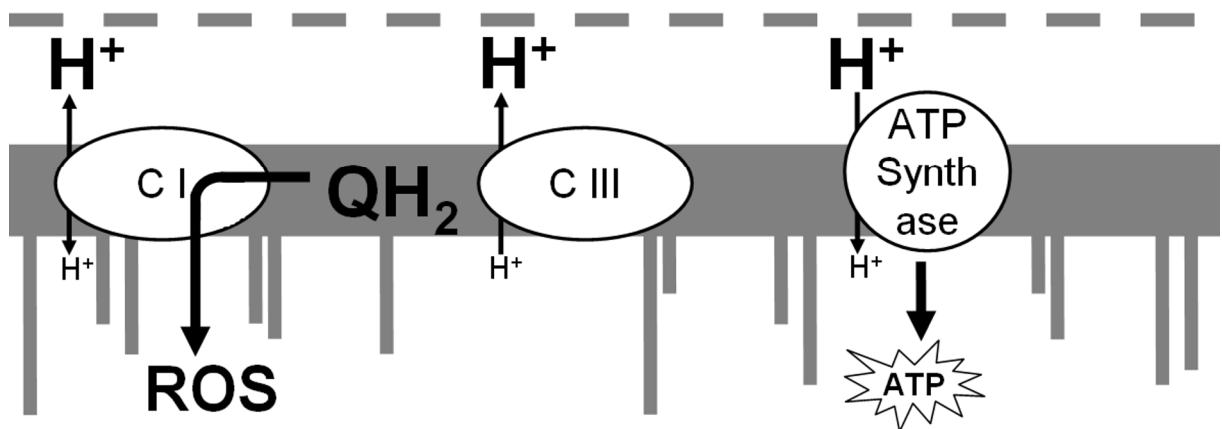
A normal conditions**B** high NADH/NAD⁺ ratio; low ATP demand**C** reverse electron transport

Figure 5: Schematic Representation of Different Modes for Mitochondrial ROS Production.

Murphy [2009] proposed three modes of reactive oxygen species (ROS) production in mitochondria. (A) Under normal conditions, low levels of ROS are produced by mitochondrial complexes I and III (C I and C III) by yet undisclosed mechanisms. (B) An increased NADH/NAD⁺ ratio combined with a low demand for ATP production promote the direct transfer of electrons from NADH to molecular oxygen at the flavin mononucleotide, i.e. the NADH-binding site, of complex I. (C) In case of high proton (H⁺) gradient ($\Delta\Psi_m$) across the inner mitochondrial membrane and a reduced CoQ₁₀ pool (QH₂), electrons can be transferred from QH₂ to molecular oxygen by reverse electron transport (RET) and thereby producing ROS.

Another mode of complex I-dependent ROS formation is induced by some inhibitors of complex I at the site of the quinone-binding pocket [Degli Esposti *et al.* 1996b, Fato *et al.* 2009]. A well-known inhibitor falling in this category, rotenone, promotes the delivery of electrons to O₂ in forward electron transfer [Treberg and Brand 2011].

Complex III has also been frequently quoted to be a major source of mitochondrial ROS formation [Cadenas *et al.* 1977, Turrens *et al.* 1985]. Other mitochondrial oxidoreductases implicated in superoxide production are α -ketoglutarate dehydrogenase (EC 1.2.4.2) [Starkov *et al.* 2004], G3PDH [Tretter *et al.* 2007], and ETFDH [St-Pierre *et al.* 2002]; however, their portion in radical generation—including that of complex III—is negligible compared to RET-driven superoxide emission by complex I [Murphy 2009].

Hence, complex I is—next to being the most important entry site for electrons into the ETC—potentially hazardous, since ROS induced by it may lead to devastating effects if protection mechanisms fail to suppress their propagation.

2.3 The Importance of the Redox Environment

Radicals were long considered to be detrimental to cells and organisms [Oliveira *et al.* 2010], but this picture altered within recent years granting them a more versatile role in cellular function than just the part of playing a detrimental agent [Schafer and Buettner 2001, Miura and Endo 2010]. Redox reactions, as well as compounds and pathways involved therein, are a prime example for the delicate, intricate and dynamic processes taking place in biological systems. Free radicals—harmful to cells when abundant above a certain threshold—are employed as messengers in signaling cascades. Changes in the redox environment can lead to altered conformations and thus functions of certain enzymes. These interactions are highly complex and important, but still far from understood.

In biological systems, radicals arise in processes involving redox reactions. Unfortunately, compounds with unpaired electrons—the so-called free radicals—might be unintentionally generated during such reactions as described for ROS production by complex I [see 2.2.4]. Their high reactivity diminishes the selectivity against reactants and thus, the sophisticated balance of cellular interactions between macromolecules of all sorts can be disrupted. Hence, tight control over redox reactions, redox-active agents and free radicals—which are merged in the term redox state [Schafer and Buettner 2001]—are absolutely necessary for a cell's function.

2.3.1 Oxidative Stress

An excess of free radicals—mostly ROS in biological systems—leads to hazardous alterations of macromolecules such as lipids and proteins by a process termed oxidative stress. Generally, chemical reactions—even if they form energetically more stable products and are thus favorable—require energy to be started. Enzymes are employed to reduce this initial energy barrier and thus, the chemical reactions of a cell to produce the needed components are catalyzed by enzymes. In contrast, free radicals are very aggressive agents which do not depend on enzymatic activity to react with other molecules: their high reactivity leads to spontaneous reactions with any molecule in its vicinity.

In the case of complex I-dependent ROS production during RET, superoxide is formed within the quinone-binding pocket which has access to the inner membrane of the mitochondria. This membrane consists of phospholipids which are susceptible to undergo redox reactions with superoxide in a process called lipid peroxidation [Figure 6]. The free radical catches an electron from a fatty acid chain of a phospholipid thereby generating a lipid radical. Addition of molecular oxygen forms a lipid peroxy radical which steals an electron and a proton of a proximate fatty acid chain resulting in the production of a lipidperoxide and a new lipid radical which in turn continues this cycle [Gutteridge and Halliwell 1990]. Thus, the formation of lipidperoxides propagates throughout the membrane.

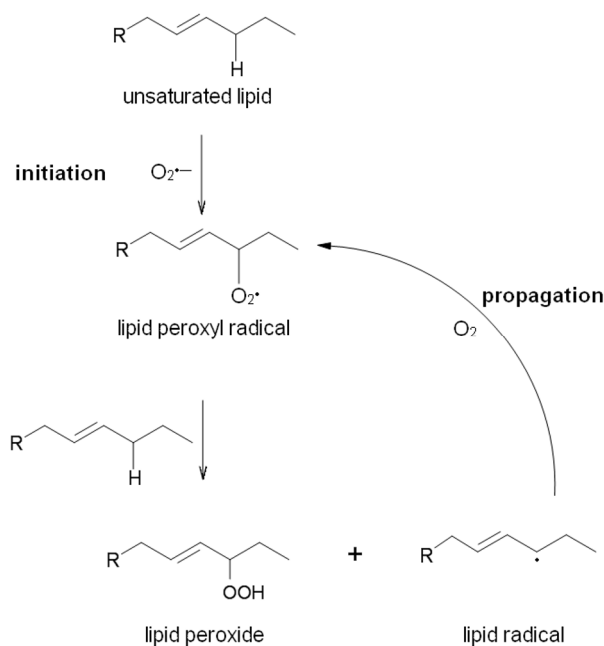


Figure 6: Schematic Representation of Lipid Peroxidation.

Lipid peroxidation is initiated by the reaction of unsaturated lipids with superoxide ($O_2^{\bullet-}$). Thereby, the unstable lipid peroxy radical is formed which reacts with an adjacent unsaturated lipid. This results in the formation of two products: (i) the relatively stable lipid peroxide with a bulky peroxide group and (ii) a lipid radical. The latter can react with molecular oxygen to produce a new lipid peroxy radical, which again reacts with another unsaturated lipid. Thus, the formation of lipid peroxides is propagated via a chain reaction. When lipid peroxidation occurs in phospholipid membranes, the bulky peroxide groups diminish membrane integrity.

The composition of fatty acids determines the stability and fluidity of a membrane. Accordingly, addition of polar, bulky components like the peroxy group alters the arrangement of fatty acids and undermines the proper function of the membrane. Due to the induced sterical hindrance, the permeability across the membrane is elevated and this can entail detrimental effects such as apoptosis.

Hence, a cell is well advised to counteract radical propagation at an early stage. Therefore, several mechanisms for capturing radicals have evolved. Control of the cellular redox state combines a myriad of transcriptional, enzymatic and small molecule-mediated actions as will be explained. For the latter, certain redox couples are especially important, such as nicotinamide adenine dinucleotide (phosphate) ($NAD(P)^+/NAD(P)H$) and glutathione ($GSSG/2\ GSH$). Linked redox couples are compounds that can be interconverted by reduction or oxidation, respectively and they are responsible for the redox environment as by definition of Schafer and Buettner [2001] is the “summation of the products of the reduction potential and reducing capacity of the linked redox couples” which are found in a given biological compartment, be it an organelle, a cell or tissue. The reduction potential is determined by the likelihood of a given chemical species to be reduced and the reducing capacity characterizes the number of electrons available.

A cell employs both enzymatic and small molecule-driven detoxifying of radicals. With cellular concentrations up to 10 mM, glutathione (L- γ -glutamyl-L-cysteinyl-glycine, GSH) represents the major agent for detoxifying oxidative species such as ROS and reactive nitrogen species (RNS) [Smith *et al.* 1996]. It consists of a tripeptide with a γ -bond between glutamate and cysteine which is suggested to be resistant against degradations by enzymes responsible for protein breakdown [Sies 1999]. The redox-active moiety of GSH is its sulfhydryl group which is employed as a reducing agent. In most instances, oxidation of GSH gives rise to glutathione disulfide (GSSG) which is the homodimer of GSH. However, GSH can also interact with cysteine residues of proteins via disulfide bonds (PSSG; whereas PSH denotes the protein (P) with the sulfhydryl group (SH) of the accordant cysteine) [Schafer and Buettner 2001]. Glutathione S-transferases (GTS; EC 2.5.1.18) catalyze the addition of GSH to pro-oxidant exogenous agents [Hayes *et al.* 2000], whereas glutathione peroxidase (EC 1.11.1.9) promotes the reaction of hydrogen peroxide to water [Park *et al.* 2011]. Depletion of GSH was shown to be fatal to cells under increased oxidative insults revealing its importance in oxidative protection [Sortino *et al.* 1999]. GSSG is recycled to GSH by the enzyme GSH reductase (EC 1.8.1.7) utilizing NADPH gained from the pentose phosphate pathway (PPP) which will be described below [2.3.2].

Other redox-reactive, antioxidant compounds are CoQ₁₀ and vitamin E; the latter being a collective name summarizing structurally similar agents, i.e. tocopherols and tocotrienols. Both molecules are highly hydrophobic and are thus well suitable for preventing the radical propagation across membranes. Vitamin E and/or CoQ₁₀ supplementation has shown to be beneficial both *in vivo* and *in vitro* [Serbinova *et al.* 1991, Shargorodsky *et al.* 2010, and Kalayci *et al.* 2011]. However, some argue that antioxidants, being redox-reactive, bear the risk of turning into pro-oxidants [Linnane *et al.* 2007, Lam *et al.* 2010]. In fact, knowledge on the properties of this class of compounds needs to be deepened.

Next to these small molecule-dependent defense mechanisms, cells also enact several enzymatic strategies to detoxify free radicals. The elimination of superoxide, a very aggressive radical agent, is carried out by a class of enzymes called superoxide dismutases (SOD; EC 1.15.1.1) which convert superoxide into molecular oxygen and hydrogen peroxide. Even though the latter remains a potential threat to cells, it is far less reactive than superoxide. Two sorts of SOD are found in cells: the zinc (Zn)-containing enzyme (ZnSOD) within the cytosol and the manganese-containing SDO (MnSOD) specifically found in mitochondria [Weisiger and Fridovich 1972]. That mitochondria employ their own form of SOD confirmed the importance of antioxidant protection of this compartment [Murphy 2009]. In mice lacking mitochondrial SOD, several detrimental pathological symptoms, which result in early neonatal death, have been described [Melov *et al.* 1998]. The hydrogen peroxide produced by SOD can be further detoxified to water by the enzyme catalase [Chelikani *et al.* 2004].

High levels of oxidative stress also trigger transcriptional changes which are also induced by exogenous toxicants. Transcription factors bind to so-called promoter regions on DNA strands and initiate or repress the transcription of genes encoded within the successive DNA sequence. A major role in the response to ROS is played by the nuclear factor (erythroid-derived 2)-like 2 (Nrf2). Under physiological conditions, Nrf2 is located in the cytosol and readily degraded; a process which is interrupted by high levels of ROS [see 2.3.2]. Then, however, Nrf2 enters the nucleus where it binds to DNA regions which contain an antioxidant response element (ARE) [Jaiswal 2000]. These can be found in promoters of genes that are involved in the detoxification of ROS. Hence, Nrf2 promotes the transcription of antioxidant enzymes and redox regulators such as GSH-related enzymes (for example GSH reductase and GSTs) and NAD(P)H:quinone oxidoreductase (NQO1; EC 1.6.5.2) [Klaassen and Reisman 2010, Sykietis and Bohmann 2011]. NQO1 is a cytosolic enzyme which is engaged in detoxifying exogenous compounds. Some detoxifying enzymes such as NADPH:cytochrome p450 reductase (EC 1.6.2.4) hold the disadvantage of employing a one-electron reduction of hazardous agents which might paradoxically result in the production of radicals. In contrast, NQO1 catalyzes a complete, two-electron reduction [O'Brien 1991, Monks *et al.* 1992]. Experiments in nrf2-mutant mice provided data for the importance of Nrf2 for inducing detoxifying enzymes, since disruption of the gene prevented the expression of GSTs and NQO1 after treatment with a pro-oxidant [Itoh *et al.* 1997].

All the described strategies help to protect cells from oxidative damage. However, when these defensive mechanisms fail to reduce the toxic threat, cells might die due to disintegration of membranes and dysfunction of enzymes. Next to the aforementioned deficiencies of glutathione or SOD, it has been shown that increased levels of pro-oxidants can overcharge cellular response mechanisms [Cardoso *et al.* 1998, Mordente *et al.* 1998].

2.3.2 Redox Environment and ROS Signaling

Nonetheless, the reputation of ROS has changed from being exclusively detrimental for they are now regarded as more versatile agents [Miura and Endo 2010]. In fact, ROS and redox reactions are fundamental for cells and cover a broad range of cellular processes. Indeed, the redox environment defines the fate of a cell to a great extent and seem to reflect or force states such as proliferation, differentiation and even death [Schafer and Buettner 2001].

The important role of redox reactions and environments can be appreciated by their prominent appearance. For example, different cellular compartments possess specific redox environments: whereas the cytosol holds reduced conditions, the functioning of some organelles such as lysosomes require on rather oxidative composition [Alberts *et al.* 2000]. Furthermore, breakdown of food molecules and energy production heavily rely on redox reactions and redox reactive agents such as NADH, CoQ₁₀ and prosthetic groups like FeS clusters [see 2.2].

Two related and pivotal redox couples are NADH and NADPH. Both—in addition to directly affect a cell's redox environment—are important co-factors in many enzymatic processes. Despite their chemical similarity—NADH and NADPH vary only in that NADPH bears a phosphate group, whereas NADH does not—their cellular functions cover fields that are quite diverse. NADH, as discussed before, is used as a carrier of high-energy electrons from glycolytic metabolism to OXPHOS. NADPH, in contrast, is employed as reducing agent in anabolic reactions such as fatty acid synthesis and in the restoration of GSH.

NADPH is mainly produced by reduction of NADP⁺ during the oxidative phase of the pentose phosphate pathway (PPP), an alternative pathway to glycolysis for the breakdown of glucose [Kruger and Schaewen 2003]. Nonetheless, PPP is rather an anabolic pathway, since not only NADPH, but also the other products, ribose-5-phosphate and erythrose-4-phosphate, are used in the synthesis of nucleotides and aromatic amino acids, respectively. The ratio of NADH/NADPH therefore represents the metabolic state of a cell [Ying 2008]. Furthermore—in accordance to its role of catabolism—the ratio of the redox couple NAD⁺/NADH is regarded as a sensor of the cell's energy status [Lin *et al.* 2004] and as such also employed in the measures against limited food supply. When there is abundant food and thus, glucose, NADH is produced on the expense of NAD⁺ and the ratio drops. However, lack of glucose shifts this equilibrium towards NAD⁺ and increases the ratio. Hence, it is not surprising that NAD⁺ is a substrate for sirtuins [Lin *et al.* 2004]. Sirtuins promote transcription of certain genes by deacetylating DNA strands. Acetylated DNA tends to be inaccessible for transcription factors and enzymes. Basically, sirtuins respond to decreased glycolytic activity by activating alternative pathways of energy production that may differ from tissue to tissue. In the liver, sirtuins stimulate gluconeogenesis. In white adipose tissue, sirtuins trigger the release of fatty acids into the blood stream. And finally, in muscle cells, sirtuins promote the expression of the transcriptional co-activator peroxisome proliferator-activated receptor gamma

(PPAR γ) coactivator 1-alpha (PGC-1 α) which in turn promotes mitochondrial genesis and fatty acid oxidation [Haigis and Sinclair 2010].

As impressive as the aforementioned consequence of the NAD⁺/NADH ratio might seem, influences of redox couples or the redox state may not always have systemic effects. They might, however, be able to direct the fate of a cell by signaling cascades or alterations of proteins. ROS signaling can be explained using the enzyme Keap1 as an example. The binding of Keap1 to Nrf2 promotes the degradation of the latter. Keap1 contains several cystein groups in the reduced form, since the protein is located within the reduced environment of cytosol. These cystein groups act as redox sensors for a decrease in reduced environment manifests in the oxidation of these groups causing the release of Nrf2 binding [Sykietis and Bohmann 2004]. As a consequence, the degradation of Nrf2 is abandoned and it can translocate into the nucleus to promote transcription of antioxidant enzymes [see 2.3.1]. Thus, defence mechanisms against oxidative stress are triggered by high levels of ROS via induction of oxidative damage to the control enzymes themselves. The resulting conformational changes are then responsible for alterations in enzyme activity. Accordingly, the redox reactive cystein groups of Keap1 are sensors for high levels of oxidative stress.

2.4 Idebenone

2.4.1 Quinones

A compound which was mentioned before in two different roles, namely as electron carrier in the ETC [2.2.2] and as antioxidant compound [2.3.1], is CoQ₁₀ [Figure 7A]. Chemically, CoQ₁₀ belongs to a class called quinones [reviewed in O'Brien 1991 and Monks *et al.* 1992]. This class includes an immense number of important and naturally occurring substances. All quinones share the same basic structure which consists of a quinoid ring system; chemically termed a fully conjugated cyclic dione structure according to IUPAC's Compendium of Chemical Terminology [2nd Edition, 1997]. Quinones are ubiquitously found in fungi, plants, animals, and bacteria in nature as essential mediators of normal cellular functions or as toxic defendants against natural enemies [Monks *et al.* 1992], but are also contained in pollutants such as cigarette smoke [Schmeltz *et al.* 1977].

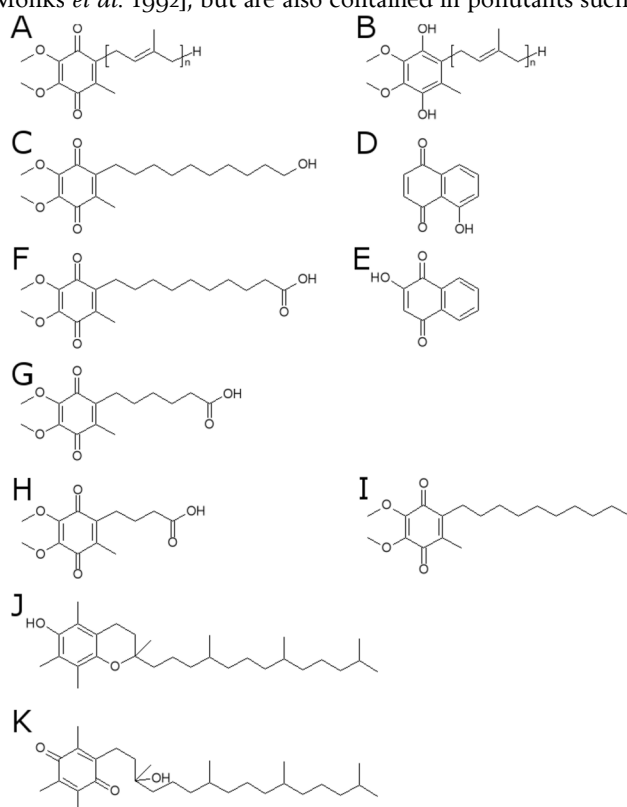


Figure 7: Chemical Structures of Selectec Quinones and Related Molecules.

The selection shows CoQ_n (for example, CoQ₁₀ represents the electron carrier in human electron transport chain,) in the oxidized (A) and reduced (B) form. Upon *in vivo* administration, idebenone (C) can be metabolized into QS-10 (F), QS-6 (G), and QS-4 (H). Decylubiquinol (decylQ; I) lacks the terminal hydroxygroup compared to idebenone. The isomeric juglone (D) and lawsone (E) feature different toxicological properties. The most common representative of vitamin E, α -tocopherol (J), is converted into a quinone after oxidation and water addition (K).

Covering such a broad range of physiological properties suggest that, despite the underlying mutual group, this class unites molecules with distinct pharmacological activities. In contrast to CoQ₁₀, for example, juglone [Figure 7D], a component found in hulls and leaves of black walnut, is highly toxic [Monks *et al.* 1992]. This characteristic of juglone is used by the black walnut to defense its territory against competitive plant species.

Hence, juglone is used mainly as an herbicide, even though its toxicity is harmful for insects or human cells as well [Paulsen and Ljungman 2005].

Surprisingly, the contradictory effects of these two molecules which belong to the same chemical class are partially defined by the chemical reactivity of this class. Quinones have three properties: first, they are oxidants, second, quinones are electrophiles and third, quinones are colored [Monks *et al.* 1992]. The color represents absorption of ultraviolet and visible light energy. Though photo-excited quinones might be fairly reactive, this reaction type might be negligible when examining effects in cells lacking direct contact to light *in vivo*. Nonetheless, this photochemical property has been taken advantage of since ancient history: an isomeric molecule of juglone called lawsone [Figure 7E] is the active ingredient of the Henna dye used since antiquity. Juglone itself exhibits a dark orange-brown color and is also used to dye hair or wool clothes or fabrics and CoQ₁₀ features a yellowish orange color [Monks *et al.* 1992].

In one potential reaction mechanism for quinones, nucleophiles can attack the partially positively charged carbon bound to oxygen. The second oxygen of the quinone, however, decreases the polarization of the quinoid ring and thereby reducing the electrophilic reactivity of the carbon atom. Hence, even though quinones are potential electrophiles, nucleophilic addition to quinones is seldom seen [Cummunings *et al.* 1990, Monks *et al.* 1992]. Instead of that, quinones are rather involved in redox reactions.

Reduction of quinones occurs at one of the partially positively charged carbon atom attached to the oxygen. The excess electron is delocated over the π -orbitals of the quinoid ring system, whereas the electronegative oxygen allures both electrons used for the former double bond to the carbon atom. Thus, one-electron reduction of a quinone leads to a semiquinone anion radical whose negative charge might be neutralized by binding to a proton (called semiquinone radical or more often just semiquinone). Donation of a second electron—attacking at the second oxygen-binding carbon atom—gives rise to the hydroquinone which is—as implied by its name—unlikely to be unprotonated. Beside the correct name hydroquinone one also might find the chemically erroneous term quinol in some publications.

Thus, quinones, semiquinones and hydroquinones are the same molecule in different oxidative states and feature different physicochemical properties. Indeed, the redox capacity of quinones is potentially their most relevant property in a biological context. For example, some quinones can oxidize cellular macromolecules such as lipids or proteins promoting their malfunctioning; whereas some hydroquinones—such as the reduced form of CoQ₁₀, H₂-CoQ₁₀—are described to be potent antioxidants [Crane 2001] that is they are able to stop the hazardous actions of oxidizing agents. Vitamin E, another antioxidant, becomes a quinone upon oxidation [Figure 7J&K]. In its reduced state, however, one oxygen atom is covalently bound to a carbon atom of the alkyl tail.

Since some quinones are toxic to cells, mechanism for their detoxification evolved. NADPH:cytochrome p450, a key enzyme in degradation of exogenous compounds, and NADH:cytochrome *b5* reductase (EC 1.6.2.2) interact with quinones in an incomplete, one-electron reduction, producing potentially hazardous semiquinones [O'Brien 1991]. Additionally, the gene family of NAD(P)H:quinone oxidoreductases (NQOs) are cytosolic flavoproteins that catalyze the reduction of highly reactive quinones and their derivatives and consists of the two members NQO1 and NQO2 (EC 1.10.99.2). Despite substantial differences in expression patterns and inhibitor sensitivity [Winger *et al.* 2009], both enzymes feature the ability to perform complete, two-electron reduction of quinones [Monks *et al.* 1992]. This reaction results in the formation of hydroquinones and hence, eliminates the production of semiquinones. Accordingly, NQOs are key detoxifying enzymes which are induced by stressors such as xenobiotics or pro-oxidants. In the promoter regions of both genes, *cis*-elements like the antioxidant response element (ARE) have been identified [Jaiswal 2000 and subchapter 2.3.1]. While NQO1 uses both NADH and NADPH as electron donor, NQO2 shows a high preference for dihydronicotinamide riboside (NRH) [Long and Jaiswal 2000].

Although—beside a very low reduction rate for CoQ₁₀ [Siegel *et al.* 1997, Dinkova-Kostova and Talalay 2010]—the physiological electron acceptors have not been identified yet, NQOs have been shown to interact with numerous pharmacologically active compounds. Among the substrates are chemicals belonging to the groups of quinone epoxides, aromatic nitro and nitroso compounds, azo dyes and Cr(VI) compounds [Colucci *et al.*, 2007]. However, NQO1 has the highest affinity towards quinones. Interestingly, the two well-described quinone substrates mitomycin C and β -lapachone exhibit their biological activity only upon NQO1-dependent reduction. In presence of functional NQO1, mitomycin C is converted into its active form which is regarded as a valuable anti-cancer candidate [Adikesavan *et al.* 2007]. Similarly, β -lapachone, a naphthoquinone, needs bio-activation by NQO1 to accomplish its anti-tumor effect [Pink *et al.* 2000]. Additionally, reduced β -lapachone is unstable and auto-oxidizes back into its parent form. Thus, this futile cycling continuously stimulates NADH oxidation. The resulting elevated NAD⁺ levels stimulates energy metabolism [Hwang *et al.* 2009 and 2.3.2]. This finding suggests that the function of NQO1 is not limited to protection against oxidative stress but is also involved in more general processes concerning physiological states of a cell. In accordance with this hypothesis, NQO1 was suggested to participate in the redox shuttling of CoQ₁₀ [Beyer *et al.* 1996].

2.4.2 Idebenone: An Overview

As became evident in the precedent chapters, CoQ₁₀ serves two beneficial functions, namely its role in energy production within mitochondria and its antioxidant effect. In disorders with either high levels of oxidative stress

or diminished OXPHOS, treatment with CoQ₁₀ might seem considerable. CoQ₁₀, however, exhibits a major limitation for clinical administration: the long, lipophilic alkyl chain decreases its absorption. For this reason, analogs have been synthesized to increase their solubility while at the same time retaining their beneficial effects.

Idebenone (2-(10-hydroxydecyl)-5,6-dimethoxy-3-methyl-cyclohexa-2,5-diene-1,4-dione) is such a less lipophilic, synthetic molecule with structural similarities to CoQ₁₀, differing from its archetype solely in the alkyl tail: instead of ten repeats of isoprenoid elements, idebenone possesses a ten-carbon alkyl tail holding a hydroxyl group at its end [Okamoto *et al.* 1988 and Figure 7C]. Idebenone was first synthesized by Takeda Pharmaceutical Company and developed for treatment of Alzheimer's disease and improvement of memory and cognitive functions.

Idebenone crosses the blood brain barrier as it has been detected within the brain [Nagai *et al.* 1985]. The distribution of idebenone in rat brains was reported to correspond to 0.5% of dosage at peak time [Nagai *et al.* 1989]. Studies in rats and dogs have revealed that radioactively labeled idebenone peaked in blood 15 min after administration [Torii *et al.* 1985]. It was found most abundantly in the stomach—which means that it remained unabsorbed—as well as in liver and kidneys. In plasma, metabolites called QS-4, QS-6 and QS-10 [Figure 7F-H] outnumbered idebenone. However, when idebenone reached the brain, a 30% was found in mitochondria (the same amount was found in the cytosol and the remaining 40% could not be allocated to). Furthermore, Torii *et al.* [1985] found no accumulation after repeated administration. In human adults, administration of 30–50 mg idebenone evoked peak plasma levels of 300–400 µg/l after one to two hours [Gillis *et al.* 1994].

Despite some reports rising concerns about potential toxicity [Lustyik and O'Leary 1990, Wempe *et al.* 2009, Tai *et al.* 2011], idebenone was considered as a safe drug in many toxicological studies [unpublished data Takeda/Santhera] and clinical trials [Bodmer *et al.* 2009, Kutz *et al.* 2009]. The objections of Lustyik and O'Leary [1990] and Wempe *et al.* [2009] hold limitations: whereas the first report used concentrations which are not achieved *in vivo*—Lustyik and O'Leary reported toxicity for concentrations higher than 75 µM—the latter employed an assay for cell viability, the so-called 3-(4,5-dimethylthiazol-2-yl)-2,5-diphenyltetrazolium bromide (MTT) assay, which interferes directly with idebenone [personal communication with M. Erb].

2.4.3 Idebenone: Preclinical Data of the Brain

Since idebenone enters the brain, several studies investigating neurological effects of the drug have been carried out. Gillis *et al.* [1994] found moderate improvements in humans suffering from a mild form of dementia. In aged rats, administration of 10 or 20 mg/kg idebenone increased levels of nerve growth factor (NGF) in hippocampus and both frontal and parietal cortices [Nitta *et al.* 1993]. On a functional basis, idebenone ameliorated memory as assessed in behavioral test such as the water maze, passive avoidance and habituation test [Yamada *et al.* 1997]. Production of NGF has also been confirmed *in vivo* with concentrations of 10–18 µM idebenone in astrocytes [Takeuchi *et al.* 1990]. Furthermore, Takuma *et al.* [2000] demonstrated protection of astrocytes after reperfusion injury by a broad range of idebenone (10 nM – 10 µM). According to the authors, this protection was not achieved by an antioxidant effect, but by production of NGF.

In addition, idebenone might also be involved in neurotransmitter action. In a rat model of cerebral ischemia, 10–100 mg/kg idebenone inhibited the decrease in acetylcholine [Kakihana *et al.* 1998]. Miyamoto and Coyle [1990] found that a single *per os* (p.o.) application of 3 or 10 mg/kg idebenone 0.5 hours prior to injection of either a kainate receptor (KAR) agonist or an 2-amino-3-(5-methyl-3-oxo-1,2-oxazol-4-yl)propanoic acid (AMPA) receptor (AMPA) agonist into the striatum protects cholinergic or γ -aminobutyric acid (GABA)-ergic neurons. However, this protection was not seen after injection of an *N*-methyl-*D*-aspartate (NMDA) receptor (NMDAR) agonist. Similarly, Kaneko *et al.* [1991] did not detect an influence of idebenone on NMDARs, but they reported augmented currents of KARs and AMPARs in presence of their agonist induced by 10 µM or higher concentrations of idebenone.

2.4.4 Idebenone: Interaction with the Electron Transport Chain

Based on the structural analogy of idebenone and CoQ₁₀, idebenone was proposed to interact with enzymes of the ETC. In fact, influence of idebenone on complexes I, II, and III were described. Sugiyama and coworkers reported that idebenone interfered with complex I, even though their data from *in vitro* and *ex vivo* experiments delivered conflicting results: in isolated rat mitochondria, *in vitro* treatment with 0.25–100 µM idebenone reduced NADH-linked respiration [Sugiyama *et al.* 1985]; whereas idebenone increased complex I-mediated respiration when administered *in vivo* (100–300 mg/kg for three days) [Sugiyama and Fujita 1985]. These data suggested that the interaction of idebenone with ETC components is far more complicated than anticipated. Imada *et al.* [1989] reported that idebenone restored both complex I- and complex II-dependent respiration in CoQ₁₀-depleted mitochondria. In healthy mitochondria, however, idebenone did not alter respiration of complex II, but it inhibited complex I-mediated respiration [Imada *et al.* 1989]. In 1996, Degli Esposti *et al.* dedicated their attention to the role of idebenone in the ETC. They described that idebenone inhibited complex I, whereas it was an effective substrate for complexes II and III. In agreement with these data, Brière *et al.* [2004] found that in presence of pyruvate and succinate, idebenone almost completely inhibited complex I activity whilst leaving the gross metabolic rate unaltered. Lenaz *et al.* [2002] confirmed that idebenone is an inhibitor of complex I using submitochondrial particles. Furthermore, they also reported that idebenone-mediated complex I-inhibition led to superoxide production.

Interestingly, despite the well documented complex I inhibition by idebenone, 69% of idebenone was reduced by mitochondria in presence of NADH [Sugiyama *et al.* 1985]. This suggests that the inhibition of complex I by idebenone might succeed its reduction by complex I; in other words: by reducing idebenone, complex I would give rise to an inhibitor of itself. Indeed, this hypothesis was further substantiated by King *et al.* [2009], who classified idebenone as a competitive substrate to CoQ₁₀ and suggested that it unfolds its inhibitory action by reacting very slowly at the active quinone binding site. The slow reactivity was explained with limited product dissociation and an augmented affinity towards the binding site. King *et al.* [2009] also suggested that idebenone, in addition to the quinone binding site, is reduced at the NADH oxidation site of complex I, since they reported not only reduction of idebenone in presence of the inhibitors of the quinone-binding site, but they also found reduced idebenone when only the NADH binding site-containing subcomplex I λ was present. Since their experiments were carried out on isolated complex I, reduction of idebenone by other oxidoreductases such as NQO1 was omitted. This finding is backed up by the report by Degli Esposti *et al.* [1996a] who showed that the reduction of idebenone is only 63% sensitive to rotenone-inhibition, suggesting an alternative reduction site for idebenone. In contrast, James *et al.* [2005] demonstrated that idebenone—apart from being a good substrate for complex II and III—elicited similar complex I activity as CoQ₂, a described complex I inhibitor [Degli Esposti 1998]. However, these data were generated using yeast which do not employ CoQ₁₀, but a shorter, six isoprenoid repeats-long CoQ as physiological electron carrier [Tran and Clarke 2007]. Therefore, it is difficult to predict if CoQ₂ maintains its inhibitory effect of complex I in this organism. Indeed, ROS production associated with the inhibition of complex I was reported for idebenone [Geromel *et al.* 2008, Fato *et al.* 2008].

In 2008, Rauchová *et al.* confirmed complex I inhibition by idebenone, but demonstrated that it also stimulates electron transfer from G3PDH to complex III, suggesting an alternative route for idebenone-mediated respiration. Indeed, idebenone improved energy production in yeast under low oxygen conditions by an increase in mitochondrial membrane potential, allowing yeast to grow similarly compared to yeast under normoxic conditions [Chapela *et al.* 2008].

2.4.5 Idebenone: Preclinical Evidence for an Antioxidant Effect

Antioxidant effects of idebenone have been described in a myriad of publications. In an artificial system for estimating antioxidant activity using superoxide quenching, 30 mM idebenone proved to be as effective as 213 mM vitamin E, a well described antioxidant [Zhai *et al.* 2008]. Abdel Baky *et al.* [2010] reported a decrease in lipid peroxidation and an increase in GSH, SOD and catalase levels by a single 100 mg/kg *intraperitoneal* (i.p.) administration in a rat hemic hypoxia model. In a rat stroke model, 30 mg/kg p.o. administration of idebenone inhibited lipid peroxidation in erythrocytes and thus, protected membrane integrity [Suno *et al.* 1989].

Since most cells can prevent ROS on their own under normal conditions *in vitro*, oxidative stress sometimes has to be induced either by adding pro-oxidant agents or by inhibiting cellular defense mechanisms. In GSH-depleted cells, viability was ameliorated by as little as 1 μ M idebenone [Sortino *et al.* 1999]. In 1999, Rustin *et al.* reported antioxidant activity of a high dose of idebenone (60 μ M) in homogenates of heart biopsies from FRDA patients. FRDA is a devastating disorder characterized by progressive muscle wasting which is elicited by a mutation in frataxin, a protein thought to be involved in the assembly of FeS clusters in mitochondria. Jauslin *et al.* [2002, 2003, and 2007] utilized the susceptibility of FRDA lymphoblasts to the GSH-depleting agent L-buthionine (S,R)-sulfoximine (BSO) which induces ROS. Idebenone rescued cells from BSO-mediated cell death with half maximal effective concentration (EC₅₀) of 0.4–0.5 μ M. Ferric iron (Fe³⁺) is another ROS-inducing compound often used to provoke oxidative stress and mitochondrial swelling *in vitro*. Idebenone was reported to reduce or even inhibit both symptoms at concentrations varying from two to 84 μ M idebenone [Suno and Nagaoka 1984a-c, Cardoso *et al.* 1998, and Mordente *et al.* 1998]. Interestingly, the beneficial effect of idebenone in this model was enhanced in presence of complex II substrate succinate [Suno and Nagaoka 1989a], suggesting that the antioxidant effect of idebenone is increased when continuing reduction of the molecule is assured. Indeed, the reduced form of idebenone *per se* was attributed with higher antioxidant capacity [Mordente *et al.* 1998].

Bile acid induces high levels of oxidative stress, mitochondrial swelling, and apoptosis. Idebenone was reported to reduce both ROS and RNS production, mitochondrial swelling, and apoptosis at concentrations of 30 or 100 μ M [Yerushalmi *et al.* 2001, Gumprich *et al.* 2002, and Sokol *et al.* 2005].

2.4.6 Idebenone: Additional Findings

However, beside the two major fields of research on idebenone, i.e. its effect as antioxidant and its role in ETC, it has been reported that the drug also modulates other cellular mechanisms. For example, idebenone has been described to inhibit neuronal (N-type Ca_v2.2) and Purkinje cell-encoded (P-type Ca_v2.1) Ca²⁺ channels at concentrations ranging from 1–100 μ M [Houchi *et al.* 1991, Kaneko *et al.* 1990, Chang *et al.* 2011, and Newmann *et al.* 2011]. In their study from 2003, Gil *et al.* reported that 1 μ M idebenone reduced intracellular Ca²⁺ levels in an *in vivo* model of apoptosis. Furthermore, idebenone inhibited platelet aggregation, prostaglandin synthesis and thromboxane B₂ production [Suno and Nagaoka *et al.* 1989c]. This was confirmed by Civenni *et al.* in 1999 when they showed that 10–20 μ M idebenone was able to inhibit cyclooxygenase (EC 1.14.99.1) and lipooxygenase (EC 1.13.11.31), two enzymes involved in prostaglandin synthesis and arachidonic acid metabolism, in astroglia and platelets. Further literature adds to a potential involvement of idebenone in this metabolism, since it was found to inhibit an enzyme involved in the regulation of arachidonic acid-mediated inflammation, phospholipase

A2 (EC 3.1.1.4), with a IC_{50} of 32 μ M [Amano *et al.* 1995]. Interestingly, similar protection against staurosporin-induced apoptosis to that elicited by idebenone was found for a phospholipase A2 inhibitor [Gil *et al.* 2003]. Tsuruo and coworkers [1994] reported that 1-3 μ M idebenone is a substrate for an NO-synthesizing NADPH diaphorase (nNOS; EC 1.14.13.39) in the brain. Although NQO1—formerly known as DT diaphorase—has a similar name, these two enzymes are distinct and should not be mixed up.

2.4.7 Idebenone: Clinical Data

According to its proclaimed antioxidant activity, idebenone was considered a possible treatment in a series of disorders with high levels of oxidative stress. It has been most prominently investigated in FRDA, a disorder characterized by deficiency of FeS complexes and high susceptibility to radicals [Rötig *et al.* 1997]. Several studies have provided data that idebenone is beneficial in FRDA patients by slowing the progression of the disease, especially in young patients [among others Hausse *et al.* 2002, Buyse *et al.* 2003, Di Prospero *et al.* 2007, Tonon and Lodi 2008, Pineda *et al.* 2008, Schulz *et al.* 2009, and Brandsema *et al.* 2010]; however, phase III clinical trials missed significant endpoints [Lynch *et al.* 2010], so the proof of efficacy needs to be substantiated. Currently, idebenone is marketed in Canada under the trade name Catena® for the treatment of FRDA and is also available in Europe under a Named-Patient Program.

Since a preclinical study using *mdx* mice showed that idebenone reduced inflammation and fibrosis in the heart and prevented death due to cardiac pump failure [Buyse *et al.* 2009], idebenone was also investigated as a treatment for DMD. In a phase IIa double-blind randomized placebo-controlled clinical trial, idebenone showed a trend towards ameliorating the cardiac phenotype and significantly increasing respiratory function [Buyse *et al.* 2011].

Furthermore, idebenone is also studied for the treatment of MELAS. In one patient, 5-month treatment of idebenone improved blood flow and mitochondrial respiration in the cerebrum [Ikejiri *et al.* 1996] and in another patient, 24-month treatment ameliorated neurological symptoms [Napolitano *et al.* 2000]. In addition, treatment with idebenone and *L*-arginine for over two years prevented stroke-like episodes in one MELAS patient with the exception of two incidences when the treatment was halted [Lekoubou *et al.* 2011]. At present, a phase IIa, double-blind, placebo-controlled clinical trial, entitled “Study of Idebenone in the Treatment of Mitochondrial Encephalopathy Lactic Acidosis & Stroke-like Episodes (MELAS)” (www.clinicaltrials.gov, NCT00887562), by Santhera Pharmaceuticals Ltd. and Columbia University, NY, is conducted.

Idebenone is also often administered to LHON patients; however, its effects are discussed controversially. Whereas Barnils *et al.* [2007] did not find an improvement by idebenone when administered in combination with vitamin C, other groups reported faster visual recovery after treatment with idebenone alone [Mashima *et al.* 1992, Carelli *et al.* 1998, and Mashima *et al.* 2000]. Recently, a significant improvement in visual performance and an arrest in visual deterioration were found in a phase II, double-blind, randomized, placebo-controlled clinical trial [Klopstock *et al.* 2011]. When patients with mitochondrial mutations 3460G>A, 11778G>A, and 14484T>C were treated with idebenone over a period of 24 weeks, changes in visual acuity of either the best eye at start and the best eye at the end of the treatment, the best eye at start of the treatment, or both eyes were ameliorated in patients with discordant visual acuities.

Finally, in line with the effects described above, idebenone showed improvement of brainstem functions, particularly respiration, in a patient with Leigh syndrome, a necrotizing encephalomyopathy with underlying mitochondrial respiratory chain deficiency [Haginoya *et al.* 2009].

2.5 Perspectives

The aim of this thesis was to shed light on the molecular effects of idebenone. Even though it has been used for the treatment of several diseases, the underlying mechanism(s) for the observed, beneficial effects remain still unclear. Data so far also do not draw a conclusive picture of its mode of action. Beside rather obvious predictions such as antioxidant activity or employment in ETC, idebenone was described to modify arachidonic acid metabolism, to block Ca^{2+} channels, and to stimulate NGF production among other fibres. Considering the range and diversity of effects attributed to idebenone, the emphasis of this work lies in the following questions: (i) of what nature is the interaction between idebenone and the mitochondria, especially in regards to the ETC, (ii) is there a difference in this mitochondrial interaction between healthy and impaired mitochondria, and (iii) which possible implications can be drawn from potential molecular mechanisms in regards to mitochondrial disorders or *in vivo*.

3 Results

3.1 Confirmation of Duchenne Muscular Dystrophy Model Systems

Duchenne muscular dystrophy (DMD) is a devastating disease which manifests in a disruption of membrane integrity and defective calcium (Ca^{2+}) homeostasis on the cellular level. In addition, involvement of reactive oxygen species (ROS) in the course of the pathology was reported [Kar *et al.* 1979, Hunter and Mohamed 1986, Ragusa *et al.* 1997, Disatnik *et al.* 1998, and Rando *et al.* 1998]. In addition, impairment of mitochondrial function and energy production was also described in DMD patients and the *mdx* mouse model [Barbiroli *et al.* 1992, Kemp *et al.* 1993, Gannoun-Zaki *et al.* 1995, Sperl *et al.* 1997, Kuznetsov *et al.* 1998, Brini 2003, Burelle *et al.* 2010, and Kinnally *et al.* 2011]. Hence, primary muscle cells from DMD patients appear to be a model system for mitochondrial involvement in pathology and appear to be suited for investigating mitochondrial effects of a particular compound.

Before setting out to use DMD cells as model system, it was imperative to characterize the cell lines used. Cultured cells might diverge from the phenotype they exhibited under the physiological conditions *in vivo*. Cells which are less affected and thus fitter than others might be more successful in proliferation. As a consequence, the impaired phenotype observed *in vivo* could be eliminated by selection *in vitro*. An additional difference of great importance between conditions *in vivo* and *in vitro* is the mode of energy production. *In vivo*, cells might rely on different ATP-generating processes depending to their function, their supply with certain types of food molecules and metabolic setup. In muscles dominated by type I fibers, mitochondrial density is high and ATP is mainly generated via oxidative phosphorylation (OXPHOS). The primary myoblasts used in the following experiments were isolated mostly from type I muscle fibers (3DMD, 5DMD, 2TE, 4TE, and 8TE) with the exception of 5TE myoblasts which were established from muscle tissue with equal distribution of fiber types I and II. Unfortunately, the accurate origin of 6DMD cannot be traced back. However, since the myoblasts in culture are derived from satellite cells and not differentiated muscle, it is possible that the changes leading to an OXPHOS-preferring metabolism *in vivo* might not be evident in cultured cells.

It has to be pointed out that, under normal cell culture conditions *in vitro*, glucose is abundant in concentrations exceeding those found *in vivo*. While glucose concentrations in blood are approximately 5 mM, standard culture media exhibit concentrations of 25 mM. Such a five-fold surplus of glucose promotes the use of glycolysis over OXPHOS and therefore diminishes mitochondrial activity [Boquist 1977]. In order to measure mitochondrial activity, glucose in medium had to be adjusted.

Therefore, the following experiments [Figure 8, Figure 9, and Table 1] were conducted in four media differing in their glucose and serum content. **Aneural media**, the growth medium for primary myoblasts, is moderate in glucose (approximately 5 mM). In contrast to the three other media used, aneural is supplemented with growth factors and non-heat-inactivated serum. The other media were based on DMEM and on heat-inactivated serum which itself contributed to estimated 0.5 mM glucose. In addition, **Hi Glu medium** contained 25 mM glucose, whereas in **Lo Glu medium** serum content contributed to 0.5 mM glucose. In order to force cells to use mitochondria but still supply adequate amounts of organic energy, in the fourth medium, glucose was substituted by galactose. Being a six-carbon sugar like glucose, galactose breakdown via glycolysis yields an equivalent amount of ATP as glucose (two molecules per molecule of sugar). However, galactose needs to be converted into glucose-6-phosphate in order to enter glycolysis by a process costing two ATP molecules [Marroquin *et al.* 2007]. Hence, glycolytic breakdown of galactose does not generate ATP directly, but provides pyruvate and NADH for OXPHOS. This so-called Gal medium utilized in the following experiments exhibited a concentration of 10 mM galactose.

Four endpoints were selected to characterize human primary myoblasts: cellular energy status as measured by ATP levels in homogenates, cytoplasmic and mitochondrial ROS production, and mitochondrial mass. To determine the levels of ROS two widely used fluorophores employed which cover distinct manifestations of oxidative stress. The mitochondrial-targeting dye MitoTracker[®] Red CM-H₂Xros—which will henceforward be abbreviate as MitoROS—indicates the abundance of mitochondrially derived superoxide ($\text{O}_2^{\cdot-}$). Superoxide is a free radical of the most aggressive type and origins mainly as toxic byproduct of respiration primarily produced by complexes I and III. A second dye called CM-H₂DCFCA is a plasma membrane-permeable compound and a rather unspecific marker that indicates general ROS levels within a cell.

Given the impaired mitochondrial function described above in patients suffering from DMD, one would expect a clear distinction between cells derived from DMD patients and those from healthy donors with regards to the selected parameters. Surprisingly, this was not the case. The amount of ATP, ROS, and mitochondrial mass could not be easily attributed to either affected or healthy cells. For example, ATP content under aneural conditions varied as much in control cells as it did in DMD cells [Figure 8]. As a result, *in vitro* impairment of energy status was not specific to DMD cells, but rather to particular cells regardless of their genotype. This was also true when observing changes in mitochondrial ROS or mass. For these parameters, differences within affected or within control cells seemed to outplay differences between affected and control cells. In contrast, cellular ROS levels were similar in most cells with the exception of one or two outliers [Figure 8], making it impossible to distinctly separate healthy for affected cells in general on the basis of mitochondrial parameters.

As a consequence, primary myoblasts from DMD patients had to be considered unsuitable as model systems to investigate mitochondrial impairment *sui generis*. The mitochondrial phenotype described by others in muscle

fibers *in vivo* [Barbiroli *et al.* 1992, Kemp *et al.* 1993, Gannoun-Zaki *et al.* 1995, Sperl *et al.* 1997, Kuznetsov *et al.* 1998, Brini 2003, Buelle *et al.* 2010, and Kinnally *et al.* 2011] failed to substantiate *in vitro*. Dysfunction of mitochondrial activity or elevated ROS levels was therefore exogenously induced in subsequent experiments.

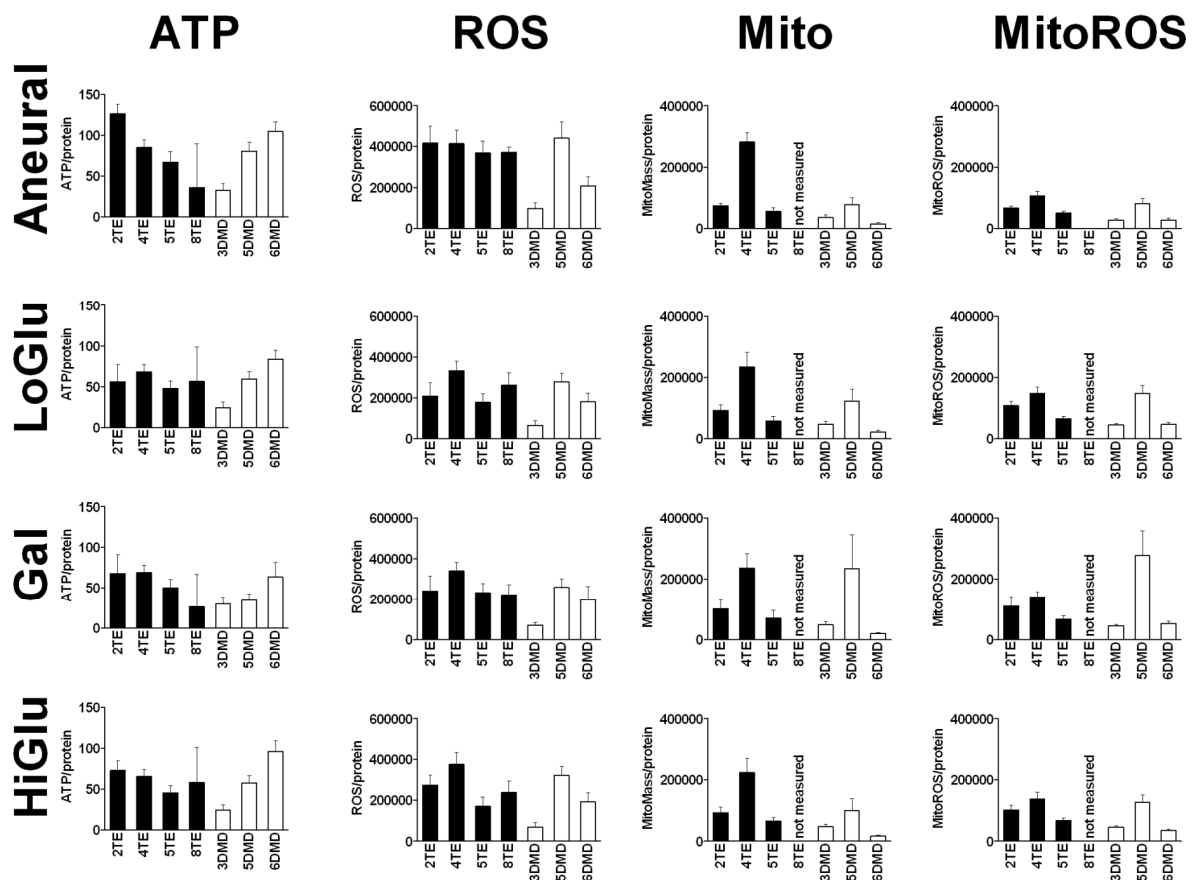


Figure 8: Primary Muscle Cells of Healthy Donors and DMD Patients Cannot Be Discriminated by Mitochondrial Mass, Energy Status or ROS Levels.

Basal levels of energy status (ATP concentration and mitochondrial mass) and oxidative stress (general and mitochondrially generated ROS levels) were analyzed in primary muscle cells from healthy donors (2TE, 4TE, 5TE, and 8TE; filled bars) or patients suffering from DMD (3DMD, 5DMD, 6DMD; empty bars). Cells were seeded in Aneural medium (10% non heat-inactivated serum, 100 ng/ml FGF, 100 ng/ml EGF and 10 μ g/ml insulin; total 5 mM glucose) at a density of 4,000 cells/well in 96-well plates. After 24 h, medium was changed to either fresh aneural medium, DMEM LoGlu (10% serum; total 0.5 mM glucose), DMEM HiGlu (10% serum, 25 mM glucose), or DMEM Gal (10% serum, 10 mM galactose; total 0.5 mM glucose). After 96-h incubation, ATP was measured using a luciferase-based luminescence assay, protein concentrations were quantified using BCA-mediated change in absorption and ROS, MitoMass and MitoROS were analyzed using specific fluorescent dyes. ATP and protein concentrations were calculated by means of standards; auto-fluorescence of cells and medium was deducted from raw values in fluorescence assays. Bars depict mean + stdev of 12 samples of one or two experiments. ATP levels are displayed as nmol per mg protein, ROS, mitochondrial mass and ROS are depicted as fluorescence units per mg/ml protein.

One could argue that ATP levels and the amount of mitochondria abundant in a cell are interconnected and not truly independent parameters. As a consequence, measuring ATP levels could substitute for measuring mitochondrial mass and vice versa. In order to confirm this hypothesis, the parameters should correlate with each other. Analyses of correlations revealed that most parameters measured are independent of one another in the cells used [Figure 9 and Table 1]. Statistically significant ($p < 0.05$), positive correlations were found between mitochondrial mass and mitochondrial ROS production independent of the type of media. This is not surprising, since mitochondrial targeting of the employed dyes is achieved through the same mechanism: both MitoTracker and MitoROS are positively charged molecules which accumulate in the negatively charged mitochondria. This correlation should be kept in mind for further data analyses.

Furthermore, a statistically significant ($p < 0.05$), positive correlation between cellular and mitochondrial ROS production was observed in all media, except for Gal medium where significance for this correlation was clearly missed ($p = 0.2818$) [Figure 9 and Table 1]. In LoGlu medium, and in this medium alone, cellular ROS production was statistically significantly ($p = 0.0422$) correlated with mitochondrial mass.

Taken together, the four parameters analyzed in these experiments could be considered as generally independent from one another, with the exception of mitochondrial ROS production and mitochondrial mass and, in some cases, cellular and mitochondrial ROS production.

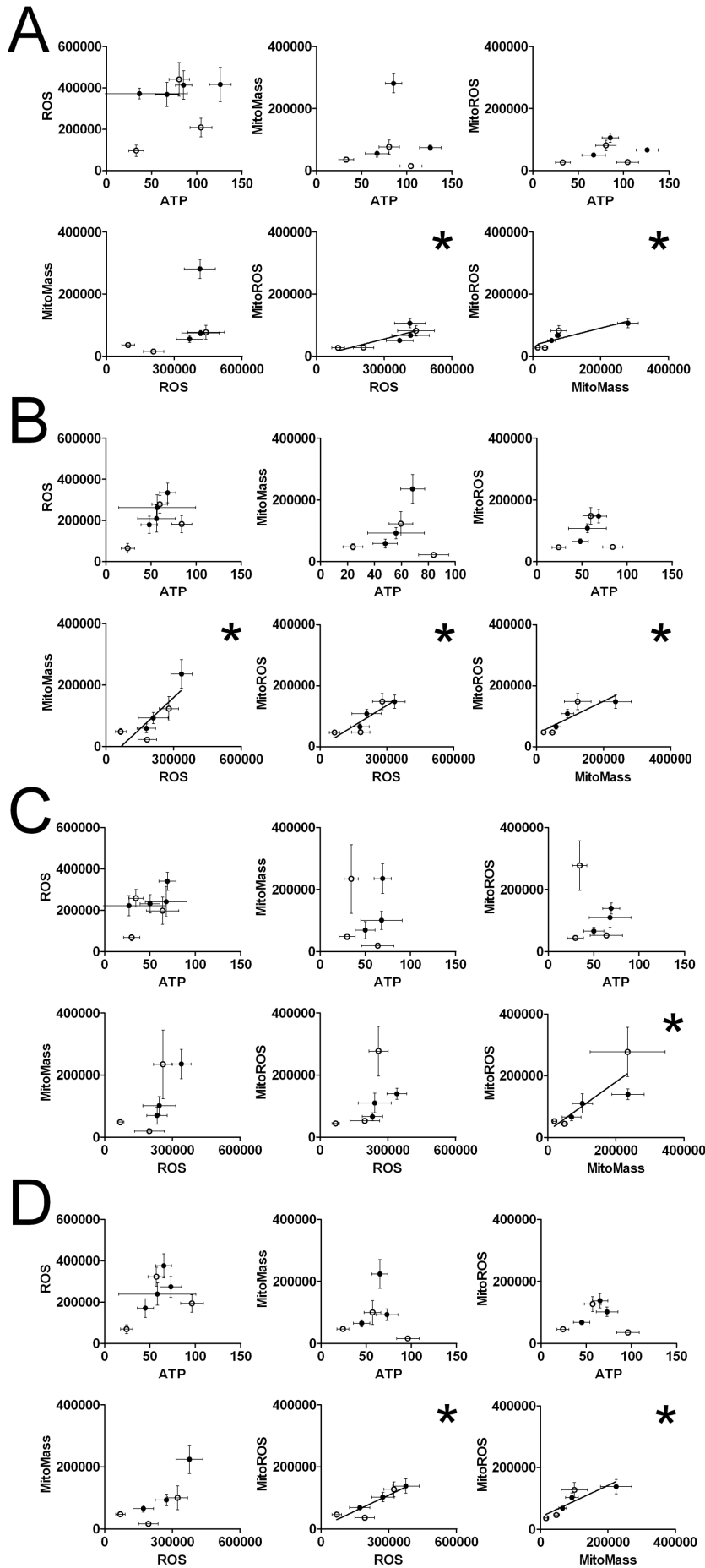


Figure 9: Correlation between ATP Levels, Cytosolic and Mitochondrial ROS Level, and Mitochondrial Mass in Primary Muscle Cells of Healthy Donors and DMD Patients.

Basal levels of energy status (ATP concentration and mitochondrial mass) and oxidative stress (general and mitochondrially generated ROS levels) were analyzed in primary muscle cells from healthy donors (2TE, 4TE, 5TE, and 8TE; filled circles) or patients suffering from DMD (3DMD, 5DMD, 6DMD; open circles). Cells were cultivated in (A) Aneural medium (5 mM), or DMEM medium containing (B) 0.5 mM glucose, (C) 10 mM galactose, or (D) 25 mM glucose. After 96-h incubation, ATP was measured using a luciferase-based luminescence assay, protein concentrations were quantified using BCA-mediated change in absorption and ROS, MitoMass and MitoROS were analyzed using specific fluorescent dyes. ATP and protein concentrations were calculated by means of standards; auto-fluorescence of cells and medium was deducted from raw values in fluorescence assays. Correlation and significance were calculated ($p^* < 0.05$; two-tailed Pearson correlation). ROS, mitochondrial mass and ROS are depicted as fluorescence units per mg/ml protein.

Table 1: Correlation Parameters for Energy Status and Oxidative Stress Levels in Primary Muscle Cells of Healthy Donors and DMD Patients.

Correlation and significance were calculated ($p^* < 0.05$; two-tailed Pearson correlation). Significant correlations are listed in bold.

Medium				R ²	p
Aneural (5 mM Glucose)	ATP	vs.	ROS	0.388	0.390
	ATP	vs.	MitoMass	0.094	0.859
	ATP	vs.	MitoROS	0.291	0.576
	ROS	vs.	MitoMass	0.499	0.314
	ROS	vs.	MitoROS	0.832	0.040*
	MitoMass	vs.	MitoROS	0.859	0.029*
Lo Glu (0.5 mM Glucose)	ATP	vs.	ROS	0.614	0.142
	ATP	vs.	MitoMass	0.204	0.698
	ATP	vs.	MitoROS	0.274	0.599
	ROS	vs.	MitoMass	0.827	0.042*
	ROS	vs.	MitoROS	0.886	0.019*
	MitoMass	vs.	MitoROS	0.864	0.027*
Gal (10 mM Galactose)	ATP	vs.	ROS	0.532	0.219
	ATP	vs.	MitoMass	0.023	0.966
	ATP	vs.	MitoROS	-0.208	0.693
	ROS	vs.	MitoMass	0.719	0.107
	ROS	vs.	MitoROS	0.528	0.282
	MitoMass	vs.	MitoROS	0.856	0.030*
Hi Glu (25 mM Glucose)	ATP	vs.	ROS	0.463	0.295
	ATP	vs.	MitoMass	-0.006	0.990
	ATP	vs.	MitoROS	0.048	0.929
	ROS	vs.	MitoMass	0.786	0.064
	ROS	vs.	MitoROS	0.900	0.015*
	MitoMass	vs.	MitoROS	0.863	0.027*

As a last parameter mitochondrial structure was investigated in DMD cells, since functional deficits could be attributed to changes in structure [Twig *et al.* 2008]. Therefore, human primary myoblasts were loaded with the fluorescent dye 5,5',6,6'-tetrachloro-1,1',3,3'-tetraethylbenzimidazolylcarbocyanine iodide (JC-1). Green fluorescent JC-1 accumulates within the mitochondria in a membrane potential-dependent manner and aggregates with a strong red fluorescence when at high concentrations. Hence, green fluorescence indicates mitochondria *per se*, whereas red fluorescence indicates a high membrane potential. However, in primary muscle cells, the dye did not demonstrate a staining pattern described for other cell types [Reers *et al.* 1991]. Red fluorescence did not accumulate in mitochondria-like as described and was thus insufficient for quantification [*data not shown*]. Nonetheless, only focusing on green fluorescence channel, the mitochondria showed distinct morphology in human primary myoblasts of either healthy donors (2TE, 4TE, 8TE) or cells obtained from DMD patients (5DMD, 6DMD, 12DMD) [Figure 10]. Whereas control cells formed tubular networks of continuous mitochondria which resembled a ring-shaped net, mitochondria in myoblasts from DMD patients were more fragmented and disjointed, indicating a higher rate of fission which would correlate with a higher proportion of depolarized mitochondria [Twig *et al.* 2008]. Nonetheless, this difference in mitochondrial morphology was not sufficient to impair mitochondrial function in a magnitude observable in functional assays [Figure 8].

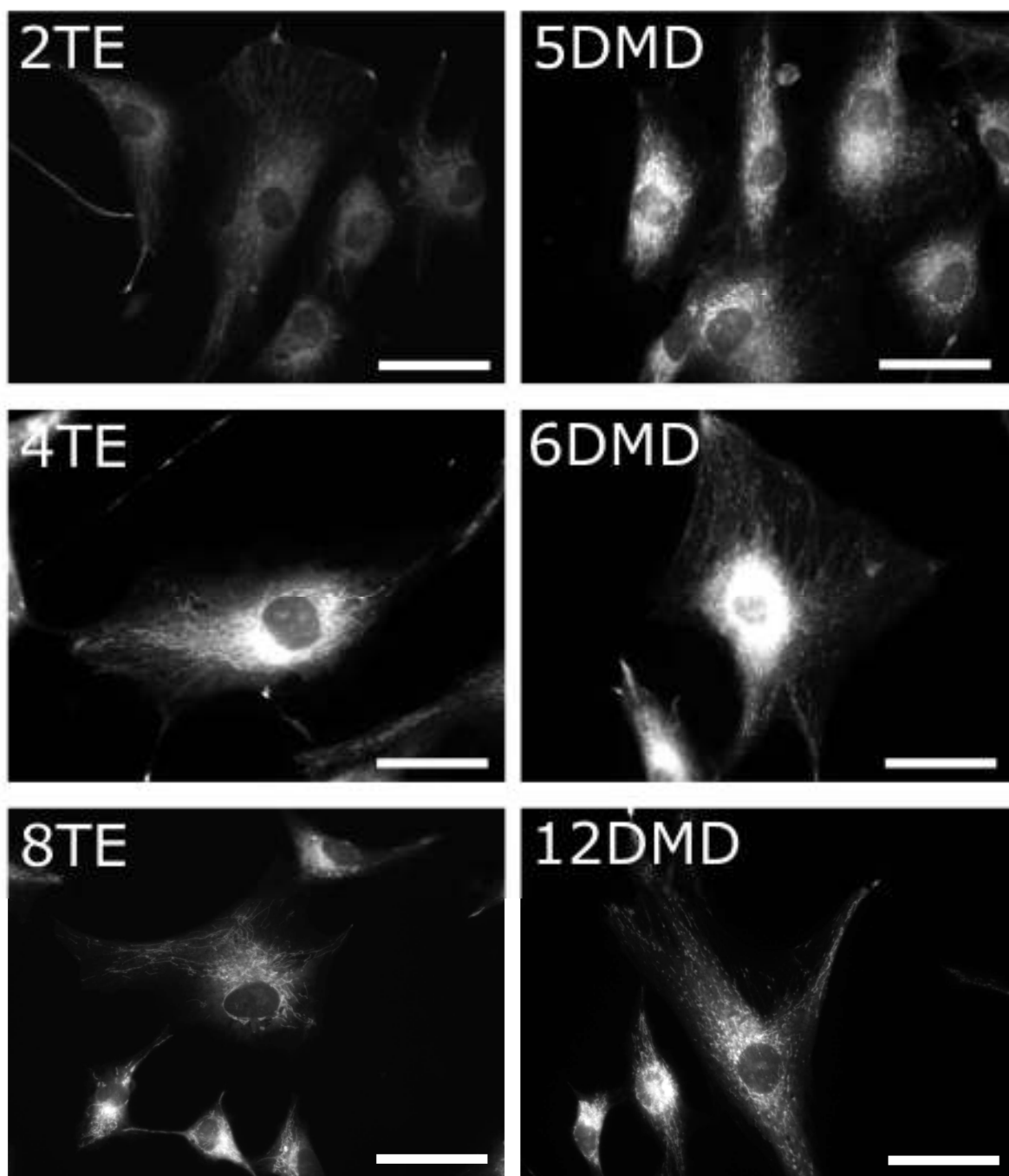


Figure 10: Mitochondrial Morphology in Primary Myoblasts of Healthy Donors and DMD Patients. Mitochondria of primary myoblasts of healthy donors (2TE, 4TE and 8TE) and from Duchenne patients (5DMD, 6DMD, and 12DMD) were stained using the fluorescent dye JC-1. Only pictures from green fluorescent channel are shown. Scale bar: 50 μ m.

Contradictory to the work by others using DMD cells [Hunter and Mohammed 1986, Barbioli *et al.* 1992], DMD cells available in our lab could not be used as an experimental model of mitochondrial dysfunction *in vitro* [Figure 8]. However, a mouse model for DMD, the *mdx* mouse [Bulfield *et al.* 1984], was also described to have an impaired mitochondrial metabolism [Gannoun-Zaki *et al.* 1995, Ragusa *et al.* 1997, and Distanik *et al.* 1998]. The *mdx* mouse possesses a mutated dystrophin gene in the genetic background of the C57Bl/10 strain [Bulfield *et al.* 1984] and shows muscle degeneration and regeneration at the age of four to six weeks [Dupont-Versteegden *et al.* 1994] which is associated with decreased membrane integrity and elevated levels of cytosolic enzymes in the blood [Bulfield *et al.* 1984]. It was thus of interest to see if reduced levels of ATP could be found in *mdx* mice.

First, wild type (WT) and *mdx* animals were genotyped to surely discriminate from one another on a genetic basis [data not shown]. Subsequently, differences in creatine kinase (CK) blood levels were analyzed in WT and *mdx* animals in order to verify differences in their phenotype [Figure 11A]. The blood level of CK, a cytosolic enzyme, is a commonly used marker for plasma membrane disruption and increased blood CK levels were

described as a hallmark phenotype in the *mdx* mouse [Bulfield *et al.* 1984]. Indeed, 6-week old *mdx* mice showed a five-fold, but nevertheless insignificant increase in blood CK levels ($573.7 \pm 314.8\%$ ¹) compared to WT animals ($100 \pm 109.8\%$). Older, WT animals showed increased blood CK levels ($298.7 \pm 434.4\%$) at 12 week compared to 6-week old WT mice. Blood CK levels of 12-week old *mdx* mice significantly exceeded those of WT animals of the same age by a factor ($1139.9 \pm 448.8\%$). Hence, the *mdx* mice in our lab showed the phenotype of elevated blood CK levels described by others [Bulfield *et al.* 1994].

After confirmation that WT and *mdx* mice are genetically and phenotypically distinct, ATP levels in different tissues were analyzed in WT and *mdx* mice at the age of six and 12 weeks. To minimize the temporal degradation of ATP, extracted tissues were immediately snap frozen in liquid nitrogen and stored at $-80\text{ }^{\circ}\text{C}$ until ATP levels of all samples were assayed simultaneously. At the age of six weeks, no differences of ATP levels were observed either in any of the tested muscles—be it *m. soleus* ($1.12 \pm 0.19\text{ }\mu\text{mol/ml protein}$ in WT and $1.22 \pm 0.17\text{ }\mu\text{g/ml protein}$ in *mdx*), diaphragm ($1.09 \pm 0.33\text{ }\mu\text{mol/ml protein}$ vs. $0.90 \pm 0.27\text{ }\mu\text{mol/ml protein}$), *gastrocnemicus lateralis* ($2.75 \pm 0.75\text{ }\mu\text{mol/ml protein}$ vs. $2.94 \pm 1.17\text{ }\mu\text{mol/ml protein}$), or the heart ($0.75 \pm 0.29\text{ }\mu\text{mol/ml protein}$ vs. $1.00 \pm 0.35\text{ }\mu\text{mol/ml protein}$)—or in the cerebellum ($0.34 \pm 0.11\text{ }\mu\text{mol/ml protein}$ vs. $0.53 \pm 0.42\text{ }\mu\text{mol/ml protein}$) [Figure 11B].

Similarly, no difference in ATP levels was found in most of the analyzed tissues² [Figure 11C] such as *m. soleus* ($0.89 \pm 0.19\text{ }\mu\text{mol/ml protein}$ in WT and $0.72 \pm 0.23\text{ }\mu\text{g/ml protein}$ in *mdx*), diaphragm ($0.41 \pm 0.13\text{ }\mu\text{mol/ml protein}$ vs. $0.33 \pm 0.24\text{ }\mu\text{mol/ml protein}$), the heart ($0.14 \pm 0.10\text{ }\mu\text{mol/ml protein}$ vs. $0.10 \pm 0.02\text{ }\mu\text{mol/ml protein}$), and the cerebellum ($0.22 \pm 0.19\text{ }\mu\text{mol/mg protein}$ vs. $0.14 \pm 0.08\text{ }\mu\text{mol/mg protein}$). In *gastrocnemicus lateralis*, however, a significant decrease of ATP levels was observable, from $1.30 \pm 1.02\text{ }\mu\text{mol/mg protein}$ to $0.39 \pm 0.24\text{ }\mu\text{mol/mg protein}$. Nonetheless, the remarkably high standard deviation of the average WT ATP level should advice caution. After a closer look at the individual values obtained from each animal [inlay figure of Figure 11C], it becomes apparent, that this difference is due to approximately half of the WT animals which showed high ATP levels in that muscle, whereas the rest showed comparable values as seen in *mdx* mice. Hence, in the selected tissues, no convincing difference in cellular ATP levels was able to discriminate WT from *mdx* mice.

The lack of mitochondrial characteristics discriminating unaffected from dystrophic animals or cells also questioned the suitability of these animals or cells as models for mitochondrial impairment. Since DMD cells and *mdx* mice showed no indications of mitochondrial malfunction *per se*, subsequent experiments were performed in cell lines with exogenously induced mitochondrial dysfunction.

¹ Results are always noted as mean \pm stdev (standard deviation) if not stated otherwise.

² ATP measurements of six- and 12-week old animals were not performed at the same time point. Therefore, a direct comparison between the two cohorts should be conducted with caution.

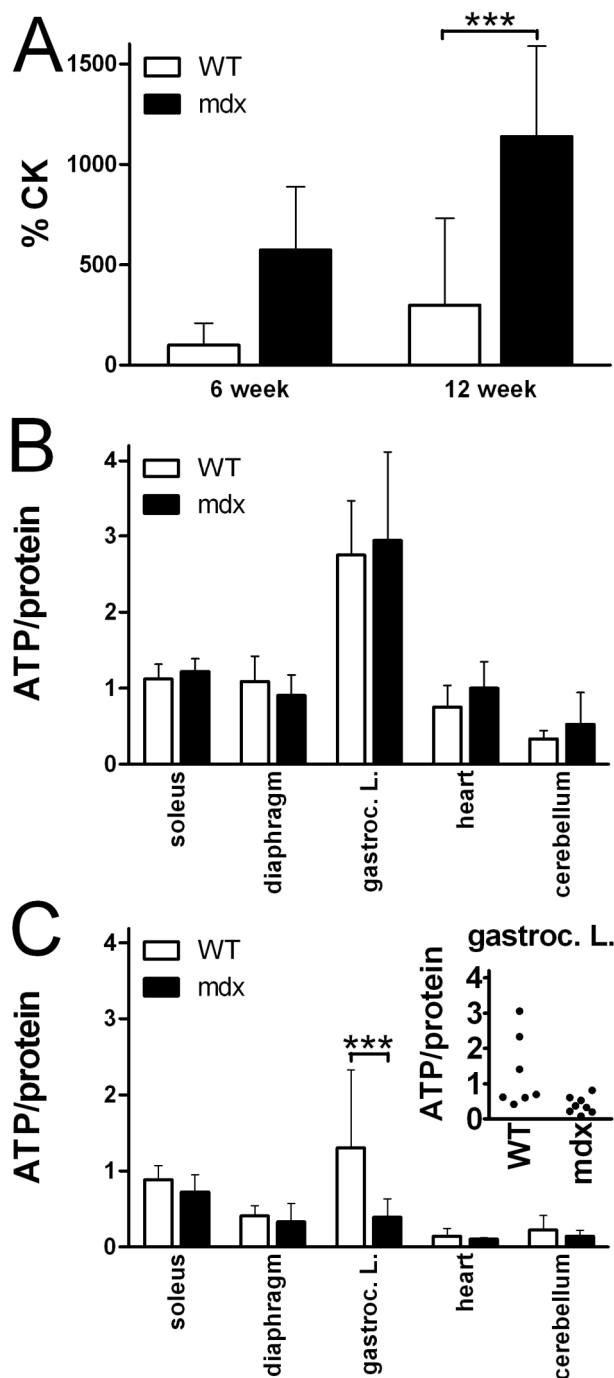


Figure 11: Blood CK and Muscle ATP Levels in Six- and 12-Weeks Old Mice.

(A) Creatine kinase (CK) levels in blood were measured in six- and 12-week old WT (empty bars) and *mdx* (filled bars) mice. ATP levels in homogenized muscle tissue of *m. soleus*, the diaphragm, *gastrocnemius lateralis*, the heart and the cerebellum were analyzed in (B) six-week and (C) 12-week old WT (empty bars) and *mdx* (filled bars) mice. ATP/protein is denoted as μM ATP per mg protein. Bars represent mean + stdev of averaged triplicates of six to eight individual mice. Insert dot-plot depicts averaged triplicates of individual mice for *gastrocnemius lateralis*. $p^{***} < 0.001$; two-way ANOVA Bonferroni's Multiple Comparison test.

3.2 Influence of Idebenone on Mitochondrial Activity

Since DMD cells showed no coherent intrinsic impairment of mitochondrial parameters such as mitochondrial mass [Figure 8], the effect of idebenone and related benzoquinones on exogenously impaired mitochondrial activity was observed in other cells. Before doing so, however, the influence of the quinones on healthy mitochondria was investigated under conditions of low mitochondrial dependency for ATP production. In cell culture, high levels of glucose cause cells to rely mainly on glycolysis for ATP generation which reduces the extent of mitochondrial activity [Vander Heiden *et al.* 2009]. If a compound which is involved in mitochondrial activities other than energy production was added to cells under high glucose conditions, it should be possible to

observe changes in parameters such as mitochondrial membrane potential ($\Delta\Psi_m$) or mitochondrial mass without impairing cellular energy production.

Therefore, idebenone and structurally related compounds were assessed in primary skin fibroblasts under high glucose conditions (25 mM glucose). Alterations in the alkyl tail of short-chain quinones had mild influence on mitochondrial parameters on $\Delta\Psi_m$ and the mitochondrial mass [Figure 12]. The changes, however, were quite small and could still lie within the limits of variation for this assay. Idebenone, for example, elevated $\Delta\Psi_m$ by 16% in fibroblasts, but at the same time decreased mitochondrial mass by 11%. In contrast, CoQ₀, which lacks an alkyl tail all together, increased both $\Delta\Psi_m$ and mitochondrial mass by 22% and 24%, respectively. CoQ₁ did alter neither $\Delta\Psi_m$ nor mitochondrial mass (102% and 100%, respectively), whereas CoQ₂ and the idebenone metabolite QS-10 [Okamoto *et al.* 1998] caused opposing effects on both parameters: whilst the first decreased $\Delta\Psi_m$ by 15% and increased mitochondrial mass by 6%, the latter increased $\Delta\Psi_m$ by 8% and decreased mitochondrial mass by 15%. CoQ₁₀ elevated $\Delta\Psi_m$ to 109% of DMSO-treated controls and reduced mitochondrial mass by 5%. Finally, DQ slightly increased both $\Delta\Psi_m$ and mitochondrial mass by 3% and 5%, respectively.

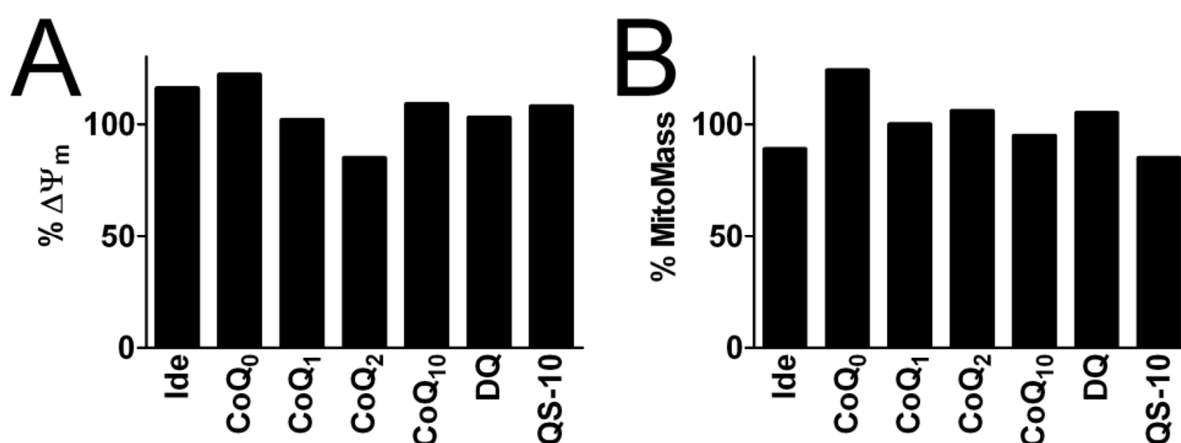


Figure 12: Quinones Only Moderately Influence Mitochondrial Parameters.

Human fibroblasts were treated with different quinones (10 μ M) in 25 mM glucose-containing medium for three days before mitochondrial membrane potential (A; $\Delta\Psi_m$) or mitochondrial mass (B) was measured using the fluorescent dyes JC-1 and MitoTracker Green, respectively. Percentage relative to values from DMSO-treated was calculated. Bars represent mean of two independent experiments.

Thus, idebenone seemed to have a slight influence on mitochondrial parameters *per se*. Since the most prominent mitochondrial function is the production of ATP, further emphasis was laid on the effect of idebenone on cellular energy status. When glucose is abundant, cells rely mainly on glycolysis as source of energy, abandoning the use of mitochondria. In absence of glucose, however, the highly effective ATP production of OXPHOS is employed in order to gain as much energy as possible from all available food molecules. Thus, compounds negatively interfering with OXPHOS are thought to reduce ATP levels when glucose concentrations are low [Figure 13]. Lymphoblastoid cells (LCL BC1) were cultured in DMEM medium containing 10% fetal bovine serum (FBS) and either none or 4.5 g/l glucose in addition (combined with the glucose from the serum, this amounts to 0.5 and 25 mM glucose in total). Idebenone slightly increased ATP production under conditions of high glycolysis (111 \pm 31% of residual ATP levels; mean \pm SEM). However, when glycolysis could not contribute sufficiently to energy production, ATP levels dropped to 63 \pm 66% compared to DMSO-treated cells under the same conditions. CoQ₁ reduced ATP levels under conditions of both high and low glucose concentrations to 12 \pm 15% and 9 \pm 20%, respectively. Both CoQ₁₀ and QS-10 increased glycolysis-mediated ATP synthesis (177 \pm 82% and 142 \pm 75%). However, whereas CoQ₁₀ also moderately increased OXPHOS-dependent ATP production (124 \pm 62%), QS-10 showed no alteration thereof (103 \pm 67%). Rotenone, a known complex I inhibitor, was used as a positive control for the suppression of OXPHOS-dependent ATP production, and indeed, under low glucose conditions, rotenone decreased ATP levels to 20 \pm 20%. When high levels of glucose were available, however, rotenone increased ATP synthesis (142 \pm 32%) [Figure 13].

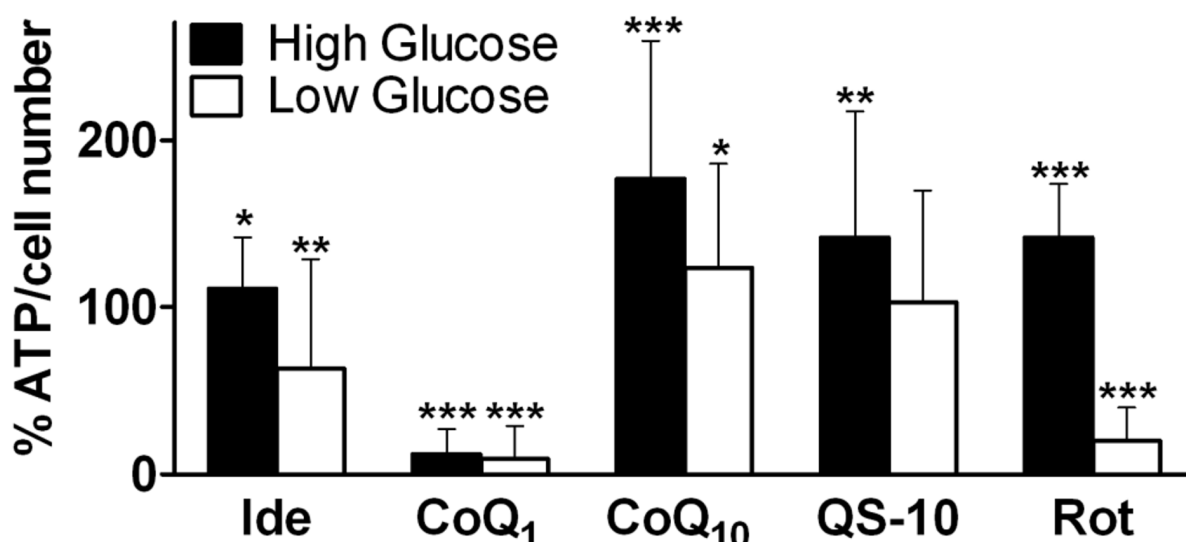


Figure 13: Influence of Quinones on Cellular ATP Status Depending on Glycolysis- or OXPHOS-Mediated Energy Production.

Human lymphoblastoid cells (LCL BC₁) were treated with 10 μ M idebenone, CoQ₁, CoQ₁₀, QS-10, and 10 nM rotenone for 72 h in DMEM medium containing 10% serum and either 25 mM glucose (high glucose; filled bars) or 0.5 mM glucose (low glucose; empty bars). The percentage difference from ATP levels of DMSO-treated control conditions were calculated for both high and low glucose conditions. Bars represent mean + SEM of triplicates from 4-15 independent experiments. $p^* < 0.05\%$, $p^{**} < 0.01\%$, and $p^{***} < 0.001\%$ relative to DMSO-treated cells in the according medium; Student t-test.

3.3 Idebenone Rescues ATP Levels under Conditions of Dysfunctional Complex I

Despite the fact that the short-tail benzoquinones idebenone and CoQ₁ reduced ATP levels after long-term incubation in glucose-deprived medium [Figure 13], some reports suggested that these compounds are able to donate electrons to the ETC when reduced [Beyer *et al.* 1996, Chan *et al.* 2001, and Audi *et al.* 2003]. To test such a possible involvement in ETC, conditions of mitochondrial dependence for energy production are required as well as a potential entry site for the electrons carried by the quinone. Most likely, this entry site is complex III, which was described to oxidize idebenone and CoQ₁ [Degli Esposti *et al.* 1996]. However, in order to see an effectual input of electrons into the ETC by hydroquinones, the actual entry sites for electrons into the ETC (i.e. complex I and II) needed to be blocked.

Guided by these demands, the following experimental conditions were established: HepG2 cells were cultured for 24 h under conditions of low glucose (DMEM medium containing 0.3 g/l glucose, 2% FBS amounts to 1.77 mM glucose) to promote mitochondrial energy production. Then, glucose was removed to force cells to use mitochondrial activity in order to produce energy. Consistently, removal of glucose alone did not alter ATP levels over a period of 90 min (without glucose, ATP levels were defined as $100 \pm 7\%$, in presence of 1.77 mM glucose, ATP levels reached $111 \pm 3\%$), indicating that the cells still had sufficient glucose and/or pyruvate available to fuel OXPHOS. Now that cells relied on mitochondria to generate ATP, controlled and specific inhibition of discrete parts of OXPHOS provided models for the interaction of quinones with mitochondrial respiration. In order to impair OXPHOS, cells were treated with known inhibitors disrupting the electron transport chain (ETC) for 60 min starting 30 min after medium change.

Treatment with the complex I inhibitor rotenone reduced ATP levels almost completely already with relatively low concentrations ($5 \pm 0\%$ of residual levels at 100 nM, $2 \pm 0\%$ at 1 μ M and $1 \pm 0\%$ at 10 μ M) [Figure 14A]. An inhibitor of complex II, 3-nitropropionate (3-NPA), did not alter ATP levels ($98 \pm 2\%$ at 100 μ M, $101 \pm 4\%$ at 1 mM and $103 \pm 2\%$ at 10 μ M) and was therefore omitted in further experiments. Blocking complex III function by antimycin A pushed ATP levels down to $5 \pm 0\%$ of residual levels at 100 nM, $2 \pm 0\%$ at 1 μ M and $2 \pm 0\%$ at 10 μ M. Oligomycin decreased ATP levels to $14 \pm 0\%$ at 100 nM, $17 \pm 0\%$ at 1 μ M and $18 \pm 0\%$ at 10 μ M by blocking the proton pump (i.e. the F₀ subunit) of the ATP synthase. Similarly, FCCP, an uncoupler decreasing the proton gradient needed for ATP production by ATP synthase, also depleted ATP levels ($64 \pm 5\%$ at 100 nM, $13 \pm 1\%$ at 1 μ M and $11 \pm 0\%$ at 10 μ M).

As a result, *in vitro* models for specific OXPHOS dysfunctions were established. These models could be used to investigate potential ameliorations in mitochondrial ATP production of a particular compound when OXPHOS was inhibited at either complex I, complex III, or ATP synthase, or through abolishing the proton gradient.

To determine if idebenone could rescue ATP levels in cells that are dependent of mitochondrial energy production which in turn exhibits impaired mitochondrial function, cells were pretreated with either DMSO or 10 μ M idebenone in glucose-deprived medium for 30 min before inhibitors of ETC were added for additional 60

min [Figure 14B&C]. Idebenone rescued ATP levels when complex I (from $10\pm 5\%$ to $88\pm 1\%$ during co-incubation with 100 nM rotenone), but not when complex III was blocked (from $8\pm 2\%$ to $6\pm 3\%$ during co-incubation with 100 nM antimycin A). Likewise, idebenone failed to restore cellular ATP levels when the function of ATP synthase was inhibited by either directly by 100 nM oligomycin (from $29\pm 1\%$ to $15\pm 1\%$ during co-incubation) or indirectly by 1 μ M FCCP (from $7\pm 3\%$ to $6\pm 1\%$ during co-incubation).

A similar picture was obtained when idebenone was substituted by CoQ₁ [Figure 14D] which only rescues ATP levels when cells are stressed by rotenone ($106\pm 2\%$ of residual levels), but not when they are treated with antimycin A ($4\pm 1\%$), oligomycin ($13\pm 2\%$) or FCCP ($18\pm 0\%$).

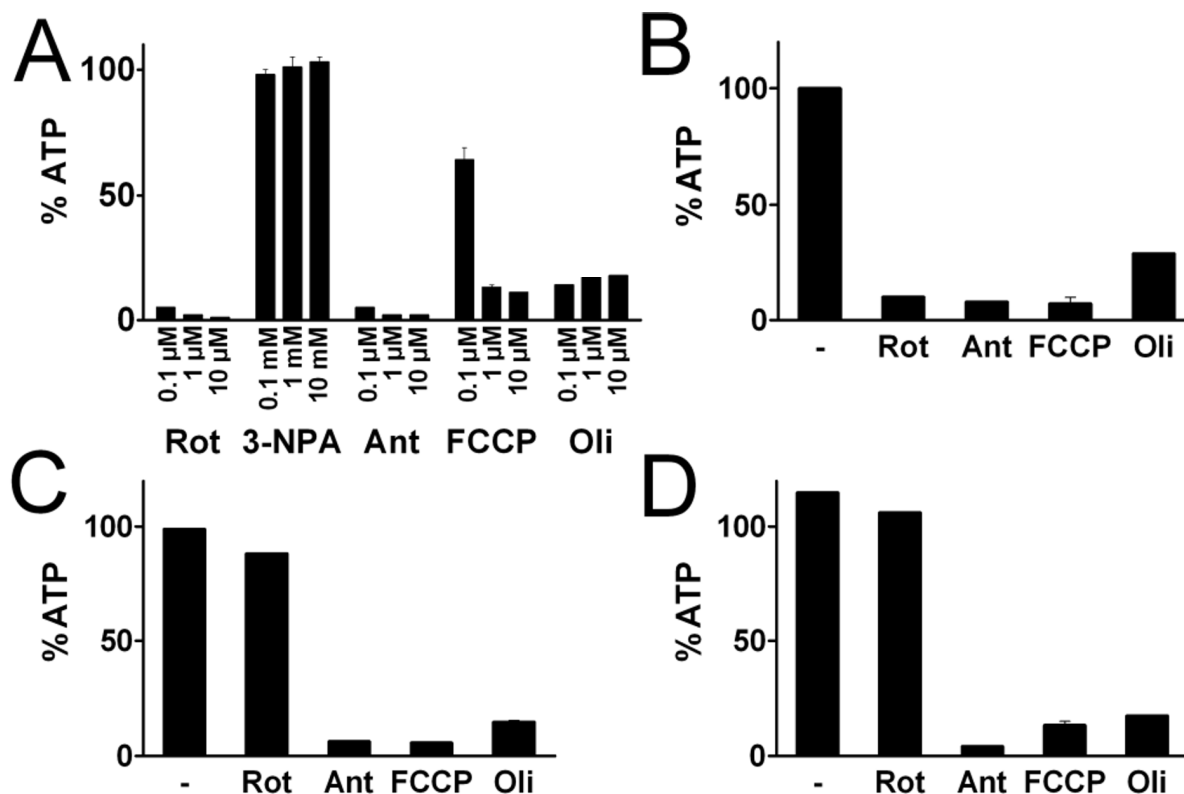


Figure 14: Influence of ETC Inhibitors, Idebenone, or CoQ₁ on ATP Levels.

HepG2 cells were kept on 1.77 mM glucose overnight before glucose was removed for 60 min. (A) Simultaneously, different inhibitors of the electron transport chain (complex I inhibitor rotenone (Rot), complex II inhibitor 3-nitropropionate (3-NPA), complex III inhibitor antimycin A (Ant), uncoupler FCCP, and ATP synthetase inhibitor oligomycin (Oli)) was added at different concentrations. ATP was measured after the 1-h incubation of inhibitors. In presence of 100 nM rotenone, 100 nM antimycin A, 1 μ M FCCP, and 100 nM oligomycin, cells were pretreated with DMSO (B), 10 μ M idebenone (C), or 10 μ M CoQ₁ (D) 30 min prior to glucose removal and addition of inhibitors. Bars represent mean + stdev of triplicates of a typical experiment.

Thus, idebenone and CoQ₁ were able to rescue ATP levels in presence of rotenone [Figure 14B-D]. Due to the similarity of their chemical structure, one could assume that this effect is intrinsic to idebenone-like benzoquinones. In order to test this hypothesis, additional to idebenone and CoQ₁, CoQ₁₀ and QS-10 were subjected to rotenone-stressed HepG2 cells [Figure 15A]. Incubation with 60 μ M rotenone for one hour reduced ATP levels to $2\pm 0\%$ of residual levels, whilst treatment with 5 μ M quinone alone for the same duration caused no substantial changes in cellular ATP content (idebenone: $91\pm 12\%$, CoQ₁: $120\pm 15\%$, CoQ₁₀: $99\pm 10\%$, and QS-10: $104\pm 9\%$ of control). When quinones and the complex I inhibitor were administered simultaneously, idebenone and CoQ₁ were able to restore ATP levels ($71\pm 6\%$ and $64\pm 6\%$, respectively); whereas CoQ₁₀ and QS-10 entirely failed to ameliorate cellular energy status ($2\pm 1\%$ for both quinones).

In order to evaluate the importance of temporal administration of idebenone to ameliorate energy status under conditions of dysfunctional complex I, 10 μ M idebenone was administered at different time points before, during or after addition of 6 μ M rotenone [Figure 15B]. ATP levels were then quantified after 1-h incubation with rotenone. As observed previously, rotenone had a detrimental effect on ATP levels ($3\pm 0\%$ of residual levels) and simultaneous administration of idebenone restored ATP levels to $73\pm 7\%$ (co-treatment). If cells were pre-treated with idebenone up to 40 minutes before rotenone challenge (total 100 -min incubation with idebenone), ATP levels were elevated to $81\pm 1\%$. Strikingly, the protection of ATP levels by idebenone was also detectable when idebenone was administered after the addition of rotenone. Incubation with idebenone for only five min which took place 55 min after rotenone was added (labeled as post-treatment), an ATP rescue to $54\pm 4\%$ of residual levels was detected [Figure 15B].

Similar results were observed in freshly isolated mouse hepatocytes. After isolation, hepatocytes were immediately treated with 60 μM rotenone in presence or absence of 5 μM idebenone. Again, idebenone protected cells from rotenone-induced ATP depletion [Figure 15C]. Although, acute incubation of primary hepatocytes with rotenone did not lead to the same striking reduction of ATP levels compared to HepG2 cells ($72 \pm 18\%$ of control), idebenone fully restored ATP levels ($106 \pm 21\%$) in this system. At the same time, in the absence of rotenone, idebenone did not alter ATP levels in these cells ($111 \pm 16\%$). This *ex vivo* activity of idebenone on ATP levels after rotenone-mediated impairment of complex I raised the question, whether this protective action could also be observed *in vivo*. Therefore, idebenone (400 mg/kg/day; p.o.) was administered to mice over a period of four weeks before hepatocytes were isolated and immediately treated with 20 μM or 60 μM rotenone for one hour as in previous experiments. In this experiment, however, idebenone was not freshly added to hepatocytes during this stress phase. Freshly isolated hepatocytes of idebenone-treated and sham-treated mice had similar basal ATP levels ($113 \pm 16\%$ and $100 \pm 21\%$ respectively) [Figure 15D]. Consistent with our *in vitro* and *ex vivo* data, rotenone led to a drop in ATP levels in hepatocytes of sham-treated animals ($45 \pm 2\%$ residual ATP levels at 20 μM rotenone, $46 \pm 8\%$ at 60 μM rotenone). However, hepatocytes of idebenone-fed mice were significantly more resistant to rotenone challenge ($81 \pm 7\%$ residual ATP at 20 μM rotenone and $77 \pm 4\%$ at 60 μM rotenone).

Recently, some evidence emerged that longer incubation periods of up to one week are required to detect some protective effects by CoQ₁₀ [López *et al.* 2010]. Therefore, we investigated whether rescue of ATP levels, as demonstrated for acute exposure to idebenone and CoQ₁, would be detectable after a 1-week treatment with CoQ₁₀ [Figure 15E]. Rescue of ATP levels could not be detected for any quinone when administered only once at the beginning of a 1-week treatment. However, further addition of quinone simultaneously to the rotenone challenge after the 1-week treatment restored ATP levels in the case of idebenone and CoQ₁, whereas under these conditions, CoQ₁₀ again failed to protect ATP levels [Figure 15E].

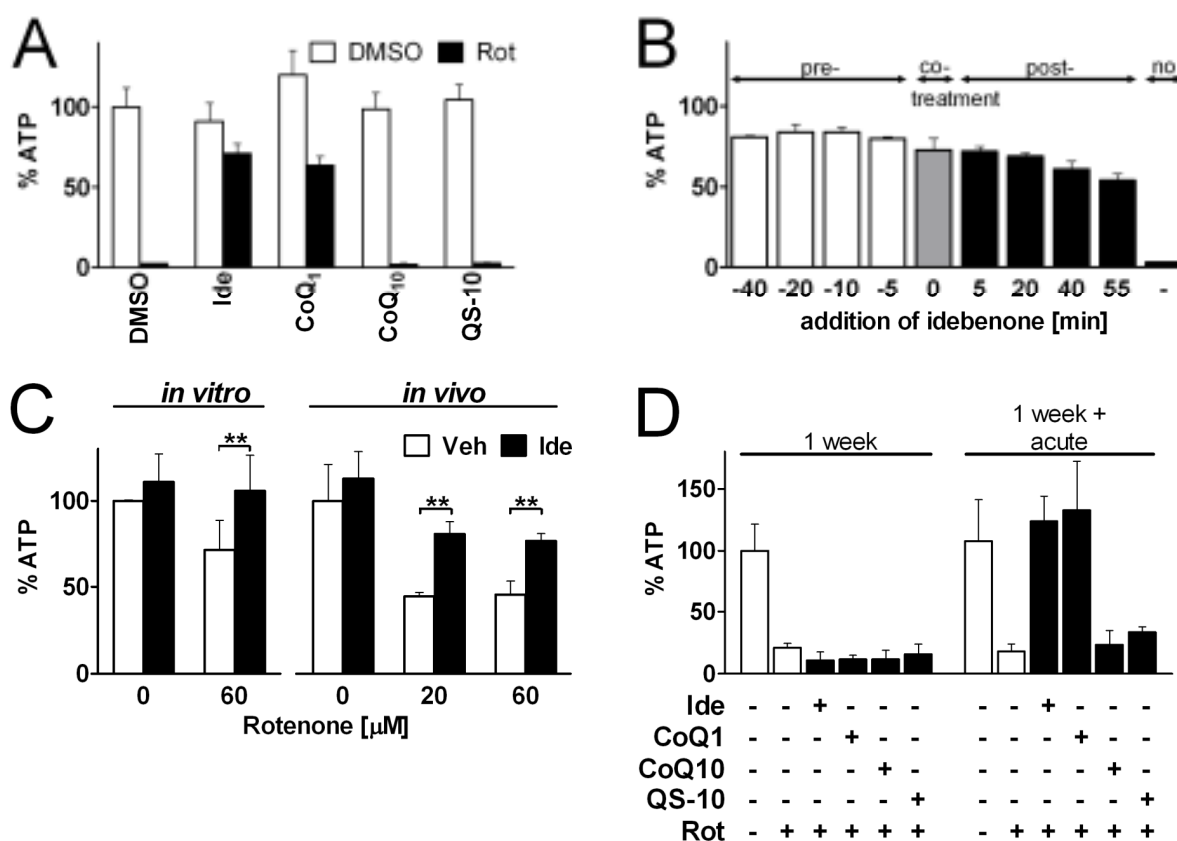


Figure 15: Idebenone and CoQ₁ Rescue ATP Levels in Rotenone-Treated HepG2 Cells.

(A) HepG2 cells were incubated with different quinones (5 μM idebenone, CoQ₁, CoQ₁₀ or QS-10) in absence (empty bars) or presence (filled bars) of rotenone (Rot; 60 μM) for one h. ATP levels were normalized to protein and expressed as percentage of DMSO-treated cells in absence of rotenone. (B) HepG2 cells were incubated with 6 μM rotenone for 60 min, while 10 μM idebenone was pre-, co- or post-incubated regarding the time point of rotenone addition. ATP levels are expressed as percentage of untreated cells. Bars represent mean + stdev of triplicates of one typical out of two independent experiments. (C) Rescue of ATP levels of rotenone-treated (20 and 60 μM) primary mouse hepatocytes by either acute *in vitro* idebenone treatment (5 μM) for one hour or four-week *in vivo* administration of idebenone. Therefore, idebenone (400 mg/kg/day; p.o.) was administered to mice over four weeks and protection of ATP levels was maintained in rotenone-treated (20 and 60 μM for one hour) primary hepatocytes *ex vivo* without acute addition of idebenone. Bars represent either mean + stdev of six independent experiments (*in vitro*) or mean + stdev of duplicates from each one idebenone- and sham-treated mouse (*in vivo*). ATP levels were normalized to cell number and expressed as percentage of sham-treated hepatocytes in absence of rotenone. (D) HepG2 cells were treated for one week with 10 μM quinones. In freshly added, glucose-free medium, ATP rescue experiment was performed using 6 μM rotenone and in absence (1 week) or presence (1 week + acute) of freshly added 10 μM quinones. Bars represent mean + stdev of one typical experiment. $p^{**}, 0.01$, $p^{***}, 0.001$; two-way ANOVA.

ATP rescue experiments were mostly performed using rotenone as inhibitor for complex I. In this series of experiments, other inhibitors of complex I were used to determine if the rescue of ATP levels mediated idebenone is dependent on a specific site of inhibiting complex I [Figure 16]. Therefore, several different inhibitors binding at specific sites were used [Table 2]. Inhibitors of quinone-binding site were classified according to the nomenclature of Degli Esposti [1998] as class A, B, or C inhibitors (binding at the site of CoQ₁₀, semiquinone, or hydroquinone interaction site of complex I). Rhein, in contrast, blocks complex I at the NADH binding site [Kean 1970]. Previously, the lowest concentration which is effective to reduce ATP levels by 30% after one hour in glucose-deficient medium was determined for each inhibitor [*data not shown*].

Table 2: Selection of Complex I Inhibitors.

A List of inhibitors according to their inhibitor class, mode of inhibition and concentrations for half maximal inhibition of complex I (IC₅₀) according to Degli Esposti [1998], if not otherwise stated. Concentrations employed in experiments are listed as well.

	class	mode of inhibition	IC ₅₀	Concentrations used	notes
berberine	-	not known		100 μM	stimulates mitochondrial permeability transition as well
capsaicin	C	QH ₂ antagonist	20-30 mM	1 mM	
coenzyme Q ₂	B	semiQ & QH ₂ antagonist upon reduction	2 μM	not used	
diphenylene iodonium	none	NADH antagonist	230 nM	not used	[Majander <i>et al.</i> 1994]
idebenone	A	Q antagonist	0.4 μM	not used	
metformin	-	indirect inhibition		50 mM	[El Mir <i>et al.</i> 2000]
pyridaben	A	Q antagonist	2.4 μM	10 nM	[Schuler 2001]
piERICIDIN	A/B	Q & semiQ antagonist	0.06 nmol/mg	not used	
rhein	none	NADH antagonist	30 μM	10 μM	[Kean 1970]
rolliniastatin	A	Q antagonist	0.06 nmol/mg	not used	
rotenone	B	semiQ antagonist	0.4 nmol/mg	6 μM	
stigmatellin	C	QH ₂ antagonist	100 nmol/mg	10 nM	inhibits complex III as well

Consistent with previous experiments, 6 μM of the class B inhibitor rotenone reduced ATP levels from 100.0±4.1% in DMSO-treated cells to 6.0±2.0%. In the presence of 10 μM idebenone, ATP levels were increased to 61.0±9.0%. In addition, idebenone rescued ATP levels to 88.2±8.5% when 50 mM metformin were used to inhibit complex I. This inhibition alone amounted to a reduction of ATP levels to 38.2±6.1%. However, the complex I inhibition by metformin was assumed to embody indirect pathways [El Mir *et al.* 2000]. Accordingly, the mode of inhibition by berberine is not described yet. However, 100 μM berberine was able to reduce ATP levels to 72.0±9.1%, and idebenone was not able to significantly rescue this drop of ATP (78.8±5.0%). Pyridaben, a class A inhibitor, acts at the quinone-binding site of the quinone-reduction pocket of complex I and potently reduces ATP levels after 1-h incubation (8.9±3.7%). In presence of idebenone, ATP levels were slightly increased to 16.7±0.0%. Two class C inhibitors, capsaicin and stigmatellin, were employed to investigate the effect of inhibitors acting on the hydroquinone-binding site in the quinone reduction pocket of complex I. Capsaicin (1 mM) reduced ATP levels to 2.0±1.2% and 1.4±0.3% in absence and in presence of idebenone, respectively. This was also seen for the second class C inhibitor, since idebenone was not able to restore ATP levels decreased by

10 nM stigmatellin (60.3% instead of $62.9 \pm 14.2\%$). However, it has to be noted that stigmatellin was also described as an inhibitor of complex III, which should be taken into account when interpreting these results [Degli Esposti 1998].

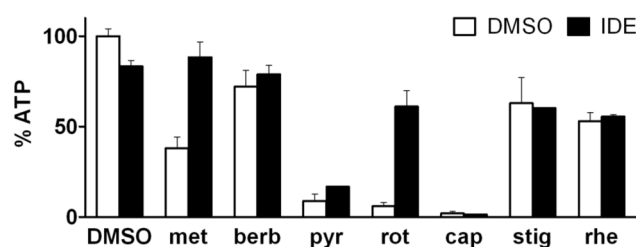


Figure 16: ATP Rescue in Presence of Different Complex I Inhibitors.

In glucose-deficient medium, HepG2 cells were treated with different complex I inhibitors for one hour and in absence (empty bars) or presence (filled bars) of 10 μ M idebenone. Inhibitors comprise metformin (met; 50 mM) and berberine (berb; 100 μ M), whose sites of inhibition are still unknown, the class A inhibitor pyridaben (pyr; 10 nM), class B inhibitor rotenone (rot; 6 μ M), class C inhibitors capsaicin (cap; 1 mM) and stigmatellin (stig; 10 nM), and NADH-binding site inhibitor rhein (rhe; 10 μ M). Bars represent average + stdev of at least three samples per condition.

3.4 Investigating the Mode of Quinone-Dependent ATP Rescue

The experiments described above showed that some quinones are able to restore ATP levels under conditions of impaired complex I [Figure 14 and Figure 15]. Confronted with these data, the question arose how idebenone and a small selection of related compounds were able to restore ATP levels under conditions of impaired complex I and if this rescue could be attributed to a certain molecular mode of action. First and foremost, idebenone is described as an antioxidant [amongst others Mordente *et al.* 1998, Jauslin *et al.* 2002, and Abdel Baky *et al.* 2010]. Furthermore, an increasing number of reports also implied that idebenone can block Ca^{2+} channels [Houchin *et al.* 1991, Chang *et al.* 2011, Kaneko *et al.* 2011, and Newman *et al.* 2011]. Both ROS production and abnormal Ca^{2+} levels are hallmarks of processes that lead to cell death. Thus, since reduced ATP levels might be a representation of rotenone-induced cell death, idebenone could rescue cells by blocking apoptotic or necrotic processes. This would imply that the idebenone-mediated restoration of ATP levels represent just an epiphenomenon of reduced cell death.

Pathways of oxidative stress, Ca^{2+} imbalance and cell death unite at a particular crossroad: the mitochondrial permeability transition pore (mPTP). The mPTP is a protein complex in the inner mitochondrial membrane which is formed upon several stimuli including stress and apoptotic- or necrosis-inducing factors [Kinnally *et al.* 2010]. The formation of the pore enables molecules up to 1.5 kDa to pass the inner membrane and thus, prolonged opening of the mPTP triggers multiple pathways leading to cell death. For example, osmotic gradients force ions and molecules to enter the mitochondria and this entails the influx of H_2O causing the mitochondria to swell. As a consequence, swelling of the mitochondria leads to a decreased integrity of the inner and outer membrane and thus, the proton gradient needed to fuel ATP synthesis becomes corrupted. Furthermore, in order to maintain the proton gradient, ATP synthase starts to catalyze the hydrolysis of ATP and thereby the levels decrease further.

Since idebenone protects cells against different stressors [Yerushalmi *et al.* 2001, Gumprich *et al.* 2002, and Jauslin *et al.* 2002, 2003, and 2007], one could hypothesize that this protective action is due to an inhibition of apoptotic or necrotic pathways such as the formation of mPTP. Consistent with this mechanism, idebenone was described to prevent mitochondrial swelling [Suno and Nagaoka 1989b, Sokol *et al.* 2005] which was attributed to its antioxidant effect. However, if idebenone interacted directly with the mPTP, swelling of mitochondria would be detained by averting the opening of the pore. Notably, rotenone deregulates intracellular Ca^{2+} homeostasis which can be reversed by cyclosporin A (CsA), an inhibitor of mPTP opening [Gieseler *et al.* 2009]. Thus, the rescue of ATP levels by idebenone in presence of rotenone could potentially originate from the inhibition of mPTP opening.

To test this hypothesis, HepG2 cells cultured for 24 h in low glucose medium were treated with different compounds known to influence the mPTP and quantified their impact on ATP levels in the absence of glucose. Compounds thought to inhibit mPTP opening were pretreated for 30 min prior to the 1-h incubation with compounds thought to open the pore.

Since Ca^{2+} promotes opening of mPTP, compounds influencing intracellular Ca^{2+} concentrations were used. The ionophore A23187 shuttles Ca^{2+} ions through the plasma membrane into the cytosol; whereas thapsigargin promotes Ca^{2+} release from the ER. In contrast, BAPTA-AM is a membrane-permeable Ca^{2+} chelator.

In preliminary experiments, the potential of Ca^{2+} concentrations-elevating agents to decrease ATP levels was assayed [Figure 17A]. In contrast, a drop in ATP levels induced by an antagonist of Ca^{2+} concentrations increase were regarded as objectionable, since their potential to reverse the negative effects of Ca^{2+} -elevating agents on ATP levels was of interest in subsequent experiments. A23187 decreased ATP levels in a dose-dependent manner ($70 \pm 5\%$ for 100 nM, $39 \pm 1\%$ for 1 μ M and $10 \pm 0\%$ of residual ATP levels for 10 μ M A23187). The second compound increasing cytosolic Ca^{2+} levels, thapsigargin, did not alter ATP levels at any concentration used ($98 \pm 6\%$ for 100 nM, $102 \pm 2\%$ for 1 μ M and $90 \pm 4\%$ for 10 μ M) and was therefore not employed in later

experiments. BAPTA-AM reduces ATP levels only at a high concentration ($9\pm 1\%$ for $100\ \mu\text{M}$); whereas lower concentrations did not alter ATP levels ($98\pm 1\%$ for $1\ \mu\text{M}$ and $95\pm 1\%$ for $10\ \mu\text{M}$) and CsA itself did not affect ATP levels ($92\pm 8\%$ for $100\ \text{nM}$, $94\pm 9\%$ for $1\ \mu\text{M}$ and $93\pm 3\%$ for $10\ \mu\text{M}$) [Figure 17A].

Subsequently, $10\ \mu\text{M}$ A23187 was used to inhibit mitochondrial ATP production instead of rotenone. Two antagonistic agents, as well as idebenone, were tested for their potential to reverse the detrimental effect [Figure 17B]. Similarly to the preliminary experiments [Figure 17A], $10\ \mu\text{M}$ A23187 reduced ATP levels to $7\pm 1\%$, whereas $10\ \mu\text{l}$ idebenone, $10\ \mu\text{l}$ BAPTA-AM, or $10\ \mu\text{l}$ CsA did not alter ATP levels after 1-h incubation ($99\pm 10\%$, $97\pm 0\%$, or $107\pm 15\%$, respectively) [Figure 17B]. Co-incubation of each of these three compounds with A23187, however, did not rescue the drop of ATP induced by A23187 alone ($5\pm 0\%$, $5\pm 0\%$, or $5\pm 1\%$, respectively).

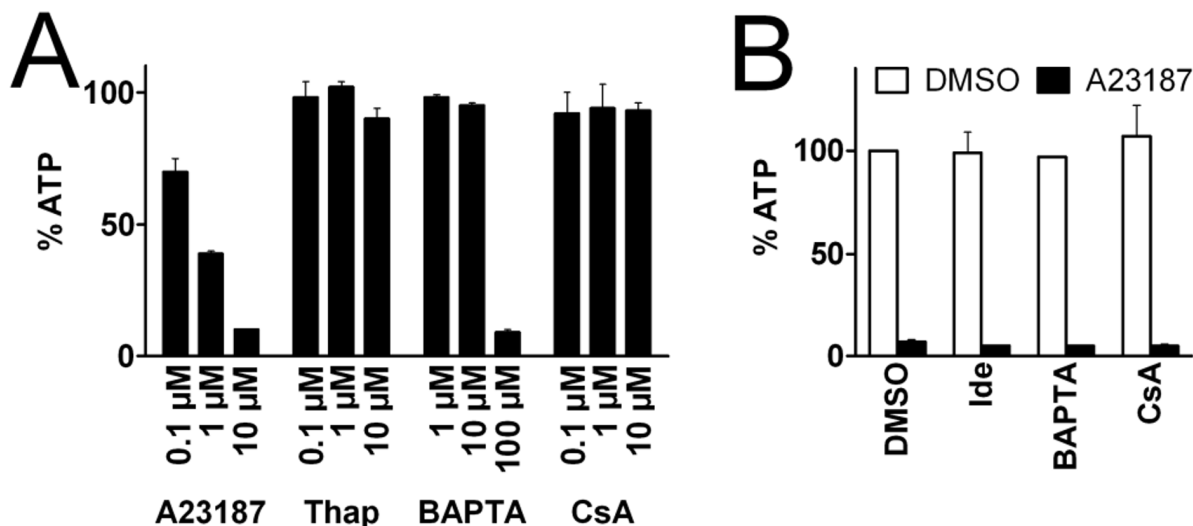


Figure 17: Influence of Calcium on Mitochondrial ATP Production.

(A) ATP levels of HepG2 cells were measured after 1-h incubation of Ca^{2+} -inducing agents A23187 and thapsigargin (Thap), cell-permeable Ca^{2+} chelator BAPTA-AM (BAPTA), and cyclosporin A (CsA), an inhibitor of mPTP opening, in glucose-free medium. (B) Under the same conditions, ATP levels were determined after treatment with $10\ \mu\text{M}$ idebenone (Ide), $10\ \mu\text{M}$ BAPTA, or $10\ \mu\text{M}$ CsA in absence (empty bars) or presence (filled bars) of $10\ \mu\text{M}$ A23187. Bars represent mean + stdev of triplicates of a typical experiment.

These results indicated that increased Ca^{2+} levels led to a massive reduction of ATP content and that idebenone was not able to restore ATP levels under conditions of elevated Ca^{2+} concentrations [Figure 17]. Since the only rescue of ATP levels by idebenone were observed when complex I was inhibited [Figure 14 and Figure 16], the mode of action of this rescue was further investigated in the presence of rotenone. As stated earlier, idebenone was suggested to act as an antioxidant, by blocking Ca^{2+} channel, or by triggering anti-apoptotic or – necrotic pathways. Therefore, well known and widely used agonists of these pathways were used in order to see if the observed rescue can be attributed to one of these functions. The antioxidants tempol and *N*-acetyl-L-cysteine (NAC), the antiapoptotic omigapil and an anti-necrotic inhibitor of poly(ADP-ribose) polymerase 1 (PARP1), PJ34 [Fiorillo *et al.* 2006] were tested for their ability to rescue ATP levels after rotenone-mediated inhibition of complex I. For the case that rotenone could mediate the ATP drop through alteration of Ca^{2+} homeostasis, the membrane-permeable Ca^{2+} chelator BAPTA-AM and the inhibitor of mPTP opening, CsA, were included in these experiments again.

When HepG2 cells were cultivated overnight in medium containing $0.3\ \text{g/l}$ glucose before 1-h incubation with these compounds in glucose-free medium, ATP levels basically remained unaltered ($108\pm 1\%$, $112\pm 2\%$, and $111\pm 3\%$ for $10\ \mu\text{M}$, $100\ \mu\text{M}$, and $1\ \text{mM}$ tempol, respectively; $86\pm 3\%$, $85\pm 3\%$, and $94\pm 3\%$ for $500\ \mu\text{M}$, $5\ \text{mM}$, and $50\ \text{mM}$ NAC; $93\pm 5\%$, $95\pm 4\%$, and $95\pm 4\%$ for $10\ \text{nM}$, $100\ \text{nM}$, and $1\ \mu\text{M}$ omigapil, respectively; and $101\pm 2\%$, $108\pm 1\%$ and $110\pm 2\%$ for $100\ \text{nM}$, $1\ \mu\text{M}$, and $10\ \mu\text{M}$ PJ34, respectively) [Figure 18A]. Influence of BAPTA-AM and CsA on ATP levels have been described previously [Figure 17A].

When cells were simultaneously treated with $100\ \text{nM}$ rotenone—beside $10\ \mu\text{M}$ idebenone ($87\pm 1\%$ of residual ATP levels) and $10\ \mu\text{M}$ CoQ₁ ($107\pm 3\%$)—only $50\ \text{mM}$ NAC ($31\pm 4\%$) was able to partially rescue ATP levels [Figure 18B]. The other compounds employed could not attenuate the detrimental effect of rotenone on ATP levels ($10\ \text{mM}$ tempol: $-7\pm 0\%$; $10\ \mu\text{M}$ BAPTA-AM: $-5\pm 0\%$; $10\ \mu\text{M}$ CsA: $-1\pm 2\%$; $10\ \mu\text{M}$ omigapil: $-3\pm 2\%$; and $10\ \mu\text{M}$ PJ34: $-4\pm 1\%$). Thus, the fact that NAC showed a mild ATP rescue compared to idebenone raised the question, if the mode of action for this rescue could be similar to the one of idebenone. Therefore, $50\ \text{mM}$ NAC were co-incubated with ATP-depleting agents ($100\ \text{nM}$ antimycin A, $10\ \mu\text{M}$ A23187, $1\ \mu\text{M}$ FCCP, and $100\ \text{nM}$ oligomycin) whose effects could not be reversed by idebenone. Interestingly, NAC showed some rescue of ATP levels regardless of the mode of respiration inhibition ($10\pm 7\%$ ATP rescue for antimycin A, $23\pm 20\%$ for A23187, $139\pm 10\%$ for FCCP, and $64\pm 13\%$ for oligomycin) [Figure 18C]. Idebenone was not able to rescue ATP levels in presence of these inhibitors [Figure 18C] which is in line with results shown before [Figure 14C].

An interesting finding was that both the quinones idebenone and CoQ₁, but not CoQ₀ ($-7\pm 1\%$ rescue) were able to rescue the rotenone-mediated drop in ATP [Figure 18B]. Hence, it was of interest to test several structurally related quinones for their ability to reduce the rotenone-induced ATP drop. As in previous experiments [Figure 15A], CoQ₁₀ and QS-10 showed no rescue ($2\pm 1\%$ and $2\pm 1\%$ ATP rescue, respectively), whereas idebenone and CoQ₁ were once more confirmed as potent rescuers ($59\pm 10\%$ and $65\pm 6\%$) [Figure 18D]. In this series of experiments, a rescue mediated by CoQ₀ was observed ($11\pm 2\%$) which, however, is negligible in contrast to the rescue ability of idebenone or CoQ₁. Interestingly, DQ and CoQ₂, two benzoquinones with an eight- and ten-carbon alkyl tail, respectively, also showed rescue values of $60\pm 6\%$ and $60\pm 10\%$, respectively, which were comparable to that of idebenone and CoQ₁. A quinone with a longer, 20-carbon chain, CoQ₁₀, failed to rescue ATP levels at all ($1\pm 1\%$).

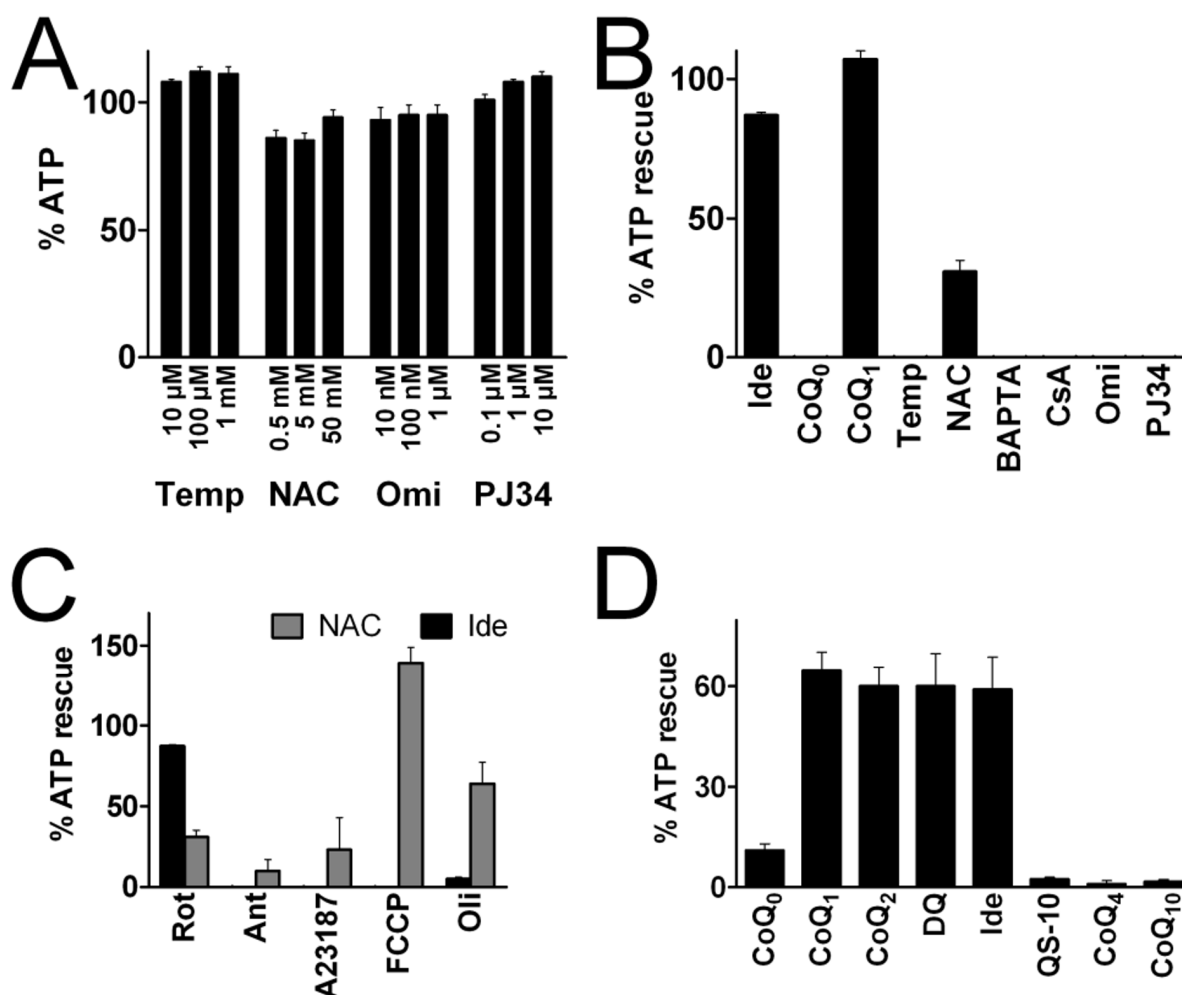


Figure 18: ATP Rescue Is Specific to Certain Short-Chain Benzoquinones.

(A) Different concentrations of tempol (Temp), *N*-acetyl-*L*-cysteine (NAC), omigapil (Omi), or PJ34 were added for one hour to glucose-depleted HepG2 cells before ATP levels were measured. Values are expressed as percentage relative to DMSO-treated controls. (B) HepG2 cells were incubated with 100 nM rotenone simultaneously with 10 μ l idebenone, 10 μ M CoQ₁, 10 mM tempol, 50 mM NAC, 10 μ M BAPTA-AM (BAPTA), 10 μ M cyclosporin A (CsA), 10 μ M omigapil, or 10 μ M PJ34 for one hour in glucose-free medium before ATP levels were measured. (C) Idebenone (10 μ M; black bars) or NAC (50 mM; grey bars) were co-incubated with 100 nM rotenone, 100 nM antimycin A (Ant), 10 μ M A23187, 1 μ M FCCP, or 100 nM oligomycin (Oli) for one hour in glucose-free medium. (D) Different quinones altering only in their alkyl chains (sorted in order of ascending chain length) such as idebenone and decylQ (DQ) were co-incubated with 6 μ M rotenone for one hour in glucose-depleted HepG2 cells before ATP was measured. Percentage ATP rescue is defined as the compound-dependent increase of ATP in presence of rotenone relative to rotenone-induced ATP drop. Bars represent mean + stdev of triplicates from one experiment (A-C) or mean + stdev of three independent experiments.

3.5 Can Idebenone Ameliorate ATP Levels Via AMPK?

Idebenone was shown influence ATP production through OXPHOS [Figure 13], to rescue of ATP levels under conditions of deficient complex I [Figure 15], but at the same time, it was also reported as an inhibitor of complex I [Sugiyama *et al.* 1985, Degli Esposti *et al.* 1996, Briere *et al.* 2004, Fato *et al.* 2008, and Rauchová *et al.* 2008, Santhera unpublished data]. Inhibition of complex I leads to a reduction of ATP synthesis and, as a consequence, to the activation of AMP-activated protein kinase (AMPK) [Hutchinson *et al.* 2007]. AMPK is a sensor for energy shortage and phosphorylation of AMPK at threonine 172 (Thr172) leads to energy-conserving processes such as glucose uptake, fatty acid oxidation, and mitochondrial biogenesis [Han *et al.* 2010].

To assess if complex I inhibition by idebenone could activate AMPK and thereby promote cellular responses to low ATP levels, phosphorylation status of AMPK in rat L6 myoblasts was assessed by western blots. To detect rapid, transcriptionally or translationally unrelated changes in AMPK activation, cells were treated with idebenone for only a very short time. Since AMPK can be activated by growth factors, cells were serum starved 24 h before treatment with idebenone [Bikman *et al.* 2010]. Phosphorylation-specific antibody against phosphorylation of AMPK at Thr172 was employed and total amount of AMPK in the sample was used as a normalizing reference [Figure 19]. Although some activated AMPK protein was observed in lysates of untreated cells, different concentrations of idebenone ranging from 100 mM to 10 μ M did not alter the total amount or the activity of AMPK evidenced by phosphorylation at Thr172. Similarly, increasing the incubation period with idebenone had no influence on phosphorylation strength, since signals from AMPK and phospho-AMPK were perfectly congruent. Furthermore, 15-min treatment with berberine, a complex I inhibitor described to activate AMPK [Han *et al.* 2010], was also not able to increase phosphorylation signal compared to untreated cells [Figure 19].

Thus, the notion that increased ATP production induced by idebenone was driven via AMPK-involving pathways is unlikely.

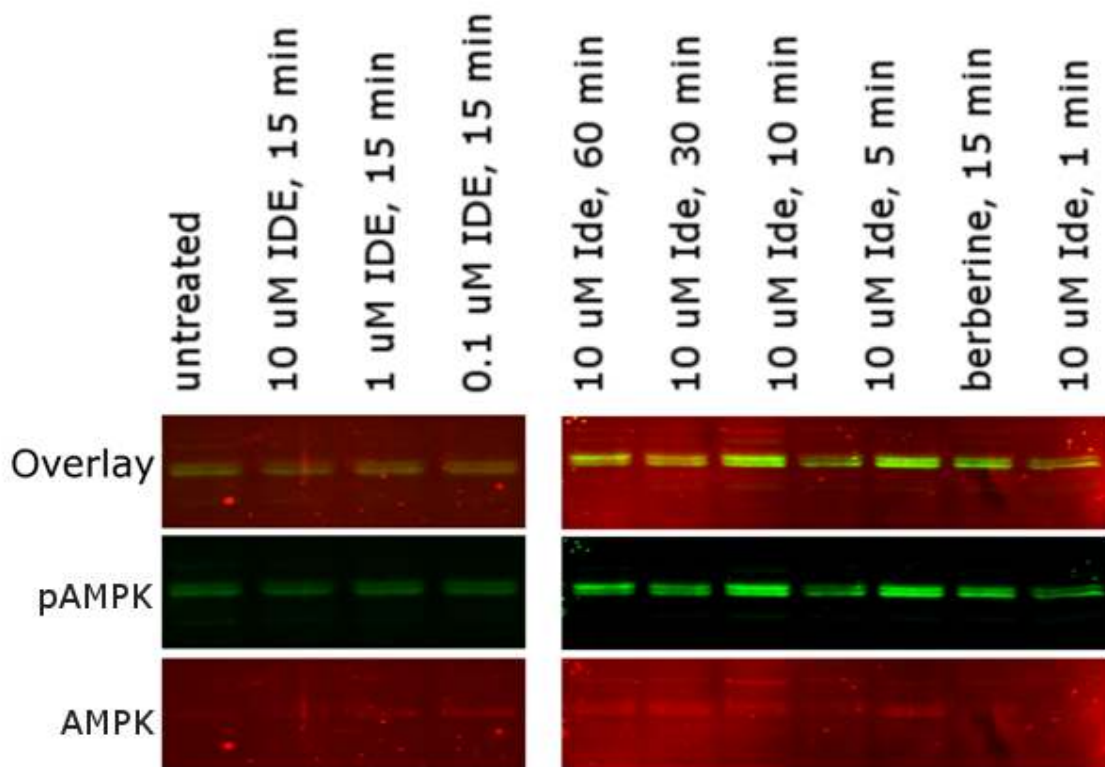


Figure 19: Idebenone Treatment Does Not Alter Phosphorylation of AMPK.

L6 cells were cultivated in medium containing 1 g/l glucose and 2% serum for 24 h before medium was replaced with serum-free 1 g/l glucose-containing medium. After 24 h, cells were treated with different concentrations of idebenone (IDE) or berberine (10 μ M) for 15 min or with 10 μ M idebenone for a duration ranging from one minute to one hour. Total AMPK protein (red) and Thr172-phosphorylated AMPK (pAMPK; green) content in cell lysates were analyzed using Western blotting.

3.6 Quinone-Dependent ATP Rescue Is Dependent on NQO1 and Complex III

Since the restoration of ATP levels under conditions of impaired complex I could not be attributed to antioxidant, Ca^{2+} homeostasis-interfering, anti-apoptotic or -necrotic, mPTP-blocking or AMPK-activating activity, a possible explanation therefore would be direct intervention of idebenone into the ETC. For doing so, idebenone would be required to induce mitochondrial electron transport in the presence of dysfunctional complex I. This would require idebenone to be reduced by (an) unknown oxidoreductase(s) and then to donate its electrons into the ETC, probably at the site of complex III since it has been described that idebenone is an excellent substrate for complex III [Degli Esposti *et al.* 1996]. Strikingly, such a mechanism was described previously for CoQ₁: Chan *et al.* [2002] reported that this quinone could be reduced within the cytosol by NQO1 and then donates its electrons to cytochrome *c* via complex III. If acting as cytosolic-mitochondrial electron carrier accounted for the ATP rescue in presence of rotenone, the rescue should be sensitive to inhibition of complex III and of the cytosolic oxidoreductase proposed by Chan and co-workers: NQO1.

Consequently, ATP rescue was performed as in previous experimental settings: after culture in 0.3 g/l glucose-containing medium supplemented with 2% FBS, HepG2 cells were deprived of glucose and treated with 60 μ l rotenone for one h. This led to the reduction of ATP levels to 2% of residual levels [Figure 20]. Idebenone and CoQ₁ restored ATP levels to 71 \pm 6% and 64 \pm 6%, respectively; whilst CoQ₁₀ and QS-10 were not able to elevate

ATP levels in presence of rotenone ($2 \pm 1\%$ for both quinones) [see also Figure 15]. Strikingly, when the inhibitors of NQO1 or complex III—dicoumarol or antimycin A, respectively—were added to cells simultaneously with rotenone, the impressive ATP rescue by idebenone and CoQ₁ was lost [Figure 20].

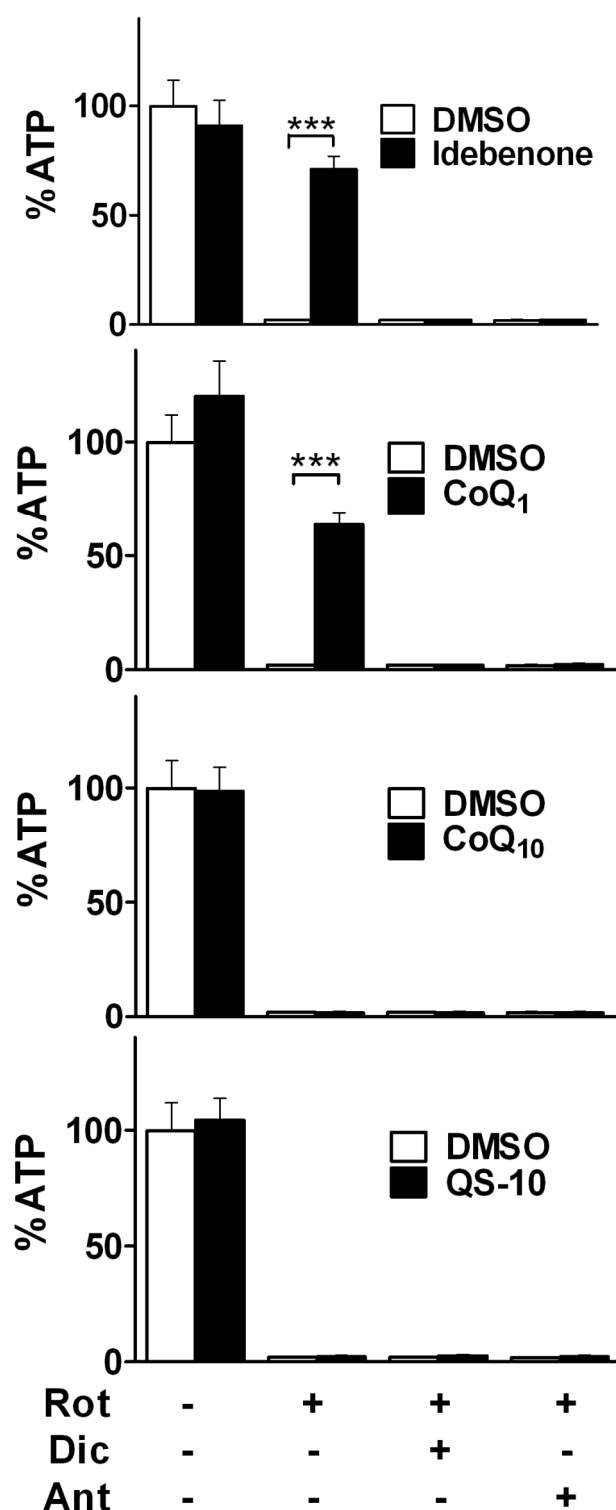


Figure 20: ATP Rescue of Idebenone and CoQ₁ Is Dependent on NQO1 and Complex III.

(A) HepG2 cells were incubated with rotenone (Rot; 60 μ M), dicoumarol (Dic; 20 μ M), and antimycin A (Ant; 6 μ M) in absence (empty bars) or presence (filled bars) of different quinones (5 μ M idebenone, CoQ₁, CoQ₁₀ or QS-10) for one h. ATP levels were normalized to protein and expressed as percentage of DMSO-treated cells in absence of rotenone. $p^{***} < 0.001$; two-way ANOVA.

This data supported the assumption, that idebenone might shuttle electrons into the ETC upon reduction in the cytosol by NQO1. However, in order to endorse this hypothesis, it was necessary to demonstrate the reduction of idebenone by NQO1. *In vitro* assays using recombinant enzyme provided a suitable model system to confirm or refute this argument.

Idebenone, CoQ₁, CoQ₁₀, and QS-10 were investigated for their ability to oxidize NAD(P)H in presence of NQO1. The loss of absorption at 340 nm after oxidation of NAD(P)H to NAD(P)⁺ was employed to determine kinetic parameters of NQO1-quinone interaction. Experiments with recombinant enzymes clearly demonstrated that these four quinones are differentially reduced by NQO1 [Table 3 and Figure 21A&B]. Generally, NQO1 demonstrated a slight preference of NADPH over NADH as electron donor with either idebenone, CoQ₁ or QS-10 as acceptor substrate [Table 3]. Whereas maximal reduction velocity (v_{\max}) for NQO1 presented in the following order: CoQ₁ > idebenone > QS-10, we could not find any evidence for a NQO1-mediated reduction of CoQ₁₀ [Table 3]. Due to poor solubility of CoQ₁₀ in aqueous solutions, we repeated the assay with different formulations of CoQ₁₀ in accordance to its lipophilic requirements. Nevertheless, when complexed with fetal bovine serum (FBS) or incorporated into phosphatidylcholine-based leptosomes [Mayer *et al.* 1985, Paolino *et al.* 2004], we were unable to detect any NQO1-dependent reduction of CoQ₁₀ [Figure 21C]. In contrast, idebenone was clearly reduced by NQO1 under all conditions tested.

NQO2, although much less studied, is reported to possess similar oxidoreductase activity with some differences in substrate specificities [Wu *et al.* 1997]. Despite similar cDNA and amino acid sequences of NQO1 and NQO2, NQO2 has different co-factor requirements [Long and Jaiswal 2000]. Indeed, using either NADH or NADPH as electron donor, NQO2 failed to reduce quinones [*data not shown*]. Thus, 1-(3-sulfonatopropyl)-3-carbamoyl-1,4-dihydropyrimidine, a synthetic analog of the NQO2 substrate dihydronicotinamide ribosid (NRH) [Knox *et al.* 2000], was employed as electron donor instead. However, before calculating turnover rates of 1-(3-sulfonatopropyl)-3-carbamoyl-1,4-dihydropyrimidine, the absorption coefficient had to be determined. Therefore, several concentrations of the compound (1, 5, 10, 50, and 100 μM) were added into a 1-cm cuvette containing reaction buffer. The difference between the absorption at A_{355} and the absorption of blanks was divided by the molar concentration, resulting in an absorption coefficient of $\epsilon_{\text{NRH-derivate}} = 4430 \text{ M}^{-1} \text{ cm}^{-1}$. For all four quinones, we found similar results with regards to the K_m and v_{\max} for NQO2-dependent reduction compared to the data generated with NQO1 [Table 3 and Figure 21D].

The use of dicoumarol as inhibitor of NQO1 was in line with publications showing that this compound selectively blocks NQO1 activity at an IC_{50} of 10 nM [Ernster 1962, Wu *et al.* 1997, and Long and Jaiswal 2000]. Nevertheless, the specificity for dicoumarol to inhibit NQO1 was confirmed in this experimental setting of NADH or 1-(3-sulfonatopropyl)-3-carbamoyl-1,4-dihydropyrimidine oxidation by recombinant NQO1 in presence of CoQ₁₀ as electron acceptor, respectively: dicoumarol (20 μM) potentially inhibited recombinant NQO1 activity (4% residual activity), while at the same time NQO2 activity was only inhibited by 14% (86% residual activity) [Figure 21E].

To analyse whether the reduction of idebenone by NQO1 is mechanistically comparable to other NQO1 substrates, idebenone was co-incubated with a widely used electron acceptor, 2,6-dichlorophenolindophenol (DCPIP), whose interaction with NQO1 was described [Cabello *et al.* 2009, Cabello *et al.* 2011]. Reduced DCPIP does not absorb at 600 nm in contrast to its oxidated form. A rise in idebenone concentration reduced the conversion of DCPIP and thus, K_m values of DCPIP increased. However, v_{\max} remained constant. This means, idebenone and DCPIP are competitive substrates for NQO1 as depicted by the conjunction on the ordinate of the linear regressions of different samples in a Lineweaver-Burk plot [Figure 21F].

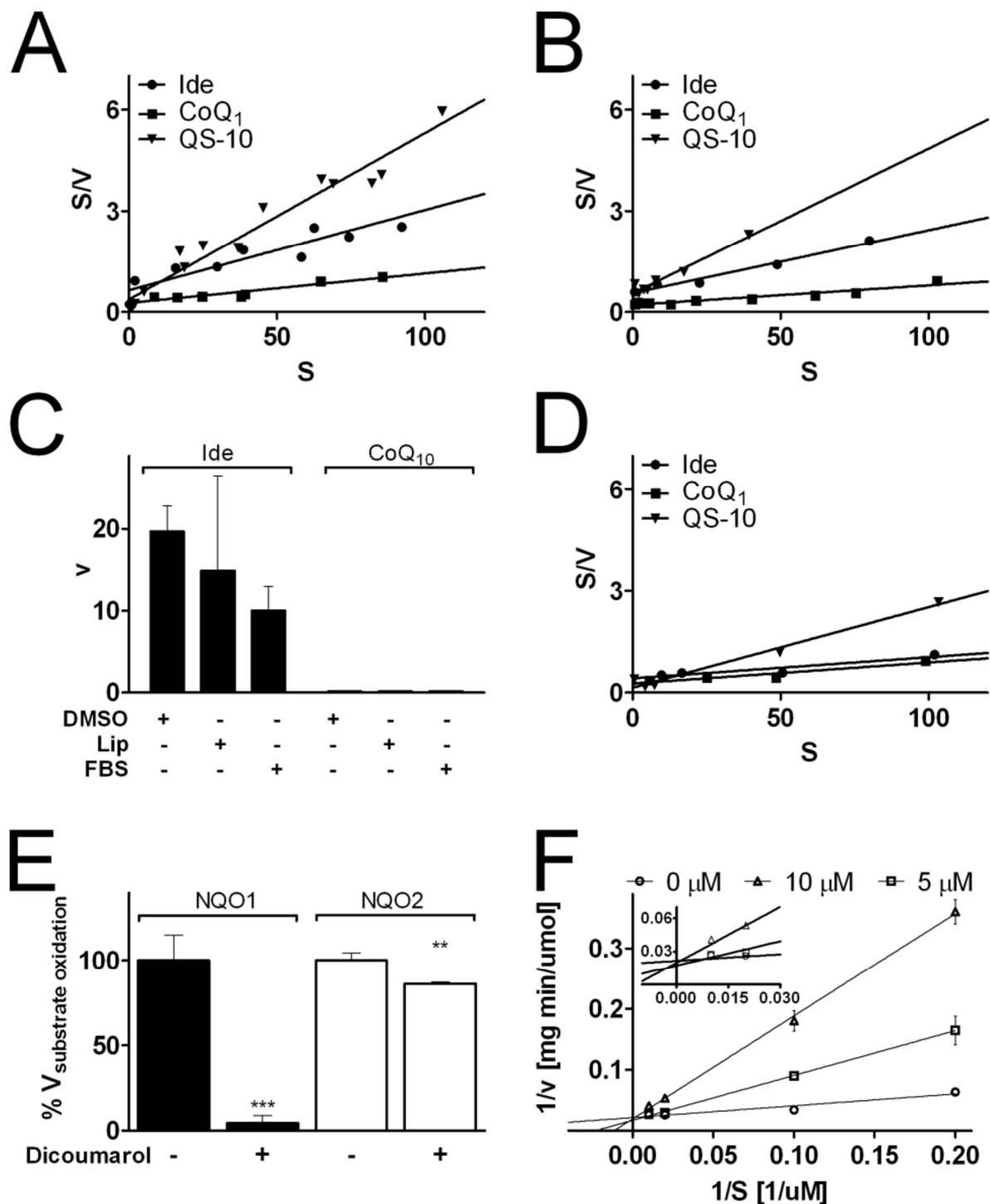


Figure 21: Idebenone and Related Quinones Are Substrates for NQO1 and NQO2.

Hanes-Woolf plots depict oxidation of NADH (A) or NADPH (B) by NQO1 in presence of different quinones as electron acceptors. Each data point represents the average of three independent measurements. (C) Effect of different quinone formulation in DMSO, liposomes (Lip) and fetal bovine serum (FBS) on metabolism by NQO1. Graph depicts electron donor oxidation rate expressed as percentage of control; mean + stdev of three independent measurements. (D) Hanes-Woolf plot of NRH-derivate dihydronicotinamide riboside oxidation by NQO2 in presence of different quinone analogs. Each data point represents the average of three independent measurements. (E) Dicoumarol (20 μ M) selectively inhibited NADH oxidation by recombinant NQO1 with CoQ₁₀ as electron acceptor (96% inhibition, filled bars) *in vitro*, whereas it reduced NQO2-mediated NRH derivative oxidation by only 14% (empty bars). Graph depicts electron donor oxidation rate (% $V_{\text{substrate oxidation}}$) expressed as percentage of control; mean + stdev of three independent measurements; $p^{***,0.001}$, $p^{**,0.01}$, two-tailed t-test. (F) Idebenone is a competitive inhibitor of DCPIP as electron acceptor for NQO1-mediated NADPH oxidation as the intersection of the ordinate in a Lineweaver-Burk plot (magnified in inlay) indicates. Each data point represents the average of three independent measurements.

Table 3: Steady-state kinetic constants of NQO1 and NQO2 with different quinones.

^{a)} For NQO2 enzymatic assays 1-(3-sulfonatopropyl)-3-carbamoyl-1,4-dihydropyrimidine (NRH-derivative) was used as electron donor as described [Knox *et al.* 2000]; ^{b)} No enzymatic activity above background could be detected for CoQ₁₀, thus, steady-state kinetics could not be calculated.

Enzyme Substrate	NQO1				NQO2	
	NADH		NADPH		NRH-derivate ^a	
	K _m [μM]	V _{max} [μmol/ mg/min]	K _m [μM]	V _{max} [μmol/ mg/min]	K _m [μM]	V _{max} [μmol/ mg/min]
Idebenone	27	41.9	30	53.4	38	97.4
CoQ ₁	31	115.5	36	172.2	47	128.0
CoQ ₁₀	- ^b	- ^b	- ^b	- ^b	- ^b	- ^b
QS-10	8	20.5	13	23.3	5	29.6

Idebenone and CoQ₁ were able to restore ATP levels in rotenone-treated cells [Figure 15] and this rescue was sensitive to the NQO1 inhibitor dicoumarol [Figure 20]. In addition, interaction of idebenone and NQO1 was verified using recombinant enzyme, demonstrating that idebenone is a good substrate for NQO1 [Figure 21]. Subsequently, it was of interest to demonstrate the reduction of idebenone by NQO1 in living cells. Tan and Berridge [2010] reported the use of the tetrazolium dye WST-1 to detect quinone-mediated NQO1 activity. In their model, quinones entering the cell are reduced by NQO1 and are then able to donate the electrons to WST-1, possibly via plasma membrane electron transport enzymes, since WST-1 is membrane-impermeable. Upon reduction, WST-1 is converted into its formazan structure which resulted in an increased absorption at 450 nm.

Hence, the WST-1 assay appeared to be a suitable instrument to measure quinone reduction *in vitro*. The assay was performed in different cells in order to detect cell-specific reduction rates of idebenone and CoQ₀. [Figure 22A]. Both quinones were reduced in almost all cells tested³, but CoQ₀ was converted at an approximately two-fold rate compared to idebenone. With regards to the expression levels of NQO1 [Haefeli *et al.* 2011 and personal communication by D. Robay], WST-1 signal and NQO1 abundance seemed to lack a correlation. Human fibroblasts C2 and C3, and human myoblast 2TE showed distinctly lower NQO1 expression levels, whereas WST-1 turnover were comparable. However, in cell lines featuring very low NQO1 expression—RGC-5, SH SY5Y, and HEK293—addition of idebenone did not result in an increase of absorption at 450 nm [Figure 22A].

In cell lines where idebenone and CoQ₀ were well converted, human HepG2 hepatic cells and rat L6 myoblastoids, three related quinones—decylQ, CoQ₁, and QS-10—were tested [Figure 22B]. None of these quinones were nearly as strongly reduced as CoQ₀, or even idebenone. The fact that each substrate for NQO1 exhibited individual turnover rates was in line with different affinities of substrates towards the recombinant enzyme [Table 3]. Intriguingly, CoQ₁, a stronger substrate for recombinant enzyme than idebenone, seemed to show a weaker response in the WST-1 assay compared to idebenone within living cells.

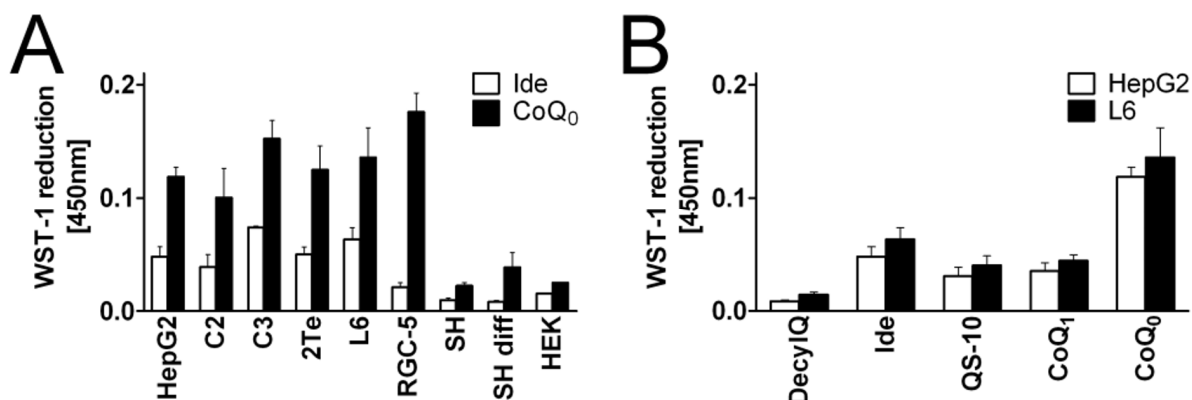


Figure 22: Idebenone and Related Quinones Are Reduced in a Selection of Cells and Cell Lines.

Quinone reduction was measured using WST-1 assay. (A) The reduction of idebenone (open bars) and CoQ₀ (filled bars) in different cells and cell lines was measured using the WST-1 assay. (B) Reduction of the selected quinones, idebenone (Ide), DecylQ, CoQ₁, CoQ₀ and QS-10, varied markedly as is shown here for HepG2 (open bars) and L6 (filled bars) cells. Bars represent mean + stdev of at least three independent experiments.

³ BC1 LCL lymphoblastoid cells were also subjected to the WST-1 assay but no usable data was obtained in this cell line, since (i) their NQO1 levels were negligible [data not shown] and (ii) the unequal distribution of suspension cells interfered with absorption measurement. Therefore, data obtained with BC1 LCL were omitted.

3.7 The Influence of Cell Medium on ATP Rescue Experiments

The fact that rotenone and other OXPHOS inhibitors were able to completely deplete cellular ATP content in the previous experiments excluded glycolytic involvement in these experimental settings [Figure 14]. Nonetheless, it was of interest to determine how elevating glycolytic activity would interfere with the observed effects. In the previous experiments investigating the ATP rescue by idebenone, glucose content was kept to a minimum in order to promote mitochondrial energy production. HepG2 cells cultivated in medium containing low glucose content (1.77 mM glucose; the so-called *Lo Glu medium*) were highly susceptible to rotenone after withdrawal of glucose and idebenone and related quinones were able to reverse rotenone-mediated ATP depletion in an NQO1-dependent manner [Figure 14 - Figure 20]. In contrast, cultivating cells in *Hi Glu medium* (25 mM glucose) promotes the use of glycolysis over mitochondrial energy production [Vander Heiden *et al.* 2009]. Thus, it is likely that after withdrawal of glucose, cells relying on glycolysis are not able to quickly shift their ATP production to OXPHOS. As a result, ATP levels would not be that strongly sensitive towards mitochondrial impairment.

In order to discriminate the influence of glycolysis and OXPHOS on the ATP levels observed in the previous experiments, glucose was substituted by galactose (25 mM galactose; the so-called *Gal medium*). Galactose, in turn, can be broken down by glycolysis; however, since activation of galactose to enter glycolysis requires two molecules of ATP and glycolysis results in two molecules ATP, the net value of glycolytic decomposition of galactose is zero. Therefore, substitution of glucose by galactose is used to force cells to rely on mitochondrial respiration.

Basal ATP levels after incubation in glucose-free medium for one hour did not differ in cells cultivated in Hi Glu, Lo Glu, or Gal medium [*data not shown*]. When cells were then subjected to 6 μ M of rotenone, the reduction of ATP levels was differently affected when comparing cells cultivated in media which promote glycolysis-dependent energy production with those relying on mitochondrial ATP synthesis. In HepG2 cells cultivated in (A) Hi Glu, 1-h incubation with rotenone did not affect ATP levels as much as in cells cultivated in either (B) Lo Glu or (C) Gal medium (63 \pm 2% of residual levels for cells cultivated in Hi Glu, 25 \pm 2% in Lo Glu, and 7 \pm 1% in Gal medium, respectively) [Figure 23A-C]. According to the mitochondrial dependency of galactose-mediated energy production, rotenone had a substantially negative effect on ATP levels in cells cultivated in Gal medium and treated in Gal medium (8 \pm 0% of residual levels) [Figure 23D]. Treatment with 20 μ M dicoumarol failed to reduce ATP levels as significant compared to rotenone (83 \pm 6% for Hi Glu \rightarrow No Glu, 81 \pm 8% for Lo Glu \rightarrow No Glu, 81 \pm 10% for Gal \rightarrow No Glu, and 94 \pm 1% for Gal \rightarrow Gal). Co-incubation of rotenone and dicoumarol, however, had a more dramatic influence on ATP levels than rotenone alone (46 \pm 2% for Hi Glu \rightarrow No Glu, 9 \pm 2% for Lo Glu \rightarrow No Glu, 3 \pm 3% for Gal \rightarrow No Glu, and 5 \pm 0% for Gal \rightarrow Gal). As anticipated, cells which ignored mitochondrial energy production during cultivation were less susceptible to OXPHOS inhibition.

Addition of idebenone emerged in an interesting picture. When cells were cultivated in Lo Glu medium and treated with either 10 μ M idebenone alone or in presence of 6 μ M rotenone, 20 μ M dicoumarol, or both, the pattern seen in previous experiments could be observed again (94 \pm 3% when treated with idebenone alone, 81 \pm 3% in presence of rotenone, 13 \pm 3% in presence of dicoumarol, and 7 \pm 1% in presence of both) [Figure 23B]. The strong negative effect on ATP levels induced by the co-treatment with idebenone, rotenone, and dicoumarol was also detected in the three other conditions tested (26 \pm 4% for Hi Glu \rightarrow No Glu, 7 \pm 1% for Gal \rightarrow No Glu, and 26 \pm 7% for Gal \rightarrow Gal) [Figure 23A,C&D].

Similar as in Lo Glu \rightarrow No Glu cells, cells cultivated in galactose were not affected by addition of idebenone, regardless of the medium in which the treatment occurred (105 \pm 8% for No Glu, 95 \pm 2% for Gal). In contrast, cells cultivated in Hi Glu showed susceptibility to idebenone when transferred to glucose-free medium as seen by decreased ATP levels (70 \pm 3%) [Figure 23A]. Addition of rotenone (62 \pm 4%) resulted in an only slightly more pronounced reduction of ATP levels. This was in line with the results obtained in glycolysis-preferring lymphoblastoids where idebenone reduced ATP levels under conditions of low glucose content [Figure 13].

An intriguing finding was observed in galactose-cultivated cells. As anticipated, idebenone rescued ATP levels of rotenone-treated cells; however, the rescue was severely reduced when cells were still incubated in Gal medium (53 \pm 6%) compared to cells transferred in No Glu medium (86 \pm 10%) [Figure 23C&D].

Interestingly, the drop in ATP levels observed in cells co-incubated with idebenone and dicoumarol in cells cultivated in Lo Glu (7 \pm 1%) was observed in cells cultivated in either Hi Glu or Gal medium to a much less prominent extent (56 \pm 1% or 49 \pm 16%, respectively). Strikingly, when Gal medium-cultivated cells were treated in the same medium with both idebenone and dicoumarol, no decrease of ATP levels could be observed (89 \pm 8%) compared to dicoumarol treatment only. These data suggest that a product of glycolysis can prevent idebenone from depleting ATP levels in presence of dysfunctional NQO1. This assumption was further supported by the fact that decrease in ATP mediated by co-incubation of dicoumarol and idebenone was attenuated in cells cultivated in Lo Glu and Hi Glu medium, suggesting that glycolysis and the drop in ATP induced by oxidized idebenone was negatively correlated.

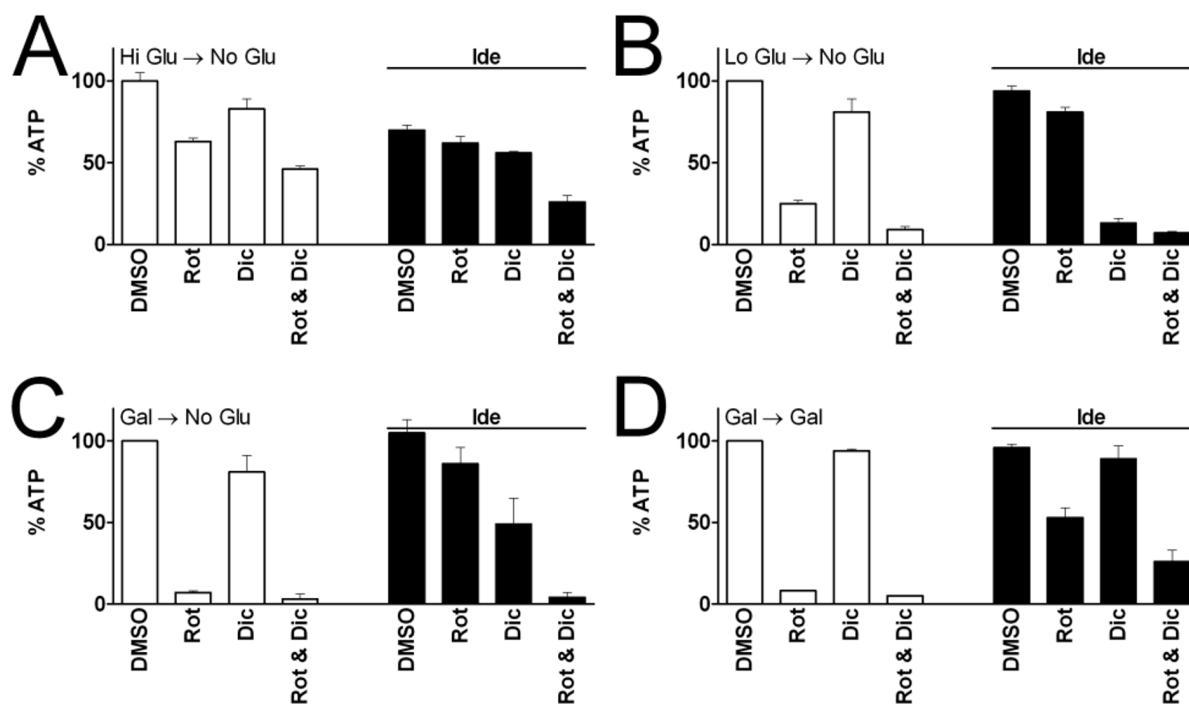


Figure 23: Influence of Media Sugar Content on ATP Rescue by Idebenone.

HepG2 cells were cultivated in medium containing either (A) 4.5 g/l glucose (Hi Glu), (B) 0.3 g/l glucose (Lo Glu), or (C&D) 4.5 g/l galactose (Gal) before medium was replaced by either (A-C) glucose-free medium (NoGlu) or (D) Gal medium. Simultaneously, cells were treated with 6 μM rotenone (Rot), 20 μM dicoumarol or both in the absence (empty bars) or presence (filled bars) of 10 μM idebenone for one h. Bars represent averaged percentage + stdev of two independent experiments.

3.8 Idebenone Reduced ATP Levels in Cells Deficient of NQO1

The NQO1 inhibitor dicoumarol was shown to inhibit the idebenone-dependent ATP restoration after rotenone incubation [Figure 20] and idebenone was demonstrated to interact with NQO1 [Figure 21 and Figure 22]. In addition to the importance of NQO1 for idebenone-mediated ATP rescue, inhibition of NQO1 in cells relying on OXPHOS caused idebenone to reduce ATP by itself [Figure 23]. It thus seemed that NQO1 activity is a pre-requisite for the beneficial effect of idebenone.

This interaction was further elaborated in a publication by our lab [Haefeli *et al.* 2011]. In this study, we demonstrated that the expression of NQO1 positively correlated with the protection of cells from rotenone-mediated energy decrease by idebenone. For example, HEK293 cells were described to be deficient of NQO1 and that this deficiency was in line with the inability of idebenone to rescue ATP levels in presence of rotenone.

The main function attributed to NQO1 for far is its role in detoxification of exogenous or pro-oxidant compounds [O'Brien 1991, Monks *et al.* 1992]. Hence, HEK293 cells are a good model to test the toxicity of exogenous compounds since the pivotal protection by NQO1 is deficient without the use of dicoumarol. HEK293 cells were cultivated in normal growth medium and incubated with 10 μl of idebenone, CoQ₁, CoQ₁₀, or QS-10 for one, 48, or 72 h [Figure 24A]. After 1-h incubation, none of the quinones altered cellular energy status. After 48-h incubation, both idebenone and CoQ₁ decreased ATP levels, however, not significantly (86±10% and 84±19% for idebenone and CoQ₁, respectively, compared to 93±5% for DMSO-treated cells relative to 100±8% of cells treated with DMSO for one h). This tendency toward a decline in ATP levels was not observed for CoQ₁₀ and QS-10 (96±7% and 91±7%, respectively) after 48 h. Again, after 72-h treatment, CoQ₁₀ and QS-10 did not lead to alterations in ATP content (108±9% and 101±10%, respectively, compared to 100±17% for DMSO-treated cells at this time point). In contrast, both idebenone and CoQ₁ reduced ATP levels to 59±5% and 45±2% after three days [Figure 24A].

It was then of interest if this reduction could also be observed in NQO1-deficient HepG2 cells. Since HepG2 cells were demonstrated to have high expression of this enzyme [Haefeli *et al.* 2011], NQO1 was inhibited using 20 μM dicoumarol and ATP levels were analyzed in absence or presence of increasing concentrations of idebenone [Figure 24A]. Otherwise, the setup of the ATP rescue experiments, i.e. the cultivation of cells in medium containing 0.3 g/l glucose and 2% FBS and the treatment of cells in glucose-free medium for one hour before ATP measurement, was maintained. Dicoumarol alone had a slightly reduced ATP levels by 15±6%. In presence of 1 μM idebenone, this reduction was similar (15±7%) [Figure 24A]. However, increasing concentrations of idebenone reduced ATP levels compared to residual levels in a dose-dependent manner (77±14% for 2.5 μM, 74±13% for 5 μM, 70±2% for 7.5 μM idebenone). Using 10 μM idebenone in presence of 20 μM dicoumarol, ATP levels were reduced to 40±6% of residual levels after one hour in glucose-free medium [Figure 24A].

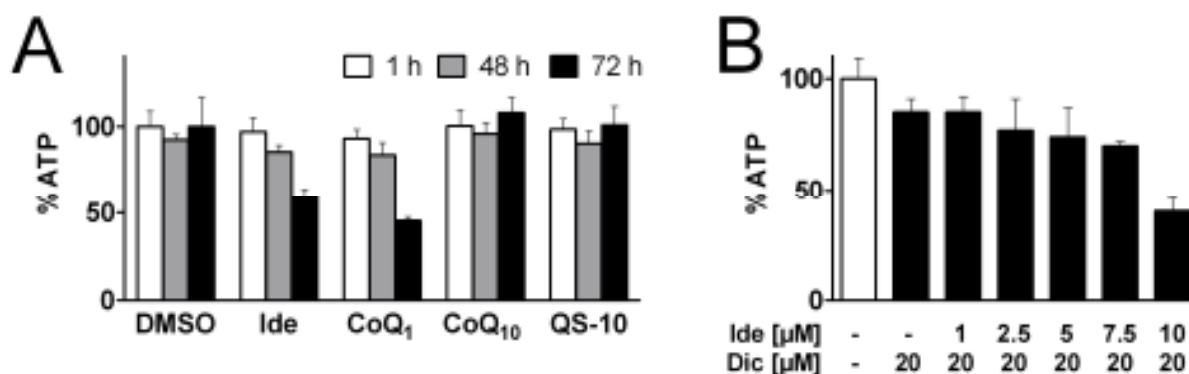


Figure 24: Idebenone and CoQ₁ Reduce ATP Levels in NQO₁-Deficient Cell Lines.

(A) HEK293 cells were cultivated for one (white bars), 48 (grey bars) and 72 (black bars) h in 25 mM glucose-containing medium in the presence of 10 μ M quinones (idebenone (Ide), CoQ₁, CoQ₁₀, and QS-10). ATP levels were normalized to amount of protein before the percentage ATP/protein levels were calculated relative to levels of DMSO-treated cells after 1-h incubation. Bars represent mean + stdev of four individual samples of a typical experiment. (B) HepG2 cells were cultivated in 0.3 g/l glucose-containing medium (Lo Glu) before medium was replaced by glucose-free medium (No Glu) and cells were incubated for one hour with different concentrations of idebenone in the presence of 20 μ M dicoumarol (Dic). Bars represent averaged mean + stdev of triplicates of one typical experiment.

To rule out objections that the idebenone-mediated decrease in ATP levels in presence of dicoumarol was not due to inhibition of NQO₁ but caused by potentially unknown effects of dicoumarol, NQO₁ activity should also be blocked without the use of an inhibitor. Therefore, NQO₁ expression was silenced using short-hairpin RNA (shRNA)-expressing lentiviral particles.

HEK293 and HepG2 cells were transduced with 20 viral particles per cell coding for shRNA against NQO₁ expression. Knock-down of NQO₁ expression was then confirmed using qPCR. HEK293 cells showed only 2.5 \pm 0.4% expression of NQO₁ compared to HepG2 cells [*data not shown*]. Nevertheless, shRNA reduced NQO₁ mRNA levels in HEK293 cells to 38 \pm 3% of basal levels [Figure 25A]. In contrast, HepG2 cells were more reluctant to NQO₁ silencing by shRNA [Figure 25B]. After transduction using 20 viral particles per cell, NQO₁ mRNA levels were still 34 \pm 8% of basal levels.

To further investigate the role of NQO₁ levels on the molecular mechanisms of idebenone, stable clones were selected using puromycin for subjecting them to functional assays. In line with the ratio of gene knock-down, dicoumarol-sensitive reduction of idebenone measured using WST-1 assay was also diminished by approximately a third. Whereas dicoumarol inhibited idebenone reduction in untransduced cells by 66 \pm 4%, dicoumarol was only able to inhibit 38 \pm 8% of idebenone reduction in stable clones expressing shRNA [Figure 25C] indicating that the amount of gene knock-down was comparable to the inhibition of enzymatic activity. Intriguingly, the ability of idebenone to rescue ATP levels in presence of rotenone was not significantly reduced in shRNA-expressing cells [Figure 25D]. Idebenone was capable to restore 70 \pm 11% of ATP depleted by rotenone in untransfected cells which was only slightly higher than the rescue observed in stable clones (59 \pm 6%).

Even though NQO₁ silencing did not substantially reduce the ability of idebenone to rescue ATP levels, it was well in line with results from cells expressing different levels of NQO₁ [Haefeli *et al.* 2011]. Indeed, the correlation between ATP rescue by idebenone in presence of rotenone and NQO₁ mRNA levels could be perfectly integrated in results of experiments with other cells.

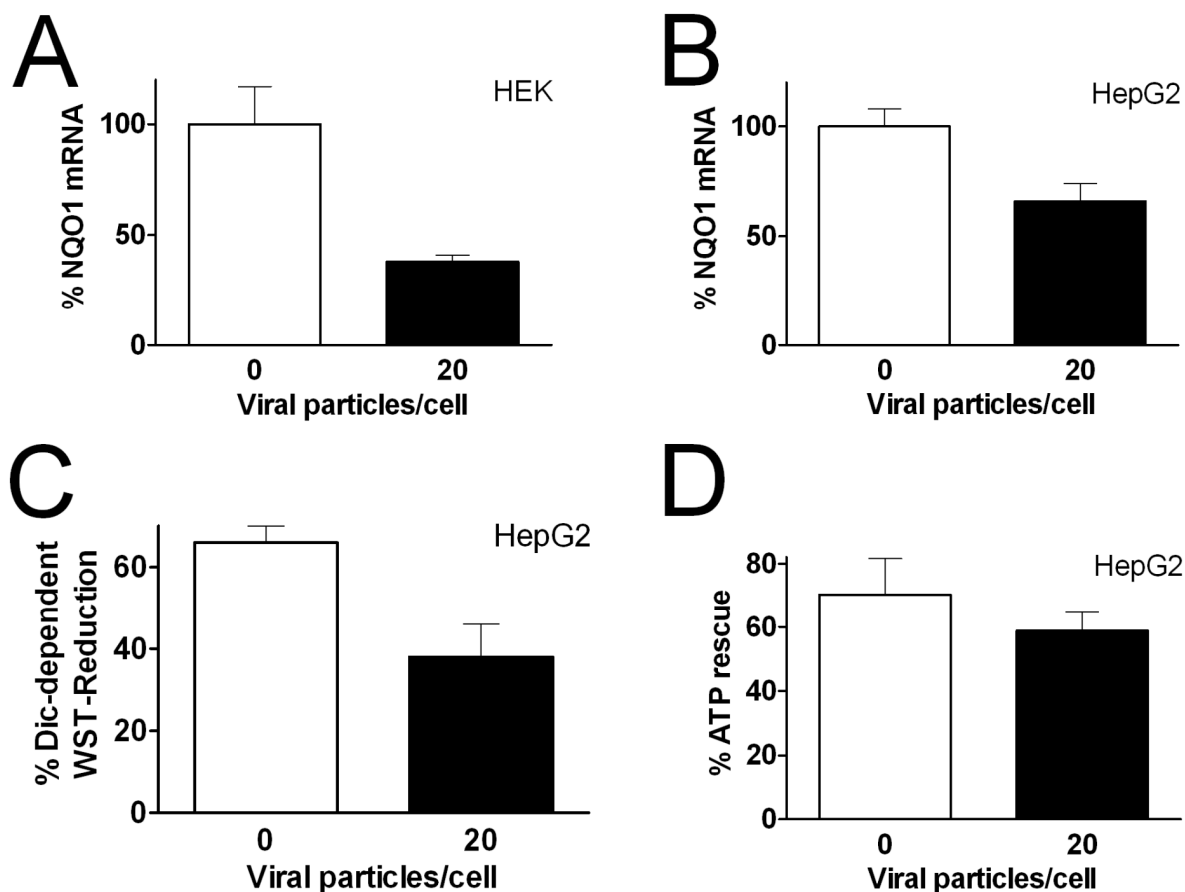


Figure 25: Knock-down of NQO1 Expression using shRNA.

HepG2 and HEK cells were transduced using 20 viral particles coding for NQO1 shRNA per cell. Gene expression of NQO1 in transduced (A) HEK and (B) HepG2 cells was quantified using qPCR with GAPDH as house-keeping gene. (C) Stable clones of transduced HepG2 cells were treated with 6 μM rotenone in presence or absence of 10 μM in glucose-deprived medium. Percentage ATP rescue was defined as the difference between ATP levels of rotenone-treated cells in presence and absence of idebenone relative to the difference between ATP levels of cells in presence and absence of rotenone. (D) WST-1 absorption in presence of 10 μM idebenone was quantified in presence or absence of 20 μM dicoumarol (Dic) in stable clones of untransfected HepG2 cells and HepG2 cells transfected with 20 viral particles per cell. Relative difference between signals in presence and absence of dicoumarol were defined percentage of dicoumarol-dependent WST-1 reduction. Bars represent mean + stdev of (A&B) two individual measurements or (C&D) four six individual measurements from a typical experiment. Data for amount of NQO1 mRNA in HepG2 cells transduced with 50,000x viral particles/well were excluded due to experimental mishandling.

3.9 Interactions of Idebenone with Additional Oxidoreductases

The previous experiments raised the question whether idebenone might be a substrate for additional oxidoreductases [Figure 25B-D]. Furthermore, absence of NQO1 did not lead to an idebenone-mediated depletion of ATP when galactose was abundant [Figure 23]. Since the glycolytic breakdown of galactose itself does not yield ATP, the missing ATP depletion by idebenone in presence of galactose could not be compensated for directly. However, it is likely, that NADH produced by glycolysis could be used to reduce idebenone via an NQO1-independent mechanism.

Oxidoreductases with a potential to reduce idebenone comprise for example NQO2, complex I, electron transfer flavoprotein dehydrogenase (ETFDH), NADH:cytochrome *b5* reductase, and NADPH:cytochrome p450 reductase and these enzymes are inhibited by imatinib, rotenone, pentachlorophenol (PCP), 4-(hydroxymercuri)benzoic acid (HMB), and diphenylene iodonium (DPI), respectively.

Specific inhibitors of the dehydrogenases are an elegant tool for the investigation of the role of these enzymes in idebenone turnover in cells. Unfortunately, since dehydrogenases have similar substrates, the specificity of their inhibitors might be undermined. Thus, to test the specificity of these six aforementioned inhibitors towards NQO1 and NQO2, the sensitivity of NADH or dihydronicotinamide riboside (NRH) turnover, respectively, in presence of CoQ, was detected [Figure 26A&B]. As expected, NQO1 was specifically inhibited by dicoumarol ($99 \pm 3\%$) [Figure 26A]. Intriguingly, the five other compounds tested partially reduced NQO1-dependent NADH oxidation by approximately a third or a fourth. Imatinib and DPI inhibited NQO1 by $23 \pm 5\%$ and $23 \pm 9\%$, respectively, HMB and PCP blocked this dehydrogenase by $28 \pm 7\%$ and $31 \pm 2\%$, respectively. The most potent inhibitor of NQO1 after dicoumarol was rotenone which suppressed its activity by $34 \pm 5\%$ [Figure 26A]. In contrast, NQO2 was inhibited more selectively, since only two of the six inhibitors tested—imatinib and DPI—blocked NRH turnover [Figure 26B]. The NQO2-specific inhibitor imatinib almost totally prevented the oxidation of NRH by NQO2 ($95 \pm 1\%$), whereas DPI inhibited NQO1 by $51 \pm 1\%$.

Thus, these results confirmed that NQO1 and NQO2 are specifically inhibited by dicoumarol and imatinib, respectively. Nonetheless, imatinib also detained NADH oxidation by NQO1. DPI, described as an NADPH:cytochrome p450 reductase inhibitor [McGuire *et al.* 1994], blocked the activity of NQO1 and NQO2 as well. The remaining three inhibitors—rotenone, PCP, and HMB—inhibited NQO1, but to a lesser extent compared to dicoumarol. In contrast, they, as well as dicoumarol, left NQO2 activity totally unaltered.

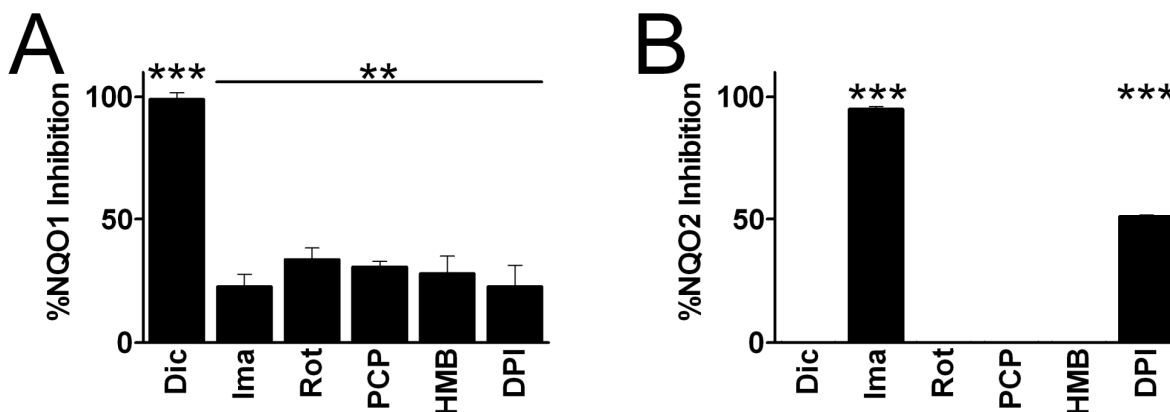


Figure 26: Specificity of Oxidoreductase Inhibitors towards NQO1 and NQO2.

Several dehydrogenase inhibitors (dicoumarol (Dic), imatinib (Ima), rotenone (Rot), pentachlorophenol (PCP), 4-(hydroxymercuri)benzoic acid (HMB), and diphenylene iodonium (DPI)) were tested for their ability to inhibit recombinant (A) NQO1 or (B) NQO2. Bars represent mean + stdev of averaged inhibition of NADH or dihydronicotinamide riboside (NRH) reduction by NQO1 or NQO2, respectively, in the presence of 50 μM CoQ₁ of three individual samples. $p^{**} < 0.01$, $p^{***} < 0.001$; one-way ANOVA with Bonferroni's Multiple Comparison test. HepG2 cells were treated with (C) 10 μM idebenone or (D) 10 μM CoQ₁ in presence of 20 μM dicoumarol, 5 μM imatinib, 6 μM rotenone, 5 μM PCP, 5 μM HMB, or 5 μM DPI. Bars represent mean + stdev of three independent experiments.

Thus, NQO1 was completely inhibited by dicoumarol and slightly inhibited by the rest of the inhibitors employed. Thus, it is important to know to what extent these inhibitors could prevent the reduction of idebenone in cells.

The reduction of idebenone or CoQ₁ in the presence or absence of different oxidoreductase inhibitors was measured using WST-1 assay in HepG2 [Figure 27A&B]. As expected, dicoumarol repressed the reduction of idebenone and CoQ₁ by $66 \pm 4\%$ and $56 \pm 12\%$, respectively. Similarly, quinone reduction was inhibited by DPI ($67 \pm 7\%$ inhibition for idebenone and $83 \pm 10\%$ inhibition for CoQ₁). Despite their ability to inhibit NADH oxidation by recombinant NQO1, imatinib, rotenone, and HMB failed to prevent the reduction of quinones in HepG2 cells. Intriguingly, treatment with PCP emerged in different pictures when idebenone or CoQ₁ was added to cells: whereas PCP did not block the reduction of CoQ₁ ($-2 \pm 5\%$ inhibition), it inhibited reduction of idebenone by $35 \pm 6\%$ [Figure 27A&B]. Thus, it seemed that PCP might selectively interfere with redox reactions concerning idebenone.

Since PCP partially inhibited the reduction of idebenone as measured using the WST-1 assay [Figure 27A], it was of importance to verify if co-incubation with idebenone had a similar effect on ATP levels as the one observed with dicoumarol [Figure 24B]. Indeed, 5 μM PCP reduced ATP levels to $91 \pm 7\%$ of residual levels [Figure 27B] and this negative effect was increased by addition of ascending concentrations of idebenone ($88 \pm 4\%$ for 1 μM , $85 \pm 1\%$ for 2.5 μM , $68 \pm 4\%$ for 5 μM , $49 \pm 8\%$ for 7.5 μM idebenone). Co-incubation of 10 μM idebenone and 5 μM PCP even led to the reduction of ATP levels to $18 \pm 4\%$ of residual levels after one hour in glucose-free medium [Figure 27C].

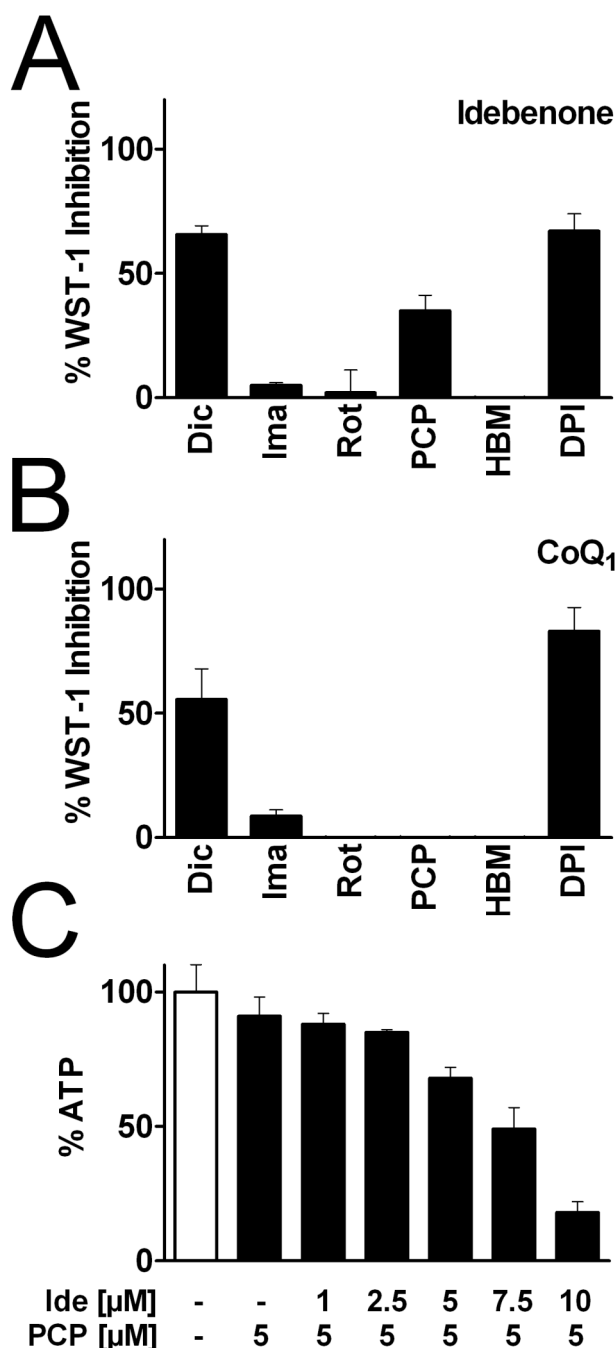


Figure 27: Pentachlorophenol Selectively Inhibits Reduction of Idebenone.

HepG2 cells were treated with (A) 10 μM idebenone or (B) 10 μM CoQ₁ in presence of 20 μM dicoumarol (Dic), 5 μM imatinib (Ima), 6 μM rotenone (Rot), 5 μM pentachlorophenol (PCP), 5 μM 4-(hydroxymercuri)benzoic acid (HMB), or 5 μM diphenylene iodonium (DPI). Inhibition of reduction of the quinone was measured using WST-1. Bars represent mean + stdev of three independent experiments. (C) HepG2 cells were cultivated in 0.3 g/l glucose-containing medium (Lo Glu) before medium was replaced by glucose-free medium (No Glu) and cells were incubated for one hour with different concentrations of idebenone in the presence of 5 μM pentachlorophenol (PCP). Bars represent averaged mean + stdev of triplicates of one typical experiment.

PCP inhibited the reduction of idebenone but not of CoQ₁ or other related quinones in HepG2 cells. To rule out the possibility that this effect was specific to HepG2 cells or to CoQ₁, the same experiment reported in Figure 27A&B was expanded by including different cells and further quinones [Figure 28]. A similar pattern was detected in human fibroblasts (C₂ and C₃), human primary myoblasts (2Te), and rat myoblastoids (L6): PCP only inhibited the reduction of idebenone whilst it had no influence on the redox reaction of the remaining quinones. These data raised the question if idebenone was a substrate of a PCP-sensitive oxidoreductase which did not interact with related quinones at all.

Furthermore, the experiments showed that reduction of all employed quinones—i.e. idebenone, CoQ₆, CoQ₁₁, QS-10 and decylQ—was preferably inhibited by dicoumarol and DPI. This was in line with reports of Tan and Berridge [2010] who reported that WST-1 assay is sensitive to both inhibitors. They explained the efficacy of DPI

to decrease WST-1 signal by its function as inhibitor of the plasma membrane electron transport chain which is exploited to transfer electrons from hydroquinones within cells to WST-1 in the supernatant.

Rotenone and HBM did not interfere with quinone reduction at all, whereas imatinib caused minor limitation of quinone turnover. Differences between decylQ and remaining quinones could be explained in regard to In comparison with the other quinones, reduction rates of decylQ were marginal in all cells used [data not shown], especially in HepG2 [Figure 22B]. Addition of oxidoreductase inhibitors could not restrict decylQ conversion; since reduction of decylQ was nearly absent in these cells *per se* [Figure 28].

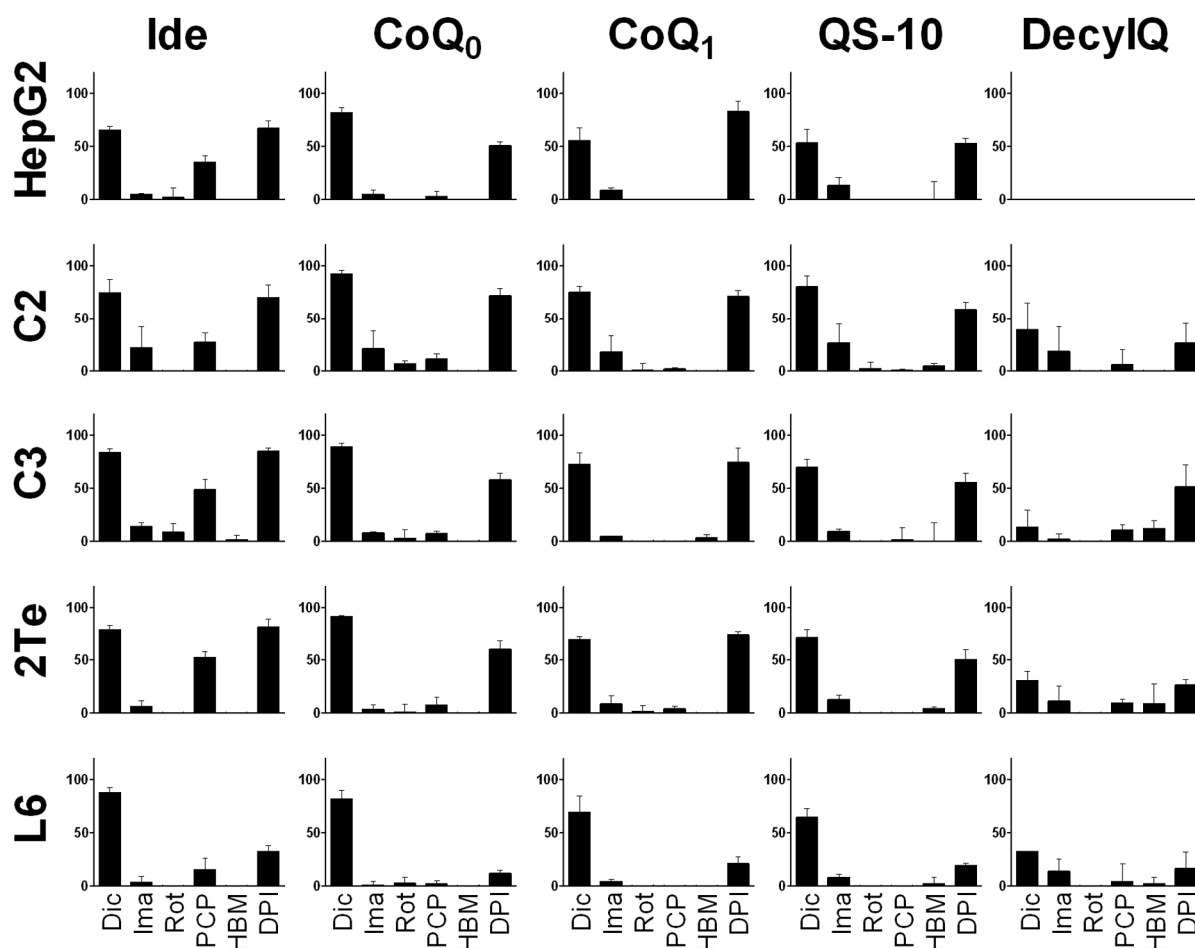


Figure 28: Reduction of Quinone Is Diversely Inhibited by Different Inhibitors, in Different Cells and in Presence of Different Quinones.

Quinone reduction was measured using WST-1 assay. The percentage of WST-1 signal inhibition induced by dehydrogenase inhibitors dicoumarol (Dic; 20 μ M), imatinib (Ima; 5 μ M), rotenone (Rot; 6 μ M), pentachlorophenol (PCP; 5 μ M), 4-(hydroxymercuri)benzoic acid (HBM; 5 μ M), or diphenylene iodonium chloride (DPI; 5 μ M) was assessed in presence of idebenone (ide), CoQ₀, CoQ₁, QS-10, and decylQ at a concentration of 10 μ M. The assay was performed in a human hepatic cell line (HepG2), human fibroblasts (C2 and C3), human primary myoblasts (2Te), and rat myoblasts (L6). Bars represent mean + stdev of at least three independent experiments.

PCP selectively inhibited the reduction of idebenone *in vitro* [Figure 28]. In a study of Šimkovič and Frerman [2004], PCP was described to inhibit ETFDH and idebenone was reported to be a good substrate for this enzyme. Similarly, they demonstrated that CoQ₁ and decylQ, two quinones whose reduction was not inhibited by PCP [Figure 28], were also converted by this oxidoreductase. Even though they assessed the enzyme-substrate interaction not in cellular systems but using recombinant enzyme, the fact that idebenone was one electron acceptor of ETFDH among others compromised the chance of finding an idebenone-specific mode of action. Nevertheless, ETFDH, which links fatty acid metabolism to the ETC, was an interesting target to take a closer look at.

If the inhibition of idebenone reduction by PCP was essentially due to blocking of ETFDH, knock-down of this enzyme should produce similar results as PCP addition. Therefore, small interference RNA (siRNA) was used to knock-down ETFDH. The employed siRNAs against ETFDH were not validated to knock-down transcription *in vitro*, but were selected for their potential efficacy *in silico* [information by manufacturer]. For this reason, two different siRNAs against ETFDH were applied; either in combination or by themselves. For NQO₁, whose knock-down by siRNA was included in this set of experiments, validated siRNA was available.

The best conditions for gene knock-down in HepG2 cells were established preliminary using siRNA for glycerol-3-phosphate dehydrogenase (GAPDH) silencing. Knock-down was quantified using an assay measuring

the conversion of NAD^+ to NADH by GAPDH. In these experiments, a concentration of 30 nM siRNA showed the best results in the trade-off of silencing GAPDH and minimizing cytotoxicity [data not shown].

Efficacy of gene knock-down was assessed using WST-1 assay with idebenone as electron acceptor [Figure 29]. Whereas negative siRNA had no influence on WST-1 signals ($104 \pm 14\%$ of basal absorption), siRNA to knock down NQO1 decreased idebenone reduction to $88 \pm 2\%$, indicating that gene silencing via siRNA was not as strong as anticipated. In contrast, addition of 20 μM dicoumarol diminished idebenone reduction by $37 \pm 4\%$. This inhibition is slightly weaker than the one observed in previous experiments ($67 \pm 4\%$) [Figure 28]. Nonetheless, the inhibition by PCP ($15 \pm 3\%$) amounted to half of that by dicoumarol in both experiments.

In contrast, transfection of HepG2 cells with siRNA against ETFDH did not inhibit idebenone reduction at all [Figure 28]: neither did transfection with single siRNA decrease WST-1 signal ($103 \pm 5\%$ for siRNA ID# 14819 and $109 \pm 9\%$ for #113116), nor did the combination of both siRNAs ($105 \pm 9\%$).

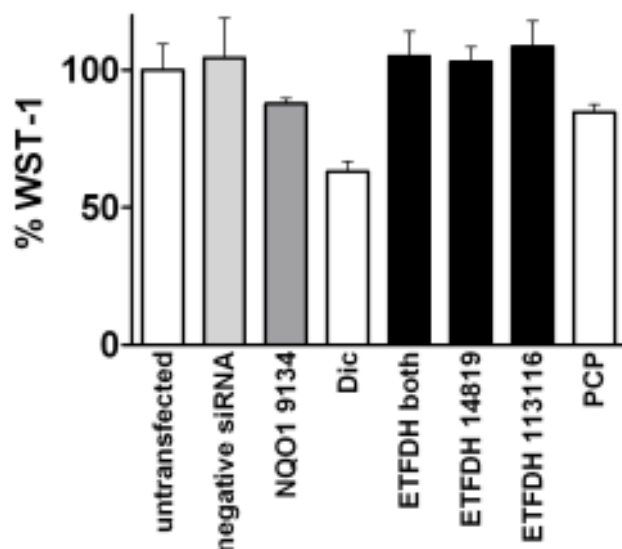


Figure 29: Knock-Down of ETFDH Expression Using siRNA.

HepG2 cells were transfected with 30 nM siRNA in order to silence ETFDH by reverse transcription; NQO1 and non-sense negative siRNA was used as control. Gene silencing was measured using WST-1 assay in presence of 10 μM idebenone. Cells were transfected with two variants of ETFDH siRNA (#14819 and #113116) or the combination thereof (black bars), negative siRNA (light grey bar) or NQO1 siRNA (#9134; grey bar). Untransfected cells (empty bars) were treated with 20 μM dicoumarol or 5 μM pentachlorophenol (PCP) as negative control. Bars represent mean + stdev of five to six individual measurements from a typical experiment.

Since PCP was described to be an inhibitor of ETFDH [Šimkovič and Frerman 2004] and PCP selectively inhibited idebenone reduction [Figure 27 and Figure 28], the question arose if idebenone contrary to CoQ_1 accepts electrons from ETFDH. Even though this question was already affirmed by Šimkovič and Frerman in experiments using recombinant enzyme [2004], confirmation of this interaction in cells was preferable. In these experiments [Figure 29], however, siRNA failed to knock down ETFDH as detected by functional analysis and thus, a functional interaction between idebenone and ETFDH in living cells could not be verified yet. Therefore, to investigate the role of ETFDH in the redox metabolism of idebenone in cells, experiments following an indirect path were conducted.

ETFDH shuttles electrons derived during β -oxidation of fatty acids into the ETC. Thus, if the inhibition of idebenone reduction by PCP occurred at the site of ETFDH, inhibition of β -oxidation—which is upstream of ETFDH—would also lead to a decreased reduction rate of idebenone. Therefore, two inhibitors of β -oxidation—3-mercaptopropionic acid (MPA) [Wang *et al.* 2010] and valproic acid (VPA) [Coudé *et al.* 1983]—were employed in WST-1 assay experiments where PCP showed efficacy to block the actions of idebenone [Figure 27 and Figure 28]. Both 2 μM MPA and 1 mM VPA did not decrease WST-1 signal ($-3 \pm 10\%$ and $-5 \pm 1\%$, respectively) [Figure 30C]. As a control, 5 μM PCP inhibited idebenone reduction by $30 \pm 0\%$ which is in line with previous experiments.

Thus, it seemed that ETFDH was not responsible for the drop in WST-1 signal when PCP and idebenone were co-incubated. Nonetheless, to refute a potential influence of ETFDH on the reduction of idebenone in living cells, another functional assay dependent on the reduced form of idebenone was employed. Since dicoumarol inhibits idebenone reduction and idebenone-mediated ATP restoration in presence of rotenone, PCP was suggested to prevent ATP rescue as well. If ETFDH was responsible for donating electrons to idebenone in this experimental setup, then blocking β -oxidation and thereby the source of electrons for ETFDH would also disable the capacity of idebenone to protect ATP content from rotenone-mediated energy depletion.

As anticipated, ATP rescue by idebenone in presence of rotenone was inhibited by 5 μM PCP ($7 \pm 1\%$ instead of $60 \pm 2\%$) [Figure 30B]. In line with their inability to reduce idebenone in WST-1 assay, the inhibitors of β -oxidation did not markedly decrease idebenone's capacity to rescue ATP levels from rotenone-mediated energy

failure ($67\pm 31\%$ for MPA, $47\pm 6\%$ for VPA, and $54\pm 16\%$ for SA). Thus, ETFDH was refuted as a target for idebenone in these experimental setups.

PCP did not only inhibit the reduction of idebenone [Figure 27 and Figure 30A], but also prevented the idebenone-mediated restoration of ATP levels after their depletion by rotenone [Figure 30B]. Since the inhibition of quinone reduction by PCP was limited to idebenone and ATP rescue seemed dependent on the reduced forms of quinones [Figure 20], it was likely that PCP inhibited ATP rescue mediated by idebenone but not by other quinones. Indeed, whereas PCP almost completely blocked the capacity of idebenone to counteract rotenone-induced ATP drop ($7\pm 1\%$), a substantial ATP rescue was observed when CoQ₁ was co-incubated with rotenone and PCP ($34\pm 24\%$) [Figure 30B]. As positive controls, ATP rescues by idebenone and CoQ₁ in the presence of rotenone only ($60\pm 2\%$ and $66\pm 14\%$) were in line with previous experiments. Similarly, when idebenone was replaced with $10\ \mu\text{M}$ CoQ₁₀, QS-10, or decylQ, the drop in ATP levels was not observed as well [*data not shown*].

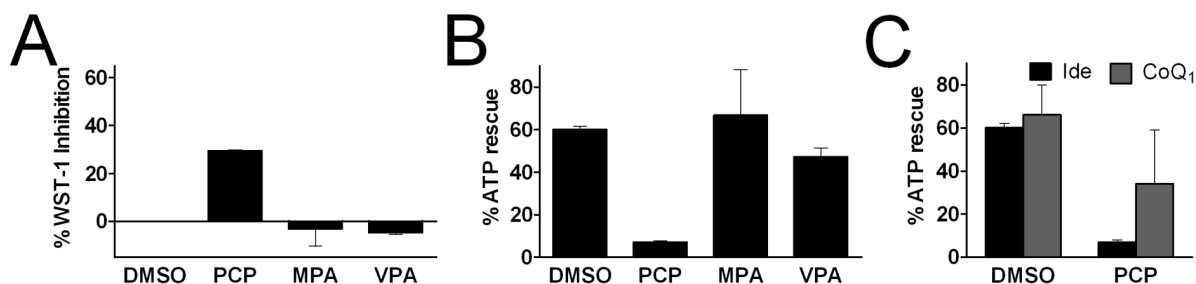


Figure 30: Inhibition of Idebenone-Mediated ATP Rescue by Pentachlorophenol Is Not Linked to β -Oxidation.

Pentachlorophenol (PCP; $5\ \mu\text{M}$) and two inhibitors of β -oxidation 3-mercaptopropionic acid (MPA; $2\ \mu\text{M}$) and valproic acid (VPA; $1\ \text{mM}$) were tested for their ability to inhibit (A) NQO₁-dependent reduction of idebenone as measured using WST-1 assay or (B) idebenone-mediated ATP rescue in presence of $6\ \mu\text{M}$ rotenone. Bars represent mean + stdev of duplicates from a typical experiment. (C) HepG2 cells were cultivated in medium containing low glucose concentrations before deprivation of glucose in presence of $6\ \mu\text{M}$ rotenone (Rot) and $5\ \mu\text{M}$ pentachlorophenol (PCP) for one hour. Simultaneously, $5\ \mu\text{M}$ idebenone (black bars) or CoQ₁ (grey bars) were added to cells. Percentage ATP rescue is defined as the compound-dependent increase of ATP in presence of rotenone relative to rotenone-induced ATP drop. Bars represent mean + stdev of duplicates from one experiment.

3.10 Potential Benefits from ATP Rescue in Disorders with Deficient Complex I

These data suggested that idebenone might be beneficial to cellular energy status under conditions where (i) complex I is dysfunctional and (ii) idebenone can be reduced. Therefore, one could assume that idebenone rescues ATP levels in cells bearing a mutation in a subunit of complex I which is the case in cells from LHON, Leigh syndrome or Kearns-Sayre syndrome.

Thus, the ability of idebenone to rescue ATP content in presence of rotenone was investigated in lymphoblastoid cell lines of LHON patients [see 2.1.2] and patients suffering from Leigh syndrome and Kearns-Sayre syndrome. Even though these cell lines featured a mutation in a subunit of complex I, they did not exhibit reduced basal levels of ATP when deprived of glucose [*data not shown*]. Hence, the suitability of these cell lines as a model for complex I deficiency was questionable. In glucose-deprived medium, 1-h incubation with $1\ \mu\text{M}$ rotenone decreased ATP levels to zero in all cell lines. Addition of $10\ \mu\text{M}$ idebenone to rotenone-treated cells failed to rescue ATP levels and this finding was also observed in three lymphoblastoid cell lines from healthy donors [*data not shown*]. Nevertheless, this failure of idebenone to ameliorate energy status of complex I-deficient lymphoblastoid cells could be explained by the generally low NQO₁ expression in lymphoblastoid cell lines [*personal communication by D. Robay*]. This confirmed the importance of the reduction of idebenone in order to improve cellular ATP production.

Another disorder characterized by dysfunctional mitochondrial respiration is called *mitochondrial encephalomyopathy, lactic acidosis and stroke-like episodes* (MELAS) [see 2.1.1]. Mitochondria of lymphoblastoid cells from MELAS patients were transferred into a mitochondria-depleted cell with cancerous nuclear background, thus generating so-called cybrids which hold the advantages of immortality and MELAS-specific mitochondria. MELAS and wild-type (WT) cybrids were a kind gift from M. Hirano and M. Davidson and cultivated in galactose-containing challenge medium which forced them to use mitochondria to produce energy.

In MELAS cells, low levels of ATP synthesis and excess lactate production were described [Pallotti *et al.* 2004]. The observed excess lactate is largely a result of increased glycolysis to maintain sufficient energy levels under conditions of defective OXPHOS. The reason for producing lactate is to regenerate NAD⁺ levels which were utilized in the initial steps of glycolysis. Without sufficient NAD⁺, glycolysis cannot proceed. Since quinone-dependent rescue of ATP levels under conditions of impaired complex I [Figure 18D] and NQO₁-dependent metabolism is described to increase NAD⁺/NADH ratio [Dragan *et al.* 2006], the role of quinones on cellular metabolism in cybrids harboring either WT mitochondria or mitochondria from MELAS patients were of interest.

Intriguingly, ATP levels in MELAS cybrids did not increase after 1-h incubation with idebenone [*data not shown*], despite reports of impaired complex I [James *et al.* 1996, Sarnat and María-García 2005, Sarasman *et al.* 2008, and Davidson *et al.* 2009]. Unlike the situation where acute short-term incubation with quinones increased ATP levels after rotenone challenge in HepG2 cells [Figure 18D], MELAS cells did not show increased

ATP levels after 48-hour treatment with idebenone or CoQ₁ [Figure 31A]. In contrast, there was a trend of slightly decreased ATP levels in presence of idebenone (87±17%) or CoQ₁ (84±12%) compared to DMSO-treated MELAS cybrids (100±21%), even though these changes did not reach statistical significance. In presence of 10 µM dicoumarol, this trend towards decreased ATP levels was abolished (106±24% and 94±8% for idebenone and CoQ₁, respectively). In WT cybrids, idebenone did not alter ATP content in presence or absence of dicoumarol (106±6% and 100±17%, respectively). Strikingly, a statistically significant drop in ATP levels was observed after 48-h incubation with CoQ₁ (51±11%) which was reversed by addition of dicoumarol (94±11%) [Figure 31A].

Even though idebenone and CoQ₁ did not restore ATP levels in rotenone-treated MELAS cybrids, an amelioration of energy production was observed in these cells. Mitochondrial impairment in MELAS led to a decrease in mitochondrial membrane potential: after two-day incubation in galactose-containing challenge medium, $\Delta\Psi_m$ was slightly lower in MELAS cybrids (85±17%) compared to WT cybrids (100±11%) [Figure 31B]. Strikingly, both idebenone and CoQ₁ substantially increased $\Delta\Psi_m$ in this experimental setup (146±26% and 120±20%, respectively) [Figure 31B]. CoQ₁₀ and QS-10—two quinones which failed to restore ATP levels in rotenone-treated HepG2 cells [Figure 20]—did not influence $\Delta\Psi_m$ (80.3±15.2% and 78.8±23.9%). Thus, these results were in line with previous experiments in healthy cell lines with rotenone-mediated complex I deficiency. In WT cybrids which contained functional mitochondria, none of the quinones led to alteration of [Figure 31B]; a result which observed in human fibroblasts before [Figure 12A].

Idebenone and CoQ₁ strengthened $\Delta\Psi_m$ of MELAS cybrids, but this beneficial effect could not be utilized by the cells to increase ATP content. The question then arose how this profitable effect of idebenone and CoQ₁ could manifest in an amelioration of cellular metabolism. Impairment of mitochondrial energy production forces MELAS cells to produce ATP via glycolysis. This process is maintained by the production of lactate which accounts for pathological symptoms described in MELAS [Kaufmann *et al.* 2004, Davidson *et al.* 2009]. It was therefore of interest, if quinones might influence lactate production.

As also reported by Davidson *et al.* [2009] who generated the MELAS cybrids used in our lab, these cells had markedly increased lactate levels (46.3±1.5 mM/mg protein) compared to WT cybrids (11.5±0.6 mM/mg) [Figure 31C]. In WT cybrids, lactate levels remained unchanged after 48-h treatment with idebenone (13.5±1.0 mM/mg), QS-10 (12.3±0.5%), or CoQ₁₀ (12.0±0.8%). In line with the massive drop in ATP levels upon 48-h treatment [Figure 31A], CoQ₁ doubled the amount of lactate production under these conditions (22.7±2.9 mM/mg) [Figure 31C].

Interestingly, both idebenone and CoQ₁ effectuated a statistically significant decrease in lactate production in MELAS cybrids (35.3±5.0 mM/mg and 19.8±2.1 mM/mg, respectively) [Figure 31C]. In contrast, neither CoQ₁₀ nor QS-10 altered extracellular lactate concentrations of MELAS cybrids (53.8±6.7 mM/mg and 49.0±5.7 mM/mg, respectively). In a subsequent experiment, the lowering of lactate levels by idebenone and CoQ₁ was confirmed (reduction to 54.2±5.1 mM/mg and 46.0±6.9 mM/mg from 74.6±16.5 mM/mg in sham-treated MELAS cybrids, respectively) [Figure 31D]. Strikingly, this reduction was significantly abrogated by inhibition of NQO1: in presence of dicoumarol, lactate production in MELAS cells was not substantially altered by idebenone (67.4±5.2 mM/mg) or CoQ₁ (59.8±7.3 mM/mg) [Figure 31D].

Thus, increased mitochondrial activity of MELAS cells induced by idebenone and CoQ₁—as manifested in the elevation of $\Delta\Psi_m$ —could actually be utilized to reduce lactate production in MELAS cybrids. As a consequence, overall ATP content did not change, but the production of lactate, the toxic byproduct to maintain glycolysis under conditions of impaired OXPHOS, could be substantially reduced by both idebenone and CoQ₁.

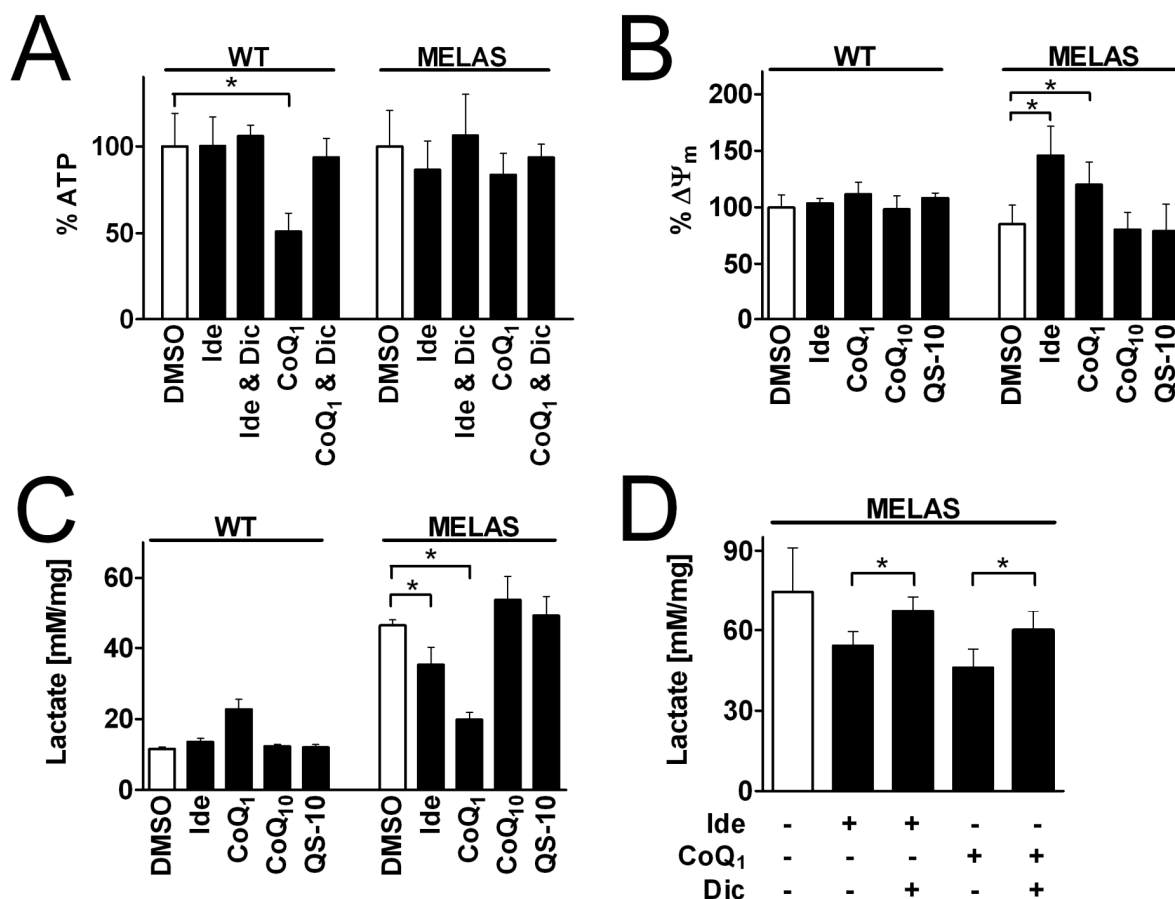


Figure 31: Effect of Quinones on Mitochondrial Membrane Potential and Lactate Production in MELAS Cybrids. (A) Effect of quinones (10 μ M) on ATP levels in wild-type (WT) and MELAS cybrid cells was assessed after two-day incubation in galactose-containing challenge media for in the presence or absence of dicoumarol (10 μ M). Data depict one typical experiment out of three and each data point represents the mean + stdev of four individual dishes. (B) Cells were cultivated in galactose-containing challenge media for two days in the presence or absence of quinones (10 μ M). Mitochondrial membrane potential ($\Delta\Psi_m$) in cybrids was measured after two-day treatment with 10 μ M quinones using TMRM. Bars represent mean + stdev of four separate wells of a typical experiment as relative percentage compared to TMRM/protein in DMSO-treated WT cybrids. (C) Quinones (10 μ M) were added to WT and MELAS cybrids for two days before lactate was measured in the supernatant and standardized to protein content. Data depict one typical experiment out of three and each data point represents mean + stdev of three individual wells. (D) Co-incubation with dicoumarol (10 μ M) partially reverses the drop of lactate levels induced by 10 μ M idebenone or CoQ₁. Extracellular lactate levels were standardized to protein content. Bars represent mean + stdev of four separate dishes within a typical experiment. $p^* < 0.05$; Student t-test $p^* < 0.05$; Student t-test.

3.11 Toxicological Analyses of Idebenone and Related Quinones

Despite the beneficial shift in energy production in MELAS cybrids induced by idebenone and CoQ₁, the latter also reduced ATP levels in WT cybrids which relied on mitochondrial ATP generation [Figure 31A]. Idebenone and CoQ₁ also decreased ATP levels in OXPHOS-dependent cells with dysfunctional NQO1 [Figure 13 and Figure 24]. These detrimental effects of the two quinones were in line with previous studies reporting that idebenone and CoQ₁ inhibit mitochondrial complex I function [Sugiyama *et al.* 1985, Degli Esposti *et al.* 1996, Briere *et al.* 2004, Fato *et al.* 2008, and Rauchová *et al.* 2008].

Even though the observed reductions of ATP content by idebenone were only visible under conditions forcing cells to use mitochondrial activity for energy production, it was of interest to see if idebenone or other quinones have detrimental effects on energy-consuming cellular functions such as proliferation. Therefore, BC₁ lymphoblastoid cells which display a high proliferation rate were treated with quinones over an extended period and the rates of population doublings were calculated. This cell line also bore the advantage of very low NQO1 expression [*personal communication by D. Robay*], making them potentially more susceptible to toxicity induced by quinones.

Proliferation rates were calculated as cumulative cell doubling (CCD) which is defined as sum of exponential growth. In a scatter plot depicting CCD vs. time, immortalized cell lines with a steady cell growth follow a perfect line as seen for DMSO-treated lymphoblastoid cells (9.7 \pm 1.5 CCD after 18 days) [Figure 32]. In agreement with effects on ATP levels, 10 μ M idebenone reduced CCD (5.1 \pm 1.2 CCD after 18 days), reaching statistical significance after seven days ($p^* < 0.05$; and $p^{***} < 0.001$ after ten days). Upon treatment with 10 μ M CoQ₁, lymphoblastoid cells died after four days [Figure 32A]. Likewise, reflecting previous experiments demonstrating that 10 μ M CoQ₁₀ or QS-10 had no negative effect on cellular energy production [Figure 13 and Figure 24A],

both compounds did not affect cumulative cell doubling either (10.2 ± 0.7 CCD and 9.6 ± 1.7 CCD after 18 days, respectively) [Figure 32A].

At a concentration of $10 \mu\text{M}$, idebenone impaired proliferation of lymphoblastoid cells. This harmful effect of idebenone, however, was dependent on the dose applied: lower concentrations of idebenone did not substantially alter proliferation rates (7.6 ± 1.6 CCD at $2 \mu\text{M}$ idebenone and 8.0 ± 0.8 CCD at $5 \mu\text{M}$ idebenone after 18 days, respectively) [Figure 32B].

Similar results were also observed in primary human myoblasts (4TE) cultured in aneural medium where $10 \mu\text{M}$ idebenone led to a drastic decrease in growth already after ten days [C]. Whereas DMSO-treated myoblasts showed linear proliferation with a 7.5 ± 0.6 CCD after 21 days, increasing concentrations of idebenone reduced proliferation (4.1 ± 0.7 CCD at $2 \mu\text{M}$ idebenone, 4.7 ± 0.5 CCD at $5 \mu\text{M}$ idebenone, and 1.7 ± 0.8 CCD at $10 \mu\text{M}$ idebenone). Since these cells had intermediate levels of NQO1 expression, the observed effect could not solely be attributed to the oxidized form of idebenone.

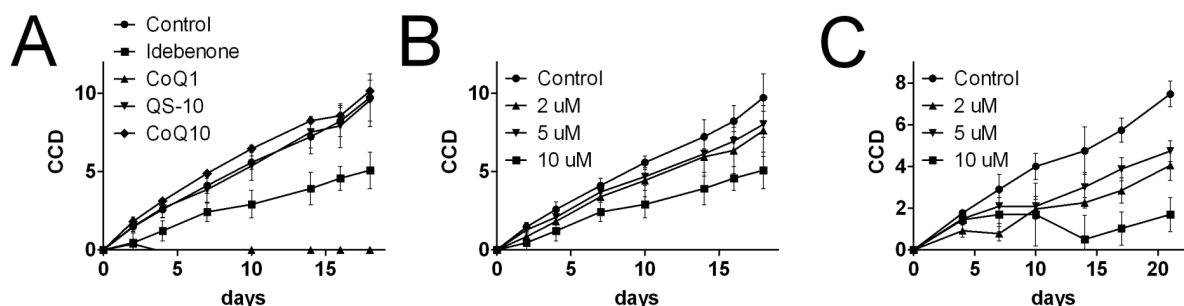


Figure 32: Alteration of Cumulative Cell Doubling by Different Quinones.

Lymphoblastoid (A&B) or human 4TE myoblast (C) cells were treated with $10 \mu\text{M}$ DMSO, idebenone, CoQ_1 , CoQ_{10} or QS-10 (A) or different concentrations of idebenone (B&C; 0, 2, 5, and $10 \mu\text{M}$). Every second to fourth day, cells were counted to calculate cumulative cell doubling rates (CCD) and to re-seeded at a density of $500,000$ cells/ml (lymphoblastoids) or $20,000$ cells/ml (myoblasts). Values represent mean \pm stdev of triplicates of cumulative cell doubling rates (CCD).

3.12 Idebenone Influences Akt-1 Status

Despite the abundance of NQO1 in primary 4TE myoblasts which is supposed to elevate the reduced form of idebenone [Merker *et al.* 2007], it could still not be ruled out that the decrease in proliferation induced by high concentrations of idebenone in these cells [Figure 32] was associated with a potential pro-oxidative effect of idebenone. One possible target, which integrates metabolism, proliferation and anti-apoptotic pathways, is Akt-1/protein kinase B (PKB). Akt-1 does not only directly inhibit apoptosis by phosphorylation of apoptosis-inducing factor B-cell lymphoma (Bcl) 2/BclX antagonist (BAD), but it also activates transcription factors such as members of the Forkhead (FoxO) family or the nuclear factor $\kappa\beta$ (NF- $\kappa\beta$) which in turn promote the expression of survival genes [Hanada *et al.* 2004]. Strikingly, beside anti-apoptotic agents such as growth factors, oxidative stress also activates Akt-1 by inducing a phosphorylation event at serine (Ser) 473 [Higaki *et al.* 2008, Nishimoto *et al.* 2010].

Western blot analysis of Akt-1 protein in human 4TE primary myoblasts revealed that neither $10 \mu\text{M}$ idebenone treatment for three days, $100 \mu\text{M}$ H_2O_2 stress for 30 min immediately before lysis, or a combination thereof had any influence on total Akt-1 protein levels⁴ [Figure 33]. Intriguingly, when SDS, a strong detergent was added to the lysis buffer an additional band at 73 kDa instead of 64 kDa was observed despite the use of a rather selective antibody against Akt-1 [Figure 33] [personal communication by M. Erb and D. Robay]. The fact that the shift of approximately 9 kDa resulted in a distinct band rather than a smear suggested that this higher molecular weight form of Akt-1 was post-translationally modified, for example by covalent attachment to small ubiquitin-like modifier (SUMO). Phosphorylation would increase the molecular weight of the protein in a lesser extent, whereas ubiquitination or glycosylation would lead to a smear in western blot analysis. Interestingly, in DMSO-treated cells, the 73 kDa band showed an over 15-fold higher signal than the 63 kDa band. Furthermore, three-day incubation with $10 \mu\text{M}$ idebenone substantially reduced the 73 kDa species by approximately 20-fold. This finding combined with the reduced proliferation observed in idebenone-treated 4TE myoblasts [Figure 32] proposes that idebenone reduces a modification necessary for Akt-1-mediated proliferation.

However, H_2O_2 completely inhibited the signal of the 73 kDa band, which suggests that the potential proliferating action of Akt-1 is reduced under oxidative stress. Indeed, H_2O_2 -mediated phosphorylation of Akt-1 at Ser473 was rather linked to anti-apoptotic pathways than cell proliferation, since pre-treatment with H_2O_2 was described to make cells less susceptible latter stress [Nishimoto *et al.* 2010]. Therefore, a potential pro-oxidative effect of idebenone on Akt-1 was anticipated to manifest in phosphorylation at Ser473 site. Therefore, the phosphorylation status of the site was analyzed using a phospho-specific antibody [Figure 33]. Since the same

⁴ Akt-1 was reported to have a molecular weight of 56-60 kDa according to the manufacturer of the antibody but manifested as 64 kDa protein. However, since GAPDH ran at a higher position than expected as well (39 kDa instead of 36 kDa), it rather seemed that the protein marker was running too quickly under the buffer conditions used.

membrane was used a second time for this antibody, the background signal was higher (as observable in the differences between the first two (overlay and phospho-Akt) and latter two (Akt-1 and GAPDH) detail sections in Figure 33), and unspecific bands slightly below the expected position emerged. As anticipated, phosphorylation of Akt-1 at Ser473 was increased after 30-min H₂O₂ treatment. This effect was independent of pre-treatment with either idebenone or DMSO. Idebenone itself did not increase Ser473 phosphorylation of Akt-1.

Taken together, these findings indicated that long-term idebenone treatment had a weaker effect on Akt-1 than acute H₂O₂ treatment. Whereas short-term addition of H₂O₂ resulted in phosphorylated Akt-1 and completely prevented the modification resulting in a 9 kDa heavier protein, three-day incubation with idebenone was not able to phosphorylate Akt-1 and reduced, but did not fully block, the 73 kDa band. Despite the lack of phosphorylation at Ser473, it can not be ruled out that idebenone could still act as a mild pro-oxidant given the strong reduction of modified Akt-1.

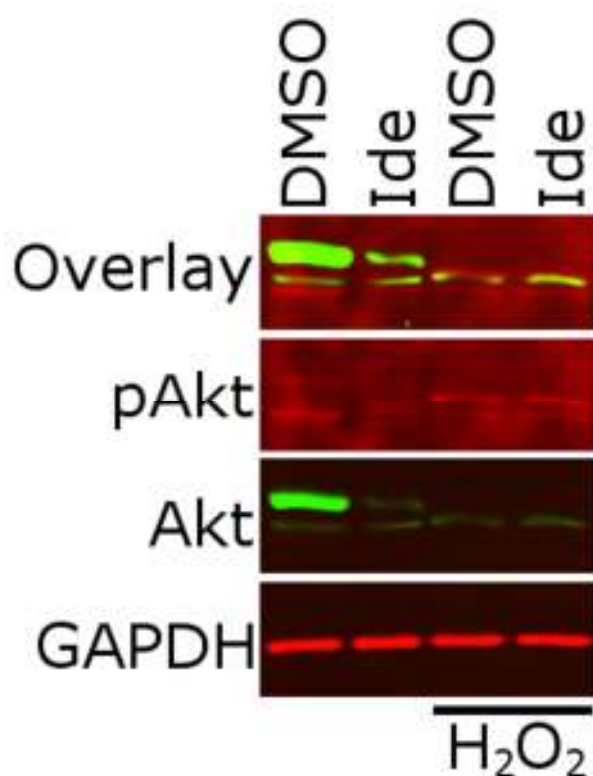


Figure 33: Idebenone Decreases Modification of Akt-1.

Primary 4TE myoblasts were treated with 10 μ M idebenone for three days in aneural medium before half of the cells were subjected to 100 μ M H₂O₂ for 30 min. Total Akt-1 protein levels were determined in a Western blot using GAPDH protein levels for normalization. In a subsequent step, a serine 473 phosphorylation-specific Akt-1 (pAkt) antibody was used on the same membrane.

Thus, the dependence of pro-oxidant properties on quinone toxicity was elaborated further using cells with high (HepG2), intermediate (4Te) and low (HEK293, SH SY5Y) levels of NQO1 [Haefeli *et al.* 2011 and personal communication by D. Robay], wherein extent of DNA damage promoted by 24-hour incubation with 10 μ M quinones in normal growth medium was investigated. Therefore, the percentage of cells positive for immunochemical staining against a phosphorylated histone, γ H₂AX, which indicates DNA double strand breaks, was counted. HepG2 cells showed a high basal level of γ H₂AX-positive cells (25%) compared to HEK293, SH SY5Y, and 4Te cells (4%, 2%, and 0.5%, respectively) [Figure 34A-D]. In HepG2 cells, impact of quinones on DNA damage levels was rather marginal: both idebenone and QS-10 showed no substantial alteration in γ H₂AX-positive cells (22% and 26%, respectively), whereas CoQ₁ slightly increased DNA damage (33%) and CoQ₁₀ even led to a decrease in of γ H₂AX signal (16%) [Figure 34A]. In contrast, CoQ₁ elicited high genotoxicity in the two cell lines with low NQO1 levels, HEK293 and SH SY5Y, as seen in the massive elevation of γ H₂AX-positive cells (34% and 10%, respectively) [Figure 34B&C]. In these two cell lines, idebenone and CoQ₁₀ did not alter γ H₂AX-positive cell number. In contrast, QS-10 elevated the number of γ H₂AX-positive cells to 14% in HEK293, but not SH SY5Y cells. [Figure 34B&C]. In a primary human 4Te myoblasts, idebenone slightly increased DNA damage-positive nuclei to 1.2% [Figure 34D]. The highest, approximately four-fold increase of DNA double strand breaks was seen in CoQ₁-treated cells (2.0%). As seen before, CoQ₁₀ and QS-10 did not alter the frequency of γ H₂AX-positive cells (0.5 and 0.7%, respectively) [Figure 34D]. A similar picture was detected in primary human fibroblasts. After 72-hour incubation with 10 μ M quinones, only fibroblasts treated with CoQ₁ were positive for

the nuclear DNA damage marker $\gamma\text{H}_2\text{AX}$, while for all other quinones, including idebenone, no increase above basal levels could be detected [Figure 34B].

Contradictory to previously stated assumptions that CoQ_1 would exhibit pro-oxidant effects in cells whose NQO1 levels are too low to detoxify the compound, CoQ_1 induced genotoxicity regardless of NQO1 expression levels in cells. Thus, promotion of DNA double strand breaks by CoQ_1 must be regarded as independent of its role in energy metabolism.

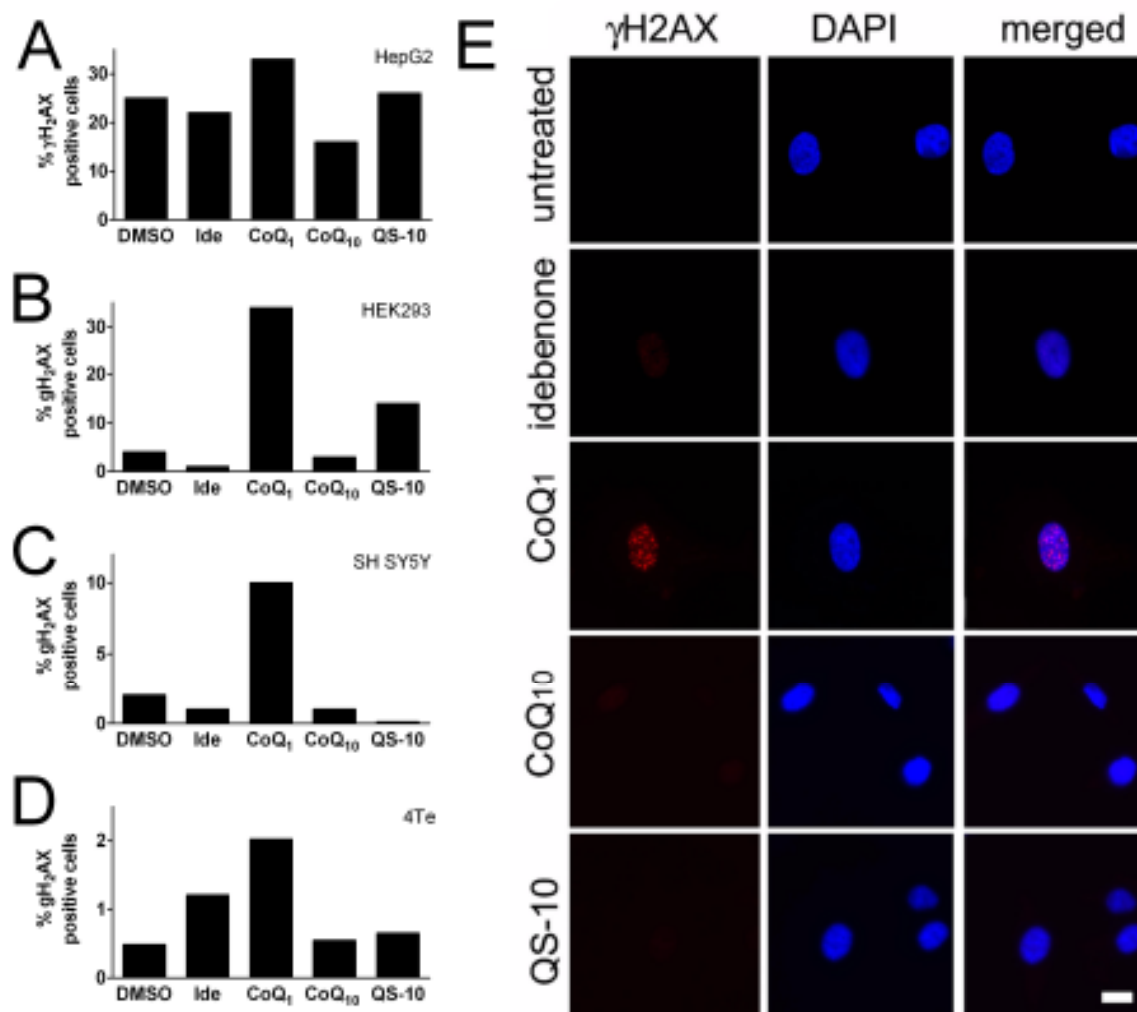


Figure 34: CoQ_1 Elicits DNA Damage Regardless of NQO1 Content.

DNA double strand breaks were stained using $\gamma\text{H}_2\text{AX}$ in (A) HepG2, (B) HEK293, (C) SH-SY5Y, and (D) 4Te cells cultured in normal growth medium. After 24-h incubation with 10 μM quinones, cells were fixed and stained against the DNA damage marker $\gamma\text{H}_2\text{AX}$. More than thousand cells per condition were counted manually for each condition and $\gamma\text{H}_2\text{AX}$ -positive cells were expressed as percentage of the total number of cells counted (stained using DAPI). (E) Human primary fibroblasts were incubated for 72 h with quinones (10 μM) under ambient conditions before cells were fixed and stained against the DNA damage marker $\gamma\text{H}_2\text{AX}$ (red). DAPI dye was used as nuclear counter stain (blue). Scale bar: 10 μM .

In addition to these data, a pro-oxidative function for some short-chain quinones such as idebenone was discussed [Degli Esposti *et al.* 1996, Lenaz *et al.* 2002, Genova *et al.* 2003, Lenaz *et al.* 2007, and Fato *et al.* 2008]. These authors suggested that idebenone and other short-chain quinones inhibited the electron transport from NADH to CoQ_{10} via complex I, but not from NADH to molecular oxygen. Thus, the pro-oxidant effect of idebenone was mainly attributed to its complex I-inhibiting characteristics. Therefore, potential adverse effects had to be assessed.

Pro-oxidative agents harm cells by demolishing their macromolecules such as proteins, DNA, or lipids. Even though idebenone was described to reduce lipid peroxidation after toxic insults *in vitro* and *in vivo* [Suno and Nagaoka 1989a&b, Suno *et al.* 1989, Cardoso *et al.* 1998, Mordente *et al.* 1998, and Abdel Baki *et al.* 2010], it was of interest if exposure to quinones could lead to increased lipid peroxidation. Therefore, human fibroblasts were incubated for three days with 10 μM quinone before the magnitude of lipid peroxidation was assayed using the fluorescent dye BODIPY. Not surprisingly, 72-h incubation with 10 μM idebenone alone did not increase lipid peroxidation in human fibroblasts ($98 \pm 2\%$) [Figure 35A]. Long-term effects on lipid peroxidation induced by other benzoquinones were investigated as well. Similar to idebenone, CoQ_{10} did not alter the degree of oxidative damage of the membrane at all ($97 \pm 2\%$). In contrast to idebenone, CoQ_1 elevated lipid peroxide levels after

three days to 176% of DMSO-treated cells. Similarly, CoQ₀ caused a massive, 2.5-fold increase in lipid peroxidation (254%) [Figure 35A].

Since quinones are redox active compounds, it was of interest to observe how they behave under conditions of elevated ROS levels. These conditions were induced by short-term addition of H₂O₂ to the cells. The reduced form of quinones, in particular idebenone, is thought to be oxidized by ROS and thereby attenuating oxidative damage [Germonel *et al.* 2002]. However, one-electron reduction of quinones gives rise to semiquinones which could in turn act to generate ROS [Monks *et al.* 1992]. Therefore, human myoblasts were pretreated with 10 μM quinone and the fluorescent dye CM-H₂DCFDA for 15 min before 10 μM H₂O₂ was added for another 15 min [Figure 35B]. Idebenone and its metabolite QS-10 both slightly aggravated this rapid oxidative damage by increasing the H₂O₂-induced fluorescence signal by 115±10% and 120±8% (mean±SEM), respectively. Interestingly, CoQ₁₀ did not substantially prevent ROS levels (95±6%). In contrast, CoQ₀, an agent otherwise described to induce ROS itself, reduced H₂O₂-induced ROS by 30±2% [Figure 35B]. Even though 10 μM idebenone slightly exacerbated ROS levels after addition of H₂O₂, lower concentrations of idebenone showed antioxidant effects [Figure 35C]. Indeed, idebenone reduced H₂O₂-induced ROS levels in a dose-dependent manner: as little as 100 pM idebenone reduced ROS levels by 12±3% (mean±SEM) and this antioxidant amelioration augmented with increasing concentrations reaching 34±3% at 1 μM idebenone [Figure 35C].

In conclusion, idebenone might have a mild pro-oxidant effect; however, this property of idebenone was not able to induce genotoxic damage or lipid peroxidation.

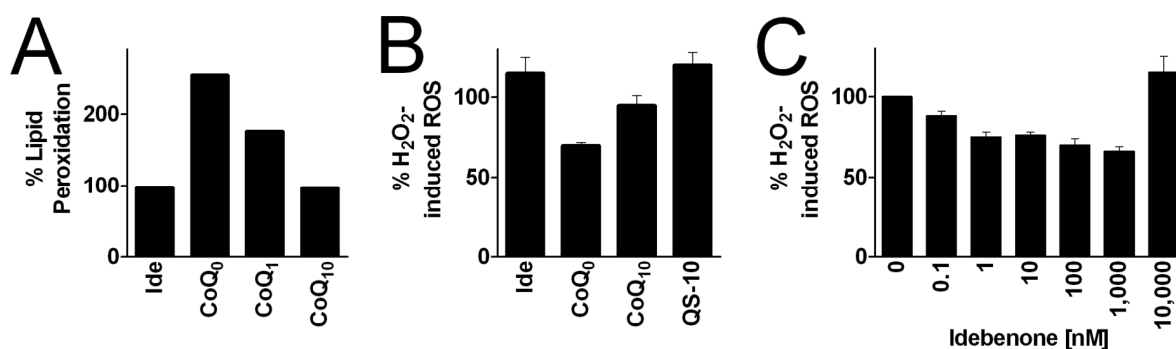


Figure 35: Quinones Affect ROS Levels Differently.

(A) Human fibroblasts were treated with 10 μM quinones for 72 h, before amount of lipid peroxidation was measured using the fluorescent dye BODIPY. Changes in fluorescence signal were calculated as percentage of values from DMSO-treated cells. In human 4TE myoblast cells, CM-H₂DCFDA fluorescent dye was co-incubated with (B) 10 μM different quinones or (C) different concentrations of idebenone for 15 min before 10 μM H₂O₂ was added for another 15 min. Bars represent (A) mean of two independent experiments or (B&C) mean + SEM of two to 15 independent experiments.

3.13 Idebenone Protects Cells from Oxidative Stress-Induced Cell Death

Idebenone had thus elicited negative effects on ATP levels [Figure 24B] and proliferation [Figure 32] in NQO1-deficient cells. However, in cells expressing significant levels of NQO1, idebenone improved resistance against energy failure induced by complex I inhibitor rotenone [Figure 15] and idebenone also reduced toxic lactate production in MELAS cybrids [Figure 31]. This is in line with a number of reports describing the rescue from cell death of exogenously stressed cells by idebenone [Yerushalmi *et al.* 2001, Gumprich *et al.* 2002, Jauslin *et al.* 2002, 2003, and 2007, Gil *et al.* 2003, and Chapela *et al.* 2008]. The authors of these reports mostly accounted a potential antioxidant effect of idebenone for averting the destruction. Therefore, idebenone-mediated survival after strong oxidative damage induced by an exogenous pro-oxidant was assessed.

When human lymphoblastoid cells were subjected to radiation-induced DNA damage after two-day cultivation, idebenone reduced cell death observed two days after radiation [*personal communication by M.F. Lavin, Queensland Institute of Medical Research, Australia*]. The same regime was selected for studying the effect on survival by idebenone with the exception that H₂O₂ was employed as stressor. Experiments were conducted in rat L6 myoblasts, since they expressed high levels of NQO1 [*personal communication by D. Robay*]. After two-day cultivation in normal growth medium, the medium was with 200 μM H₂O₂ in PBS replaced for 30 min, before old medium was restituted again. Idebenone (10 μM) was added at different time points relative to the stress. Two days after the toxic insult, survival was assayed using two fluorescent dyes which exploited the loss in membrane integrity found in dead cells. The cell-permeable calcein exhibits green fluorescence upon cleavage by cytosolic esterases. The red ethidium homodimer binds to DNA but is not able to cross membranes. Thus, red nuclei represented dead cells, whereas green cell bodies stained living cells.

As anticipated, PBS-treated control cells showed no signs of cell death or even impaired proliferation; the cells developed their characteristic spindle-shaped form regardless of the presence of idebenone in the medium [Figure 36]. In contrast, a majority of cells subjected to H₂O₂ treatment were dead 48 h after pro-oxidant exposure. The same result was observed when 10 μM idebenone was added to the cells at 30 min or 24 h after stress. In contrast, when cells were pre-treated with 10 μM idebenone either 1 or 24 h prior to H₂O₂ stress the number of surviving cells substantially increased [Figure 36], indicating a protective effect of idebenone on

survival. However, the morphology of cells still alive differed dramatically from cells not subjected to H_2O_2 treatment: instead of the normal elongated spindle shape they appeared rounded up, suggesting that the cells were in a vulnerable condition. Nevertheless, the survival of total cells by pre-treatment with idebenone was impressive. When idebenone was administered simultaneously with H_2O_2 , however, the rescue was even more pronounced for cells were not only almost completely protected from cell death but they also showed normal morphology [Figure 36].

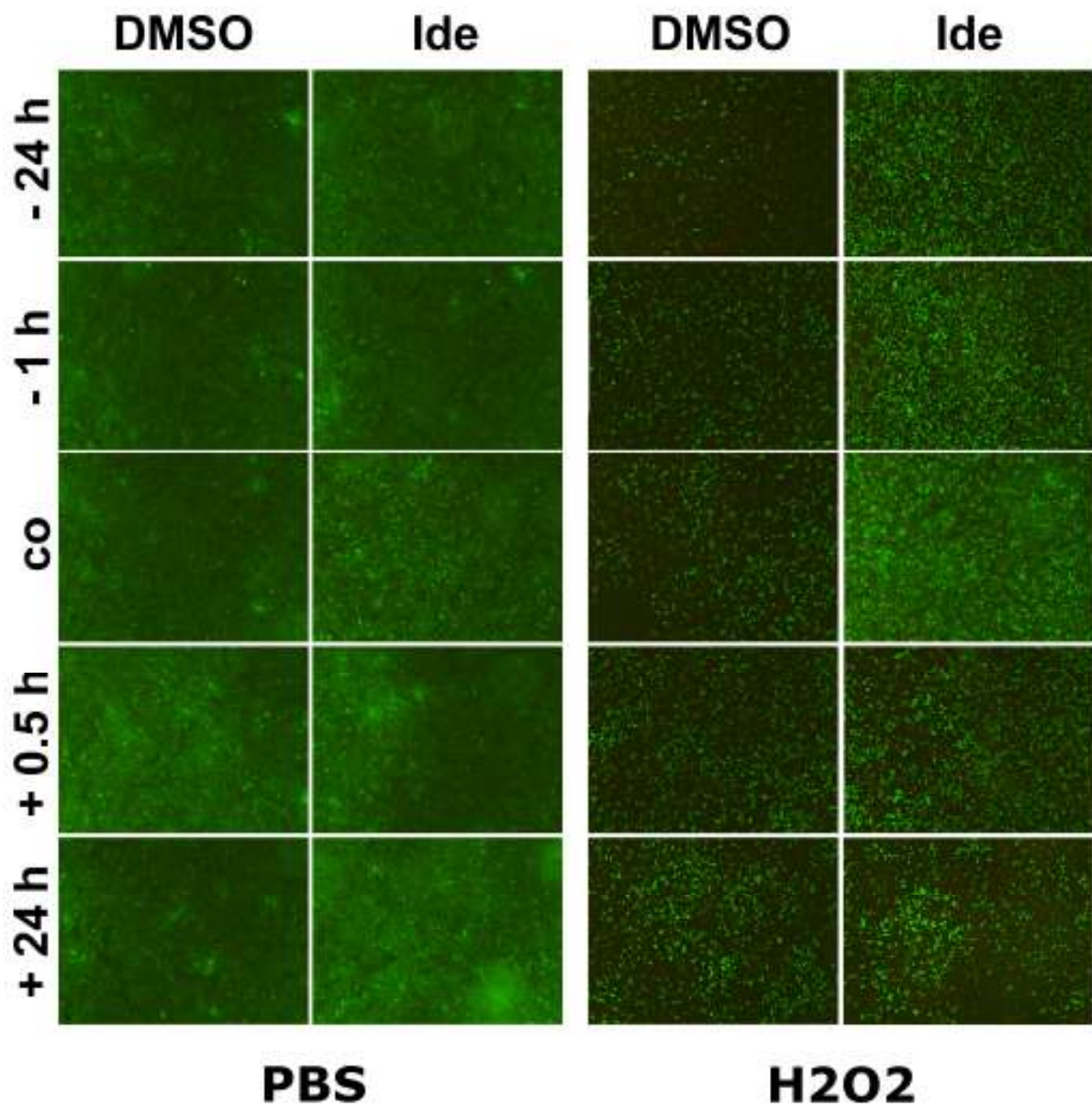


Figure 36: Pre-Treatment with Idebenone Increases Survival of Myoblastoids after Hydrogen Peroxide Stress.

L6 myoblasts were treated with DMSO or 10 μ M idebenone either one (-1 h) or 24 h (-24h) prior, simultaneously to (co), or 30 min (+0.5 h) or 24 h (+24h) after a 30-min stress with PBS or H_2O_2 . Cells were allowed to recover in the previous medium for 48 h after the stress, before cells were stained for survival. Calcein (green) labeled living cells, whereas ethidium homodimer (red) was used to tag dead cells. Scale bar: 500 μ M.

The observation of idebenone-mediated protection against cell death induced by H_2O_2 was then also quantified by calculating the percentage of living cells relative to the total amount of cells. In absence of idebenone, the percentage survival amounted to nearly 50% after cells were stressed for 20 min by H_2O_2 [Figure 37A]. When 10 μ M idebenone was added after H_2O_2 treatment, similar proportions of viable cells were observed (50 \pm 15% and 50 \pm 12% when idebenone was added six or 24 hours after stress, respectively). As observed under the microscope [Figure 36], pre- and co-treatment of idebenone with H_2O_2 led to an increase in cell survival [Figure 37A]. Pretreatment with idebenone elevated survival with statistic significance (78 \pm 8% (**p < 0.01) and 75 \pm 6% (*p < 0.05) when idebenone was added 24 or one hour prior to H_2O_2 shock, respectively). Intriguingly, simultaneous administration of idebenone and H_2O_2 led to only 72 \pm 13% viable cells, despite the clearly visible protection observed under the microscope [Figure 36]. This surprisingly low proportion could be partially explained by the relatively higher area which was covered by morphologically healthy cells.

In fibroblast subjected to 15-min H_2O_2 treatment, idebenone concentrations lower than $10\ \mu\text{M}$ showed a much better antioxidant effect [Figure 35C]. Thus, a dose dependency of idebenone on cell survival was of interest as well. In contrast to the short-term antioxidant effect in fibroblasts, dilution of idebenone did not increase its capacity for protection [Figure 37B]. On the contrary, the proportion of surviving cells gradually decreased with descending concentrations. When cells were pre-treated with idebenone 24 h before treatment with H_2O_2 , a concentration of $3.33\ \mu\text{M}$, $1.11\ \mu\text{M}$, or $0.37\ \mu\text{M}$ idebenone solely amounted for $72\pm 4\%$, $70\pm 3\%$, or $63\pm 6\%$ survival, respectively, in contrast to $51\pm 9\%$ survival in absence of idebenone [Figure 37B].

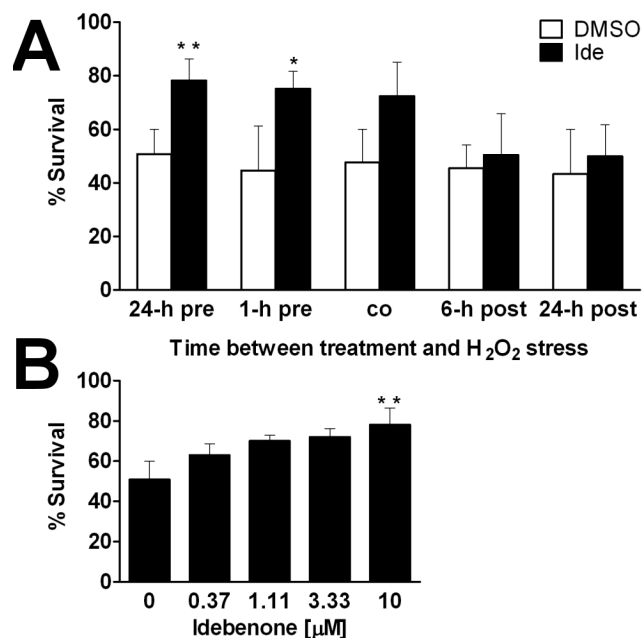


Figure 37: Survival of Rat Myoblasts after Hydrogen Peroxide Stress.

Cultured rat L6 myoblasts were seeded in 96-well plates in normal growth medium. After 48 h, cells were treated with $200\ \mu\text{M}$ H_2O_2 in PBS for 30 min before cells were allowed to recover in the medium they were cultivated seeded in before H_2O_2 shock for additional 48 h. Percent Survival was calculated as percentage of live cells relative to the sum of live and dead cells as detected using the fluorescent dyes calcein and ethidium homodimer. (A) Cells were treated with $10\ \mu\text{M}$ idebenone at different time points (one or 24 h before or six or 24 h after H_2O_2 shock, or simultaneously with H_2O_2 shock). $p^* < 0.05$, $p^{**} < 0.01$, two-way ANOVA with Bonferroni's Multiple Comparison tests. (B) Cells were pretreated with different concentrations of idebenone ($0.37 - 10\ \mu\text{M}$) 24 h prior to H_2O_2 shock. $p^{**} < 0.01$, one-way ANOVA with Bonferroni's Multiple Comparison test.

The surprising finding that contrary to all other combinations tested, co-treatment of idebenone and H_2O_2 over the short period of 30 min protected cells almost completely from toxicity could be attributed to a potential direct interaction of these two compounds. In this scenario idebenone would directly interact and detoxify H_2O_2 outside the cell, so that in essence the cells are not exposed to H_2O_2 at all. To investigate this possibility, a redox-sensitive dye, CM- H_2DCFDA , was employed for investigating this issue. First, the proper detection of H_2O_2 by CM- H_2DCFDA was analyzed. In a cell-free assay, $2.45\ \text{M}$ H_2O_2 yields a 10-fold higher fluorescence than PBS control [Figure 38A]. This high concentration was used, since lower concentrations—as the one employed for the survival assays ($200\ \mu\text{M}$)—did not detectably alter dye fluorescence [*data not shown*]. Second, a potential perturbing interference of idebenone with the dye was excluded, since idebenone did not change CM- H_2DCFDA fluorescence at the henceforward used concentrations [Figure 38A].

Surprisingly, but consistent with the observation from cell based assays, increasing concentrations of idebenone markedly reduced the H_2O_2 -mediated oxidation of CM- H_2DCFDA [Figure 38B]. At an approximately 25 million-fold molar excess of H_2O_2 in comparison to idebenone ($10\ \mu\text{M}$), the quinone suppressed the fluorescence signal to nearly half of control, which implies a catalytic mode of action.

Since its quinone ring is already fully oxidized, classical chemistry would suggest that idebenone could solely be oxidized at the hydroxyl group of the alkyl tail. Hence, if the reduced fluorescence was the result of direct oxidation of idebenone at its primary alcohol group by H_2O_2 , both decylQ and QS-10 would not be converted by H_2O_2 , since decylQ lacks the primary alcohol moiety and the corresponding carbon of QS-10 is already fully oxidized. However, both decylQ and QS-10 behaved similarly as idebenone in this assay [Figure 38B]. To exclude involvement of the two methoxy substituents at the quinone ring, the plastoquinone analogs of idebenone (SNT₂₁₀₄₈₆) and decylQ (SNT₂₁₀₂₀₁), in which the methoxy groups are interchanged by methyl groups were also tested and again showed no deviant characteristics.

Another H_2O_2 -sensitive dye, MitoSOXTM Red mitochondrial superoxide indicator or MitoSOX in short, was used to eliminate artifacts derived by a putative interaction between idebenone and CM- H_2DCFDA . Again, the same results were obtained with this chemically different dye [Figure 38C].

An interesting finding is the velocity of the reaction between quinone, H_2O_2 and dye. If one assumed that oxidation of the dye under the experiment's conditions was irreversible, an accumulation of fluorescence signal

over time would occur in sham-treated samples. Not only was that the case for the controls, but also for quinone containing samples [data not shown]. In addition, the reduced fluorescence signal of quinone-treated samples in contrast to controls abated after prolonged incubation as well [Figure 38D], suggesting that the interaction between quinone and H_2O_2 could decelerate, but not prevent the total oxidation of dye.

Chemically, these findings were challenging to discuss, since there is no reasonable mechanism by which an oxidized quinone and H_2O_2 could interact. Nonetheless, these results suggest that idebenone is able to detoxify H_2O_2 in solution and that therefore, a protection during co-treatment of idebenone and H_2O_2 —even at an approximately 10,000-fold lower concentration than used in this assay—cannot be attributed to cellular mechanisms but possibly cell-independent interactions of these compounds in the medium. Thus, the increased survival of rat myoblastoids observed when idebenone and H_2O_2 were added to cells simultaneously [Figure 36] has been dismissed for further experiments investigating the cellular causes for prevention of cell death.

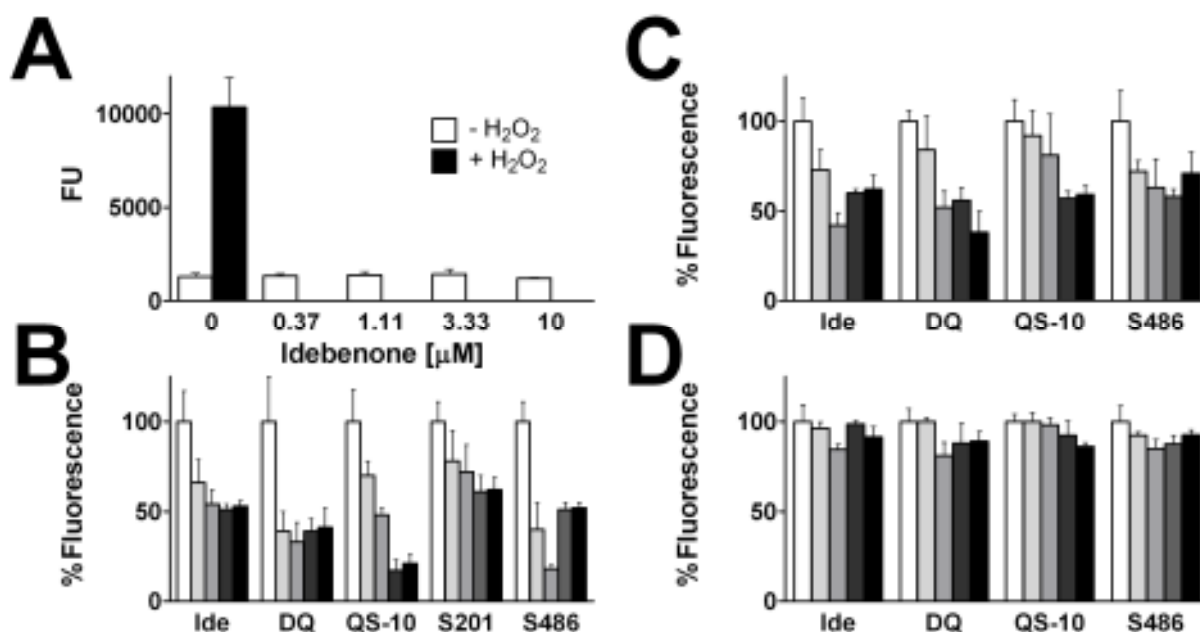


Figure 38: Idebenone Reduces Hydrogen Peroxide in Solution.

H_2O_2 causes oxidation of redox-active fluorescent dyes such as CM- H_2 DCFDA (1.7 μ M) and MitoSOX (1 μ M). (A) Treatment with 2.45 M H_2O_2 (black bar) massively increases fluorescence signal from CM- H_2 DCFDA; whereas idebenone (white bars) does not interact with the dye. Bars represent mean \pm SD of four simultaneous measurements. (B) Different quinones such as idebenone (ide), decylQ (DQ), QS-10 as well as two plastoquinone derivatives produced in-house, SNT₂₁₀₂₀₁ (S201) and SNT₂₁₀₄₈₆ (S486); reduce the ability of H_2O_2 to oxidize CM- H_2 DCFDA in a dose dependent manner. (C) Consistently, the same result was observed with MitoSOX as fluorescent dye after 1 min. (D) After 10 min, the reaction was completed. Fluorescence signal was normalized to the control (white bars) and the concentrations used were 0.37 μ M (bright grey), 1.11 μ M (grey), 3.33 μ M (dark grey) and 10 μ M quinone (black bars). Bars represent mean \pm SD of three to six (0 and 10 μ M quinone) simultaneous measurements.

It was then of interest if the cell survival mediated by pre-treatment with idebenone in NQO1-expressing L6 myoblasts was mediated by an antioxidant effect or by ameliorating a potential decrease in ATP induced by H_2O_2 . Treatment with 10 μ M idebenone for 30 h did not affect ATP levels in 25 mM glucose-containing medium ($101.6 \pm 3.0\%$ compared to $100.0 \pm 7.5\%$ in DMSO-treated cells) [Figure 39A]. Interestingly, neither did the incubation with 200 mM H_2O_2 for up to 30 min, when ATP levels were measured immediately after this stress. However, when cells were allowed to recover for 30 min in the medium they were incubated with before the stress after 30-min incubation with 200 mM H_2O_2 , ATP levels dropped to $11.3 \pm 0.3\%$ and did not improve if time for recovery was prolonged to six h ($12.4 \pm 9.6\%$). In cells pretreated with idebenone, ATP levels also decreased to $7.7 \pm 1.3\%$ after 30-min recovery. However, after 6-h recovery following 30 min of H_2O_2 stress, ATP levels were rescued to $73.9 \pm 13.0\%$ only when cells were pretreated with idebenone [Figure 39A].

Since H_2O_2 is a potent pro-oxidant, it is conceivable that idebenone reduces oxidative damage induced by H_2O_2 via an antioxidant mechanism [Figure 39B]. Indeed, ROS levels were increased already after 1-min incubation with H_2O_2 by $55.4 \pm 13.2\%$, and after 5 min, ROS levels were doubled ($201.8 \pm 26.5\%$ compared to $100.0 \pm 7.9\%$ in untreated cells). After 10 min, a plateau of a four-fold increase in ROS was achieved ($403.7 \pm 93.8\%$), which was also detectable after 30 min ($415.1 \pm 18.3\%$). Pre-treatment with 10 μ M idebenone dramatically protected from this short-term increase in ROS: up to 20-min incubation with H_2O_2 , idebenone prevented an increase in ROS ($104.5 \pm 8.7\%$). After 30 min, however, ROS levels were doubled ($203.0 \pm 51.9\%$); an effect observed after as little as five minutes in cells not pre-treated with idebenone. Interestingly, cells which were allowed to recover after the 30-min stress with H_2O_2 showed less oxidative damage than cells not distressed by H_2O_2 [Figure 39B].

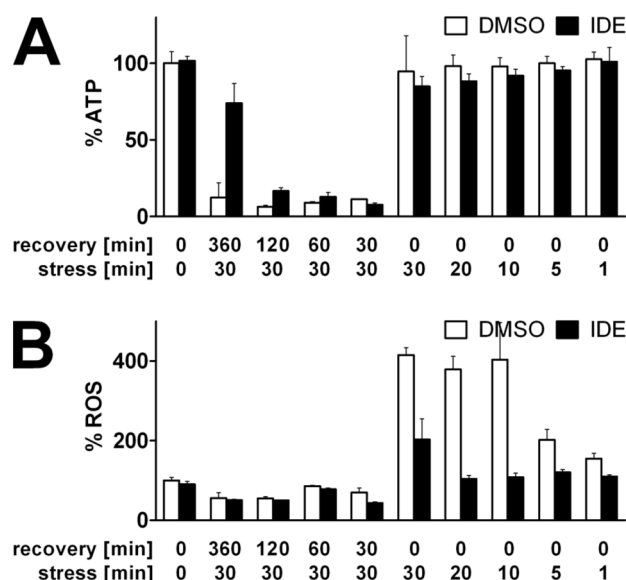


Figure 39: ATP and ROS Levels after Hydrogen Peroxide Stress:

L6 myoblasts were pretreated with DMSO (empty bars) or 10 μ M idebenone (filled bars) for 24 h before they were stressed with 200 mM H_2O_2 for up to 30 min. After that, cells were allowed to recover for different time intervals before (A) ATP and (B) ROS (CM- H_2 DCFDA) levels were measured and standardized to protein levels. Bars represent average + stdev of triplicates from a typical experiment.

These results raised the question whether the H_2O_2 -induced acute oxidative damage is followed by energy-demanding repair mechanisms after removal of the pro-oxidant which possibly could involve a transcriptional/translational response. To see if such mechanisms depend on protein synthesis or gene expression, the translation inhibitor cyclohexin and the transcription inhibitor actinomycin D were administered together with 10 μ M idebenone 24 h prior to H_2O_2 treatment [Figure 40A&C]. It was further of interest, if inhibition of NQO1 by dicoumarol could reduce the capacity of idebenone to protect cells from death by increased oxidative stress. In this series of experiments, 24-h pre-treatment with 10 μ M idebenone again showed a statistically significant protection against H_2O_2 -induced cell death ($79 \pm 2\%$ compared to $60 \pm 8\%$ living cells in DMSO-treated cells; $**p < 0.01$) [Figure 40A]. Intriguingly, pre-treatment with cyclohexin and actinomycin D increased the probability of survival by $25 \pm 3\%$ or $12 \pm 7\%$, respectively. Addition of idebenone to these cells did not significantly ameliorated survival further ($89 \pm 3\%$ and $86 \pm 2\%$, respectively). Inhibition of NQO1 by dicoumarol did not affect the protective effect of idebenone ($81 \pm 4\%$ living cells). Thus, pre-treatment with idebenone did not seem to induce expression of protective genes which in turn could attenuate the harm done by a latter oxidative stress as induced with H_2O_2 .

However, idebenone could also promote the expression of genes involved in repair mechanisms after H_2O_2 treatment. To test this, cyclohexin and actinomycin D were added immediately after the 30 min stress paradigm [Figure 40B&D]. Idebenone protected cells from dying to an extent comparable to previous experiments ($79 \pm 9\%$ living cells) [Figure 38A and Figure 40A], but since an unusually high percentage of DMSO-treated control cells subjected to the same stress survived as well ($65 \pm 7\%$), the protection against cell death mediated by idebenone was not statistically significant. Similarly to the results obtained when pre-treating cells with cyclohexin and actinomycin D, the two inhibitors protected L6 myoblastoids from H_2O_2 -induced cell death when administered after the stress as well ($80 \pm 5\%$ and $75 \pm 15\%$ living cells, respectively). Again, cyclohexin and actinomycin D did not reduce the ability of idebenone to protect cells from death ($78 \pm 9\%$ and $90 \pm 4\%$ living cells, respectively, with idebenone added to cells 24 h before H_2O_2 stress).

To check whether idebenone might elicit its cytoprotective action via interaction with NQO1 explicitly after addition of H_2O_2 , the enzyme was inhibited by dicoumarol only posterior to the 30-min H_2O_2 incubation. Similarly as when administered before H_2O_2 stress, post-treatment with dicoumarol did not alter the cytoprotective effect of idebenone ($76 \pm 7\%$ living cells). Dicoumarol itself did also not influence the number of living cells *per se* ($63 \pm 7\%$) [Figure 40B].

As expected, pre-treatment of cells with cyclohexin and actinomycin D reduced the total cell number from approximately 1,000 cells per image to roughly 500 or 550 cells per image, respectively [Figure 40C]. In contrast, when cyclohexin and actinomycin D were added after two-day cultivation and 30-min H_2O_2 -stress, the cell number did not vary compared to control cells [Figure 40D]. This suggested that after two-day cultivation, that proliferation had ceased and cells were in G_0 phase of the cell cycle. Idebenone or dicoumarol had no influence on total cell number regardless of the time point of administration [Figure 40C&D].

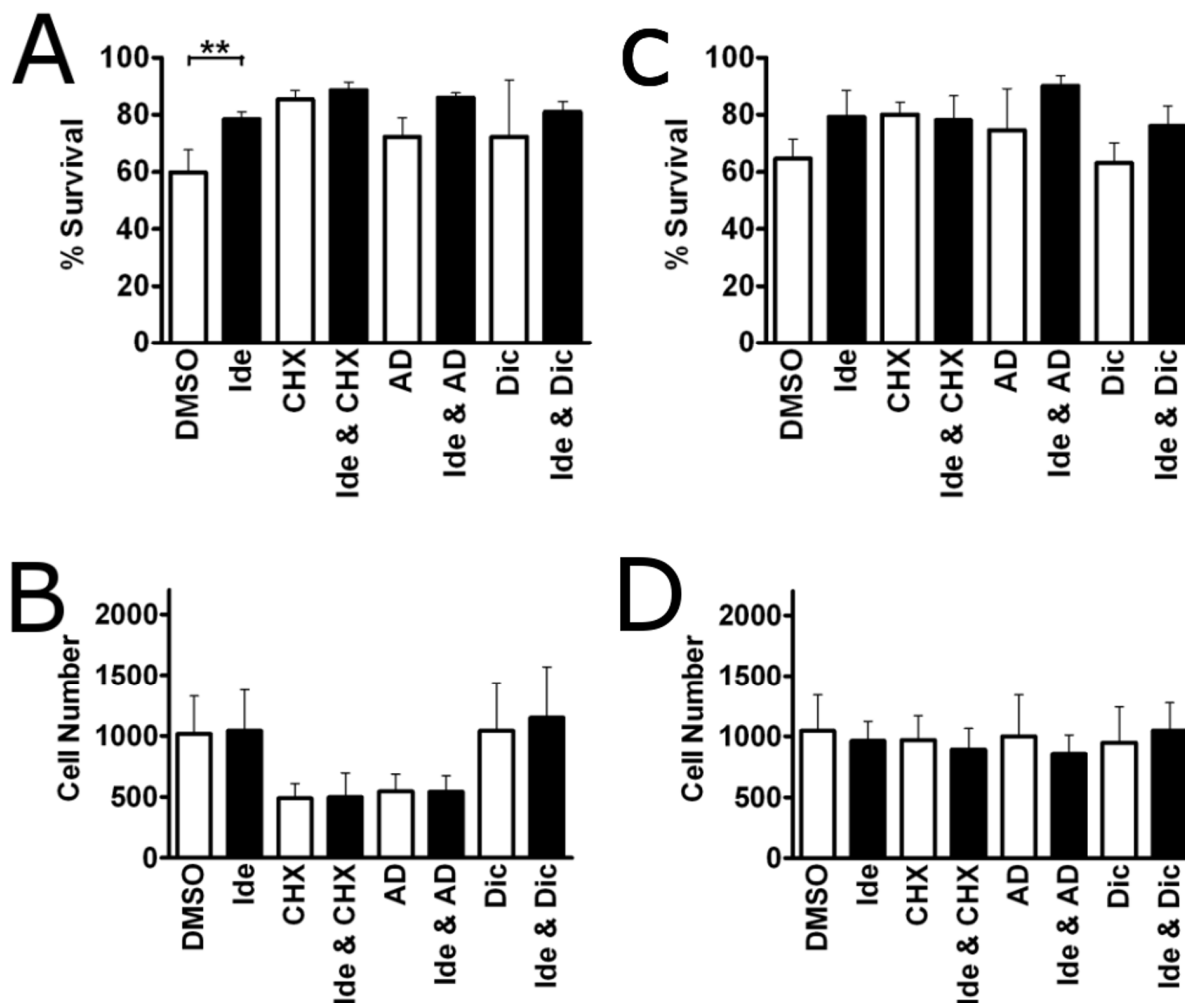


Figure 40: Idebenone-Mediated Survival Is Independent of Transcription, Translation and NQO₁ Enzymatic Activity.

Cultured rat L6 myoblasts were seeded in 96-well plates in normal growth medium. After 24 h, cells were treated with 10 μ M idebenone and subsequently, 24-h after that, cells were treated with 200 μ M H₂O₂ in PBS for 30 min before cells were allowed to recover in the medium they were cultivated seeded in before H₂O₂ shock for additional 48 h. An inhibitor of transcription, actinomycin D (AD; 1 μ g/ml), an inhibitor of translation, cyclohexin (CHX; 1 μ g/ml), and an NQO₁ inhibitor, dicoumarol (Dic; 20 μ M) were added either simultaneous with idebenone (A&B) or together with resuspending in the old medium after H₂O₂ shock (C&D). (A&C) Percent survival was calculated as percentage of live cells relative to the sum of live and dead cells as detected using the fluorescent dyes calcein and ethidium homodimer. Sum of live and dead cells are depicted as total cell number in (B&D). $p^{**} < 0.01$, two-way ANOVA with Bonferroni's Multiple Comparison tests.

3.14 Alteration in Gene Expression as a Mode of Action of Idebenone?

Even though idebenone-mediated survival of rat myoblastoids two days after H₂O₂ treatment *in vitro* was independent of translation and transcription [Figure 40], it was of interest whether long-term administration of idebenone might still initiate expression of specific genes *in vivo*. To find out which genes or pathways—if any—were differently expressed after treatment with idebenone, 200 mg/kg *p.o.* idebenone was administered to healthy mice for three weeks and differences in gene expression between treated and untreated control groups was analyzed using gene chip-based micro arrays. The strain C57Bl/6 was selected since it is one of the most widely used inbred strains. Thus, three advantages were taken by this choice: (i) individuals of inbred strains do not vary largely in their genome, (ii) since C57Bl/6 mice is a common background for transgenic mice, further studies with transgenic animals based on this strain could be compared to this one, and (iii) potential results obtained in this experiment then could be more easily evaluated in regard to findings of others due to the high usage of this strain. Animals were started to be given idebenone at the age of nine weeks when development was thought to be completed and thus, genetic programs involved in development did not interfere with the results. To avoid potential differences in individual gene regulation dependent on the female reproduction cycle only male animals were used. In humans, idebenone was described to reduce cardiac hypertrophy in left ventricles of FRDA patients [Hausse *et al.* 2002] and ameliorate cardiac parameters in the *mdx* mouse [Buyse *et al.* 2009], indicating that idebenone not only reached the heart but also accumulated in sufficient concentrations to induce observable alterations. Furthermore, due to the high energy demand of the heart muscle, and therefore a high density of mitochondria, suggested that it was likely to observe a potential effect of idebenone in this tissue.

After treatment of male C57Bl/6 mice with 200 mg/kg idebenone for three weeks, gene expression patterns induced by idebenone compared to sham treatment ($n = 5$) in the left ventricle of the heart were analyzed using one Affymetrix mouse gene chip per animal to ensure statistical power. First, the potency of idebenone treatment was investigated using principal component analysis (PCA), a statistical method reducing the dimensionality of thousands of possibly correlated variables to three uncorrelated components which can be visualized in a three-dimensional Cartesian coordinate system. The more distinct the spatial separation between the ellipsoids enclosing the representatives of two groups the more pronounced are the differences between these groups. Idebenone, in this tissue and using this treatment regime, appears to have a moderate effect on gene expression, since its ellipsoid overlaps widely with the one of the mock-treated group [Figure 41A]. The homogenous distribution of the single points representing individual animals also excludes the possibility of responder vs. non-responder groups.

Thus, PCA indicated that the effects of idebenone on gene expression were to be found in a small number of genes if at all. Indeed, when expression patterns between idebenone and control groups were analyzed using analysis of variances (ANOVA) models on the basis of single genes, no differently expressed genes were detected. Lowering the barrier by employing a less solid statistical method, the Student's *t*-test, a small number of genes was found to be expressed differently in animals treated with idebenone. Using Partek[®] software, 677 genes exhibited significantly altered scores ($p^* < 0.05$); with a maximum fold change of 1.85 compared to control animals. Another program, Agilent Genespring GX 10, was employed for confirmation of these results and presented comparable results: 616 differentially expressed genes and a maximum fold change of 1.79 ($p^* < 0.05$). Results of single gene analysis were visualized in a volcano plot which localized samples according to the binary logarithm of the fold change in the abscissa and the decimal logarithm of the statistical *p*-value in the ordinate [Figure 41B]. Thereby, samples which exceed (i) a certain arbitrarily set threshold in fold change of expression levels between groups and (ii) a required statistical significance could be visually separated from samples which did not meet the demands. A selection of the 54 genes which were expressed differently with statistical significance ($p^* < 0.05$, Student's *t*-test) and exceeding a cut-off of ± 1.3 -fold change as computed using Partek[®] software are listed in Table 4. However, some genes identified such as the testis-specific *H1fnt* or the sperm-specific *Odf3l1*, for example, were not expected to be expressed in heart tissue at all. Furthermore, many olfactory receptors were found to be differently expressed [omitted in Table 4].

The genes which were selected due to their statistically significant ($p < 0.05$; Student's *t*-test) difference in expression exceeding $\pm 30\%$ between idebenone- and vehicle-treated groups were then further analyzed on the basis of individual expression levels in each animal. In a so-called heat-map, binary logarithm-transformed signal intensities—i.e. the expression level as assayed by the binding strength on the chip—of a particular gene from a particular animal were arrayed in a matrix spanned by single animals in vertical and single gene in horizontal direction [Figure 41C]. Hence, the heat-map can be viewed as a sequence of color-coded dot-plots in a two-dimensional space [Figure 41D].

The amount of distinction between red and blue quadrants in heat maps is a measure for the discrimination between groups according to differences in their gene expression. Since statistical significance was only reached with a rather inapt model (Student's *t*-test) and the fold change between averaged expression levels of particular genes was rather low (maximum fold change was 1.79 or 1.85 using either Partek[®] or Agilent Genespring GX10 software, respectively), the separation into two times two uniformly colored rectangles fell below desired proportion [Figure 41C].

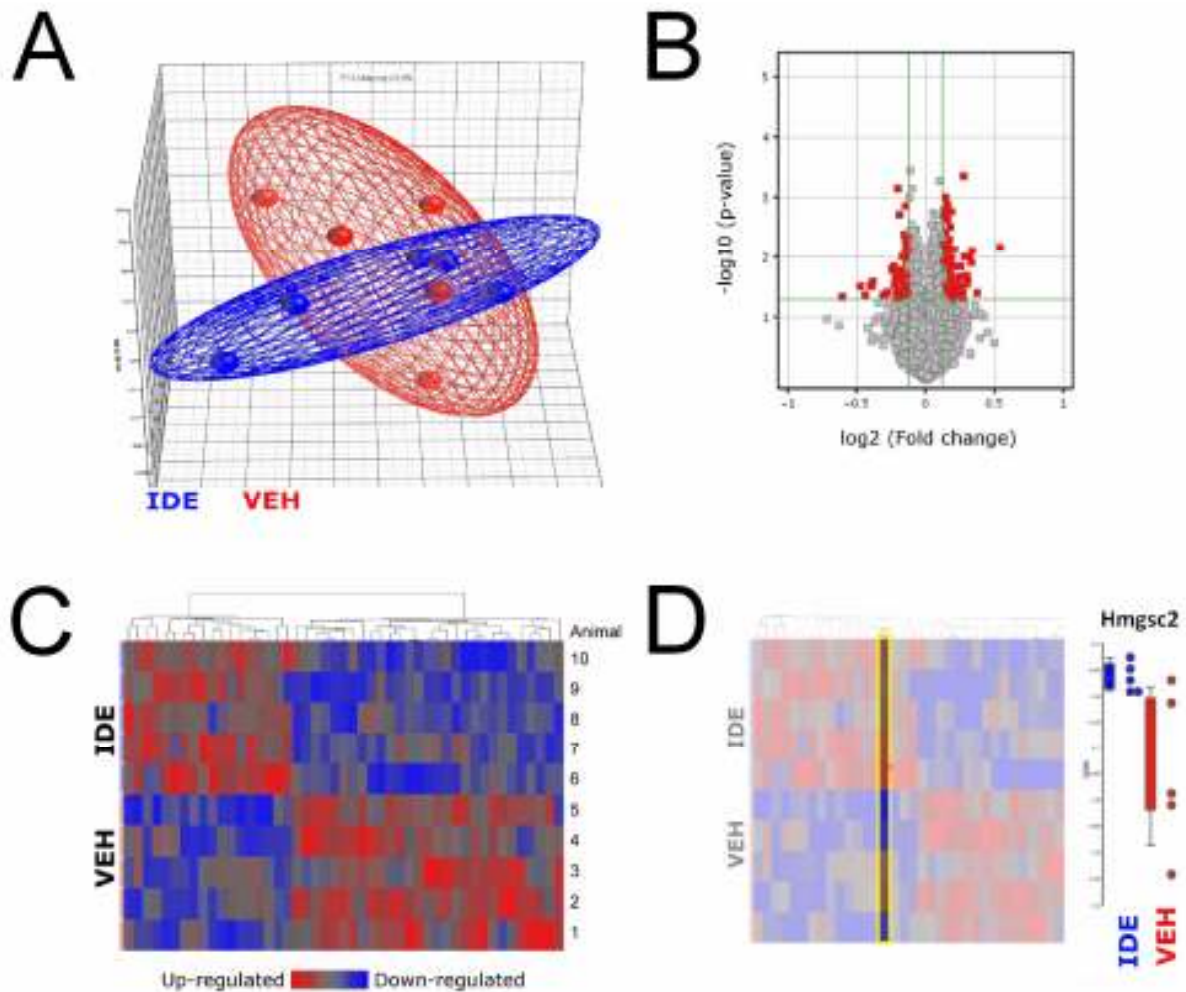


Figure 41: Quality Control of Micro Array Data.

(A) Principal component analysis is a statistical method used to reduce the dimensionality of thousands variables to three uncorrelated components. Single dots represent components for individual animals either treated with idebenone (blue) or vehicle (red). Ellipsoids incorporate points of individual animals of a group. (B) Volcano plot was used to visually separate single genes that are differently expressed. Green lines indicate cut-offs for p-value of 0.05 and for fold change of 1.3. Red dots indicate probes that are significantly differently expressed more than ± 1.3 -fold compared to control and (C) were further analyzed for the expression in individual animals using a heat map. Individual animals and hierarchically clustered genes are mounted in rows and columns, respectively, with log₂-transformed signal intensities indicated by color code. (D) The differential expression for a single gene can also be depicted in a dot plot with arbitrary units for expression levels, as shown for the gene *hmgsc2*. Dots represent individual animals treated with idebenone (blue) or vehicle (red) whereas boxes extend from the first to the first to the third quartile with a mark for the median and the whiskers represent the 10th and 90th centile of each treatment. Calculations and visualizations were computed using (A; dot plot in D) Partek[®] Genomic Suite and (B-D) Agilent Genespring GX 10 software.

Table 4: List of Genes Differently Expressed by Idebenone Treatment Selected for Fold Change Exceeding Factor 1.3.

Genes found to be differently expressed after three-week idebenone treatment in mouse hearts exceeding 1.3-fold change from control animals and reaching significance ($p < 0.05$) as assessed using Partek® Genomic Suite™ software. Fold change is relative to control levels.

Gene Symbol	Gene Name	Fold change	p-value
Mapksp1	MAPK scaffold protein 1	1.85	0.0281
Nfyc	nuclear transcription factor-Y gamma	1.81	0.0470
Ifnk	interferon kappa	1.61	0.0125
Dub2a	deubiquitinating enzyme 2a	1.53	0.0445
Xpo7	exportin 7	1.47	0.0097
Hmgcs2	3-hydroxy-3-methylglutaryl-Coenzyme A synthase 2	1.46	0.0370
Med29	mediator complex subunit 29	1.43	0.0257
Tdg	thymine DNA glycosylase	1.36	0.0462
Ccdc12	coiled-coil domain containing 12	1.35	0.0454
Fgf18	fibroblast growth factor 18	-1.30	0.0085
Zfp68	zinc finger protein 68	-1.31	0.0014
Pcdhb15	protocadherin beta 15	-1.31	0.0004
Mpzl2	myelin protein zero-like 2	-1.32	0.0499
Odf3l1	outer dense fibre of sperm tails 3-like 1	-1.33	0.0333
H2-DMb2	histocompatibility 2, class II, locus Mb2	-1.33	0.0354
Ctla2a	cytotoxic T lymphocyte-associated protein 2 alpha	-1.33	0.0080
Il17rd	interleukin 17 receptor D	-1.33	0.0375
V1rd20	vomer nasal 1 receptor, D20	-1.35	0.0270
Resp18	regulated endocrine-specific protein 18	-1.36	0.0085
Gng8	guanine nucleotide binding protein (G protein), gamma 8	-1.36	0.0137
Etd	embryonic testis differentiation	-1.36	0.0059
Sfrs12ip1	SFRS12-interacting protein 1	-1.36	0.0412
H1fnt	H1 histone family, member N, testis-specific	-1.37	0.0003
Sap18	Sin3-associated polypeptide 18	-1.38	0.0228
Ppbb	pro-platelet basic protein	-1.38	0.0455
Hist1h4h	histone cluster 1, H4h	-1.41	0.0316
Tcstv1	2-cell-stage, variable group, member 1	-1.42	0.0085
Cd24a	CD24a antigen	-1.43	0.0322
Fbxw14	F-box and WD-40 domain protein 14	-1.46	0.0000
Dnajc17	DnaJ (Hsp40) homolog, subfamily C, member 17	-1.47	0.0200
Eml5	echinoderm microtubule associated protein like 5	-1.49	0.0103
V1rc22	vomer nasal 1 receptor, C22	-1.50	0.0291
Hist1h1b	histone cluster 1, H1b	-1.58	0.0071
Krtap5-4	keratin associated protein 5-4	-1.76	0.0089

The failure to find differently expressed genes after idebenone treatment using ANVOA-based statistical models and the finding of differently regulated genes alien to heart tissue using Student's t-test questioned whether the list of genes in Table 4 was trustworthy. In order to test if the significantly differently regulated genes found using gene chip micro arrays were reliable; a selection thereof was again checked using quantitative real time polychain reaction (qPCR). Therefore, complementary DNA (cDNA) from left heart ventricle samples, on which the micro array was performed, was used as a template to quantify changes in gene expression using qPCR. Intriguingly, from the selection of 17 genes found differently expressed in micro array experiments, only three genes (i) showed comparable expression levels in gene chip and qPCR experiments and (ii) reached statistically significance ($p < 0.05$) [Table 5]. These three genes encode the 3-hydroxy-3-methylglutaryl-Coenzyme A synthase 2 (HmgCoA; +46% or +41% up-regulated by idebenone in gene chips or qPCR experiments, respectively), a key enzyme in ketogenesis; thymine DNA glycosylase (Tdg; +36% or +53% up-regulated by idebenone in gene chips or qPCR experiments, respectively), an enzyme central for the defence against DNA damage; and pro-platelet basic protein (Ppbb; -38% or -33% up-regulated by idebenone in gene

chips or qPCR experiments, respectively), a growth factor also involved in immunological responses [Table 5]. The other genes tested in qPCR experiments did neither reach significance nor exhibited comparable values of fold change in gene expression levels. Thus, up- or down-regulation of the remaining 14 genes tested with qPCR seemed to be false positives.

These results combined with PCA findings and the demand to use Student's t-test in order see differently regulated single genes, led one to conclude that idebenone treatment did not lead to an alteration in gene expression on the basis of single genes.

Table 5: Confirmation of Micro Array Data using qPCR.

The fold change in gene expression induced by three-week treatment with 200 mg/kg idebenone as quantified using gene chip micro array was controlled using quantitative real time polychain reaction (qPCR) in homogenates of left heart ventricle from 12-week old male C57Bl/6 mice.

	Micro Array		qPCR	
	fold change	p	fold change	p
Mapksp1	1.85	0.028	0.96	0.349
Nfyc	1.81	0.047	0.93	0.085
Olf550	1.74	0.030	1.19	0.307
Xpo7	1.47	0.010	1.05	0.525
HmgCoA	1.46	0.037	1.41	0.044
Med29	1.43	0.026	1.01	0.757
His1h1b	0.42	0.007	0.92	0.463
Tdg	1.36	0.046	1.53	0.037
Ccdc12	1.35	0.045	0.95	0.325
Fgf18	0.70	0.008	0.96	0.676
Zfp68	0.69	0.001	0.95	0.225
Pcdhb15	0.69	0.000	0.96	0.618
Pbbp	0.62	0.045	0.67	0.030
Hist1h4h	0.59	0.032	0.94	0.328
cd24a	0.57	0.032	0.84	0.223
Dnajc17	0.53	0.020	1.04	0.481
Eml5	0.51	0.010	0.99	0.846

Since idebenone did not seem to reliably influence gene expression on the basis of single genes, it was of interest if there were at least changes in gene expression by idebenone on the basis of parts or even the whole genome. In other words: did idebenone—despite failure in changing expression levels of single genes—transcriptionally affect entire pathways? That is: were there changes in expression levels of a set of particular genes whose products are annotated to a biological pathway which were slight and insignificant on the basis of single gene expression but not on the basis of the entire pathway? In order to address these questions, two gene ontology analysis models were employed which were based on a larger set of genes. The first computed which biological functions were transcriptionally affected by idebenone treatment based on changes in gene expression of the whole genome [see Table 8 on page 161 in the appendix]. This analysis disclosed that idebenone affected the expression of genes which are involved in biological functions involved in calcium homeostasis and lipid metabolism, amongst others. Using a second calculation model for finding gene ontology of biological functions which was based solely on the genes which reached significance in the Student's t-test, similar results were obtained [Table 7 on page 162 in the appendix].

Thus, the finding that lipid metabolism seemed to be involved in the transcriptional reaction to idebenone treatment combined with the finding that HmgCoA—an enzyme which is employed to produce ketone bodies from fatty acids as energy source when glucose levels are low—was significantly up-regulated after three weeks of idebenone administration, led to the question if idebenone might somehow shift energy consumption from using glucose to using fatty acids and ketone bodies as fuel.

3.15 Metabolic Effects of Idebenone *in Vivo*

The gene chip experiments provided some hints that idebenone might slightly alter energy consumption *in vivo*. Since idebenone was involved in mitochondrial energy production *in vitro* as well [see 3.3], it was of interest if idebenone might also lead to alterations of ATP levels *in vivo*. In order to see if idebenone might change

OXPHOS *in vivo*, a tissue with levels of mitochondria such as *m. soleus* was selected for analysis. The experimental setup and treatment regime was identical to the gene chip experiment.

Three-week incubation of male C57Bl/6 mice with 200 mg/kg idebenone had no influence on ATP content of *m. soleus* in two independent experiments called 0319 and 0350 [Figure 42A&B]. In experiment 0319, vehicle- and idebenone-treated showed practically identical ATP levels ($100 \pm 17\%$ and $97 \pm 23\%$ ATP/protein; mean \pm SEM). In experiment 0350, ATP levels in *m. soleus* were slightly decreased in idebenone-treated mice ($77 \pm 23\%$ ATP/protein) compared to sham-treated control animals ($100 \pm 59\%$ ATP/protein) but this difference did not reach statistical significance ($p = 0.43$). Thus, total ATP levels in muscle tissue of *m. soleus*—a prototype of muscles rich in mitochondria—was not significantly altered by idebenone.

Nevertheless, the quantity of ATP found in a tissue does not reveal the manner of energy production in that given tissue. Since idebenone seemed to slightly increase expression of HmgCoA [Table 4 and Table 5], a protein involved in ketogenesis, there was a possibility that the animal's metabolism could be shifted towards the use of ketone bodies as alternative energy source instead of glucose. Ketone bodies are mainly produced in the liver and then transported to consuming tissues via the blood stream.

Thus, the blood level of ketone bodies was assessed by measuring the concentration of β -hydroxybutyrate (β -HB) in plasma [Figure 42C]. Daily administration of 200 mg/kg idebenone for two weeks had no effect on blood β -HB levels (0.59 ± 0.30 mM β -HB compared to 0.49 ± 0.15 mM β -HB in vehicle-treated animals; mean \pm SEM). After another seven days of treatment, however, control animals had still comparable blood levels of β -HB (0.59 ± 0.22 -M β -HB) in contrast to idebenone-treated mice in which a trend towards higher levels of ketone bodies in the blood emerged (1.06 ± 0.37 mM β -HB). Nevertheless, the difference between idebenone- and sham-treated animals did not reach statistical significance [Figure 42C].

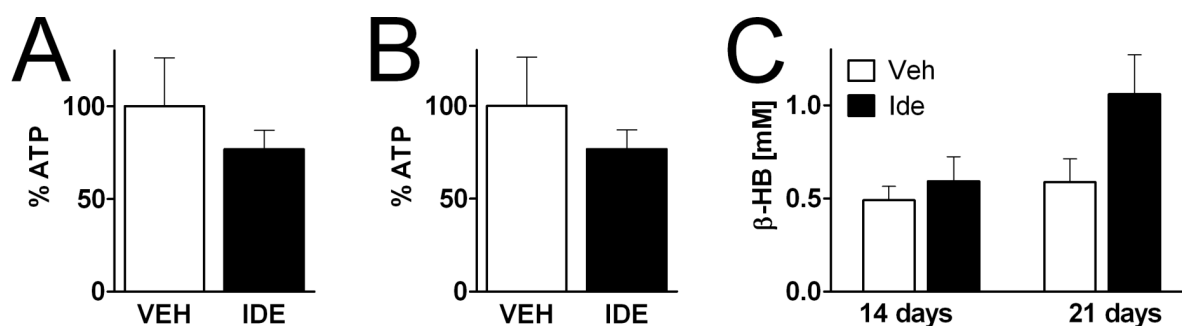


Figure 42: Idebenone Does Not Affect ATP Levels in Muscle Tissue with High Mitochondrial Density or Serum β -Hydroxybutyrate Levels *in Vivo*.

ATP levels (μ M/mg protein) were measured in *m. soleus* of male C57Bl/6 mice treated with 200 mg/kg idebenone for three weeks (filled bar) in experiment (A) 0319 or (B) 0350. Blood levels of β -hydroxybutyrate (β -HB) were measured after 14 or 21 days of experiment 0350, respectively. Bars represent mean + SEM for five animals (for β -HB, outlying values (values which were more than four times higher than average of remaining values) were not considered; n was at least equal three). No significance was seen using unpaired t-test (A, B) or two-way ANOVA with Bonferroni's Multiple Comparison test (C).

Since idebenone was suspected to interfere with energy consumption and metabolism, two elementary parameters of overall metabolic behavior were quantified: body weight of animals and their energy intake. Since idebenone was administered via food, total food intake was composed of (i) the amount of the food in which idebenone or vehicle was dissolved and (ii) the intake of supplementary food to which animals had access *ad libitum*. Intriguingly, in the same experiment in which three-week administration of 200 mg/kg/day idebenone had no significant influence on ATP levels in *m. soleus* or blood β -HB levels of male C57Bl/6 mice, the sum of supplementary food intake was substantially increased by idebenone with statistically significance after ten days [Figure 43A]. At the end of the three-week experiment, idebenone-treated mice had a significantly higher amount of supplementary ingested food (43.2 ± 4.0 g compared to 30.7 ± 5.4 g of sham-treated animals). A similar difference was observed in animals which were allowed access to a running wheel at all the time: although the total amount of supplementary food intake was increased by the physical activity (40.6 ± 4.7 g), idebenone still elevated the food consumption (50.8 ± 5.2 g) [Figure 43A].

Hence, idebenone led to a substantial increase in food intake which should have been mirrored in body weight. Strikingly, this was not the case. Treatment with idebenone did not result in a higher body weight (2.1 ± 0.3 g increase in body weight in idebenone-treated mice after three weeks compared to 2.2 ± 0.5 g increase in body weight in control animals) [Figure 43B]. After three-week administration of idebenone in the group with access to running wheels, the increase in body weight (1.4 ± 0.2 g) was not significantly higher than in control animals (0.7 ± 0.4 g).

These findings were then integrated by normalization of the supplementary food intake to the body weight [Figure 43C]. As anticipated from the previous findings, idebenone increased relative food intake in a statistically significant manner.

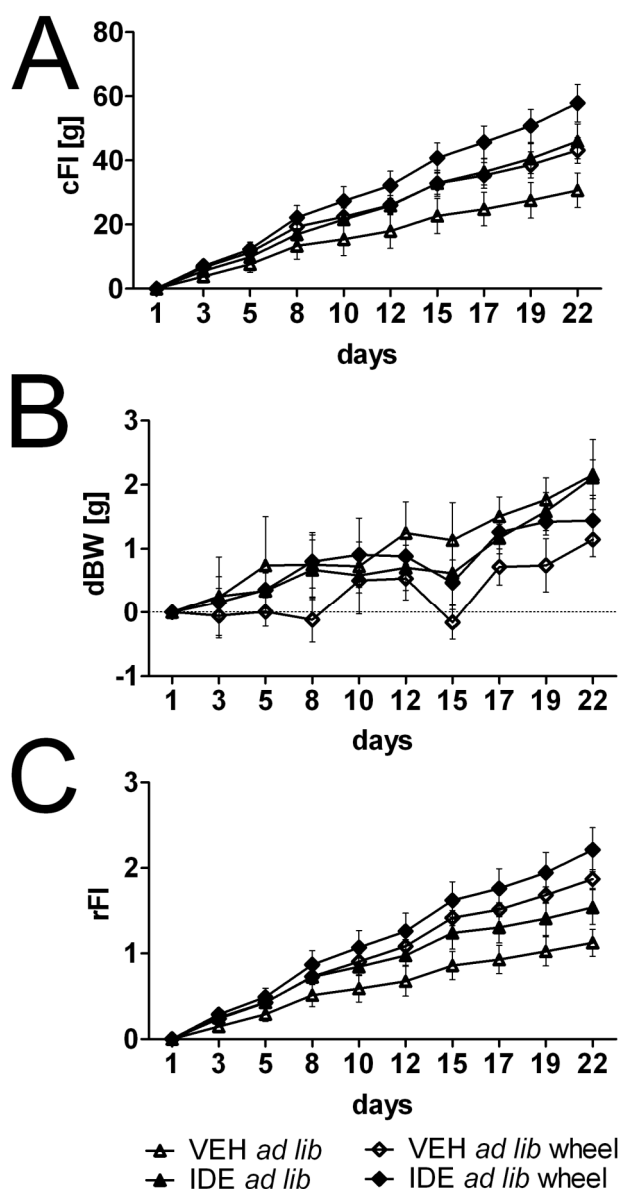


Figure 43: Idebenone Promotes Increased Food Intake but Does Not Affect Body Weight *in Vivo*.

Male C57Bl/6 mice (age 9 weeks at start of experiment; $n = 5$) were treated with 200 mg/kg idebenone (IDE; filled) or vehicle (VEH; empty) *p.o.* in food for three weeks. Animals had access to food *ad libitum* (*ad lib*) which was weighted to calculate (A) their cumulative supplementary food intake (cFI). Body weight was also measured to calculate (B) differences in body weight (dBW) and (C) the relative cumulative food intake (rFI) which was defined as difference in food intake divided by body weight. Two out of four groups had also access to a wheel all the time for voluntary locomotion.

Similar experiments as the gene chip experiment (called experiment 0319) or the one described above (0350 [Figure 43]) were conducted to see if idebenone-induced changes in food intake by simultaneously leaving body weight unchanged was also observed when parameters such as age, duration, strain, or dose were altered. Experimental setups and results of individual experiments were listed in Table 6 and data of each experiment were depicted in separated figures in the appendix [Figure 54 throughout Figure 59 on pages 163 to 168]. Out of eight experiments, comparable results were obtained in six cases, whereas in two experiments (0423 and 0436), idebenone had no influence on either food intake or body weight [Table 6]. The unresponsiveness of animals in these two experiments could be explained by the use of a different chow with a deviant composition of vitamins⁵ (KLIBAG NAFAG 3436 instead of Teklad 2018S; experiment 0423) or the higher age of animals (experiment 0436 was conducted in 14 to 18-week old mice).

In most additional experiments, however, idebenone increased food consumption without changing body weight. The only exception was found in experiment 0319 which was also used for gene chip analyses, where idebenone did in fact not increase food intake but abolished the weight gain usually observed in mice at that age. Thus, the better part of these experiments suggested that idebenone decreased the coupling of food intake to

⁵ Chow used in experiment 0423 possessed 40 mg/kg vitamin C compared to no vitamin C in chow used in other experiments. However, this chow possessed only half of the amounts of vitamins A, D₃, B₆, one fourth of vitamin B₁, pantothenic and folic acid, and biotin, and one fiftieth of vitamin K₃ [Table 10 in the appendix].

body weight. This finding was not specific to the strain, since it was observed in C57Bl/10 *mdx*, C57Bl/6, and RjHan:NMRI mice. Nevertheless, RjHan:NMRI mice showed a statistically significant increase in food intake only after almost four weeks of treatment with idebenone.

Table 6: Overview on Different *in Vivo* Metabolism Experiments.

^{a)} *Ad lib* indicates that animals had access to *ad libitum* food during entire experiment. ^{b)} A running wheel for voluntary physical activity was available during entire experiment. ^{c)} The daily dosage of idebenone mixed in food is indicated as mg/kg. ^{d)} Duration of the experiment in weeks. ^{e)} The age in weeks of mice at the start of the experiment. Mouse strains refer to ^{f)} C57Bl/10 *mdx*, ^{g)} C57Bl/6 JRj, and ^{h)} RjHan:NMRI. ⁱ⁾ Day of experiment from which on values continuously differed with statistical significance of $p < 0.05$ (two-way ANOVA with Bonferroni's Multiple Comparison test). ^{j)} Absolute and relative food intake differed from day 10 or days 15 or 19 for groups without or with wheel, respectively.

<i>ad lib</i> ^a	wheel ^b	IDE	0305	0319	0350	0423	0436	0444	0459a	0459b
○			-	-	-	0	-	-	-	-
●		+	-	-	-	200	-	-	-	-
△	+		-	0	0	0	-	-	-	-
▲	+	+	-	200	200	200	-	-	-	-
□	+		0 ^c	-	-	-	0	-	-	-
■	+	+	400	-	-	-	400	-	-	-
◇	+	+	0	-	0	-	0	0	0	0
◆	+	+	400	-	200	-	400	400	400	400
		Duration ^d	4	3	3	4	4	4	4	4
		Age ^e	7	9	9	8	8	6	6	6
		Strain	<i>mdx</i> ^f	Bl/6 ^g	Bl/6	Bl/6	Bl/6	Bl/6	Bl/6	NMRI
		n =	8	5	5	10	10	10	6	6
		Food intake (cFI)	+	0	+	0	0	+	+	+
		p < 0.05 from day ^j	7	ns	10/15 ⁱ	ns	ns	10	17	26
		Body weight (dBW)	0	-	0	0	0	0	0	0
		p < 0.05 from day	ns	21	ns	ns	ns	ns	ns	ns
		Relative FI (rFI)	+	0	+	0	0	+	+	+
		p < 0.05 from day	7	ns	10/19 ⁱ	ns	ns	7	12	28

Uncoupling of food consumption and weight gain could be achieved by higher energy expenditure which would manifest itself in either higher body temperature or increased agitation. The latter was quantified by measuring locomotion. Analyses of the use of running wheels in some experiments indicated that administration of idebenone did not increase locomotion [*data not shown*]. Similarly, body temperature was not increased in animals treated with idebenone compared to vehicle treated mice [*personal communication by C. Anklin*]. Increase in body temperature is achieved by uncoupling of mitochondrial respiration, i.e. that the proton gradient is not used to produce ATP but heat. Another explanation for the reduction in intake-mediated weight gain could be a change in body composition. Therefore, lean and fat mass was studied in a series of experiments using magnetic resonance imaging (MRI). However, both idebenone- and vehicle-treated animals showed similar fat content which amounted to approximately 8% of body weight. Thus, the effect of idebenone on systemic metabolism could not be explained by any of these three potential causes.

Nevertheless, another pathway involved in metabolic changes might be influenced by idebenone. Insulin is released from pancreatic β -cells in response to elevated blood glucose levels. This response is mediated by an elegant but elaborate mechanism: glucose enters the cells and is degraded by glycolysis; thereby producing a huge amount of ATP which in turn leads to the closing of ATP-dependent potassium channels. The resulting depolarization forces voltage-gated Ca^{2+} channel to open and intracellular Ca^{2+} concentrations rise (this effect is even amplified by IP_3 -dependent Ca^{2+} release from the endoplasmic reticulum). Similar to neurons, the high Ca^{2+} levels cause vesicles filled with insulin to fuse with the plasma membrane, thus releasing insulin into the blood stream [Campbell and Reece 2005]. Since idebenone was reported to inhibit voltage-gated Ca^{2+} channels by various authors [Kaneko *et al.* 1990, Houchi *et al.* 1991, Chang *et al.* 2011, and Newman *et al.* 2011], an influence on systemic metabolism by interfering with insulin pathways was assumed as a possible mode of action. Hypothetically, administration of idebenone would inhibit the release of insulin and this would then prevent glucose release from the liver and a shift in using fat over glucose as a fuel for muscle cells.

Glucose tolerance test is used to observe insulin-mediated metabolic changes. When fasted individuals ingest glucose, blood concentrations of glucose increase rapidly. Insulin then promotes uptake of glucose by muscle cells, thus lowering amount of glucose in blood over time. Inhibition of insulin release would impede the reduction of blood glucose. In order to investigate if idebenone interferes with the insulin pathway, overnight fasted mice were subjected to the glucose tolerance test after administration of 200 mg/kg idebenone simultaneously with 2 g/kg glucose [Figure 44A]. In this experiment, olive oil was employed as a vehicle due to the good solubility of idebenone therein. As anticipated, glucose administration increased blood glucose levels after 30 and 60 min ($72 \pm 49\%$ and $46 \pm 45\%$ of basal levels). When idebenone was administered simultaneously with glucose, a statistically indistinguishable increase in blood glucose concentrations compared to glucose treatment alone was observed ($101 \pm 65\%$ and $76 \pm 38\%$ of basal levels after 30 and 60 min, respectively). Accordingly, idebenone was not able to prolong the increased blood glucose levels, since two hours after glucose administration, blood levels were comparable in presence and absence of idebenone ($10 \pm 29\%$ and $-4 \pm 19\%$ of basal levels, respectively) [Figure 44A]. Thus, these findings suggested that idebenone did not inhibit the release of insulin.

Furthermore, a variation of this experiment was able to demonstrate a potential effect of idebenone as an inhibitor of complex I *in vivo*. Metformin was described as an inhibitor of complex I activity and treatment with metformin prevented hepatic glucose production and glucose release from liver [Periello *et al.* 1994, Inzucchi *et al.* 1998, and Brunmair *et al.* 2004]. In addition, metformin was reported to increase the use of glucose turnover in peripheral tissues and both, lower glucose production and higher rates of glucose consumption, resulted in lower blood glucose levels [Baily and Turner 1996]. Thus, the capacity of idebenone to inhibit complex I would be mirrored in a reduction of glucose levels in the blood. Male RjHan:NMRI mice were treated with 400 mg/kg idebenone *p. o.* after overnight fasting. Vehicle-treated animals (0.5% carboxymethyl cellulose) showed no variations of blood glucose levels after 20, 40, and 60 min [Figure 44B]. Indeed, the small increase in plasma glucose concentration after 20 min ($13 \pm 16\%$; mean \pm SEM) reproduced the findings obtained in C57Bl/6 mice [Figure 44A]. In contrast, 200 mg/kg idebenone transiently decreased blood glucose levels of fasted animals after 20 min with statistical significance ($-11 \pm 6\%$; $p < 0.05$) [Figure 44B]. However, one hour after administration of idebenone, blood glucose levels of idebenone- and sham-treated mice did not differ from values evaluated before treatment ($-6 \pm 18\%$ and $-1 \pm 9\%$, respectively). Metformin (300 mg/kg) was added as a positive control as a blood glucose-reducing agent [Foretz *et al.* 2010]. Indeed, metformin significantly ($p < 0.05$) reduced blood glucose levels in fasted mice after one hour by $27 \pm 13\%$. Thus, idebenone transiently reduced blood glucose levels which might explain the higher demand for food intake observed in idebenone-treated mice.

The *in vivo* experiments described in the previous subchapters revealed that idebenone is involved in metabolic functions. Not only did idebenone induce a transient decrease in blood glucose levels shortly after its administration, but also led chronic administration of idebenone to increased food intake. Interestingly, the higher demand for calories was not reflected in weight gain. This alteration of metabolism could be caused by inhibition of complex I. To understand more of its pharmacological properties, it was necessary to dissect some of the activities of idebenone with regards to its chemical moieties.

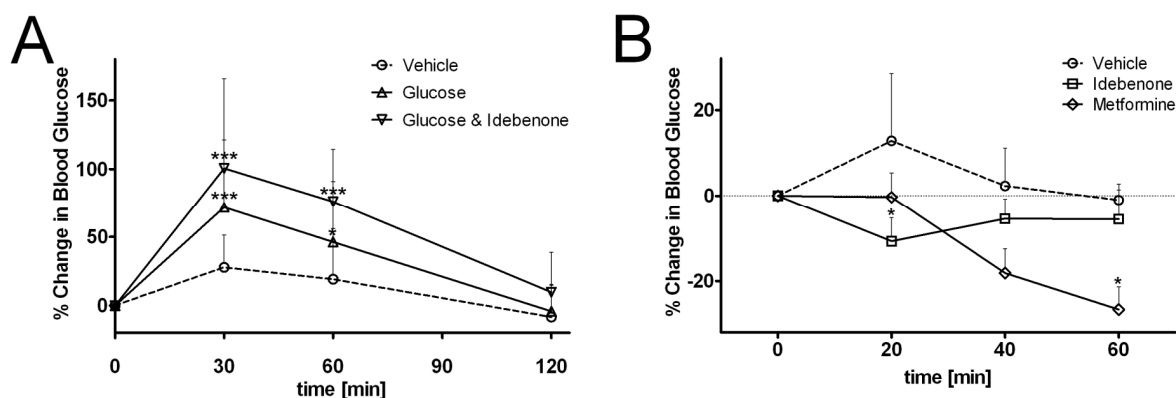


Figure 44: Idebenone Transiently Decreases Blood Glucose Levels Via an Insulin-Independent Mechanism.

(A) Male C57Bl/6 mice or (B) Male RjHan:NMRI mice were fasted overnight for 16 h and randomized after basal blood glucose levels as determined using a glucometer (Contour, Bayer). Mice were then given an oral gavage dose of (A) 200 mg/kg idebenone and 2 g/kg glucose (upside-down triangles), 2g/kg glucose alone (upright triangles), or vehicle (olive oil; circle) or (B) 300 mg/kg metformin (diamond), 400 mg/kg idebenone (square) or vehicle (circle; 0.5% CMC). Blood glucose levels were measured every 20 or 30 minutes for one to two hours. Single points depict mean \pm SEM for $n = 7-20$ (A) or $n = 6-7$ (B); $p^* < 0.05$, $p^{***} < 0.001$, two-way ANOVA with Bonferroni's Multiple Comparison test.

3.16 Characterization of Idebenone Analogs

Experiments concerning the capacity of benzoquinones to rescue ATP levels under conditions of rotenone-inhibited complex I showed that small chemical modifications of the compounds altered their behavior *in vitro* [Figure 18]. It was therefore of interest to see if chemically similar compounds to idebenone also exhibited different behaviors in other functional assays as well.

Since idebenone is a synthetic compound sharing the quinone head with CoQ₁₀, this compound and analogs thereof with shorter alkyl chains (CoQ₁₁, CoQ₂, CoQ₄, and the chain-less CoQ₀) were also included in the assays, as well as two analogs of idebenone differing in the oxidation state of the terminal carbon atom, decylQ and QS-10. Vitamin E and derivatives thereof, i.e. α -tocopherol (SNT209202), α -tocopherol quinone (SNT210202), α -tocotrienol (SNT210522), and α -tocotrienol quinone (SNT210521) were also included. The difference between tocopherols and tocotrienols is the degree of saturation of their alkyl tail: whereas the tocopherols possess only saturated bonds, alkyl tails of tocotrienols consists of three isoprenoid entities. α -Tocopherol quinone can be converted into α -tocopherol upon reduction and condensation which is also true for α -tocotrienol quinone and α -tocotrienol, respectively. Since idebenone might act as an inhibitor of complex I, rotenone was employed as a positive control. The remaining 51 compounds tested in various assays were synthesized in-house by the Chemistry Department of Santhera Pharmaceuticals. For reasons of patent protection, the chemical structures are not disclosed in this work; however, some structure activity relationships (SARs) will be discussed. Most of the assays used for screening of idebenone analogs were described before. Toxicological assays were performed by F. Schärer and B. Cardell (Santhera Pharmaceuticals) and are listed for completeness.

Influence of idebenone analogs on ATP levels in glycolysis or OXPHOS was assessed in human lymphoblastoid cells under conditions of high or low glucose content in media, respectively. In the experiment identical with the one reported in Figure 13, cells were incubated with 10 μ M compound for 72 h [Table 7]. Interestingly, depending on the quinone administered to cells, ATP levels markedly varied. Whereas idebenone reduced ATP levels when cells relied on OXPHOS ($63 \pm 17\%$, mean \pm SEM) but left ATP levels unchanged under conditions of glycolytic energy production ($104 \pm 10\%$), CoQ₀ and CoQ₁ were highly toxic to ATP production in both scenarios ($7 \pm 5\%$ and $6 \pm 3\%$ in high glucose medium, respectively, and $1 \pm 0\%$ and $2 \pm 1\%$ in low glucose medium, respectively). Intriguingly, analogs with comparable chain lengths to idebenone, decylQ and CoQ₂, showed a similar effect in low glucose medium as idebenone ($54 \pm 16\%$ and $67 \pm 30\%$, respectively), however, they drastically increased glycolytic ATP production ($294 \pm 115\%$ and $215 \pm 84\%$, respectively).

Another interesting finding was the influence of redox status on the *in vitro* behavior of vitamin E derivatives. Whereas α -tocopherol and α -tocotrienol moderately elevated ATP levels under mitochondrial energy production ($135 \pm 30\%$ and $168 \pm 37\%$, respectively), the α -tocopherol quinone and α -tocotrienol quinone dramatically depleted ATP content under these conditions ($2 \pm 1\%$ and $2 \pm 0\%$, respectively) [Table 7].

When complex I of glucose-starved HepG2 cells was inhibited by rotenone, idebenone and some analogs with similar chain lengths reversed the depletion of ATP levels [Figure 15A]. In the series of experiments whose results were listed in Table 7, the capacity for rescuing ATP levels under these conditions was slightly lower than in previous experiments ($61 \pm 9\%$ ATP rescue in contrast to approximately 80% in other experiments) [Table 7]. From all the analogs tested, about half showed an ATP rescue. Nonetheless, idebenone was one of the strongest agents in regard of restoring ATP levels in presence of rotenone with only two analogs exceeding its capacity for ATP rescue (SNT210407: $72 \pm 0\%$ ATP rescue and SNT210486: $80 \pm 9\%$ ATP rescue). Interestingly, there were two types of compounds which were not able to reverse ATP depletion by rotenone: whereas one class of compounds exhausted ATP content *per se*, the second class—including the four derivatives of vitamin E—left ATP levels unchanged in absence of rotenone. The mechanism for the observed ATP rescue in presence of rotenone seemed to be a reaction on complex I inhibition, since not a single quinone which was able to reverse rotenone-induced ATP depletion was able to elevate ATP levels after one hour incubation in absence of rotenone.

The influence of idebenone analogs on mitochondrial parameters such as membrane potential, $\Delta\Psi_m$, and mitochondrial mass when cells did not rely on mitochondria for energy production was assessed in human fibroblasts. Therefore, cells were incubated with 10 μ M compound in 25 mM glucose-containing medium for three days. As described before for idebenone, decylQ, CoQ₀, CoQ₁, CoQ₂, CoQ₁₀, and QS-10 [Figure 12], effects on these two parameters were only moderate. Even after inclusion of a much broader variety and number of quinones into experiments, the two parameters remained basically unaltered [Table 7]. Nonetheless, two exceptions are noteworthy: SNT210546—which resembled idebenone covalently linked to a peptide for mitochondrial targeting via an ester bond at the hydroxyl group of idebenone—massively increased $\Delta\Psi_m$ to 180% relative to DMSO-treated cells. On the other side, SNT210371, a compound which will be discussed below due its high pro-oxidant activity, increased mitochondrial mass after incubation for three days to 170% compared to control cells.

Short-term antioxidant capacity of idebenone analogs was assayed in human 4TE myoblasts. Cells were subjected to a 15-min stress with 10 μ M H₂O₂ 15 min after 10 μ M quinone was added. Then, the levels of cellular ROS was measured and compared to sham-treated myoblasts. As described before [Figure 35B], idebenone and QS-10 slightly aggravated exogenously induced ROS levels ($115 \pm 10\%$ and $120 \pm 8\%$ CH₂-CMDCFDA signal (mean \pm SEM), respectively), whereas CoQ₁ reduced ROS levels ($70 \pm 2\%$ CH₂-CMDCFDA signal) [Table 7]. CoQ₁₀ had no influence on ROS after short-term H₂O₂ treatment ($95 \pm 6\%$ CH₂-CMDCFDA signal). Additional analogs had effects in a similar range from $75 \pm 7\%$ (SNT210523) to $132 \pm 16\%$ (SNT210380) CH₂-CMDCFDA signal. Surprisingly, the magnitude of aggravation or diminution of exogenously induced ROS levels seemed to be independent of the pro-oxidant capacity of a particular quinone. This capacity was quantified as the induction of lipid peroxidation after three-day incubation with 10 μ M compound in human fibroblasts as described before [Figure 35A]. Intriguingly, most idebenone analogs showed no or—if any—only minor pro-oxidant activities [Table 7]. Exceptions were CoQ₀ and CoQ₁, whose pro-oxidant abilities were reported before [Figure 35A], as

well as the two compounds SNT₂₁₀₃₇₈ (282% lipid peroxidation) and SNT₂₁₀₄₃₆ (257% lipid peroxidation) [Table 7]. These two compounds did not only share a similar structure (the hydroxyl group at the terminal carbon of the alkyl tail of idebenone was replaced by a methylpiperazinyl or a pyrrolidinyl group, respectively), they also were detrimental to ATP levels in lymphoblastoid cells after three-day incubation in high ($3\pm 2\%$ and $3\pm 1\%$ lipid peroxidation, respectively) and low ($3\pm 1\%$ and $2\pm 1\%$ lipid peroxidation, respectively) glucose-containing medium and in HepG2 cells after one hour in glucose-starved medium ($5\pm 1\%$ and $28\pm 31\%$ lipid peroxidation, respectively) [Table 7]. The combination of being a strong inhibitor of cellular energy production and high pro-oxidant abilities were also observed for CoQ₀ and CoQ₁. Interestingly, a structurally similar compound, SNT₂₀₁₃₇₉, whose terminal hydroxyl group was replaced with a morpholinyl group, excessively reduced ATP production in lymphoblastoids after 72 h ($6\pm 4\%$ and $0\pm 0\%$ lipid peroxidation in high or low glucose medium, respectively), but did not show toxicity towards ATP content in glucose-deficient HepG2 cells after one hour ($80\pm 5\%$) or pro-oxidant capacity after three days in fibroblasts (116% lipid peroxidation). The two compounds showing the largest responses to short-term exogenously induced ROS, SNT₂₁₀₅₂₃ and SNT₂₁₀₃₈₀, had only marginal effects on lipid peroxidation after three days (92% and 95% lipid peroxidation).

low glucose ($p^{***} < 0.001$) [Figure 45A], ATP levels in lymphoblastoids after three-day incubation in high glucose and mitochondrial membrane potential after three days in human fibroblasts and lipid peroxidation after three-day incubation in fibroblasts (both $p^* < 0.05$) [Figure 45B&E], between mitochondrial membrane potential after three days in human fibroblasts and ATP levels in lymphoblastoids after three-day incubation in low glucose ($p^* < 0.05$) [Figure 45G], ATP rescue after one hour in HepG2 cells and ATP levels in lymphoblastoids after three-day incubation in low glucose ($p^* < 0.05$) [Figure 45K], and lipid peroxidation after three-day incubation in fibroblasts and mitochondrial mass after three days in human fibroblasts ($p^{**} < 0.01$) [Figure 45Q]. Despite the calculated statistical significance, critical observation of plots revealed that in none of these plots—with the exception of Figure 45A—reliable correlations were evident. This finding was also mirrored in the coefficient of determination (R^2) which is a measure for variability. R^2 ranges from zero and one and the higher R^2 , the better is the fitting of a linear regression between two data sets. As anticipated by critically looking at the data, R^2 for most of the statistically significant regressions—with the exception of the one depicted in Figure 45A ($R^2 = 0.555$)—the coefficient of determination was very low (R^2 ranged from 0.078 (Figure 45K) to 0.1842 (Figure 45Q)). Nevertheless, even an R^2 of 0.555 questions the reliability of a linear regression.

The finding that structural modifications of quinones led to incoherent outcomes in different assays indicated not only that most of these assays measure independent parameters, but also that the analogs of idebenone might not only have one common mode of action. Thus, these quinones are likely to have multiple targets and unique modifications might strengthen the affinity to one target whilst lowering another. As seen before with the example of the closely related compounds STN₂₁₀₃₇₈ and SNT₂₁₀₃₇₉, simple SAR could not be identified. Both quinones were equally detrimental to ATP levels in lymphoblastoids after three-day incubation regardless of glucose content of media, whereas pro-oxidant activity was only exhibited by one of two.

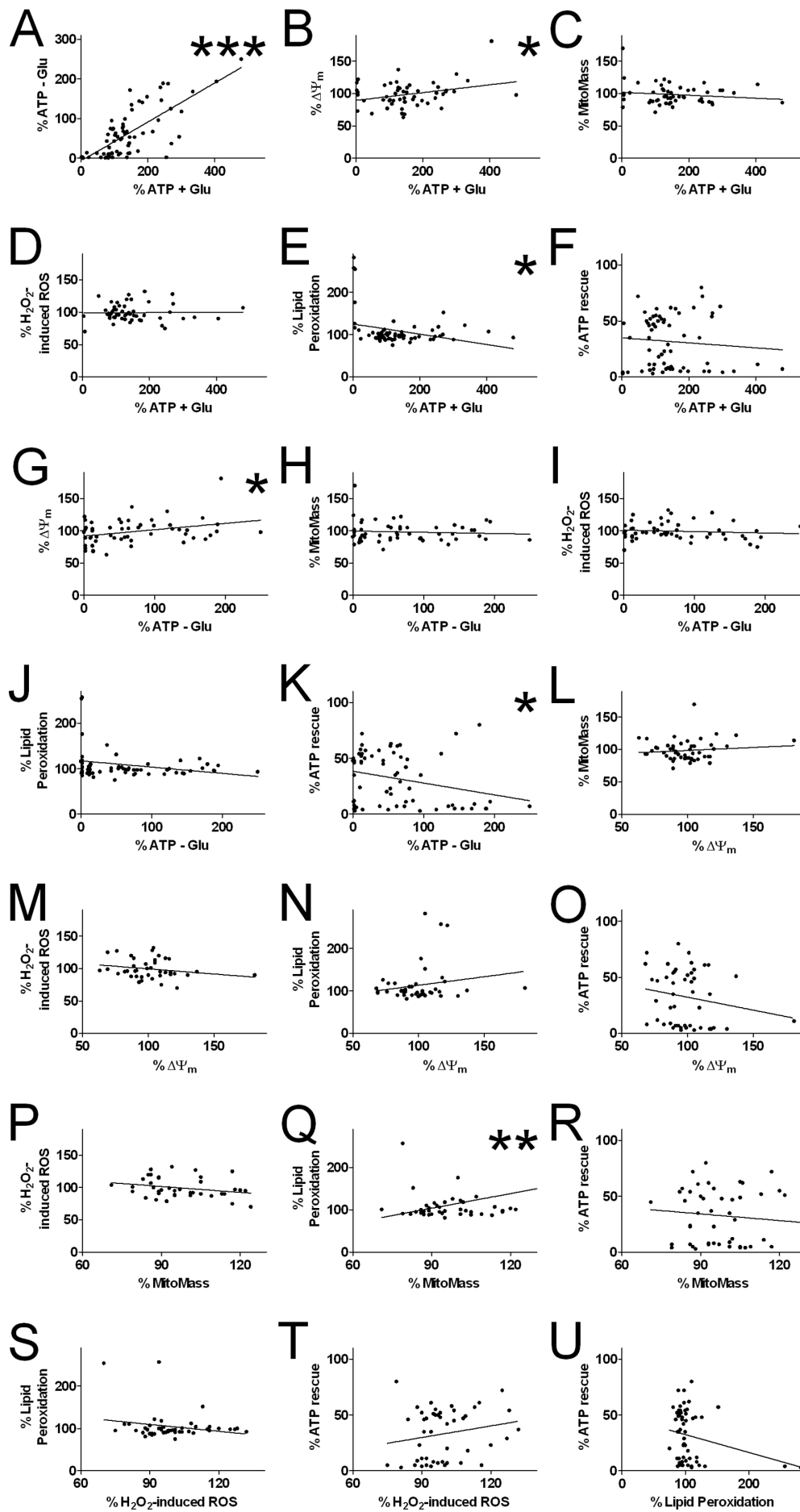


Figure 45: Correlations of Parameters Quantified for Idebenone Analogs.

Idebenone and a variety of analogs (10 μM) were subjected to different functional assays as described in Table 7. Assays include (A-F) ATP levels in lymphoblastoid cells after three day incubation in medium containing high ("+"; 25 mM) or (A, G-K) low ("-"; 0.5 mM) glucose (Glu); (B, G, and L-N) mitochondrial membrane potential ($\Delta\Psi_m$); (C,H, L, P, and Q) mitochondrial mass (MitoMass); (D, I, M, P, S, and T) ROS production after co-treatment with hydrogen peroxide (H_2O_2); (E, J, N, Q, S, and U) lipid peroxidation levels after three day incubation; and (F, K,O, R, T, U); and ATP rescue in presence of rotenone. Correlations were calculated using Pearson's correlation test with $p^* < 0.05$, $p^{**} < 0.01$, and $p^{***} < 0.001$.

In summary, several assays have shown that idebenone is able to interact with mitochondrial energy production as an inhibitor of OXPHOS, or by restoring ATP production under conditions of dysfunctional complex I via NQO1-dependent reduction. This modulation of mitochondrial function was also suggested as mode of action for the observations *in vivo*, where idebenone increased calorie intake, but left body weight unchanged. Furthermore, idebenone rescued cells from H_2O_2 -induced death. Characterization of a vast number of idebenone analogs showed complicated structure activity relations of this class of compounds in biological systems and the overall good properties of idebenone in these assays. This set of data opens the possibility to develop analogs for customized solutions in specific disorders, and for the search for new indications of idebenone.

4 Discussion

Currently, no effective treatment strategies are available in the short term to patients suffering from mitochondrial disorders. While approaches that aim to correct the underlying inherited defect, such as gene therapy, are certainly promising in their scope, these therapies are still many years away from the clinic. Thus, there is an urgent need to supply patients with safe drugs that can at least ameliorate some of the symptoms associated with their particular phenotype. Idebenone is a synthetic compound sharing structural analogies to CoQ₁₀, and has originally been developed by Takeda for the treatment of Alzheimer's disease.

Importantly, idebenone showed promising results in clinical trials in several disorders with a mitochondrial phenotype such as MELAS, LHON, and DMD [Mashima *et al.* 1992, Ikejiri *et al.* 1996, Carelli *et al.* 1998, Mashima *et al.* 2000, Napolitano *et al.* 2000, Buysse *et al.* 2011, Klopstock *et al.* 2011, and Lekoubou *et al.* 2011]. However, most studies investigating the molecular mode of action of idebenone, with regards to mitochondrial function, generated contradictory results dependent on the model system or whether idebenone was tested *in vitro* or *in vivo*. Furthermore, unlike CoQ₁₀, a rather controversial interaction of idebenone with the mitochondrial respirators complexes was described. In fact, it seems that on the one hand, idebenone inhibits complex I and on the other hand, it is a good substrate for other complexes [Shinamoto *et al.* 1982, Yu *et al.* 1982, Sugiyama *et al.* 1985, Sugiyama and Fujita 1985, Imada *et al.* 1989, Nagaoka *et al.* 1989, Degli Esposti *et al.* 1996a, Degli Esposti 1998, Kakahana *et al.* 1998, Lenaz *et al.* 2002 and 2007, Brière *et al.* 2004, Rauchová *et al.* 2008, and King *et al.* 2009, and Watze *et al.* 2010].

The goal of this thesis was to elucidate the role of idebenone in mitochondria, to rationalize its clinical use in different mitochondrial disorders and to explain the sometimes conflicting data in the literature.

4.1 Choice of Suitable Model Systems

In order to generate data relevant to clinically observed conditions, it is very important to work with suitable model systems that replicate the molecular pathology of a specific disease. Primary cells from patients with genetic disorders are often used as suitable model systems to understand the underlying molecular mechanisms and to find a potential treatment strategy. Duchenne muscular dystrophy (DMD) is devastating disorder characterized by progressive muscle wasting. A loss of function mutation of the structural protein dystrophin leads to an increased sensitivity of the muscle sarcolemma towards mechanical damage. A transient injury of the sarcolemma membrane in response to muscular contraction stress is believed to elevate levels of intracellular calcium (Ca²⁺) and to increase production of reactive oxygen species (ROS) which finally leads to mitochondrial impairment. In the case of DMD, previous work associated primary myoblasts from these patients with impaired mitochondrial function [Barbiroli *et al.* 1992, Kemp *et al.* 1993, Camiña *et al.* 1995, Gannoun-Zaki *et al.* 1995, Sperl *et al.* 1997, Kuznetsov *et al.* 1998, Brini 2003, Burelle *et al.* 2010, and Kinnally *et al.* 2011].

Surprisingly, my data showed that the only difference between primary myoblast from DMD patients and healthy donors was observed in the morphology of mitochondria. Mitochondria in dystrophic myoblasts showed a higher degree of fragmentation *in vitro* compared to those in muscle cells from healthy donors. Mitochondrial fragmentation is conducted by a process called fission and occurs mainly as a response to isolate dysfunctional parts of mitochondria [Twig *et al.* 2008]. Furthermore, mitochondrial fission was described to play a fundamental role in muscle wasting [Romanello *et al.* 2010]. In contrast, tubular networks of ring-shaped mitochondria formed by fusion were associated with maximization of OXPHOS-dependent energy production and their formation was shown to protect mitochondria from degradation [Rambold *et al.* 2011]. Since fusion and fission were reported to regulate intracellular Ca²⁺ signaling, fragmentation of mitochondria could be a potential adaptation to impaired Ca²⁺ homeostasis in DMD [Diaz and Moraes 2007].

Intriguingly, despite the observed difference in mitochondrial morphology between dystrophic and healthy primary myoblasts, the data presented here indicate that the mitochondrial function in these cells was indistinguishable. Mitochondrial parameters such as ATP levels, mitochondrial reactive oxygen species (ROS) production, or mitochondrial mass were investigated. Furthermore, ROS levels in the cytosol of primary myoblasts from DMD patients were indistinguishable from healthy myoblasts. The lack characteristic changes in dystrophic myoblasts appears to be in contrast to previous reports [Kar *et al.* 1979, Hunter and Mohamed 1986, Barbiroli *et al.* 1992, Kemp *et al.* 1993, Camiña *et al.* 1995, Gannoun-Zaki *et al.* 1995, Sperl *et al.* 1997, Ragusa *et al.* 1997, Disatnik *et al.* 1998, Kuznetsov *et al.* 1998, Rando *et al.* 1998, Brini 2003, Burelle *et al.* 2010, and Kinnally *et al.* 2011]. However, none of these studies were conducted in cultured myoblasts from biopsies of DMD patients. For example, when Camiña *et al.* [1995] reported decreased ATP levels, muscle homogenates from DMD patients were used rather than cultivated cells.

The lack of quantifiable parameters associated with the DMD cells *in vitro*, i.e. elevated ROS levels, reduced cellular ATP content, or mitochondrial mass, could simply be due to unsuited assays to detect these parameters. Although, these assays showed reliable results in other cell lines as discussed below, the JC-1 dye showed a poor performance in primary myoblasts. Thus, cell type-specific dysfunctions of this particular assay cannot be excluded. Nevertheless, since conditions *in vitro* deviate substantially from the physiology *in vivo*, it is likely that these parameters do not manifest fully *in vitro* in intact cells. *In vivo*, affected muscle cells are (i) post-mitotic cells, whereas cultured primary myoblasts divide. The more severe the pathology is in a particular cell, the less likely is the probability for it to proliferate. Thus, this hurdle decreases the degree of pathology observed *in vitro*

over time. In addition, damage is associated with (ii) stress from stretching of sarcolemma, which is not replicated under standard culture conditions. Furthermore, (iii) many experiments on mitochondrial changes in DMD were conducted in subcellular systems. For example, a recent conference submission [poster from Sobreira *et al.* EuroMit 2011, Zaragoza, Spain] reported that specific mitochondrial complexes of the respiratory chain are dysfunctional in muscle homogenates. Thus, it seems likely that intact cultured cells can compensate for their mitochondrial impairment in contrast to cells *in vivo* or isolated mitochondria. Thus, the relevance of cultured myoblasts of DMD patients for studying mitochondrial dysfunction is questionable. Finally, the absence of a detectable pathologic phenotype *in vitro* is reflected by the lack of literature on these parameters in cultured myoblasts of DMD patients.

Thus, since intact primary myoblasts of DMD patients did not manifest characteristics of impaired mitochondrial function in culture, the use of these cells as model system for understanding the molecular effects of idebenone in a disorder including mitochondrial impairment had to be dismissed. As a result, many experiments were conducted in model systems using both healthy, undisturbed cells or animals and cells in which specific pathways or enzymes/enzyme complexes were exogenously disabled by inhibitors or by RNAi-based knock-down approaches. These experiments revealed that the action of idebenone in healthy cells or animals differ fundamentally from its action in conditions of impaired mitochondrial function. Whereas idebenone induced signs of energy shortage in systems with healthy mitochondria, it had beneficial effects on metabolism in cells with dysfunctional complex I, as will be discussed below.

It has to be noted however, that in comparison with primary cell lines, model systems using artificial manipulation of mitochondria hold certain disadvantages: (i) exogenously induced modifications can never fully represent the phenotype of the disorder but only single aspects of it. This is particularly true for DMD whose complex cellular entanglements are still not fully disclosed [McArdle *et al.* 1995, Zhou *et al.* 2006, and Deconinck and Dan 2007]. Thus, inhibition of a single enzyme may only imitate one underlying cause of the disorder and never replicate the whole picture. In addition, (ii) compounds which mimic symptoms associated with a certain disorder may have different underlying causes that lead to a similar phenotype. Additionally, inhibitors are thought to (iii) interact with the target enzyme at a specific binding site for which a given compound could be competitive. Thus, a compound's ability to counteract the effects of an enzyme inhibitor is no proof that it is also able to ameliorate the pathology of a disorder in which the corresponding enzyme is dysfunctional. A further limitation is that (iv) any inhibitor might not only bind to the desired enzyme, but also interacts with unspecific off-targets. To avoid these implicated difficulties, certain precautionary measures were taken in the experiments of this thesis. For example, specificity of inhibitors against NQO1 was assessed, or ATP rescue experiments were performed in presence of complex I inhibitors other than rotenone.

On the other hand, artificial model systems hold many advantages: they (i) provide a defined setting which focuses on only one aspect of a disease. In DMD, for example, failures in Ca²⁺ homeostasis, membrane integrity, elevated oxidative stress and mitochondrial dysfunction overlap and influence each other. This makes it very difficult to attribute a potential beneficial effect of a compound to the underlying mode of action. The employment of an inhibitor facilitates the distinction of molecular mechanisms. In addition, artificial systems can be set up in cell lines that are not associated with problems of primary cells such as (ii) senescence, (iii) unsteady or diminishing growth rates, or (iv) limited transfection capacity. Furthermore, the use of cell lines (v) facilitates the reproducibility of results in different labs.

As a consequence, most experiments of this thesis concerning the mode of action of idebenone were conducted in healthy cell lines or mice which could be selectively manipulated. The main exceptions were the employment of the dystrophin-deficient *mdx* mouse model and MELAS cybrid cells. MELAS cybrids combined the mitochondrial genotype of MELAS cells and the nuclear genetic background of an osteosarcoma cell line. Findings in MELAS cybrids will be discussed below [see 4.11].

Like human DMD patients, *mdx* mice have a mutation in the dystrophin gene [Bulfield *et al.* 1984]. Nevertheless, the phenotype in these mice is much milder compared to the human disorder [Vainzof *et al.* 2008] most likely due to differences in telomere length between mice and humans. At the age of six to 12 weeks, the pathological symptoms of *mdx* mice were described to peak [Villalta *et al.* 2009]. Indeed, my data confirmed that blood levels of creatine kinase, a cytosolic enzyme which can be found in the blood when plasma membranes are disrupted, were increased in six- and 12-week old mice compared to animals without the mutation in the dystrophin gene, but with the otherwise same genetic background (wild-type (WT) mice), even though the difference in the younger animals did not reach statistical significance. The certification of the described phenotype by these experiments permitted further experiments to find disease-specific differences.

Since a 50% reduction of the activity of mitochondrial respiration complexes in *mdx* mice was described [Kuznetsov *et al.* 1998], a decrease of ATP in tissues of *mdx* compared to WT animals was expected. Intriguingly, ATP levels in dystrophic and healthy animals did not alter in different muscle types varying in the amount of mitochondria or in the cerebellum. However, a fundamental difference to the experiments described herein was that Kuznetsov's lab measured oxygen consumption directly in isolated mitochondria. Whereas these findings suggested that respiration is impaired in mitochondria of *mdx* mice, my data revealed that these animals were able to compensate the anticipated drop of ATP in tissues. Furthermore, Braun *et al.* [2001] challenged the data by Kuznetsov *et al.* [1998] by reporting that the maximal capacity of oxidative phosphorylation was undistinguishable between muscle tissues of *mdx* and WT mice.

Since no drop in ATP levels was found in *mdx* mice, DMD was abandoned as a model system for investigation of the role of idebenone in mitochondrial impairment. The dismissal of DMD as a model system does not imply

that idebenone might not be beneficial in this disorder. On the contrary, idebenone showed promising results in the *mdx* mouse model [Buyse *et al.* 2009] and in clinical trials [Buyse *et al.* 2011] and is still under investigation in this indication and potential mechanisms how idebenone could counteract the pathology of DMD are discussed below [see 4.11]. However, since the emphasis of this work was the modulating activity of idebenone on mitochondrial function, DMD appeared unsuited to answer these questions.

Despite the surprising finding that primary DMD myoblasts are unsuited to test mitochondrial impairment, an interesting result from these experiments could be obtained: the assays employed to measure mitochondrial parameters such as ATP production when oxidative phosphorylation (OXPHOS) was required, mitochondrial mass, and ROS production seemed to be independent of one another. Similar results were obtained when the effects of idebenone analogs were assessed. The certainty that the employed assays measure independent parameters was important to discriminate effects induced by idebenone and other compounds.

4.2 Influence of Idebenone on Mitochondrial Parameters in Healthy Mitochondria

Since idebenone and CoQ₁₀ share structural analogy, idebenone was suggested to interact with enzymes of the mitochondrial electron chain. In fact, interaction with complexes I, II, and III was described for idebenone. But whereas idebenone acts as a good substrate for the latter two, it inhibited both the proton pumping and redox activity of mitochondrial complex I [Sugiyama *et al.* 1985, Sugiyama and Fujita 1985, Degli Esposti *et al.* 1996a, Brière *et al.* 2004, Rauchová *et al.* 2008, and King *et al.* 2009]. Contradictory data were published by James *et al.* [2005], who described idebenone as a good substrate for not only complex II and III, but also for complex I. However, these results should be regarded with caution, since they normalized the measured activities to those elicited by CoQ₂ which is also described to be an inhibitor of complex I [Degli Esposti 1998].

Due to this differential interaction with the electron transport chain (ETC), it was important to know whether idebenone changes mitochondrial function *per se* in healthy cells when the cells do not depend on ETC for energy production. When demand for ATP is high, cells employ mitochondrial respiration in order to efficiently retrieve as much energy stored in glucose molecules as possible. In contrast, high abundance of glucose alleviates the need for mitochondrial energy production and cells undergo aerobic glycolysis in which only a small fraction of ATP is mitochondrially generated [Vander Heiden *et al.* 2009 and Mathupala *et al.* 2010; and Figure 49]. Under these conditions, enforced by addition of excess glucose to the medium, influence of compounds on mitochondria can be investigated without provoking interference with ETC-mediated energy production. Indeed, three-day incubation of lymphoblastoid cells with rotenone, an inhibitor of complex I, in medium containing a five-fold excess concentration of glucose compared to physiological conditions did not affect ATP content under these conditions, indicating that mitochondrial respiration was not required in order to produce energy. Hence, potential alterations of mitochondrial parameters found were independent of mitochondrial respiration. Similarly to rotenone, long-term treatment of human lymphoblastoid cells with idebenone did not affect ATP levels under these conditions. Accordingly, long-term treatment with idebenone in an aerobic glycolysis-based cell model did not result in alterations of either mitochondrial membrane potential ($\Delta\Psi_m$) or mitochondrial mass in human fibroblasts, suggesting that idebenone does not change mitochondrial function *per se*.

In contrast, depriving cells of glucose enforces their use of mitochondrial energy production. Thus, in an experiment with identical conditions as the one described above (three-day idebenone treatment of lymphoblastoid cells) except for a decrease in medium glucose content to physiological conditions would reveal the influence of idebenone on mitochondrial respiration. As anticipated by the described inhibitory effect of idebenone on complex I [Sugiyama *et al.* 1985, Sugiyama and Fujita 1985, Degli Esposti *et al.* 1996a, Brière *et al.* 2004, Geromel *et al.* 2008, Fato *et al.* 2008, Rauchová *et al.* 2008, and King *et al.* 2009]. ATP levels of glucose-deprived cells dropped by almost a third in presence of idebenone in long-term experiments. Rotenone, one of the most potent inhibitors of complex I known [Degli Esposti 1998], had a more severe effect on mitochondrial ATP production, suggesting that the blocking of ETC by idebenone was only partial. Indeed, the potency of idebenone to inhibit complex I is reported to be hundred-fold lower than that of rotenone [Degli Esposti 1998].

4.3 Idebenone Is an Inhibitor of Complex I

In line with works by others, these data confirmed that idebenone moderately inhibits mitochondrial respiration, probably via complex I⁶ [Sugiyama *et al.* 1985, Sugiyama and Fujita 1985, Degli Esposti *et al.* 1996a, Brière *et al.* 2004, Geromel *et al.* 2008, Fato *et al.* 2008, Rauchová *et al.* 2008, and King *et al.* 2009]. In order to elucidate interaction of idebenone with complex I, a short overview of the biochemistry of complex I would be of help. The mammalian complex I is composed of 46 subunits whereof seven are encoded in mtDNA and form the lipophilic part of the protein [Brandt *et al.* 2003]. This multi-subunit complex accomplishes three different enzymatic functions: (i) a dehydrogenase activity to oxidize NADH in the mitochondrial matrix, (ii) a

⁶ Of course, the setup of these experiments does not allow speculating on a mode of action how blocking mitochondrial ATP synthesis is achieved. Nevertheless, a plethora of work described idebenone as a complex I inhibitor and a good substrate for complexes II and III. In addition, the fact that the ATP rescue in complex I-deficient cells was sensitive to antimycin A, a complex III inhibitor, indicated that idebenone is efficiently oxidized by this mitochondrial complex.

hydrogenase activity embedded in the lipid bilayer to reduce CoQ_{10} , and (iii) a membrane-spanning translocation of protons out of the matrix. The two former activities are mainly carried out by several iron-sulfur clusters which transfer the electrons obtained from NADH to CoQ_{10} . Under normal conditions, two electrons per each NADH molecule are passed to CoQ_{10} and four protons are removed from the mitochondrial matrix during this process. The reduction of CoQ_{10} occurs within an active pocket of the enzyme complex; however, the propagation of the two electrons to the final acceptor is thought to take place at two different catalytic sites [Brandt *et al.* 2003].

The active pocket for CoQ_{10} reduction is seated within—and opened towards—the lipid bilayer of the inner mitochondrial membrane and is due to its complex configuration not well deciphered [Figure 46]. From electron paramagnetic resonance (EPR) experiments, three different binding sites for CoQ_{10} have been suggested [Ohnishi and Salerno 20005]. It is assumed that electrons are passed along different iron-sulfur clusters from NADH to the last of these clusters, called N2, and from there to the physiological quinone acceptor, CoQ_{10} . After receiving one electron, the resulting semiquinone covalently binds a proton. Subsequently, it receives another electron from N2. As a consequence, it incorporates a second proton from the matrix side and hence, a hydroquinone is formed which in turn provokes a conformational change which allows for the release of the reduced CoQ_{10} from the active pocket [Fato *et al.* 2008 and Figure 46]. The different binding sites of quinone, semiquinone, and hydroquinone were also used to characterize inhibitors of the complex I corresponding to their assumed binding sites [for a review see Degli Esposti 1998, Figure 46 and Table 2]: class A inhibitors include pyridaben, piericidin A, and rolliniastatin-1/2 and bind to the site where CoQ_{10} attaches upon entrance into the active pocket. Class B inhibitors include rotenone and two derivatives thereof (deguelin, tephrosin), piericidin B, and—as was suggested by Degli Esposti [1998]—idebenone, and they are assumed to bind at the semiquinone binding site and block the transfer of the first electron from the N2-cluster to the protein-bound quinone. Class C inhibitors, capsaicin or stigmatellin, block the hydroquinone binding site where the second electron is delivered to the semiquinone and finally, reduced CoQ_{10} is released from the active pocket. Most class C compounds are simultaneously classic complex III inhibitors. Given the narrow space occupied by the quinone, semiquinones, and hydroquinone binding sites, the three classes of complex I inhibitors possess partially overlapping binding domains [Okun *et al.* 1999]. In addition, complex I can also be inhibited at the prosthetic flavin site where electrons are donated from NADH. This mechanism is employed by diphenylene iodonium [Majander *et al.* 1994] and rhein [Kean 1970]. Other compounds, such as berberine and metformin, are also described as complex I inhibitors [El Mir *et al.* 2000], although their mode of action is unknown [Figure 46 and Table 2].

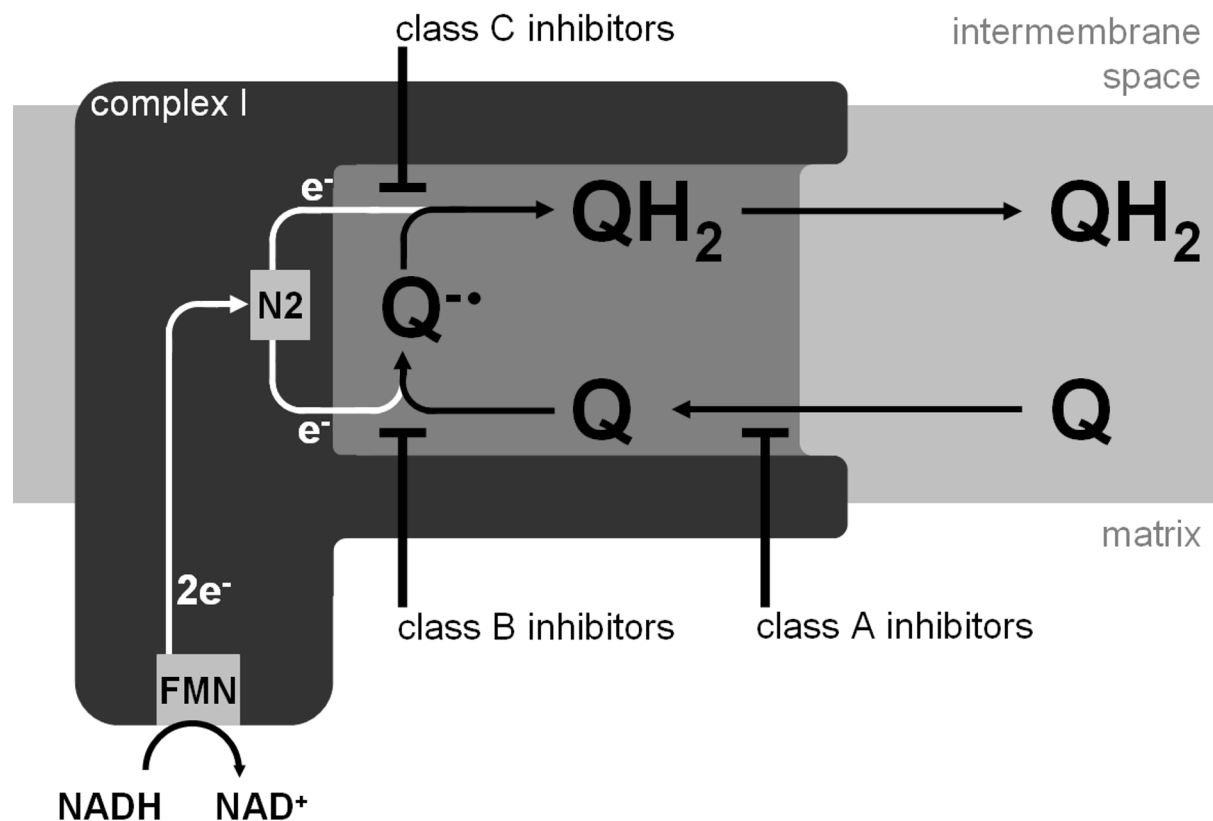
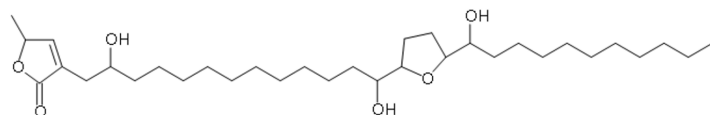


Figure 46: Schematic Representation of Electron Transfer in Complex I and Proposed Inhibition Sites.

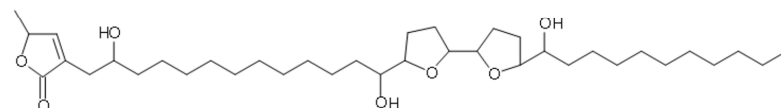
Electrons from NADH reduction at a prosthetic flavin side (FMN) are transferred along several iron-sulfur clusters (not depicted) of complex I (dark grey) to the final acceptor iron-sulfur cluster, N2. CoQ_{10} (Q) enters the active pocket (grey) from the inner mitochondrial membrane (light grey). There, receiving a first electron from the N2 cluster converts Q into a semiquinone ($\text{Q}^{\bullet-}$). The transfer of a second electron results in the formation of the hydroquinone form (QH_2) which can be—after the release of the active pocket of complex I—re-oxidized by complex III. Different classes of inhibitors might block the binding site for the quinone, semiquinone, or hydroquinone.

Considering the structures of some type A and B inhibitors, one can hypothesize how idebenone might interact with complex I. First, the difference of piericidin A and piericidin B lies in one single substitution in their alkyl tails: whereas piericidin B has a methoxy group at carbon C₁₀ of the tail, piericidin A possesses a much more reactive hydroxyl group at this position [Figure 47]. Likewise, rolliniastatin-1 and -2 exhibit a hydroxyl group at a similar position, i.e. at carbon C₁₃ of their tails, suggesting this to be a prerequisite for type A inhibition [Degli Esposti 1998]. Second, comparison between structures of piericidins and rotenone and its derivatives deguelin and tephrosin, which also inhibit complex I, reveals that they share a similar structure: all compounds feature a planar ring with six delocalized π electrons⁷ which possess two methoxy groups in ortho position [Figure 47]. Thus, from a structural point of view, idebenone, which possesses both the head group similar to rotenone and piericidin, would be considered a class A or B inhibitor. The hydroxyl group at C₁₀ of its alkyl tail, however, makes it more likely to act as class A inhibitor. Nevertheless, idebenone was suggested to act as a class B inhibitor [Degli Esposti 1998], and other publications added up to a more complex mode of action.

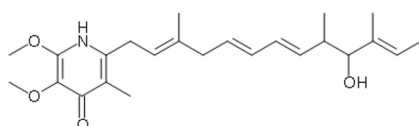
Class A Inhibitors



rolliniastatin-1

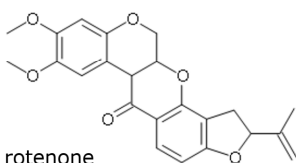


rolliniastatin-2

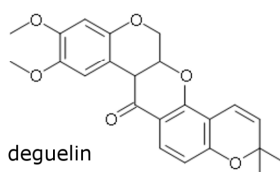


piericidin A

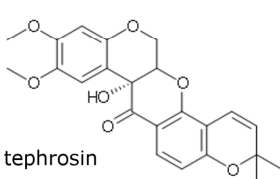
Class B Inhibitors



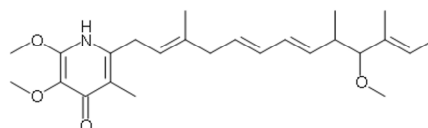
rotenone



deguelin

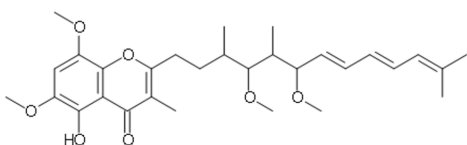


tephrosin

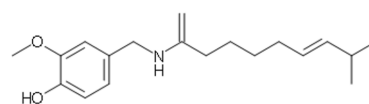


piericidin B

Class C Inhibitors



stigmatellin



capsaicin

Figure 47: Chemical Structures of Complex I Inhibitors.

Complex I inhibitors are classified on the basis of their binding sites within the CoQ₁₀-binding pocket of complex I according to Degli Esposti [1998]. Class A inhibitors (rolliniastatin-1/2 and piericidin A) block the quinone-binding site, class B inhibitors (rotenone, deguelin, tephrosin, and piericidin B) block the semiquinone-binding site, and class C inhibitors (stigmatellin and capsaicin) block the hydroquinone-binding site.

⁷ π (π) bonds are covalent chemical bonds between p-orbitals. Thus, π electrons are located in the aromatic ring of benzoquinones and in double bonds between carbon atoms and between carbon and oxygen atoms of its hydroquinone form.

Rauchová *et al.* [2008] using cytochrome *c* and 2,6-dichlorophenol indophenol (DCIP) as final electron acceptors in sub-mitochondrial fractions contributed an important experiment to find out more about the site of complex I inhibition of idebenone. In contrast to cytochrome *c* which is reduced downstream of complex I altogether, DCIP is reduced within the active pocket of the CoQ₁₀ dehydrogenase, namely at the site of type B inhibitors [Fato *et al.* 2008a]. Whereas idebenone inhibited cytochrome *c* reduction by 67%, DCIP reduction was inhibited only by 25% [Rauchová *et al.* 2008]. This indicates that idebenone might act as a type A or B inhibitor. This results were in line with previous work by Sugiyama *et al.* [1985] who registered a decreased NADH:cytochrome *c* reductase activity, and is in line with the observation that the activity of idebenone as electron acceptor at complex I was 63%-sensitive to rotenone-inhibition [Degli Esposti *et al.* 1996a].

Consistent with this finding, 69% of idebenone was reduced by mitochondria in presence of NADH [Sugiyama *et al.* 1985] as mentioned in the Introduction [see 2.4.4]. King *et al.* [2009] added to the picture that the limited dissociation of reduced idebenone blocks the active pocket for the entrance of CoQ₁₀. This view is supported by own experiments which suggests that the quinone (oxidized) and hydroquinone (reduced) form of idebenone exhibit different capacities towards complex I inhibition. In NQO1-expressing cells relying on mitochondrial respiration for energy production, idebenone had no influence on cellular ATP levels⁸. However, in the presence of dicoumarol, a dramatic drop in ATP content induced by idebenone was detected⁹, indicating that only oxidized idebenone is able to block complex I activity.

In addition, King *et al.* [2009] suggested that idebenone can also be reduced at the NADH binding site exposed to the mitochondrial matrix. This incomplete, one-electron reduction of idebenone, generating semiquinones radicals, could explain the ROS production associated with the inhibition of complex I [Fato *et al.* 2008, Geromel *et al.* 2008]. Contradictory to these results however, inhibition of complex I by idebenone was paralleled by a decrease of *in vitro* lipid peroxidation [Sugiyama *et al.* 1985a].

In conclusion, idebenone inhibits electron transfer from NADH to CoQ₁₀ carried out by complex I via many different modes. Internal data from Santhera Pharmaceuticals in collaboration with Scientific Devices (Heidelberg, Germany) revealed that for isolated mitochondrial membranes the half maximal concentration (IC₅₀) for inhibition of complex I was 5.9 μM which is in line with the concentrations resulting in a decrease in ATP levels used in the experiments of this thesis.

4.4 Idebenone Restores ATP Levels under Conditions of Impaired Complex I

In contrast to the experiments in cells with normal mitochondrial functional, which revealed that idebenone has either no effect on mitochondrial activity in aerobic glycolysis or inhibits complex I during OXPHOS, it was of interest to investigate the role of idebenone in mitochondria with a specific, exogenously inflicted dysfunction. Clinical data in MELAS [Ikejiri *et al.* 1996, Napolitano *et al.* 2000] and LHON [Mashima *et al.* 1992, Carelli *et al.* 1998, and Mashima *et al.* 2000] patients suggested that idebenone might be beneficial in disorders with a mitochondrial phenotype. Therefore, it was essential to establish an *in vitro* model in which mitochondrial respiration could be selectively inhibited.

In order to force cells to use mitochondria for energy production, a hepatic cancer cell line, HepG2, was cultured under low glucose conditions (1.77 mM) for 24 h before they were deprived of glucose for one hour. Cells were still able to maintain their cellular ATP levels over that short period of time unless their mitochondrial function was fundamentally disrupted.

Compounds blocking ATP synthase activity, i.e. via reduction of the proton gradient by the uncoupler FCCP or by direct inhibition using oligomycin, ATP levels dropped to 10% of residual levels. Upon treatment with inhibitors of the mitochondrial complexes I and III, rotenone and antimycin A, respectively, ATP levels decreased to practically zero compared to residual levels after one hour in absence of glucose. Since an inhibitor of complex II, 3-nitropropionate, was unable to decrease ATP at all, it seemed that this respiratory complex accounted for only minute contributions to total energy production in these cells.

In presence of antimycin A, FCCP, or oligomycin, idebenone was not able to restore ATP levels. However, idebenone was able to rescue ATP levels when complex I was inhibited with rotenone. This is especially noteworthy, since (i) complex I is dysfunctional in LHON and MELAS [Mackey *et al.* 1996, James *et al.* 1996, Kirby *et al.* 2004, McKenzie *et al.* 2004, and Malfatti *et al.* 2007], and (ii) idebenone was reported to ameliorate some symptoms in these patients [Mashima *et al.* 1992, Ikejiri *et al.* 1996, Napolitano *et al.* 2000, Carelli *et al.* 1998, and Mashima *et al.* 2000]. Hence, by inhibiting complex I in HepG2 cells relying on mitochondrial energy production, a potential disease-relevant model system to test the mode of action of idebenone was established.

The drop of ATP induced by complex I inhibition could be counteracted by two possible modes: idebenone either blocked the inhibitory effect of rotenone or enabled the synthesis of new ATP independent of complex I. To rule out the possibility that the observed rescue in ATP levels by idebenone was not an artifact of rotenone administration, but was indeed specific to complex I deficiency, six other inhibitors of complex I were employed in the same model system [Table 2]. Interestingly, the beneficial effect of idebenone was observed only when

⁸ NQO1 promotes the reduction of idebenone.

⁹ A similar effect was also observed when dicoumarol was substituted with PCP. Drop in ATP levels induced by oxidized idebenone was only observed when glycolysis was suppressed, since in presence of galactose (whose conversion into pyruvate by glycolysis does not yield in net ATP generation), depletion of ATP content after dicoumarol and idebenone treatment was not observed.

rotenone, metformin, or—to a lesser extent—pyridaben were used to inhibit complex I. However, this was not surprising, since some of these inhibitors are known to bind to different targets which might be involved in the mode of action of idebenone-mediated ATP recovery. For example, class C inhibitors, i.e. stigmatellin and capsaicin, also block complex III activity as well [Degli Esposti 1998] and both berberine and rhein inhibit several oxidoreductases related to NADH:cytochrome P450 oxidoreductase [Tang *et al.* 2009, Zhou *et al.* 2011]. Rescue in presence of pyridaben was only minor; however, pyridaben was described to be a stronger inhibitor of complex I than rotenone [Degli Esposti 1998]. Thus, the fact that the ATP rescue was still observable in presence of two complex I inhibitors other than rotenone suggests that this model system is in fact based on complex I inhibition. Since the ATP rescue mediated by idebenone was independent of the mode of complex I inhibition, it seemed likely that idebenone promotes *de novo* synthesis of ATP. Indeed, idebenone rescued ATP levels when given to cells long after rotenone addition. For example, 5-min treatment with idebenone of cells subjected to rotenone for 55 min resulted in ATP levels that were only slightly lower than those induced by simultaneous administration of idebenone and rotenone. This also suggests that idebenone is quickly absorbed and that restoration of decreased ATP levels can occur extremely fast.

Hence, an *in vitro* model system for *de novo* ATP synthesis in complex I-deficient cells was established which showed promising relevance in regards to clinical phenotypes of mitochondrial disorders.

4.5 ATP Restoration in Presence of Dysfunctional Complex I Is Carried Out by Cytosolic-Mitochondrial Electron Shuttling

It was then of interest to find out how this restoration of ATP content in cells with dysfunctional complex I was achieved by idebenone. The difficulty of this task lies in the fact that idebenone is a multi-target drug for it has been reported to modify various cellular pathways and interact with several enzymes and enzyme complexes. Among others for example, idebenone was described to block voltage-gated Ca^{2+} channels [Houchi *et al.* 1991, Chang *et al.* 2011, Kaneko *et al.* 2011, and Newman *et al.* 2011]. Nevertheless, the main characteristic assigned to idebenone is its function as an antioxidant [amongst others Mordente *et al.* 1998, Jauslin *et al.* 2002, and Abdel Baky *et al.* 2010]. Interestingly, there is evidence that inhibition of complex I by rotenone increases ROS levels [Lenaz *et al.* 2002, Fato *et al.* 2008], and that rotenone fatally disrupts Ca^{2+} homeostasis which could also be a trigger for rotenone-induced cell death [Wang and Xu 2005, Freestone *et al.* 2009]. It was therefore plausible to question if the restoration of ATP levels induced by idebenone in presence of rotenone resembled inhibition of necrotic or apoptotic pathways activated by rotenone treatment, antioxidant detoxification of rotenone-induced damage, or amelioration of Ca^{2+} homeostasis deranged by rotenone [Figure 48A].

Idebenone could also directly block the inhibitory action of rotenone [Figure 48B]. However, since idebenone was able to rescue ATP levels in presence of complex I inhibitors other than rotenone, it is unlikely that this effect is dependent on the mode of complex I inhibition.

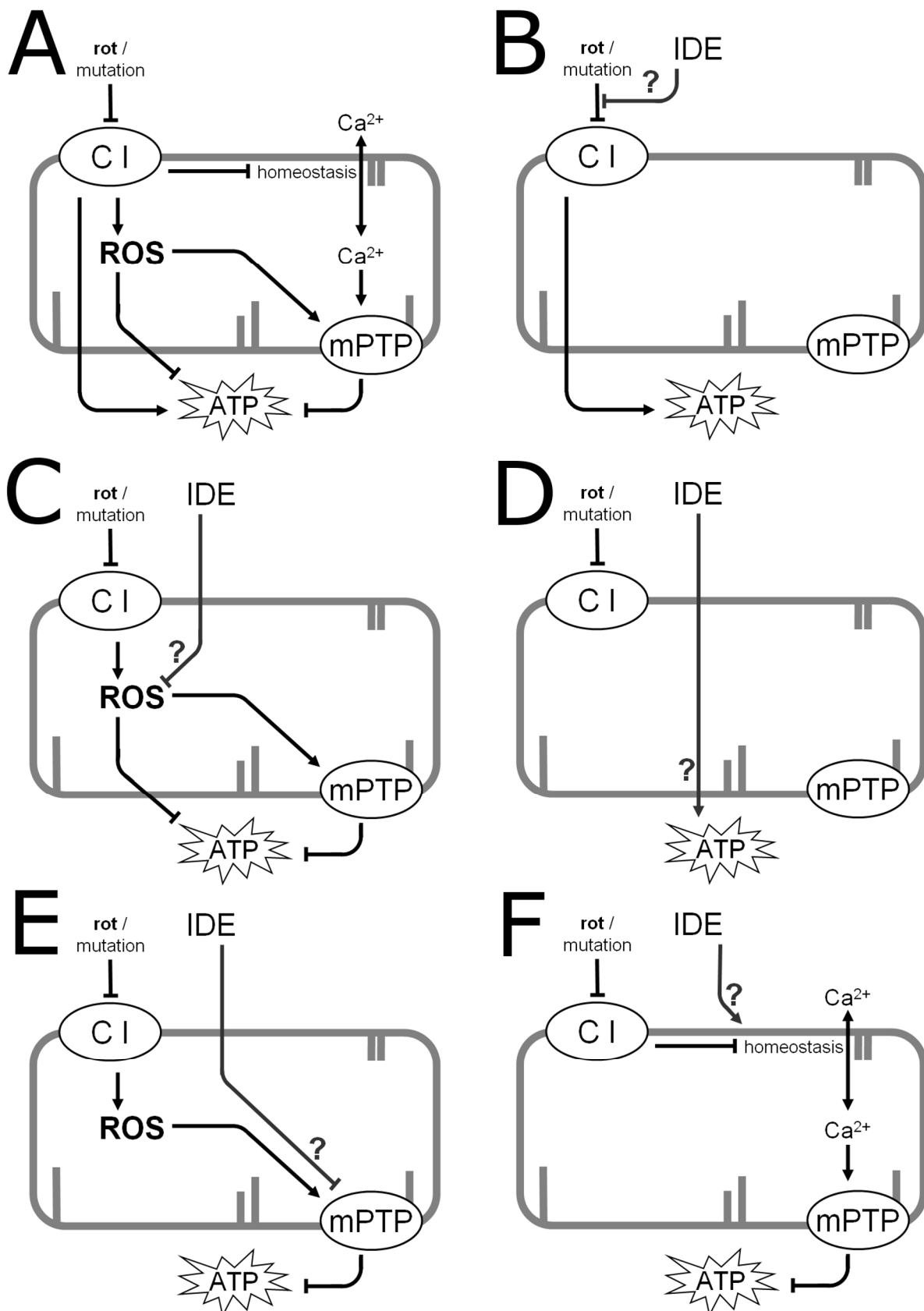


Figure 48: Potential Scenarios and Targets for Idebenone-Mediated ATP Rescue in Complex I-Deficient Cells.

(A) In cells with a deficient complex I (CI), either by reason of rotenone (rot) inhibition or mutation, several pathways are reported to be altered: ATP production is reduced [*own data*], reactive oxygen species (ROS) levels are elevated [Lenaz *et al.* 2002, Fato *et al.* 2008], and calcium (Ca²⁺) homeostasis is disturbed [Wang and Xu 2005, Freestone *et al.* 2009]. Increased levels of ROS and intracellular Ca²⁺ force the mitochondrial permeability transition pore (mPTP) to open which in turn leads to cell death [Gieseler *et al.* 2009, Kinnally *et al.* 2011]. This multitude of possible pathways for rotenone-induced ATP depletion suggests that idebenone (IDE) might rescue ATP levels by preventing the inhibition of complex I by rotenone (B), via an antioxidant effect (C), directly (D), by blocking the opening of mPTP (E), or by maintaining Ca²⁺ homeostasis (F).

The antioxidants *N*-acetyl-*L*-cystein (NAC) and tempol were added to glucose-deprived cells in presence of rotenone to see whether they might restore ATP levels comparable to idebenone. Controversially, whereas tempol was not able to counteract the drop in ATP, NAC showed a small, but significant rescue of ATP levels. However, this increase was not specific to complex I inhibition by rotenone, since NAC ameliorated cellular energy levels also in presence of an uncoupler of mitochondrial respiration or when complex III or ATP synthase were dysfunctional. In contrast, idebenone was not able to show a beneficial effect under these conditions. Therefore, it seemed that NAC might employ a mode of action not related to that of idebenone, and—in line with the inefficacy of tempol—the observed restoration of ATP levels in complex I-deficient cells by idebenone was not associated to its antioxidant effect [Figure 48C].

A second possibility for the ATP rescue in presence of rotenone was a connection between rotenone toxicity and cellular Ca^{2+} imbalance [Gieseler *et al.* 2009 and Figure 48F]. The Ca^{2+} ionophore A23187, which enables Ca^{2+} influx into cells, indeed decreased ATP levels. A23187 seemed to severely disturb Ca^{2+} homeostasis for even a membrane-permeable Ca^{2+} chelator, BABTA-AM, was not able to prevent the detrimental energy crisis triggered by Ca^{2+} overload. For that reason, Ca^{2+} was likely to activate secondary pathways which were fatal to both cells and mitochondria: increased levels of intracellular Ca^{2+} increase the probability for mitochondrial permeability transition pore (mPTP) to open which then triggers both necrotic and apoptotic pathways [Kinnally *et al.* 2010]. For example, opening of mPTP allows cytochrome *c* to enter the cytosol where it activates caspase 9, a protease involved in apoptosis [Lee *et al.* 2008]. Furthermore, ions and molecules intrude mitochondria through the mPTP following a concentration gradient and entrain H_2O which causes mitochondria to swell. Swelling disrupts the mitochondrial membrane and thereby destroys the proton gradient required to generate ATP. In addition, cellular ATP levels are further decreased by hydrolysis in order to maintain the proton gradient [Gardew *et al.* 2010]. Accordingly, rotenone could induce Ca^{2+} -mediated opening of the mPTP [Gieseler *et al.* 2009] which could account for the observed ATP drop.

Intriguingly, idebenone prevented mitochondrial swelling in isolated mitochondria [Suno and Nagaoka 1989b, Sokol *et al.* 2005] and CoQ_0 and decylQ were described as inhibitors of mPTP opening comparable to cyclosporin A [Fontaine and Bernardi 1999]. These findings suggested that the restoration of ATP content by idebenone in presence of rotenone might be due to inhibition of mPTP opening. However, both cyclosporine A and CoQ_0 were not able to rescue ATP levels under these conditions. In line with this, idebenone did not rescue ATP levels in cells treated with A23187. Thus, it seemed unlikely, that the mode of action of ATP rescue was dependent on Ca^{2+} imbalance and mPTP opening [Figure 48E&F].

A further potential mechanism responsible for induction of ATP synthesis is via the AMP-activated protein kinase (AMPK). Energy shortage activates AMPK by phosphorylation of threonine 172 (Thr172) which in turn promotes the employment of alternative sources of energy production by increasing glucose and fatty acid uptake, β -oxidation, and induction of mitochondrial biogenesis [Hutchinson *et al.* 2007, Han *et al.* 2010, and Kelly *et al.* 2010]. Since the ATP-conserving effect of idebenone was conducted already after a short time, phosphorylation of Thr172 was analyzed after 15 min. However, phosphorylation pattern of AMPK was not affected by idebenone treatment.

Hence, it seemed that the drop in ATP levels was solely due to inhibition of complex I-dependent ATP synthesis and the antagonizing effect of idebenone was conducted by actuating *de novo* ATP synthesis [Figure 48D]. Several groups reported that idebenone is a good substrate for complex III [Sugiyama *et al.* 1985, Sugiyama and Fujita 1985, Degli Esposti *et al.* 1996a, Rauchová *et al.* 2008]. This enzyme complex plays a pivotal role in the ETC. Not only does it re-oxidize $\text{H}_2\text{-CoQ}_{10}$ converted by any of the many mitochondrial quinone oxidoreductases, but also adds to the proton gradient across the inner membrane. Given that idebenone was not able to rescue ATP levels when complex I was inhibited by class C inhibitors such as stigmatellin, which also blocks complex III activity, led to the assumption that the *de novo* ATP synthesis by idebenone could be promoted via complex III. In order to test this hypothesis, the ATP rescue experiment was conducted in presence of the complex III inhibitor antimycin A. Indeed, antimycin A successfully blocked the restoration of ATP levels by idebenone, indicating that complex III is required for this beneficial effect.

The involvement of complex III elucidated the mode of action by which idebenone is able to restore ATP levels in complex I-deficient cells. In order to interact with complex III, idebenone has to be reduced. Reduced idebenone is thought to donate electrons to cytochrome *c* via complex III and might thereby maintain mitochondrial respiration as a substitute for CoQ_{10} . However in this scenario it is imperative to elucidate how idebenone is reduced prior to its interaction with complex III.

In contrast to the lipophilic physiological electron carrier of the ETC, CoQ_{10} , idebenone is an amphiphile—i.e. it is both lipophilic and hydrophilic¹⁰—and could therefore be reduced by both cytosolic and membrane-bound oxidoreductases. Experiments by King *et al.* [2009] confirmed that idebenone could interact with both the CoQ_{10} -binding pocket of complex I (which requires entrance via the lipophilic inner mitochondrial membrane) and the NADH binding site of complex I (which is exposed to the aqueous mitochondrial matrix).

One of the main oxidoreductases to reduce quinones in cellular systems is NAD(P)H:quinone oxidoreductase (NQO1) [O'Brien 1991, Monks *et al.* 1992] and NQO1-dependent reduction of idebenone analogs CoQ_0 and

¹⁰ Calculated log D values (Advanced Chemistry Development Software Package, Version 12, ACD Labs, Toronto, Canada) for idebenone and CoQ_{10} are 3.91 and 19.12, respectively [Haefeli *et al.* 2011]. Log D values are a measure for lipophilicity incorporating ionization of the compound in which small values indicate affinity for the aqueous phase.

CoQ₁ were previously confirmed *in vitro* [Chan *et al.* 2002, Audi *et al.* 2003]. Indeed, when cells with exogenously blocked complex I were subjected to the NQO₁ inhibitor dicoumarol, idebenone failed to restore ATP levels.

Although suggestive as a model, a direct interaction of idebenone and NQO₁ had to be confirmed. In experiments with recombinant NQO₁ protein, idebenone was able to oxidize both NADH and NADPH, the reductive substrates of NQO₁. Turnover rates of idebenone were comparable to those of CoQ₁, and in line with previous reports of CoQ₁ reduction by NQO₁ [Beyer *et al.* 1996]. In addition, idebenone was shown to competitively inhibit 2,6-dichlorophenolindophenol (DCPIP) reduction, whose role as electron acceptor for NQO₁ was described by Cabello *et al.* [2009 and 2011], indicating that both compounds are converted by the same mechanism.

Thus, idebenone is a substrate for recombinant NQO₁. Nevertheless, reduction of idebenone by NQO₁ had also to be confirmed *in vitro*. Tan and Berridge [2010] presented an assay measuring NQO₁-dependent conversion of a hydrophilic quinone which based on a reduction-dependent change in absorption of the tetrazolium dye WST-1. The authors demonstrated that WST-1 is converted only in the presence of functional NQO₁, since inhibition of enzymatic activity by dicoumarol abolished WST-1 reduction. Furthermore, the dye was potently reduced in cells expressing NQO₁, but failed to change absorption in NQO₁-deficient cells such as CHO cells. Indeed, results of WST-1 assays revealed that idebenone was reduced by NQO₁ *in vitro* in a dicoumarol-sensitive manner.

Although dicoumarol was described to be a selective NQO₁ inhibitor [Ernster *et al.* 1962], WST-1 is supposedly only reduced in presence of NQO₁, and dicoumarol potently inhibited recombinant NQO₁ activity in consistency with previous reports [Wu *et al.* 1997, Long II and Jaiswal 2000], the possibility of interference with potential off-targets *in vitro* could not be completely excluded. In order to attribute the findings in ATP rescue and WST-1 experiments to NQO₁, inhibition of NQO₁ activity was achieved by short hairpin RNA (shRNA)-mediated knock-down. Even though gene silencing using shRNA-expressing lentiviral particles did not result in a complete knock-down of NQO₁, the rate of *in vitro* reduction of idebenone and its capacity to restore ATP content in presence of rotenone decreased.

Experiments in cells varying in NQO₁ content were in line with this finding, since the capacity to restore ATP levels in presence of rotenone was dependent on NQO₁ levels quantified by qPCR [Haefeli *et al.* 2011] and western blot [*personal communication with D. Robay*], providing additional evidence that the beneficial effect of idebenone was in fact associated to this oxidoreductase. For example, in NQO₁-deficient cells (HEK293 and SH SY5Y), neither ATP rescue in presence of rotenone or reduction of idebenone was observed with the latter mirroring results described for CHO cells devoid of NQO₁ [Tan and Berridge 2010]. However, with increasing levels of NQO₁, the amount of restoration of ATP levels depleted by rotenone was elevated again, suggesting a pivotal role for NQO₁ in idebenone-induced ATP *de novo* synthesis in complex I-deficient cells. In addition, the fact that this mechanism was observed as well in other NQO₁-expressing cells than HepG2 indicated that this beneficial effect of idebenone was not cell type-specific [Haefeli *et al.* 2011]. Even more, ATP rescue was also observed in freshly isolated mouse hepatocytes treated with rotenone and idebenone.

In conclusion, the previous results concerning how idebenone restores ATP levels in cells with dysfunctional complex I could be incorporated into a mechanistic mode of action [Figure 49]. As the experiments pointed out, ATP rescue was dependent on complex III and NQO₁. A substantial amount of literature confirmed that idebenone is readily oxidized by complex III [Sugiyama *et al.* 1985, Sugiyama and Fujita 1985, Degli Esposti *et al.* 1996a, Rauchová *et al.* 2008], whereas interaction of idebenone with NQO₁ was shown here for the first time and the reduction of idebenone by NQO₁ was proven by various independent experiments. Since the amphiphilic idebenone can be found in both aqueous and lipid environment, it seems likely that it is first reduced within the cytosol by NQO₁ and subsequently re-oxidized by complex III within the inner mitochondrial membrane. Thereby, electrons from cytosolic NAD(P)H are transferred into the ETC and—by circumventing complex I—mitochondrial ATP synthesis can be accomplished. Since the reduced idebenone is oxidized back into its quinone form by complex III, a new cycle can be triggered resulting in a idebenone-driven electron shuttle from cytosolic NAD(P)H to mitochondrial cytochrome *c* [Figure 49].

This mode of action requires an amphiphilic quinone which can easily commute between cytosol and mitochondria. In this regard, the lipophilic CoQ₁₀ should not be able to restore ATP levels in the described model system. Indeed, when CoQ₁₀ was added to rotenone-treated HepG2 cells, ATP content remained depleted after one hour. In additional experiments, CoQ₁₀ was not reduced by NQO₁ in both cells and when given to recombinant enzyme; not even when complexed with fetal bovine serum (FBS) or incorporated into phosphatidylcholine-based liposomes to increase its solubility in water [Mayer *et al.* 1985, Paolino *et al.* 2004]. The reason for the extremely poor reduction of CoQ₁₀ by NQO enzymes most likely originates from compartmentalization of enzyme and substrate. While NQO₁ and NQO₂ are strictly cytosolic enzymes [O'Brien 1991, Long II and Jaiswal 2000], CoQ₁₀ is only found integrated into biological membranes under physiological conditions [Lenaz 2001]. Therefore, CoQ₁₀ cannot participate in this cytosolic-mitochondrial shuttling of electrons. Consistently, even prolonged cellular exposure to CoQ₁₀ for up to one week failed to trigger an ATP rescue when complex I was dysfunctional.

This proposed mechanism can rationalize the observed beneficial effects of idebenone in two disorders with impaired complex I, MELAS and LHON [see 4.11]. Given the central role of NQO₁ for the beneficial effects of idebenone, it is imperative to point out that multiple polymorphisms in the NQO₁ gene are described in the general population. Of 200 single nucleotide polymorphisms described for NQO₁ (NCBI;

<http://www.ncbi.nlm.nih.gov/projects/SNP>), 11 change the coding sequence. Out of those, the 609C>T (Ser187) polymorphism is the most intensively studied, since it destabilizes the NQO1 protein. NQO1 activity is reduced to 50% in heterozygous carriers and almost completely eliminated in homozygous carriers, respectively [Guha *et al.* 2008]. Heterozygosity of the allele is prevalent in approximately 50% of the Chinese population and one sixth of Caucasians, whereas homozygous carriers amount to 5-20% in all ethnics. The high prevalence of just this single polymorphism indicates that overall a big portion of the general population might harbour polymorphisms within NQO1 that could affect their response to idebenone. Therefore, this possibility should be considered in future clinical trials to expose a functional difference within patient populations in responder analysis approaches.

For a mechanistic understanding of this mode of action, findings obtained with idebenone were expanded to other short-chain quinones. For CoQ₁, both NQO1-dependent reduction and cytosolic-mitochondrial shuttling were described [Chan *et al.* 2010] and confirmed in own experiments. Reduction by NQO1 was also found for the idebenone metabolite QS-10 [Okamoto *et al.* 1998] using recombinant enzyme or WST-1 conversion in a cellular system. Despite turnover rates comparable to idebenone and CoQ₁ (although slightly reduced), QS-10 was not able to restore ATP levels in cells with dysfunctional complex I. QS-10 is significantly more hydrophilic than idebenone and CoQ₁, as manifested in a smaller log D value (3.91 for idebenone, 2.41 for CoQ₁, and 1.18 for QS-10). It is therefore less likely that reduced QS-10 can pass through the lipophilic mitochondrial membrane to donate the electrons to complex III. This could also account for the failure of the highly polar CoQ₀ to restore ATP content in rotenone-treated cells. In contrast, both CoQ₂ and decylQ, which have comparable polarity to idebenone and CoQ₁, were also able to show ATP rescue and were reduced by NQO1 *in vitro*. Similarly to CoQ₁₀, the lipophilic CoQ₄ did not restore ATP levels in rotenone-treated cells.

Thus, these findings imply several requirements for this form of cytosolic-mitochondrial respiration. Not only is it necessary for quinones to enter the cytoplasm and show efficient reduction by NQO1, these compounds must also be able to enter the mitochondria. Then, within the mitochondria, they must be able to interact with complex III of the respiratory chain and release electrons that contribute to the mitochondrial proton gradient which is necessary for ATP synthesis [Figure 49].

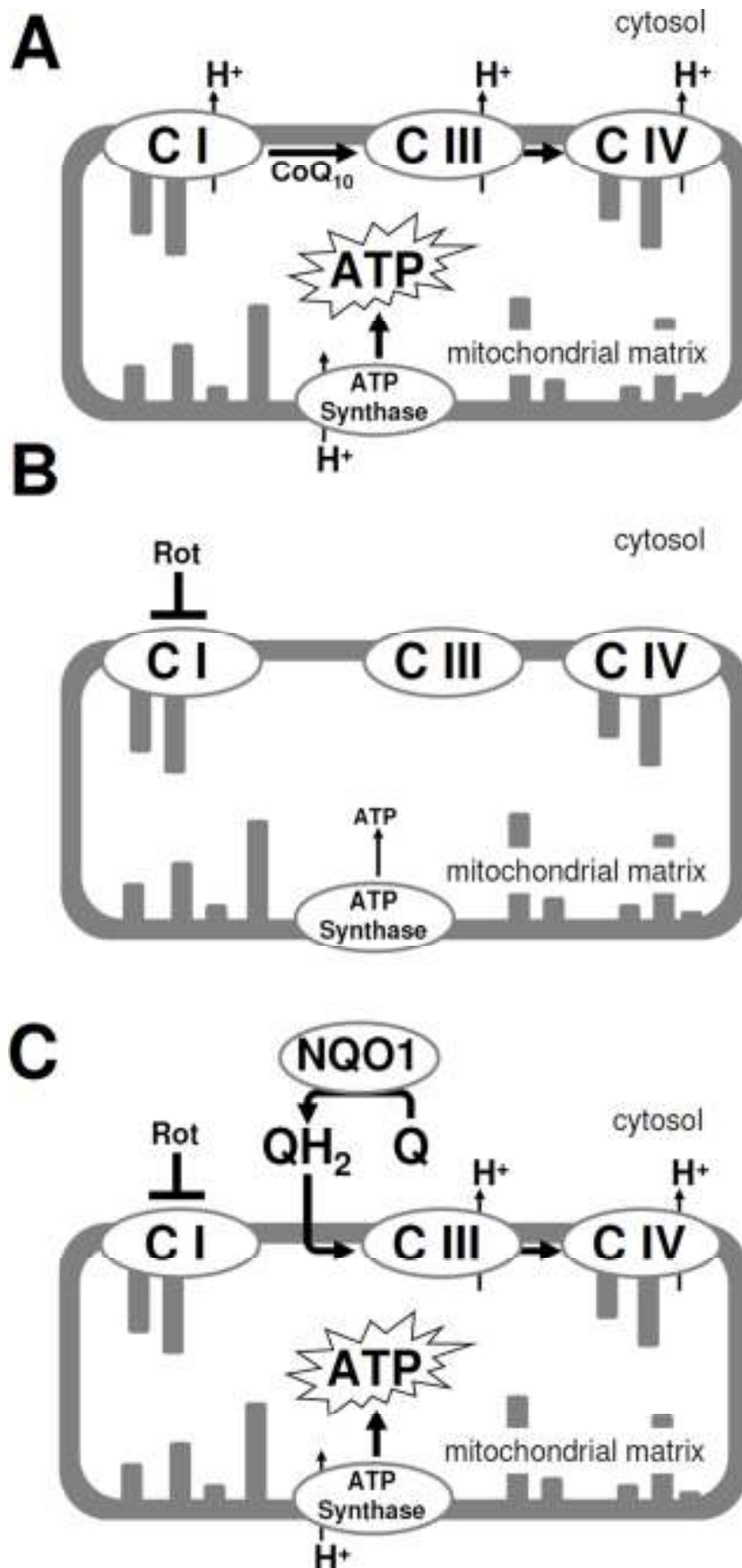


Figure 49: Schematic representation of NQO1-dependent cytosolic-mitochondrial electron shuttling.

(A) During oxidative phosphorylation under normal conditions, CoQ_{10} transports electrons from complex I (CI) to complex III (CIII) and cytochrome *c*, reduced by complex III, transfers them to complex IV. As a consequence of this electron propagation, all three complexes translocate protons (H^+) across the mitochondrial membrane, thus generating a proton gradient. ATP synthase utilizes the energy stored in this electro-chemical gradient to generate ATP. (B) Upon rotenone-induced (Rot) inhibition of complex I, ATP levels decrease dramatically. (C) Some short-chain quinones (Q) such as idebenone or CoQ , can bypass complex I inhibition via a cytosolic-mitochondrial shuttling of electrons. Upon reduction by cytosolic NQO1 (QH_2), these quinones can feed electrons into the mitochondrial respiratory chain in a complex III-dependent manner, thereby restoring ATP production.

4.6 Idebenone Is Reduced by Other Oxidoreductases than NQO1 as Well

Although the reduction of idebenone by NQO1 was thoroughly demonstrated in various experiments, it seemed unlikely that NQO1 was the only cytosolic oxidoreductase reacting with idebenone, regarding the vast number of oxidoreductases and even more considering that idebenone was reported to interact with mitochondrial oxidoreductases. Besides the aforementioned associations with complexes I, II, and III; glycerol-3-phosphate dehydrogenase (G3PDH) was also shown to reduce idebenone [Rauchová *et al.* 2008 and 2011]. G3PDH is used to shuttle electrons from cytosolic NADH onto CoQ₁₀ or quinone analogs such as idebenone which are in turn oxidized by complex III. In addition, Frerman and Šimkovič [2004] reported that idebenone was a good substrate for electron-transferring-flavoprotein dehydrogenase (ETFDH), the enzyme responsible for the donation of electrons from β -oxidation to the ETC via CoQ₁₀.

Furthermore, due to their reactivity, many quinones exhibit toxic features that are sometimes employed by organisms on purpose in order to protect themselves from natural enemies [Monks *et al.* 1992]. On this account, several enzymes used for detoxifying xenobiotics are able to reduce quinones. Among these detoxifying enzymes are not only NQO1 or NQO2, but also NADH:cytochrome p450 oxidoreductase and NADH:cytochrome b₅ reductase. In order to test if the ATP rescue mediated by idebenone in cells with dysfunctional complex I was not only dependent on NQO1, but also other oxidoreductases, this experiment was conducted in presence of inhibitors for ETFDH, NQO2, NADH:cytochrome p450 oxidoreductase, and NADH:cytochrome b₅ reductase. However, since many of these enzymes share structural analogies, a common problem of these inhibitors is a lack of specificity. Indeed, all of the tested inhibitors partially inhibited the activity of recombinant NQO1. In addition, diphenylene iodonium (DPI) which blocks NADH:cytochrome p450 was also described to inhibit complex I [Degli Esposti 1998]. Interestingly, reduction of idebenone measured by WST-1 assay and ATP restoration mediated by idebenone in presence of impaired complex I was not blocked by any of these inhibitors – with the exception of pentachlorophenol (PCP). This is noteworthy, since PCP showed the same degree of NQO1 inhibition in experiments with recombinant enzyme as the remaining inhibitors and therefore, the objection that the prevention of idebenone-mediated cytosolic-mitochondrial electron shuttling was due to inhibition of NQO1 could be abandoned. Intriguingly, this effect of PCP was only observed when idebenone was used, whereas in presence of CoQ₁₀, PCP failed to impede both ATP rescue and CoQ₁₀ reduction.

Hence, these experiments revealed a specific connection between PCP and idebenone. PCP was used to inhibit ETFDH for which idebenone was described as a good substrate [Frerman and Šimkovič 2004]. Strikingly, also CoQ₁₀, CoQ₂, and decylQ were converted by ETFDH in a comparable rate as idebenone, but PCP did not prevent reduction of these quinones *in vitro*, suggesting that not ETFDH was responsible for the specific link between PCP and idebenone, but another mechanism.

Nevertheless, involvement of ETFDH could not be excluded *a priori*. Therefore, ETFDH was knocked down using small interference RNA (siRNA). In cells subjected to ETFDH siRNA, idebenone was still reduced. Even though, these results should be regarded carefully, since siRNA-induced knock-down of NQO1 prevented reduction of idebenone less effectively than dicoumarol. Thus, the objection, that knock-down effects were too weak to sufficiently reduce enzyme expression, cannot be eliminated completely.

For this reason, the activity of ETFDH was blocked upstream. ETFDH links β -oxidation with the ETC [Frerman 1987]. During β -oxidation, the electron carrier FADH₂ is produced which donates its electrons onto electron-transferring flavoprotein (ETF). ETFDH catalyzes the electron transfer from ETF onto CoQ₁₀ which in turn supplies the electrons onto complex III. Using its (i) role as a conjunction between lipid metabolism and the ETC and (ii) the requirement of electrons derived from β -oxidation for its oxidoreductase activity, inhibition of β -oxidation should diminish reduction of idebenone if ETFDH was responsible for the effects observed in presence of PCP. However, inhibition of β -oxidation by 3-mercaptopropionic acid (MPA) or valproic acid (VPA) did not result in patterns comparable to the use of PCP in either WST-1 or ATP rescue experiments. Although each experiment on its own did not provide sufficient evidence to completely rule out the possibility of involvement of ETFDH in idebenone reduction or idebenone-mediated ATP rescue in rotenone-treated cells, the combination of both experiments made it unlikely, even more so since substrate affinity towards this enzyme did not substantially vary between idebenone and related quinones.

Unfortunately, the nature of the special relationship between idebenone and PCP could not be resolved in this thesis due to time constraints. Nevertheless, the finding that the redox properties of idebenone were specifically interconnected with PCP *in vitro* whilst leaving the conversion of analogous short-chain quinones unaltered provides sufficient indication for separating the action of idebenone from those of analogs. Despite structural similarities, short-chain quinones might vary substantially in their biologic activities [see 4.9]. Hence, further research of this topic is not only desirable, but very much required in order to identify an exclusive mode of action for idebenone.

4.7 Idebenone Inhibits Complex I *in Vivo* and Thereby Changes Metabolism

In vitro experiments revealed that idebenone is highly involved in mitochondrial energy production: not only by inhibiting complex I activity, but also to provide alternative mechanisms of ATP synthesis when complex I is dysfunctional. These mechanisms involve NQO1 activity and the glycerolphosphate shuttle [Rauchová *et al.* 2008 and 2011]. *Ex vivo* experiments in mouse hepatocytes revealed that idebenone-treated animals still

exhibited the capacity to restore ATP levels when subjected to rotenone. This is surprising, given the facts that (i) idebenone has a short half life *in vivo* with a peak around 15 min after administration [*pharmacokinetic reports from Takeda and data by F. Heitz*] Furthermore, this problem was replicated *in vitro* where (ii) idebenone was unable to rescue ATP levels in cultured cells when administered one week before the rotenone challenge. However, a potential explanation for this discrepancy will be discussed within this subchapter. This hypothesis was directly indicated by the results obtained when investigating possible metabolic changes *in vivo* by idebenone and represents a totally new mode of action for this molecule.

In the literature, only few studies reported any impact of idebenone on *in vivo* metabolism, and a great many thereof were conducted in ischemia models, suggesting that idebenone attenuated ischemic harm by increasing energy metabolism and reducing oxidative damage [Nagaoka *et al.* 1989, Kakihana *et al.* 1998, and Abdel Baky *et al.* 2010]. Solely Sugiyama and Fujita [1985] investigated metabolism-related effects of idebenone on healthy animals and surprisingly reported an increase in complex I-mediated mitochondrial respiration in isolated mitochondria of idebenone-treated rats.

On the contrary, the vast majority of literature examining the relation of idebenone and complex I, including experiments described in this work, favor an inhibitory role on complex I activity of idebenone [Sugiyama *et al.* 1985, Degli Esposti *et al.* 1996a, Brière *et al.* 2004, Geromel *et al.* 2008, Fato *et al.* 2008, Rauchová *et al.* 2008, and King *et al.* 2009], suggesting that complex I inhibition could also occur *in vivo*. *In vitro*, usage of idebenone or rotenone to block complex I activity resulted in a general ATP decrease. Adopting these findings to *in vivo* experiments would suggest that ATP content in tissue would be decreased in idebenone-treated animals; which however was not found. In this context it has to be pointed out that, *in vivo* impairment of mitochondrial respiration is usually compensated by the organism by engaging alternative sources of energy supply. The easiest mechanism for providing cells with sufficient energy would be to increase glucose uptake and glycolysis, probably by increasing the food intake.

Indeed, in mice treated with idebenone for three to four weeks with 200-400 mg/kg/day idebenone mixed in food, food intake was significantly elevated by idebenone, whilst body weight did not increase compared to control group. Although this uncoupling of calorie intake and weight gain was robust and reproducible¹¹, and seemed to be a consequence of the reported complex I inhibition by idebenone, this *in vivo* effect of idebenone was described for the first time in this thesis. Additional affirmation was obtained by experiments with another complex I inhibitor, metformin, for which lower hepatic glucose release and higher rates of glucose consumption in peripheral tissues—and thus, decreased blood glucose levels—were reported [Periello *et al.* 1994, Baily and Turner 1996, Inzucchi *et al.* 1998, and Brunmair *et al.* 2004]. Indeed, single-dose *p.o.* administration of idebenone resulted in a transient reduction of blood glucose levels, the timing of which was in line with its short half life *in vivo*. Considering the route of administration in experiments measuring the influence of idebenone on food intake and body weight—i.e. idebenone is administered constantly during feeding—complex I inhibition would not be a short-lived, once-a-day event, but coincide with food intake and thus, incessantly promote supplementary food intake.

The dependency on a mechanism involving complex I inhibition for the increase the food intake relative to body weight by idebenone was further consolidated by the dismissal of other potential explanations. In my experiments, idebenone did not increase energy expenditure by promoting higher locomotion or by elevation of body temperature which is usually accomplished by mitochondrial uncoupling [Richard and Picard 2011]. In addition, idebenone did not induce a change in body composition between fat and muscle tissue which could account for compensating measurable weight. Finally, the observed increase in relative food intake was not explained by any inhibition of insulin release.

The combination of excess food intake and unchanged body weight observed in idebenone-treated mice led to the assumption that idebenone-mediated complex I inhibition mimicked calorie restriction (CR) by a molecular mechanism. Indeed, in mice given limited amounts of food which solely allowed for maintenance of body weight, administration of idebenone led to weight loss [*personal communication by R. Dallmann*]. Furthermore, CR was reported to increase blood concentrations of β -hydroxybutyrate (β -HB) in C57Bl/6 mice. β -HB is a ketone body which can be used as an alternative source of energy [McGarry and Foster 1980]. Strikingly, β -HB was reported to rescue mitochondrial respiration in a Parkinson's disease model based on the complex I inhibitor 1-methyl-4-phenyl-1,2,3,6-tetrahydropyridine (MPTP) [Tieu *et al.* 2003]. Intriguingly, subchronic idebenone treatment of C57Bl/6 mice led to a trend of increased blood β -HB levels and to a slightly increased expression of 3-hydroxy-3-methylglutaryl-coenzyme A synthase 2 (HmgCoA), the enzyme responsible for β -HB production, in heart tissue. Ketone bodies give rise to acetyl-CoA, the starting product for the citric acid cycle (TCA). In this regard, it is noteworthy that idebenone was described to be a good substrate for complex II, a member of TCA [Sugiyama *et al.* 1985, Sugiyama and Fujita 1985, Imada *et al.* 1989, and Degli Esposti *et al.* 1996a]. Nevertheless, findings concerning ketone body synthesis induced by idebenone are disputable in regards to their poor statistical validity.

Hypothetically, transient idebenone-induced CR could account for the finding that idebenone prolonged life span in the nematode *caenorhabditis elegans* [*personal communication M. Ristow*]. Several studies showed that a

¹¹ In two out of seven experiments, idebenone did not induce an increase in food intake. However, some parameters varying in these experiments from others were accounted for the lack of this effect, as will be discussed below. Comparable results in experiments conducted in different mouse strains further confirmed that the effects were reliable.

decrease in calorie intake increases longevity in different species [Skinner and Lin 2010, Smith *et al.* 2010a] and several compounds such as the complex I inhibitor metformin are thought to mimic this effect [Anisimov *et al.* 2008, Smith *et al.* 2010b]. CR activates different pathways which promote mitochondrial biogenesis and energy production, and a shift in energy source from glucose to fatty acid consumption [Guarente 2008]. A pivotal role in these pathways is played by sirtuins which enable the expression of required genes by deacetylation of certain regions of DNA. As a consequence, sirtuins were implicated in life span extension by the CR-mimetic resveratrol in yeast, *c. elegans*, fruit flies, and mice [Howitz *et al.* 2003, Wood *et al.* 2004, and Baur *et al.* 2006]. Sirtuins require NAD^+ as a substrate in order to deacetylate DNA and an increase in NAD^+/NADH ratio was shown to activate sirtuin-dependent gene expression [Lin *et al.* 2004]. It is important to point out here that reduction of idebenone by NQO1 rapidly produces NAD^+ , as was measured using the fluorescent dye resazurin [Haefeli *et al.* 2011]. Hence, idebenone could not only initiate CR-related pathways by direct mimicking of CR, but also via NQO1-dependent sirtuin activation.

Ristow and Zarse [2010] proposed a pro-oxidant-driven mechanism for longevity which is related to CR pathways. According to this, sub-pathological doses of pro-oxidants provoke a mitochondrial-dependent adaptive response—called mitohormesis—which in turn increases the resistance to stress. Indeed, Nishimoto *et al.* [2010] reported that minor concentrations of H_2O_2 made cells less susceptible to stress at a later time point. In contrast, antioxidants were reported to block mitohormesis [Ristow and Zarse 2010]. This concept is noteworthy given the fact that idebenone might also exhibit mild pro-oxidant properties [see 4.8]. It also could explain why idebenone failed to show recovery in LHON patients when administered in combination with the antioxidant vitamin C [Barnils *et al.* 2007] which is contrary to reports showing that idebenone alone ameliorated the LHON phenotype [Mashima *et al.* 1992, Carelli *et al.* 1998, and Mashima *et al.* 2000, Klopstock *et al.* 2011]. In line with these findings, the relative food intake was not increased in idebenone-treated mice in an *in vivo* experiment using a food chow containing vitamin C (experiment 0423 [Table 10 in Appendix]). The results from Jauslin *et al.* [2007], who reported that a combination of idebenone and the antioxidant vitamin E was more potent in protection against oxidative stress-induced cell death, are not contradictory to this hypothesis. Whilst idebenone might indeed act as an antioxidant in the presence of oxidative damage, its mild pro-oxidant function could promote mitohormesis under physiological conditions. In this regard, it is noteworthy that pre-treatment with idebenone *in vivo* suppressed the formation of ROS induced by ischemic reperfusion injury in pig livers, whereas *ex vivo* treatment with idebenone could not counteract oxidative damage [Schütz *et al.* 1997, Wieland *et al.* 2000].

CR-induced longevity was found to be a conserved pathway in many species. In a simplified model, organisms mainly require energy for reproduction and maintenance of their own life and they have to divide their limited amount of energy between the two. In periods of reduced food supply, it would be disadvantageous to produce offspring due to (i) the high associated energy demand and (ii) their reduced survival chances due to a limitation of available nutrition. Thus, organisms must wait until environmental conditions become more suitable for breeding. By reducing energy consumption, CR does not only increase life span (and thus, the probability to reproduce when food supply becomes more promising), but it also represses reproductive functions [Grandison *et al.* 2011]. On the basis of single-cell organisms, this property of CR would translate in a reduction of proliferation. Indeed, idebenone suppressed proliferation in a highly dividing cell line, proving further evidence for this hypothesis.

The slight shift in energy source to the use of ketone bodies could also account for the finding that idebenone administered *in vivo* was still able to rescue ATP levels in isolated hepatocytes *ex vivo*. With regards to the short half life of idebenone *in vivo* [pharmacokinetic reports from Takeda and data by F. Heitz], it can be assumed that idebenone tissue levels at the time of the experiment were negligible from tissue and thus, the proposed cytosolic-mitochondrial electron shuttle should not have been functional anymore. However, as response to complex I inhibition or pro-oxidant activity of idebenone, cells could potentially shift their energy metabolism away from complex I-dependent respiration to the use of ketone bodies and fatty acids. Through this adaptation, inhibition of complex I by rotenone would not be as detrimental to cells as when they mainly rely on complex I.

Nevertheless, great efforts are still required to verify this hypothesis. A yet unsolved question, for example, is how idebenone could manage to promote transcription- and translation-dependent alterations when it barely altered gene expression as observed in micro array experiments. However, it is possible that the lack of observable gene expression was due to a timing effect of idebenone administration, since isolation of tissues was conducted several hours after last idebenone treatment [Figure 50]. It is likely that idebenone rapidly induces a transient transcriptional response in line with its PK profile. However, since some metabolism-related gene products display longer half lives of several hours, the induced proteins would be still present and functional after a rapid degradation of the corresponding mRNAs. This hypothesis can explain results which are otherwise difficult to reconcile with previously described modes of action of idebenone. Besides offering clues for a CR/mitohormesis hypothesis, animal experiment data provided for the first time significant evidence that complex I inhibition by idebenone described *in vitro* takes also place *in vivo*.

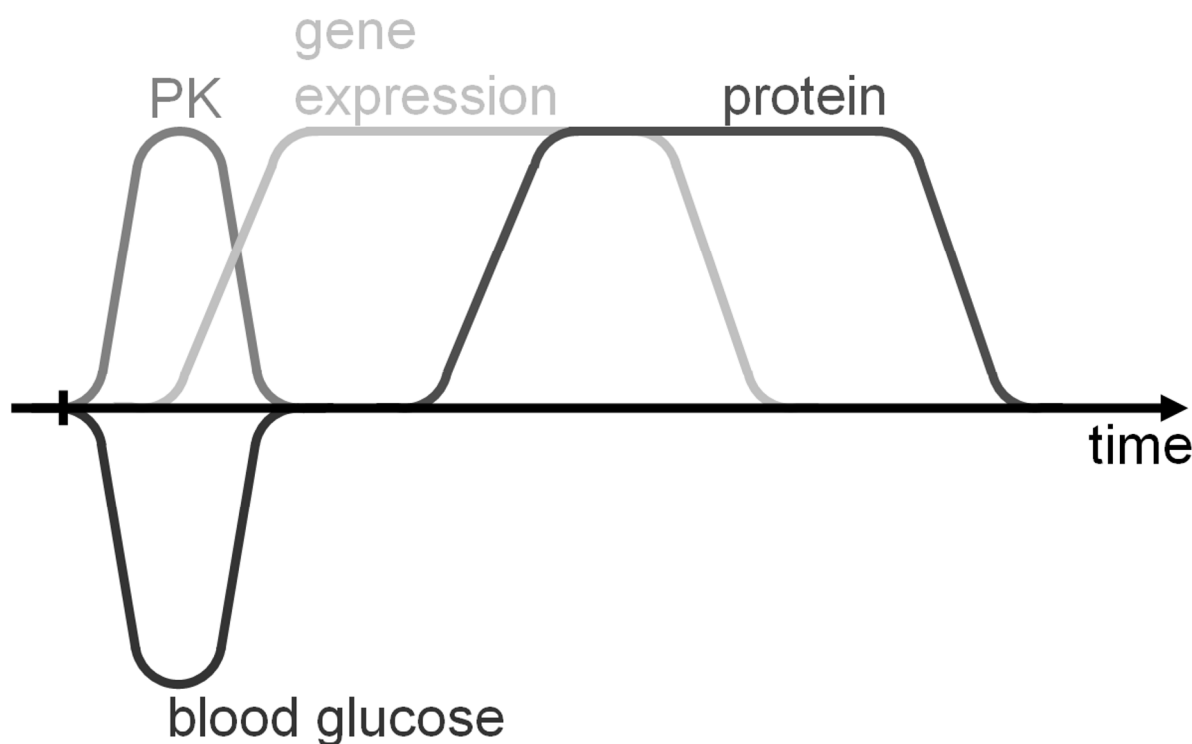


Figure 50: Timing Effects of Idebenone Administration and Suggested Development of Gene Expression and Protein Half Lives.

When given orally, pharmacokinetic experiments revealed that idebenone peaks around 15 min (PK). Consistent with this, blood glucose levels transiently drop 20 minutes after administration. Gene expression was not observed in tissue several hours after last idebenone administration. However, idebenone could still promote short-term transcription whose protein products would be functional long after administration.

4.8 Idebenone Is a Mild Pro-Oxidant

As consequence of complex I inhibition, idebenone was suggested to also act as pro-oxidant under certain conditions [Degli Esposti *et al.* 1996, Geromel *et al.* 2000, and Fato *et al.* 2008]. Indeed, some results described in this thesis support the notion that idebenone exhibits pro-oxidant properties. Nonetheless, these effects were only minor compared to exclusively pro-oxidant compounds such as hydrogen peroxide (H_2O_2) or to other short-chain quinones such as CoQ₁.

For example, chronic treatment with idebenone also seemed to have a similar, but milder effect on Akt-1 compared to short-term H_2O_2 stress *in vitro*. In fact, idebenone did not phosphorylate Akt-1 in contrast to H_2O_2 . Nonetheless, a modification of Akt-1 resulting in a 9 kDa heavier, yet unpublished protein was reduced by both H_2O_2 and idebenone. In contrast to idebenone, however, H_2O_2 prevented this modification completely. The difference in molecular weight and the distinctiveness of the according band in western blot analysis suggested that this modification was due to posttranslational modification of Akt-1 such as the ligation to a small ubiquitin-like modifier (SUMO). Intriguingly, further experiments in our lab demonstrated that this modified Akt-1 was only observed when cells were lysed using SDS which solubilizes all membranes and most higher order protein complexes [personal communication with M. Erb and D. Robay]. In this regard, it is noteworthy that SUMOylation of proteins is associated with their cytosolic-nuclear transport [Matunis *et al.* 1996]. Nevertheless, characterization of the modification and the resulting implications to the bioactivity of idebenone would have exceeded the scope of this work. The important conclusion drawn from this experiment is, however, that idebenone indeed showed a mild pro-oxidant effect.

In contrast to results suggesting a pro-oxidant function of idebenone, there is ample evidence that the picture is more complex. Pro-oxidants damage cellular macromolecules such as lipids or DNA. However, idebenone is most prominently known for its action as antioxidant. In fact, it was described to reduce lipid peroxidation *in vitro* and *in vivo* under conditions of oxidative stress [Suno and Nagaoka 1989a&b, Suno *et al.* 1989, Cardoso *et al.* 1998, Mordente *et al.* 1998, and Abdel Baky *et al.* 2010] and own experiments showed that idebenone did not increase lipid peroxidation when given to unchallenged cells. Further investigations revealed that idebenone did not induce DNA double breaks in different cell types regardless of NQO1 expression levels. NQO1 reduces idebenone and thereby, detoxifies a potential pro-oxidant effect. Indeed, NQO1 produces equilibrium between quinone and hydroquinone, whereat increasing levels of NQO1 lead to a higher concentration of hydroquinone [Merker *et al.* 2007]. In contrast, an idebenone analog, CoQ₁, for which pro-oxidant effects were assumed as well [Lenaz *et al.* 2002] increased both DNA damage and lipid peroxidation.

Furthermore, a striking concentration-dependency towards the shift in pro- and antioxidant properties of idebenone was found. Whereas concentrations up to 1 μM idebenone reduced H_2O_2 -induced ROS, 10 μM

idebenone led to a completely contrary result. H₂O₂ treatment was assumed to increase mitochondrially generated ROS, and the pro-oxidant function of idebenone was associated to its inhibition of complex I [Fato *et al.* 2008, Geromel *et al.* 2008]. Considering the IC₅₀ of 5.9 μM for complex I inhibition by idebenone, one could argue that the amplification of H₂O₂-induced ROS levels is achieved by increasing mitochondrial ROS production.

In conclusion, idebenone might both exhibit pro- and antioxidant activity; however, pro-oxidant properties of idebenone seem to be rather minute and are not sufficient to question its good safety record.

4.9 Idebenone Analogs Exhibit a High Disparity in Biological Function

Next to the unusual dose effect in scavenging or promoting H₂O₂-induced ROS, the activities of idebenone are not easy to characterize. This is due to the multi-target properties of idebenone covering a broad range of cellular functions [Table 11 in the appendix] including **(i)** action as an antioxidant [Suno and Nagaoka 1989a&b, Suno *et al.* 1989, Amada *et al.* 1995, Cardoso *et al.* 1998, Mordente *et al.* 1998, Rego *et al.* 1999, Rustin *et al.* 1999, Sortino *et al.* 1999, Wieland *et al.* 2000, Yerushalmi *et al.* 2001, Gumprich *et al.* 2002, Jauslin *et al.* 2002, 2003, and 2007, Gil *et al.* 2003, Sokol *et al.* 2005, Rauchová *et al.* 2006, and Abdel Baky *et al.* 2010], **(ii)** altering energy status, probably by interaction with the ETC [Shinamoto *et al.* 1982, Yu *et al.* 1982, Sugiyama *et al.* 1985, Sugiyama and Fujita 1985, Imada *et al.* 1989, Nagaoka *et al.* 1989, Degli Esposti *et al.* 1996a, Degli Esposti 1998, Kakihana *et al.* 1998, Lenaz *et al.* 2002 and 2007, Brière *et al.* 2004, Rauchová *et al.* 2008, and King *et al.* 2009, and Watze *et al.* 2010], **(iii)** inhibition voltage-gated Ca²⁺ channels [Houchi *et al.* 1991, Chang *et al.* 2011, Kaneko *et al.* 2011, and Newman *et al.* 2011], **(iv)** protection from cell death [Miyamoto *et al.* 1990, Houchi *et al.* 1991, Sortino *et al.* 1999, Yerushalmi *et al.* 2001, Gumprich *et al.* 2002, Jauslin *et al.* 2002, 2003, and 2007, Gil *et al.* 2003], **(v)** blockage of arachidonic acid metabolism and prostaglandin synthesis [Suno and Nagaoka 1989c, Tsuruo *et al.* 1994, Civenni *et al.* 1999], **(vi)** promoting nerve growth factor (NGF) [Takeuchi *et al.* 1990, Nitta *et al.* 1993, and Takuma *et al.* 2000], **(vii)** augmentation currents of kainate receptors and 2-amino-3-(5-methyl-3-oxo-1,2-oxazol-4-yl)propanoic acid (AMPA) receptors [Miyamoto *et al.* 1990 and Kaneko *et al.* 1991], and **(viii)** mild amelioration of memory [Nagaoka *et al.* 1989 and Yamada *et al.* 1997]. Focusing on interactions with enzymes and enzyme complexes, idebenone was described to interact with G3PDH [James *et al.* 1995, Rauchová *et al.* 2008 and 2011], ETFDH [Frerman and Šimkovič 2004], cyclooxygenase and lipoxygenase [Civenni *et al.* 1999] and with complex I, II, and III [Sugiyama *et al.* 1985, Sugiyama and Fujita 1985, James *et al.* 1995, Degli Esposti *et al.* 1996a, Brière *et al.* 2004, Rauchová *et al.* 2008, and King *et al.* 2009]. Additional to these manifold interaction partners of and pathways influenced by idebenone, this thesis showed that idebenone is a substrate for NQO1 and NQO2 and might act as an electron carrier between the cytosol and the mitochondria.

A further difficulty in characterization of idebenone lies in its chemistry: minor structural changes lead to (partially) unpredictable alterations in bioactivity as observed in various experiments in this thesis. In contrast to this, quinones that are analogous to CoQ₁₀ in the substitution pattern of their quinone moiety have often been proposed to share its biological activity. For example, Villalba *et al.* [2010] suggested idebenone to be a good substitute for CoQ₁₀ in different diseases. However, such predictions are questionable, since structural variances entail different chemical and physicochemical properties. Indeed, data presented in this thesis showed that idebenone and CoQ₁₀ behaved differently *in vitro*. For example, CoQ₁₀ is not reduced by recombinant NQO1 and NQO2, nor is it able to reduce WST-1 by an NQO1-dependent mechanism in cellular systems. Consequently, the failure of CoQ₁₀ to rescue ATP levels in presence of rotenone was ascribed to its high lipophilicity which prevented cytosolic reduction required for cytosolic-mitochondrial electron shuttle. Furthermore, being the physiological electron carrier of the ETC, CoQ₁₀ did not inhibit complex I was observed and reported for idebenone. In line with these results, idebenone was also not able for substituting a lack of CoQ₁₀ since no idebenone-dependent rescue of ATP levels was observed in CoQ₁₀-deficient fibroblasts [López *et al.* 2010]. Clinical data also supported the notion of a substantial difference between idebenone and CoQ₁₀, since idebenone ameliorated respiratory function in a patients suffering from Leigh syndrome, where high-dose CoQ₁₀ had no effect [Haginoya *et al.* 2009]. In conclusion, despite structural analogies, idebenone and CoQ₁₀ exhibit completely different biological activities and cannot substitute for each other.

Similarly, short-chain analogs of CoQ₁₀ which share a more comparable lipophilicity to idebenone than CoQ₁₀ showed disparate activities *in vitro* as could be assumed by the differences described for CoQ₆, CoQ₁₁, CoQ₂₂, decylQ, and idebenone in their affinity towards respiratory complexes [James *et al.* 1995, Degli Esposti *et al.* 1996]. Even though short-chain quinones such as CoQ₁₁, CoQ₂₂, and decylQ were reduced by NQO1 and restored ATP levels after their depletion by idebenone, they showed different results in other assays. For example, CoQ₁₁, but not idebenone triggered substantial DNA damage in different cell types. This clearly indicates that, despite sharing the protective activity against acute rotenone toxicity, CoQ₁₁ causes DNA damage in contrast to idebenone after long-term administration. Furthermore, CoQ₆ and CoQ₁₁, but not idebenone, showed depletion of ATP levels when given to cells in normal growth medium and markedly increased lipid peroxidation after long-term treatment *in vitro*, demonstrating yet other toxic properties of these compounds. These findings are in line with reports on complex I inhibition and ROS production associated to short-chain quinones [Lenaz *et al.* 2008, Geromel *et al.* 2002, and Fato *et al.* 2008]. On the other hand, QS-10, one of the first metabolites of idebenone *in vivo* [Okamoto *et al.* 1998], did not reduce ATP levels in glucose-deprived cells, was not able to restore ATP levels in presence of rotenone, or did not manifest genotoxic or pro-oxidant effects.

Furthermore, the importance of substituents became obvious when characterizing 51 idebenone analogs newly synthesized by the Chemistry Department of Santhera Pharmaceuticals in eight biological assays. These compounds vary from idebenone in some minor changes, mainly in substitution of the alkyl tail. Due to patent protection, chemical structures cannot be disclosed. Nevertheless, comparing the profiles of single compounds it became evident that they vastly deviate from each other in regards to their biological effects and that predictions with regards to their biological function on the basis of minute structural changes seem nearly impossible. This was revealed by a lack of correlation between functional assays and by direct comparison of single molecules. For example, a slightly different substitution of a six-membered ring at the terminal carbon atom of the alkyl tail (a methyl-piperazine instead of a morpholine) led to a dramatic increase in toxicity by depleting cellular energy stores.

In addition to the broad range of responses induced by the different idebenone analogs, the generated profiles provide a valuable tool for the selection of customized solutions in various indications. These findings also highlight the influence of modifications to the alkyl tail or to substitutions at the quinoid head group of short-chain quinones on their biological activity.

4.10 Idebenone Protects From Oxidative Stress-Induced Cell Death

Gil *et al.* [2003] demonstrated that idebenone protected chicken embryonic retinal neurons against staurosporin-induced apoptosis. Staurosporin is a bacterially derived antibiotic that inhibits protein kinases, increases intracellular ROS and Ca^{2+} concentrations and activates caspases. Gil *et al.* showed that one-day pre-treatment with 1 μM idebenone reduced ROS levels, ameliorated intracellular Ca^{2+} status and blocked caspase-3 activity. As a result, idebenone prevented apoptosis which was suggested to be due to its antioxidant effect. However, not only did other antioxidants such as glutathione-ethylester or trolox show similar results, but also inhibition of oxidative phosphorylation by a rotenone/oligomycin solution or a phospholipase A_2 inhibitor, arachidonyl trifluoromethyl ketone (AACOCF₃), led to comparable findings [Gil *et al.* 2003]. This is noteworthy in the respect that idebenone does inhibit mitochondrial complex I, as showed in this thesis and elsewhere [amongst others Degli Esposti *et al.* 1996, Lenaz *et al.* 2002], and idebenone was also described as an inhibitor of phospholipase A_2 [Amada *et al.* 1995]. Considering the tightly linked interaction of Ca^{2+} , ROS and apoptotic pathways, the finding that idebenone blocks Ca^{2+} channels [Houchi *et al.* 1991] further broadens the range of potential targets for advocating its beneficial effect. Thus, the rescue from cell death described by Gil *et al.* could not be exclusively accounted to one exact mode of action. Nonetheless, their publication provided the relevant information of idebenone effectively preventing apoptosis at a concentration that can be achieved *in vivo* [Nagai *et al.* 1986].

Idebenone-dependent protection against toxic insults was also described in a body of work by Jauslin *et al.* [2002, 2003, and 2007]. The authors worked with an *in vitro* model using L-buthionine (S,R)-sulfoximine (BSO) which is an inhibitor of γ -glutamyl cysteine synthase, the rate-limiting enzyme for *de novo* synthesis of glutathione. In its presence, recycling of GSH via reduction of GSSG using NADPH was still possible [Griffith *et al.* 1979]. In fibroblasts of healthy donors, concentrations up to 100 μM BSO did not alter cell viability; whereas at already half of this concentration (i.e. 50 μM), cell survival was dramatically reduced to less than 10% in fibroblasts of Friedreich's ataxia (FRDA) patients [Jauslin *et al.* 2002]. The increase of necrosis—disrupted plasma membranes were detected by nuclear inclusion of ethidium homodimer dye—was attributed to the increased ROS levels in FRDA cells. Idebenone rescued cell viability of BSO-treated FRDA fibroblasts with an EC_{50} , i.e. the half maximal effective concentration, of 0.5 μM . The studies demonstrated that this protection was not based on prevention of BSO-induced depletion of GSH levels, since both idebenone- and sham-treated FRDA cells exhibited similarly reduced GSH levels eight hours after BSO addition [Jauslin *et al.* 2002]. Vitamin E showed a similar efficacy as idebenone in this assay [Jauslin *et al.* 2007]. Even though, the results can not solely be assigned to the antioxidant effects of these two compounds, since two other antioxidants, trolox (6-hydroxy-2,5,7,8-tetramethylchroman-2-carboxylic acid) and astaxanthin (3,3'-dihydroxy-4,4'-diketo- β -carotene), were unable to rescue viability of FRDA fibroblasts.

Studies carried out by Takuma *et al.* [2000] provided further evidence that idebenone is able to protect against cytotoxicity. When cultured rat astrocytes were subjected to a 30-min hydrogen peroxide (H_2O_2) insult, post-treatment with 1 μM idebenone or higher increased cell survival. In addition, seven-day pre-treatment with idebenone rescued cells similarly at even lower doses: as little as 10 nM idebenone was sufficient to significantly increase viability [Takuma *et al.* 2000]. In their work, Takuma *et al.* considered a contribution of idebenone's antioxidant effect possible for the observed protection. However, they placed emphasis on an active involvement of idebenone in the production of neurotrophic factors. Indeed, idebenone has been reported to induce nerve growth factor (NGF) both *in vitro* in cultured mouse astroglial cells [Takeuchi *et al.* 1991] and *in vivo* in aged rat brains [Nitta *et al.* 1993]. As a matter of fact, antagonizing NGF by an antibody prevented the beneficial effect of idebenone [Takuma *et al.* 2000]. Furthermore, inhibitors of the mitogen-activated protein (MAP)/extracellular signal-regulated kinase (ERK) kinase, 2'-amino-3'-methoxyflavone, or of the phosphatidylinositol-3 (PI_3) kinase, wortmannin, as well as blocking protein synthesis by cycloheximide blocked the beneficial effect on viability induced by idebenone. Whether this was factually linked with the NGF pathway as it was suggested by the authors, or if it involved totally independent routes with even new targets of interactions for idebenone remained unclear from their study.

In addition, Prof. Lavin from Queensland Institute of Medical Research in Brisbane, Australia, reported radioprotection by idebenone [*personal communication M.F. Lavin and N. Gueven*]. Ataxia-telangiectasia (A-T) is a neurodegenerative disorder which is characterized by extreme radiosensitivity at the cellular level. After a two-day pre-incubation with 1 μ M idebenone, A-T cells were irradiated and survival after two additional days was significantly increased by idebenone. In this thesis, a similar regime was used for assessment of protective action of idebenone against oxidative damage induced by H₂O₂. In this model system, a high concentration of H₂O₂ was added to rat myoblast cells for 30 min, before medium was added back to cells. Two days after this toxic insult, only about half of the cells remained alive. However, their morphology attested severe impairment. Idebenone markedly increased viability after H₂O₂ insult when administered to cells one or more hours before H₂O₂ stress. Pre-treatment with 10 μ M idebenone did not fully abolish cell death induced by oxidative stress, but markedly reduced the extent observed. The morphology of cells which survived due to idebenone testified that they were in a stressed condition. Nonetheless, about 80% of cells survived in this model system, which amounted to an increase in protection of about 60% compared to sham-treated cells. Interestingly, the duration of pre-treatment did not seem to substantially alter the beneficial effect of idebenone, since the number of surviving cells did not vary between one, six, or 24 hours pre-incubation time with idebenone prior to H₂O₂ stress. In contrast, the presence of idebenone before H₂O₂ addition was necessary for its protective effect; when idebenone was administered to cells which were already harmed by H₂O₂ before, rates of cell death were unaltered in the presence of idebenone. These findings were in line with studies showing that pre-treatment with idebenone, but not administration of idebenone after the induction of oxidative damage, was able to reduce oxidative stress in pig livers after ischemic reperfusion injury [Schütz *et al.* 1997, Wieland *et al.* 2000].

In contrast to the work of Takuma *et al.* [2000] and Jauslin *et al.* [2002], which found cyto-protective effects of idebenone at concentrations of 10 or 500 nM, respectively, lower concentrations than 10 μ M idebenone showed no statistical significant prevention of cell death in the model system used in this thesis. Even though statistical significance was not reached for concentrations below 10 μ M, pre-treatment with a dilution series from 370 nM to 10 μ M idebenone for 24 hours showed a trend towards dose-dependency.

An intriguing finding was observed when idebenone and H₂O₂ were added simultaneously. Co-incubation of idebenone with the oxidative stressor almost completely prevented cell death and impairment of the morphology of surviving cells. This finding questioned whether idebenone might directly interact with and detoxify H₂O₂ before the latter could execute its fatal properties. Indeed, a series of cell-free experiments using two different redox-active dyes revealed a decrease in oxidative force of H₂O₂ by idebenone which is challenging to explain using chemical principles. It is believed from multiple studies that it is the reduced form of idebenone (hydroquinone) that acts as antioxidant, therefore further oxidation of oxidized idebenone which was employed in these assays is solely possible at the hydroxyl group at the tip of its tail. However, this possibility was ruled out, since two derivatives of idebenone, decylQ and QS-10, similarly reduced the oxidative capacity of H₂O₂. These two quinones differ from idebenone in the substitution of the carbon C₁₀ of their alkyl tail. In DecylQ, the terminal hydroxyl group of idebenone is replaced by a single hydrogen atom, forming a weakly reactive alkan moiety; whereas C₁₀ of QS-10 is fully oxidized and thus, a part of a carboxylic acid group. Additional derivatives of idebenone were also tested in this assay to rule out involvement of the two methoxy substituents of the quinone ring. Plastoquinones share the quinone head with CoQs with the exception, that the methoxyl groups are replaced by methyl groups. SNT₂₁₀₂₀₁ and SNT₂₁₀₄₈₆ are the plastoquinone analogs of decylQ and idebenone, respectively. The fact that these two quinones again provoked a decrease in ability of H₂O₂ to oxidize the fluorescent probes suggested that the functional group for interaction with H₂O₂ might be the dione structure of the quinone. However, even though the experimental data supposed that quinones directly interact with H₂O₂ and lower the latter's capacity as an oxidizing agent; any chemical explanation therefore would be adventurous, if not precarious. However, the search for chemical explanations for this would exceed the scope of this biological work. The relevant information of these results was that the near-absence of cell death observed when H₂O₂ was co-incubated with idebenone might not be due to defense mechanisms occurring at a cellular level, but to direct interaction of idebenone and H₂O₂ within the medium.

The protective effect of idebenone was independent of gene expression, since inhibition of both transcription and translation did not decrease the ability of idebenone to rescue cells from death. These findings are in line with the results of micro array data which revealed that chronic idebenone treatment *in vivo* had—if any—only minor influence on gene expression patterns. Furthermore, idebenone-mediated survival after H₂O₂ treatment was not sensitive to dicoumarol, indicating that the previously described cytosolic-mitochondrial electron shuttle was not involved in the protective action of idebenone. This is not surprising, considering that H₂O₂ is not reported to inhibit complex I.

Nevertheless, the protective effect of idebenone seemed to be associated to a quicker recovery of energy levels. However, the data do not allow for speculation whether the elevated ATP levels six hours after oxidative insult were part of the mechanism by which idebenone rescues cell survival or whether they are a secondary result of the protective effect by idebenone. Interestingly, during the incubation in H₂O₂, ATP content was not altered; but immediately after restitution of medium to cells, energy levels were depleted. A similar incident is observed in ischemic reperfusion injury (IRJ), even though the form of the stress during ischemia is diametrically contrary to oxidative insult by H₂O₂¹²: the detrimental effect—i.e. the substantial reduction of ATP levels after

¹² In ischemia, interruption of blood supply leads to a reduction of oxygen (hypoxia) in the tissue.

IRJ—occurs not until the restoration of normal conditions, be it that the blood supply returns in IRJ or culture medium is restituted in survival experiments [Gündüz *et al.* 2006, Szondy *et al.* 2006]. Considering these parallels, it is noteworthy that idebenone was described to attenuate detrimental effects of IRJ: in isolated pig livers treated with idebenone *ex vivo* or in isolated livers of pigs treated with idebenone *in vivo*, idebenone increased energy metabolism [Schütz *et al.* 1997]. Nevertheless, the nature of stress in ischemia and these survival experiments is completely different. In the latter, ROS formation was markedly increased during H₂O₂ treatment and declined to physiological levels as soon as medium was restituted. These findings are in clear opposition to both (i) the time point of ATP drop in IRJ and these experiments and (ii) generation of oxidative damage only after restored blood supply in IRJ. Nonetheless, idebenone markedly reduced the degree of ROS formation during H₂O₂ treatment, suggesting that an antioxidant activity of idebenone could in fact account for the protection against H₂O₂-induced cell death.

This is in line with numerous studies by others, in which idebenone was repeatedly described to exhibit potent protection against oxidative stressors [Sortino *et al.* 1999, Takuma *et al.* 2000, Yerushalmi *et al.* 2001, Gumprich *et al.* 2002, Jauslin *et al.* 2002, 2003, and 2007, and Gil *et al.* 2003]. The survival experiments of this thesis added to this impressive body of work and confirmed once more that idebenone rescues cell survival after oxidative insult.

4.11 Implications of this Thesis on Mitochondrial Diseases: DMD, MELAS, and LHON

In conclusion, the data presented in this thesis show that idebenone (i) is able to restore ATP levels when complex I is dysfunctional via an NQO1-dependent cytosolic-mitochondrial electron transport, (ii) inhibits complex I in accordance with previous publications [Sugiyama *et al.* 1985, Sugiyama and Fujita 1985, Degli Esposti *et al.* 1996a, Brière *et al.* 2004, Rauchová *et al.* 2008, and King *et al.* 2009], (iii) protects from H₂O₂-induced cell death, (iv) shows both mild pro- and stronger antioxidant capacity, and (v) changes in cellular redox status (NAD⁺/NADH ratio). The question then arrived how beneficial effects of idebenone in several disorders could be explained. Thus, it has to be noted that idebenone is not a classical pharmacophore with one mode of action—such as kinase inhibitors, for example—but orchestrates several different cellular responses. With regards to the differences in pathologies, one particular aspect might be more relevant in one disorder compared to another one.

4.11.1 Duchenne Muscular Dystrophy

Pre-clinical and clinical data reported an amelioration of pathologic symptoms in the *mdx* mouse model and in DMD patients [Buyse *et al.* 2009 and 2011]. Unfortunately, both cell and animal models were not suitable for studying effects of idebenone on mitochondrial activity in DMD [see 4.1]. Thus, it can only be speculated how idebenone could ameliorate the DMD phenotype on a molecular level.

DMD is characterized by a loss of functional structure protein dystrophin. It was assumed that DMD cells are more susceptible to mechanic stress against the plasma membrane which results in transiently disrupted membranes and thereby influx of Ca²⁺ into the cells [Petrof *et al.* 1993, and Straub *et al.* 1997]. Increase in intracellular Ca²⁺ concentrations causes a depolarization of cells and thus, opening of voltage-gated Ca²⁺ channels which further increase Ca²⁺ levels. Several studies reported higher activities of Ca²⁺ channels showed in DMD patients [Hopf *et al.* 2007, Williams and Allen 2007] and König *et al.* [2011] linked abnormalities in voltage-gated Ca²⁺ channels to cardiomyopathy in DMD. In dystrophic muscle cells, elevated intracellular Ca²⁺ concentrations are antagonized by mitochondrial uptake of Ca²⁺ [Chen *et al.* 2000] and are detrimental to mitochondrial function, promoting depletion ATP levels and elevated ROS production [Brini 2003, Gardew *et al.* 2010, and Kinnally *et al.* 2011; and Figure 51A]. The fragmentation of mitochondria observed *in vitro* could also account for an imbalance in Ca²⁺ homeostasis [Diaz and Moraes 2007]. Indeed, decreased mitochondrial respiration and oxidative stress were observed in DMD patients and *mdx* mice [Barbiroli *et al.* 1992, Kemp *et al.* 1993, Camiña *et al.* 1995, Gannoun-Zaki *et al.* 1995, Tidball and Wehlings-Hendrick 2007, Sperl *et al.* 1997, Kuznetsov *et al.* 1998, Brini 2003, Burelle *et al.* 2010, and Kinnally *et al.* 2011].

Just recently, specific deficiencies of mitochondrial complex I and complex IV were described [poster from Sobreira *et al.* EuroMit 2011, Zaragoza, Spain; and personal communication C. Sobreira and N. Gueven]. Whereas impairment of complex I would be a precondition for a NQO1-dependent cytosolic-mitochondrial electron transfer driven by idebenone, the lack of complex IV negates such a mechanism: cytochrome *c* which accepts electrons from idebenone in the proposed model via complex III is re-oxidized by complex IV. Therefore, it seems unlikely that idebenone could ameliorate respiration by transporting cytosolically generated electrons into mitochondria by the suggested NQO1-dependent mechanism.

Thus, the action of idebenone in DMD is likely to be independent of direct interactions with mitochondria. Idebenone was described to inhibit voltage-gated Ca²⁺ channels [Houchi *et al.* 1991, Chang *et al.* 2011, Kaneko *et al.* 2011, and Newman *et al.* 2011]. Hence, idebenone could prevent the secondary influx of Ca²⁺ through these channels and thereby attenuate the negative effect of high intracellular Ca²⁺ on mitochondria [Figure 51B]. Second, idebenone might reduce oxidative stress either by a direct antioxidant radical scavenging

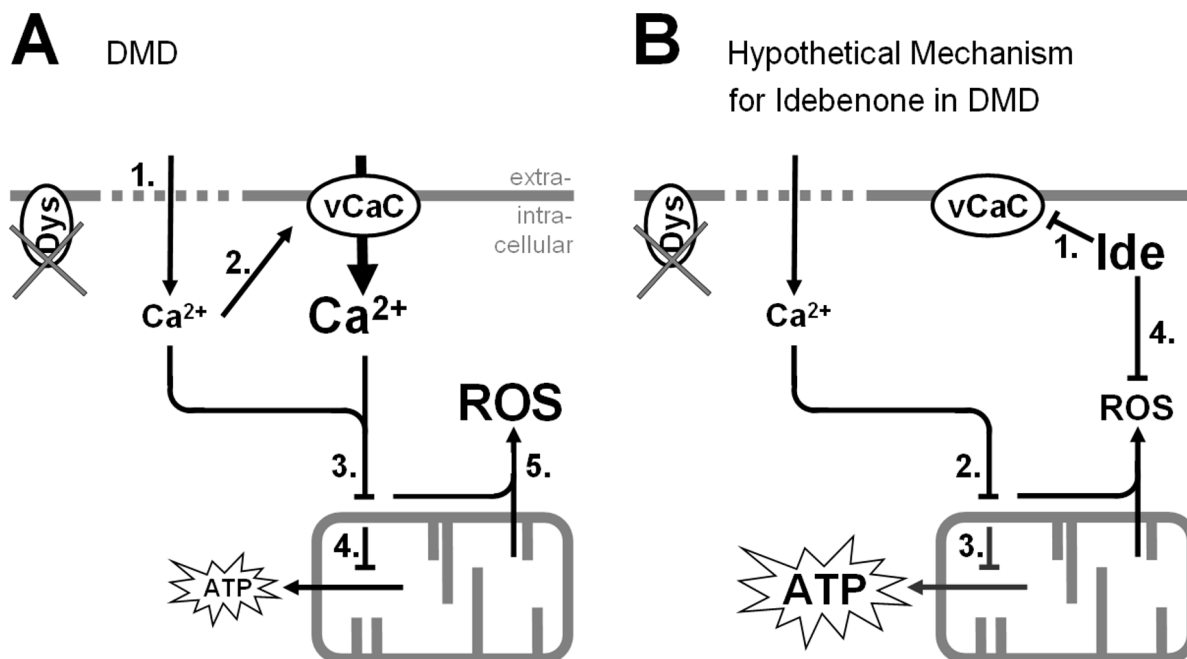


Figure 51: Schematic Representation of Duchenne Muscular Dystrophy (DMD) Pathology and Suggested Mechanisms of Idebenone.

(A) Absence of functional structure protein dystrophin (Dys) leads to a (1.) disruption of plasma membrane under mechanical stress and thus, influx of calcium ions (Ca^{2+}). The resulting depolarization (2.) activates voltage-gated Ca^{2+} channels (vCaC) which further add to intracellular Ca^{2+} concentration. Elevated Ca^{2+} levels (3.) are detrimental to mitochondria, thus leading to (4.) decreased respiration (i.e. ATP generation) and (5.) increased levels of oxidative stress-generating reactive oxygen species (ROS). (B) Idebenone might (1.) inhibit vCaCs and thus reduce Ca^{2+} influx into cells. Therefore, (2.) Ca^{2+} -driven disruption of mitochondrial function might be attenuated and (3.) energy deficiency might be less severe. Furthermore, idebenone might (4.) reduce oxidative stress by direct antioxidant capacity.

4.11.2 Mitochondrial Encephalomyopathy, Lactic Acidosis, and Stroke-like Syndrome

In contrast to DMD, results obtained in this thesis were directly applied to the pathomechanism of MELAS and can explain the observed beneficial effect of idebenone. Most MELAS patients harbor the 3243G>A mutation in the mitochondrial gene for a tRNA which affects impairs translation of mitochondrially encoded proteins [Testai and Gorelick 2010]. An impairment of transcription would assume that all mitochondrial complexes whose subunits are encoded by mtDNA would be affected similarly. However, complex I holds the majority of seven mitochondrially encoded subunits, compared to only one subunit of complex III, three of complex IV, and two of ATP synthase. Thus, on a purely statistical basis, complex I is more likely to be impaired in its function than the other three enzyme complexes. Indeed, besides decreased complex I activity, reduced function of complexes III and IV and ATP synthase was discovered [Sarnat and Maria-García 2005, Sarasman *et al.* 2008, Davidson *et al.* 2009]. In contrast, normal or increased activities of complexes III and IV and ATP synthase, but not of complex I, were described in MELAS patients harboring the 3243A>G mutation [Sano *et al.* 1995, Malfatti *et al.* 2007]. In addition, three mutations in subunit ND1 of complex I also caused a MELAS phenotype [Kirby *et al.* 2004]. These controversial data suggest that complex I is indeed dysfunctional in MELAS cells, however, the remaining members of the ETC might either be functional or dysfunctional.

Nevertheless, the impairment of complex I forces MELAS cybrid cells *in vitro* to rely on anaerobic glycolysis in order to generate sufficient ATP, since mitochondrial respiration is decreased [Figure 1]. The price for increased glycolysis is the excessive production of lactate which is responsible for lactic acidosis, a hallmark of the MELAS phenotype [Kaufmann *et al.* 2004, Davidson *et al.* 2009]. It is interesting to note in this context that the main function of lactate production from pyruvate is entirely focused on regenerating NAD^+ that is needed as co-factor for glycolysis [Figure 52]. Alternatively, NAD^+ can be generated by NQO-dependent reduction of idebenone. Indeed, experiments in cells with rotenone-mediated complex I deficiency revealed that idebenone is able to transfer electrons from NADH into the ETC and thereby, allowing for mitochondrial respiration without the need of complex I. An additional benefit of this electron shuttle is the restoration of NAD^+ pool which eliminates the need for lactate production in order to run glycolysis.

MELAS cybrids (3243A>G) possess a dysfunctional complex I. As described before, the status of the other respiration complexes is controversially discussed. Nonetheless, idebenone-treated MELAS cybrids showed reduced lactate levels and an increased mitochondrial membrane potential which is an indicator for mitochondrial respiration. These findings clearly suggest that idebenone is able to ameliorate mitochondrial energy production, possibly via the proposed NQO1-dependent cytosolic-mitochondrial electron shuttle. The observation that at the same time idebenone was unable to increase ATP levels in cybrid cells suggests that MELAS cells are switching their metabolism from anaerobic glycolysis to mitochondrial respiration in order to

generate the same levels of ATP. Since excess lactate production is considered to be one of the main pathological events in MELAS, this switch could be sufficient to alleviate some of the problems associated with the disease.

Although still some uncertainties about the conditions of complexes III and IV and ATP synthase remain, these data provide for the first time a rationale for the treatment with idebenone and the observed amelioration of symptoms in MELAS patients [Ikejiri *et al.* 1996, Napolitano *et al.* 2000, and Lekoubou *et al.* 2011].

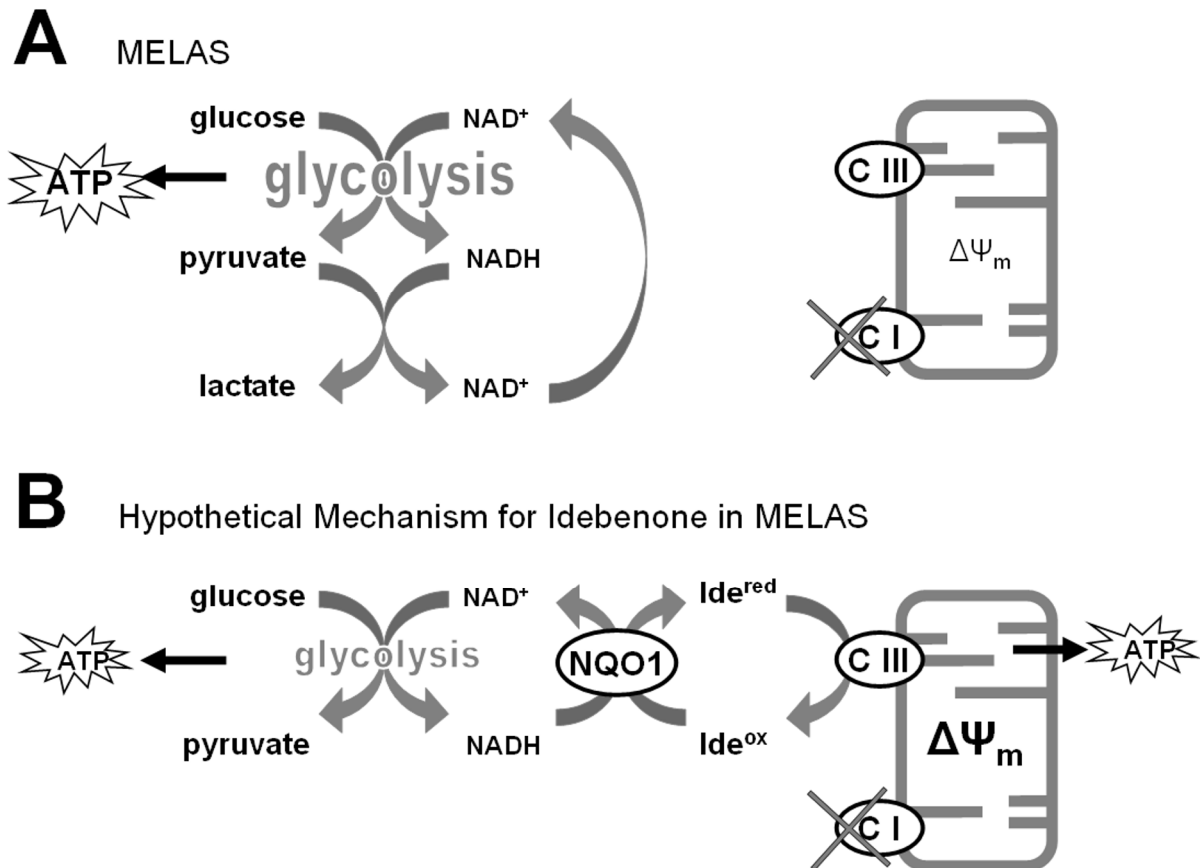


Figure 52: Schematic Representation of Energy-Related Pathology of *Mitochondrial Encephalomyopathy, Lactic Acidosis, and Stroke-like Syndrome* (MELAS) and a Suggested Mechanism of Idebenone.

(A) Dysfunctional complex I (C I) forces MELAS cells to rely mainly on glycolysis in order to produce energy (ATP). Glycolysis is the degradation of glucose which results in the production of pyruvate and NADH. In healthy cells, NADH donates its electrons onto complex I, thereby initiating the ATP-producing mitochondrial respiration. As a by-product of this NADH oxidation, NAD⁺ is formed which can then be used again in glycolysis. In MELAS, dysfunction of complex I leads to shut-down of mitochondrial respiration. Thus, NADH cannot donate its electrons into complex I. In order to restore NAD⁺ levels for maintenance of glycolysis, pyruvate is reduced to lactate which is responsible for the pathologic lactic acidosis observed in MELAS patients. (B). Idebenone (Ide) is able to restore NAD⁺ by NQO1-dependent reduction of NADH. Reduced idebenone can then transfer the electrons onto complex III (C III). Mitochondrial respiration is restored by this cytosolic-mitochondrial electron shuttle which circumvents dysfunctional complex I. Consequently, proton gradient (ΔΨ_m) is increased and ATP can be generated by both glycolysis and mitochondrial respiration. As a result, the need to produce the harmful lactate is eliminated.

4.11.3 Leber's Hereditary Optic Neuropathy

In a clinical trial with patients harboring the LHON mutations 3460G>A, 11778G>A, and 14484T>C—which all affect subunits of complex I [Mackey *et al.* 1996]—idebenone attenuated the pathology associated with these mutations [Klopstock *et al.* 2011]. It can be assumed that mutations in complex I subunits impair the function of complex I and that this dysfunction leads to the observed phenotype. Since complex I seems to be the main impairment in LHON, idebenone could increase the mitochondrial respiration by bypassing complex I and transferring electrons from the cytosol via NQO1 directly to cytochrome *c*.

However, own experiments with LHON lymphoblastoid cells showed that they were able to compensate glucose-deprivation, supposedly by increasing activities of other respiratory complexes. These findings were in line with previous reports showing no reduction in ATP levels *in vitro* and *ex vivo* [Beretta *et al.* 2004, Baracca *et al.* 2005, and Pommer *et al.* 2008]. Even when complex I was inhibited by rotenone, idebenone was not able to restore ATP levels which was attributed to the poor NQO1 expression in these cells. Therefore, the hypothesis of an NQO1-dependent electron shuttle from cytosolic NADH to cytochrome *c* could not be demonstrated. Nevertheless, the possibility that idebenone might act via this mode of action is plausible in the light of a report of Cortelli *et al.* [1997]. They showed that idebenone treatment of a patient harboring the 11778G>A mutation led to a decrease of serum lactate levels, suggesting that idebenone might in fact ameliorate energy levels in a mechanism similar to the one proposed in MELAS.

However, the main reason for the LHON pathology might not be due to an ATP synthesis defect, but rather to elevated oxidative damage in retina cells. Indeed, Wong *et al.* [2002] reported that upon differentiation, neuron-like LHON-NT2 cybrid cells exhibited elevated ROS, suggesting that dysfunctional complex I might have a more severe effect in neuronal tissue. Surprisingly, the observed ROS levels in these differentiated cybrids could be rescued by the complex I inhibitor rotenone. While rotenone generally leads to an overproduction of ROS in human skin fibroblasts, higher concentrations of rotenone cause cell death displaying some of the characteristics of apoptosis. The data by Wong *et al.* [2002] suggests that LHON mutations in a neuronal environment directly cause elevated ROS production by complex I dysfunction. This finding provides a second point of action where idebenone, a class B complex I inhibitor as rotenone [Degli Esposti 1998], could effectuate its beneficial impact.

Nevertheless, Wong *et al.* [2002] admit that their data do not rule out the possibility that ROS are produced by a secondary event downstream of complex I dysfunction. The hypothesis of excess ROS in LHON is particularly attractive, since it could explain the three-fold excess of LHON in males versus females [Emery 1991]. In laboratory animals it has been observed that male animals show higher levels of mitochondrially produced ROS compared to females. Indeed, females appear protected from A β -induced mitochondrial ROS production by an estrogen-dependent mechanism [Viña *et al.* 2007, Borras *et al.* 2007] and in LHON cells, estrogen also shows a clear protective activity [Giordano *et al.* 2010 and *personal communication between V. Carelli and N. Gueven*]. Hence, idebenone might also reduce oxidative damage in LHON on behalf of its antioxidant effect.

4.12 Conclusions

Idebenone is a versatile compound described to interact with different enzymes, enzyme complexes and pathways and its mode of action in disorders where it showed promising effects or attenuation of pathology is still under investigation [Figure 53]. Although the observed effects of idebenone are mainly attributed to its antioxidant function and an interaction with the ETC, new models described herein expand our understanding how idebenone can lead to the alleviation of symptoms.

With my work, emphasis was primarily laid on the role of idebenone in mitochondrial respiration. I confirmed that idebenone inhibits complex I and, for the first time, described implications of this inhibition *in vivo*. Idebenone forces mice to increase their food intake in order to maintain their physiological weight and leads to a transient drop in blood glucose, supposedly by blocking complex I activity. Further research on these effects is required to see if this mechanism for example could be exploited for the treatment of obesity.

I also showed for the first time that idebenone is reduced by NQO1, both in a cell-free system and in cells [Figure 53]. Based on this reduction, I provided evidence that idebenone is able to transfer electrons from the cytosol to mitochondria and thereby enables mitochondrial respiration when complex I is dysfunctional. This new mechanism allows for a rationale of the use of idebenone in MELAS for the first time.

My data also separates idebenone from structurally analogous quinones, including CoQ₁, CoQ₁₀, and 50 novel compounds, in different biochemical assays. These experiments do not only show that the modes of action employed by idebenone are distinct from other short-chain analogs, but also strongly distinguish idebenone from CoQ₁₀ which was suggested to act similarly to idebenone. Furthermore, the characterization of 50 novel idebenone analogs allows for their potential development in new indications.

In addition, I showed that idebenone prevents cell death induced by hydrogen peroxide. This adds to the great body of work ascribing protection against several toxic and pro-oxidant stressors to idebenone. Despite this defensive effect which is also in line with the antioxidant capacity of idebenone, moderate pro-oxidant effects of idebenone were described.

Finally, based on my research, I proposed possible mechanisms how idebenone could achieve the observed amelioration in diseases with a mitochondrial phenotype such as Duchenne muscular dystrophy, *Mitochondrial Encephalomyopathy, Lactic Acidosis, Stroke-like episodes* (MELAS), and Leber's Hereditary Optic Neuropathy (LHON).

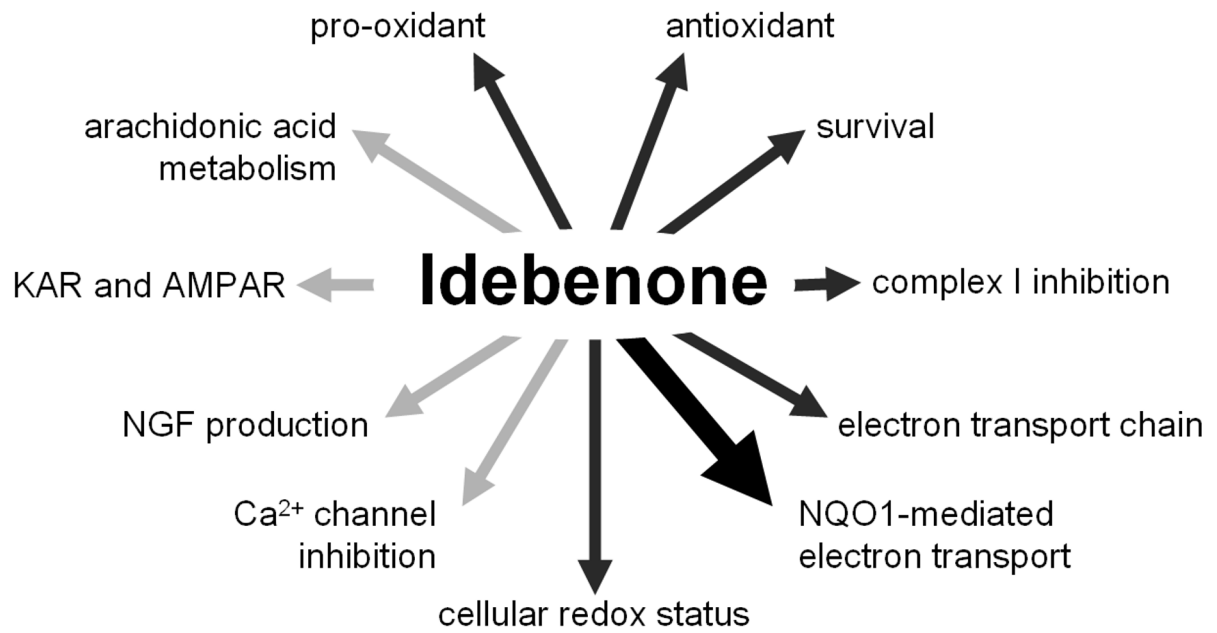


Figure 53: Relevant Molecular Interactions of Idebenone.

Idebenone is not a typical pharmacophore with one specific target, but is able to interact with various pathways, enzymes, and enzyme complexes. Involvement of idebenone in arachidonic acid metabolism, kainate or 2-amino-3-(5-methyl-3-oxo-1,2-oxazol-4-yl)propanoic acid (ARMA) receptors (AMPA), nerve growth factor (NGF) production, or calcium (Ca²⁺) channel inhibition were not investigated in this thesis (light grey arrows). Instead, pro- and antioxidant effects, protection from cell death and survival, complex I inhibition, interactions with other enzyme complexes of the electron transport chain, and alteration of cellular redox status were confirmed (dark grey arrows). In addition, a new mechanism of NQO1-dependent cytosolic-mitochondrial electron shuttle was described in this thesis for the first time (black bold arrow).

5 Methods

5.1 Enzyme Kinetics

5.1.1 NQO1 and NQO2 Activity

Recombinant NQO1 and NQO2 activity in presence of different quinones was measured according to a modified protocol by Ernster [Ernster 1967]. Reactions were performed in 1-ml disposable cuvettes at room temperature in reaction buffer (25 mM Tris-HCl pH 7.4, 0.7 mg/ml bovine serum albumin (BSA), 1 µg/ml enzyme, 10 µM quinone). The reaction was started by addition of NAD(P)H (for NQO1) or 1-(3-sulfonatopropyl)-3-carbamoyl-1,4-dihydropyrimidine (a NRH-derivate, for NQO2) [Knox *et al.* 2000]. Enzyme activity was measured as decrease of A_{340} for NAD(P)H and A_{355} for the NRH-derivate, respectively, during 30 sec in a spectrophotometer. All assays were performed in triplicate. Electron donor concentrations at start of linear phase of the decrease of absorbance were calculated using the absorbance coefficient ($\epsilon_{\text{NADH}} = 6300 \text{ M}^{-1} \text{ cm}^{-1}$; $\epsilon_{\text{NADPH}} = 6200 \text{ M}^{-1} \text{ cm}^{-1}$; $\epsilon_{\text{NRH-derivate}} = 4430 \text{ M}^{-1} \text{ cm}^{-1}$). Reduction rates per mg enzyme were calculated during the linear phase of the reduction. Since NQO1 possesses a single quinone-binding site [Dinkova-Kostova and Talalay 2010], steady-state kinetic constants were calculated using the Michealis-Menten equation combined with Hanes-Woolf plot because of its independence towards variability at high substrate levels. To determine the dicoumarol sensitivity of enzymes, reactions were performed in triplicate in the presence or absence of 20 µM dicoumarol in reaction buffer (25 mM Tris-HCl pH 7.4, 0.7 mg/ml BSA, and 1 µg/ml enzyme) containing 50 µM CoQ₁ and started with 100 µM NADH or 1-(3-sulfonatopropyl)-3-carbamoyl-1,4-dihydropyrimidine, respectively. Electron donor consumption rate was calculated as described above and expressed as percentage of the rate in the absence of dicoumarol. For complexing quinones with serum, powdered quinones were dissolved in heat-inactivated FBS by vortexing for 1 min. Alternatively, quinones were formulated in liposomes as described [Mayer *et al.* 1985, Paolino *et al.* 2004]. Briefly, L- α -phosphatidylcholine and quinone were dissolved in PBS at a final concentration of 25 mg/ml lipid in a molar drug/lipid fraction of 0.05 (final quinone concentration: 1.6 mM). The mixture was then subjected to five repetitive freeze-thaw cycles.

5.2 Cell Culture

5.2.1 Culturing of Cells

All cell lines and primary cells were cultivated under normal culture conditions (37 °C, 5% CO₂, and 90% relative humidity [rH]). All media were supplemented with antibiotics and glutamate was administered to media at the same time as serum in order to enhance shelf-life of media. Antibiotics and glutamate were added as 1% of volume in a mixed solution to a final concentration of 100 units/ml penicillin, 1 µg/ml streptomycin, and 292 mg/l L-glutamine. Phosphate-buffered Saline without Ca²⁺ or Mg²⁺ (PBS) and Hank's Buffered Saline Solution (HBSS) were supplemented with 1% penicillin-streptomycin. Fetal Bovine Serum "GOLD" from the European Union (FBS) was used as serum if not otherwise stated. Cells were handled under sterile conditions in a workbench with laminar air flow. Aspirated medium was sterilized by bleaching in Javel water and plastic waste was autoclaved for 10 min at 121 °C.

Adherent cells were cultivated in either 10-cm dishes containing 10 ml medium or 20-cm dishes containing 15 ml medium. Cells in suspension were cultivated in flasks of different sizes (25 cm², 75 cm², or 150 cm²) with maximum one third of the volume filled with medium.

Primary human fibroblasts from a 32-year old healthy male (called C₂) and from a 19-year old healthy female (called C₃), human neuroblastoma cell line SH-SY5Y, spontaneously transformed human keratinocyte cell line HaCaT, human embryonic kidney cell line HEK293, rat L6 myoblasts, and human hepatic cell line HepG2 cells were cultured in Dulbecco's modified Eagle's medium (DMEM) containing 4.5 g/l glucose supplemented with 10% FBS.

Wild-type (RN236, WT, homoplastic) and MELAS (RN164, A3243G homoplastic) cybrid cells were cultured in DMEM, 7% FBS, and 50 µg/ml uridine. The cybrids were gifts from M. Hirano and M. Davidson (Columbia University, New York NY, USA).

Primary human myoblasts were cultured in minimal essential medium Eagle (MEM EBS; E15-024; Omnilab, Mettmenstetten, Switzerland) supplemented with 25% Medium 199 EBS, 10% non heat-activated FBS, 10 µg/ml insulin, 100 ng/ml EGF, 100 ng/ml FGF. Primary human myoblasts were extracted from biospies kindly donated by the Association Française contre des Myopathies (AFM, Evry, France) and muscle cells were selected using monoclonal anti-NCAM antibody and magnetic beads-based cell sorting (MACS). Biopsies were named as following: 2TE myoblasts originated from the paravertebral muscle of a healthy 16-year old female, 4TE myoblasts originated from the paravertebral muscle of a healthy 12-year old female, 5TE myoblasts originated from the grand dorsal muscle of a healthy 14-year old male, 6TE myoblasts originated from the quadriceps of a healthy 9-year old male, 8TE myoblasts originated from the paravertebral muscle of a healthy 15-year old female, 5DMD myoblasts originated from the paravertebral muscle of a 12-year old male Duchenne's Muscular Dystrophy patient (DMD), 6DMD myoblasts originated from the striated muscle of a 13-year old male DMD patient, 7DMD myoblasts originated from muscle of a 9-year old male DMD patient, 9DMD myoblasts originated from muscle of a 14-year old

male DMD patient, 12DMD myoblasts originated from the striated muscle of a 16-year old male DMD patient, and 18DMD myoblasts originated from the tibialis anterior muscle of a 15-year old male DMD patient.

Lymphoblastoid cells (GM15851; Coriell, Camden NJ, USA and cells from LHON, Kearns-Sayer syndrome, and Leigh syndrome patients listed in 6.4.2) were cultured in Rosewell Park Memorial Institute medium 1640 (RPMI 1640; E15-039; Omnilab, Mettmenstetten, Switzerland), 10-20% FBS.

5.2.2 Thawing and Freezing of Cells

Cells stored in liquid nitrogen were thawed at 37 °C in a water bath and resuspended in growth medium to a final volume of 5 ml. After harvesting by centrifugation (700 \times g; 5 min; RT) using a swinging bucket centrifuge, the cells were resuspended in their growth medium and seeded in the designated repository.

For cryopreservation of cells, harvested cells [see 5.2.2 for details] were resuspended in DMEM (E15-011; Omnilab, Mettmenstetten, Switzerland) supplemented with 8% DMSO and 10% FBS and transferred into cryotubes at concentrations of 1,000,000 cells/ml. In a first step, cells were slowly frozen at -80 °C in a isopropanol-containing tube box for 24 h and then transferred to liquid nitrogen for long-term storage.

5.2.3 Passaging of Cells

Confluent adherent cells were washed once with PBS to remove FBS and cellular debris. Cells were then incubated in 1 mg/ml EDTA solution for 1 min at RT before detachment using 1 or 2 ml 0.5 mg/ml trypsin in 1 mg/ml EDTA/PBS for 10- or 15-cm dishes, respectively. Detached-cells were resuspended in a nine-fold excess of HBSS and harvested (700 \times g; 5 min; RT) using a swing-out bucket centrifuge. Suspension cells exceeding a density of 10^6 cells/ml were harvested (200 \times g; 5 min; RT) using a swing-out bucket centrifuge without trypsination. Cells were resuspended in their growth medium [see 5.2.1 for details] and split at a ratio of 1:3 to 1:10 depending on cell type, growth behaviour and passage number.

5.2.4 Seeding of Cells into Plates

Resuspended cells after harvesting [see 5.2.2 for details] were counted manually using disposable counting chambers and diluted in the required medium to the desired density (1,000-20,000 cells/well according to assay). Subsequently, cells were seeded in 6-, 12-, or 24-well plates, or various models of 96-well plates in volumes of 2 ml, 1 ml, 0.5 ml or 100 μ l, respectively.

5.2.5 Treatment of Cells

Compound solutions for treatment of cells were prepared as follows. Most compounds were stored as 1,000 \times stocks at -20 °C in DMSO; except for acids (in H₂O), dicoumarol (in 0.1% sodium hydroxide), and metformin (as 200 \times stock in HBSS). Stock solutions were diluted 5-fold in PBS or DMSO, depending on the solubility of the compound. For example, rotenone precipitates in PBS at concentrations higher than 100 μ M. Compounds and controls administered parallel to rotenone were accordingly diluted in DMSO for comparability reasons. The resulting 200 \times dilution was diluted 10-fold in PBS. A twentieth of medium volume was added on top of the cells, resulting in a final 1 \times concentration of the compound in 0.1 or 0.5% DMSO (v/v), respectively.

5.2.6 Cell Growth Rates

Under normal conditions, immortalized cell lines proliferate at a constant rate, whereas primary cells undergo senescence and their proliferation rate decreases with increasing passage number. However, exogenous compounds bear the risk of negatively altering cell growth rates. To investigate how a selection of quinones influences proliferation, human primary myoblasts (4TE) and Epstein-Barr virus (EBV)-immortalized lymphoblastoid cells (BC₁ LCL) were cultivated over a long period in absence or presence of the quinones at different concentrations. Therefore, cells were seeded in 12-well plates in normal growth medium at concentrations of 1,000-20,000 cells/well according to assay. Cells were passaged every three to four days. After washing with PBS, adherent cells were incubated in 100 μ l 0.5 mg/ml trypsin in 1 mg/ml EDTA/PBS and resuspended in a 900 μ l HBSS before harvesting (200 \times g; 5 min; RT). Suspension cells were harvested (200 \times g; 5 min; RT) without trypsination. Subsequently, cells were resuspended in normal growth medium and counted manually using disposable counting chambers. The cells were then diluted to the density at start of the cultivation, freshly supplemented with compounds and seeded into 12-well plates for another three to four days. Proliferation rates were expressed as cumulative cell doubling (CDD) which is defined as the binary logarithm of the quotient of the cell density from counted after three or four days relative to the cell density at seeding.

5.3 Assays

5.3.1 Determination of ATP Levels

Cellular ATP levels were quantified by an ATP-driven enzymatic reaction of luciferase (enzyme) with luciferin (substrate) which results in a quantifiable change of the luminescent signal. Two different buffer systems with the same underlying reaction have been used. Although a high luminescence output kit system was commercially available, due to poor availability and unreliable delivery, a second buffer system was

developed in-house. When using the same samples, the two buffer systems differed only quantitatively in their signal magnitude, whereas qualitatively, the two systems showed no difference.

Initially, a commercially available method (CellTiter-Glo® Luminescent Cell Viability Assay) using the mono-oxygenation of luciferin by luciferase, ATP and molecular oxygen was used as recommended by the manufacturer. Briefly, cells cultured in a 96-well plate and treated as described in the Results section were washed once with 200 µl PBS. After addition of 50 µl PBS to each well, the cells were lysed by an addition of 25 µl lysis buffer (CellTiter-Glo® buffer). The lysate was thoroughly mixed (15 min; 300 rpm; RT), and then 10 µl thereof was transferred into the corresponding well of a 96-well plate designed for luminescence measurements. As a standard, ATP diluted in 1x PBS (concentrations: 0, 1, 2, 4, 6, and 8 µM) were added into the 96-well plate. After addition of 80 µl PBS each well, the reaction was started by 25 µl of substrate buffer (5 ml CellTiter-Glo® buffer added to the CellTiter-Glo® substrate). The reaction is thoroughly mixed on a shaker for 1 min at 300 rpm at RT and the luminescence signal was immediately quantified in a multimode plate reader (integration time: 100 ms, settle time: 10 ms; attenuation: OD₁). ATP levels were calculated according to the linear range of the standard and values were standardized to protein levels determined by BCA assay [see 5.3.9 for details].

The second buffer system was developed in-house and used as follows. Briefly, cells cultured and treated as described in the Results section were lysed in a volume of 50 µl (4 mM EDTA, 0.2% Triton X-100) for 5 min at RT. In 96-well plates designed for luminescence measurements, 100 µl of ATP measurement buffer (25 mM HEPES pH 7.25, 300 µM D-luciferin, 5 µg/ml firefly luciferase, 75 µM DTT, 6.25 mM MgCl₂, 625 µM EDTA and 1 mg/ml BSA) was combined with 10 µl lysate to start the reaction. ATP measurement buffer was stored as separate substrate (25 mM HEPES pH 7.25, 600 µM D-luciferin, 75 µM DTT, 6.25 mM MgCl₂, 625 µM EDTA and 1 mg/ml BSA) and enzyme solutions (25 mM HEPES pH 7.25, 10 µg/ml firefly luciferase, 75 µM DTT, 6.25 mM MgCl₂, 625 µM EDTA and 1 mg/ml BSA) at -80 °C. Shortly before the assay, aliquots of both solutions were thawed at 37 °C in a water bath and mixed at a 1:1 ratio only just before the assay. Luminescence was quantified immediately as described for the CellTiter-Glo Assay.

Adjustments of these standard protocols for experiments in different cells types are described in the following paragraphs.

Since idebenone inhibits complex I [Degli Esposti 1996, King *et al.* 2010, and James *et al.* 2005], idebenone and some analogs synthesized in-house were screened for their ability to decrease cellular ATP levels under conditions where cells rely less on glycolysis and are forced to generate ATP by oxidative phosphorylation. Therefore, human lymphoblastoid cells were incubated with the compound over three days in medium with low glucose content. Briefly, cells were seeded in a 24-well plate at a density of 5*10⁵ cells per ml in different media containing 25 mM glucose as a control (high glucose medium; DMEM 4.5 g/l glucose) and 500 µM glucose as mitochondrial activity medium (low glucose medium; DMEM without glucose). Both media were supplemented with 10% fetal bovine serum—which accounts for approximately 0.1 g/l (0.5 mM) glucose—and 1% Penicillin/Streptomycin and L-glutamine. Cells were treated with 0.1% (v/v) of compounds (10 mM in DMSO; final concentration: 10 µM) and incubated for 72 h under normal culture conditions (37 °C, 5% CO₂, and 90% rH). After dissociation by pipetting up and down, cells were counted before clearing (5 min; 200 x g) using a tabletop centrifuge. Cells were lysed in a volume of 500 µl (4 mM EDTA, 0.2% Triton X-100) for 15 min on ice. After thorough vortexing, a triplicate of 10 µl of the mixture was added into a 96-well plate designed for luminescence measurements. The reaction was started by adding 100 µl reaction mix (300 µM D-Luciferin, 5 µg/ml firefly luciferase, 75 µM DTT, 25 mM HEPES, 6.25 mM MgCl₂, 625 µM EDTA and 1 mg/ml BSA). The luminescence signal was immediately quantified in a multimode plate reader (integration time: 100 ms, settle time: 10 ms; attenuation: OD₁). The concentration of cellular ATP was calculated for each well and then, triplicates were averaged and normalized to cell number. Average and standard error of mean were calculated from percentages of DMSO control for cell density and ATP/cell density and of individual experiments. A new batch of BC₁ LCL was thawed after every 1.5-2 months to get reproducible results. Results showing aberrations which could be attributed to either a loss of normal LCL behaviour or loss of compound activity due to continued thaw-freeze cycles, and from experiments in which control compounds failed to show efficacy were omitted from final calculation. Rotenone (10 nM) and idebenone were always included as positive controls.

Freshly isolated hepatocytes [see 5.7.1 for details] were lysed in 200 µl lysis solution (4 mM EDTA, 0.2% Triton X-100) and results were standardized to cell number.

5.3.2 Determination of Reactive Oxygen Species

Membrane permeable derivatives of reduced fluorescein can be used to detect reactive oxygen species within live cells. The commercially available 5-(and-6)-chloromethyl-2',7'-dichlorodihydrofluorescein diacetate, acetyl ester (CM-H₂DCFDA) possesses chloromethyl groups which react with thiols of proteins and thus enhance its localization within the cell. Upon cleavage by intracellular esterases, a redox-active moiety is released. Only by oxidation of this moiety by cytosolic reactive oxygen species (ROS) the compound reveals its fluorescence. The dye was used according to the manufacturer's instructions. Briefly, adherent cells were seeded in black 96-well plates and treated as described in the Results section. On the day of the assay, cells were washed with 100 µl PBS. One vial (50 µg) of CM-H₂DCFCA was supplemented with 100 µl DMSO (concentration: 865.4 µM) and diluted in PBS (final concentration: 865.4 nM). The reaction is started by adding 100 µl of the diluted dye to each well. After a 5-min incubation at normal culture conditions (37 °C, 5% CO₂, and 90% rH), the cells were washed once with 200 µl PBS. Each well was supplemented with 50 µl PBS and the fluorescence signal was quantified in a

multimode plate reader (excitation: 496 nm (bandwidth: 5nm); emission: 535 nm (bandwidth: 5nm); 50x 400 Hz flashes (settle time: 10 ms) gain: 255). Mean background fluorescence values from cell-free wells incubated dye were subtracted from signals in individual wells before signal of each well was normalized to its protein content [see 5.3.9 for details].

5.3.3 Measurement of Mitochondrial Mass

The fluorescent dye MitoTracker® Green FM was used to quantify the number of mitochondria in live cells. The dye accumulates in active mitochondria where it reacts with thiol moieties of proteins and forms a fluorescent conjugate. The dye is not only useful in live cells, but is also retained after fixation. The method was performed as instructed by the manufacturer. Briefly, adherent cells were seeded in black 96-well plates and treated as described in Results section. On the day of the assay, cells were washed with 100 µl HBSS. An aliquot of 1 mM MitoTracker® Green FM in DMSO stored at -80 °C was thawed at RT and diluted in HBSS to a final volume of 50 nM. Cells were incubated in a volume of 100 µl per well thereof for 30 min at normal culture conditions (37 °C, 5% CO₂, 90% rH). Subsequent, cells are washed twice with 50 µl PBS and fluorescence signals were measured immediately in 50 µl PBS (excitation: 490 nm (bandwidth: 10 nm); emission: 520 nm (bandwidth: 10 nm); 50x 400 Hz flashes (settle time: 10 ms) gain: 150). Mean background value from cell-free wells incubated dye was subtracted from signals in individual wells before signal of each well was normalized to its protein content [see 5.3.9 for details].

5.3.4 Measurement of Mitochondrial ROS Production

The non-fluorescent MitoTracker® Red CM-H₂XRos passively diffuses into cells and accumulates in mitochondria where it is covalently anchored after reaction with thiols. Upon oxidation by superoxide and other reactive oxigene species produced by mitochondria it changes to a fluorescent confirmation. The method was performed as instructed by the manufacturer. Briefly, adherent cells were seeded in black 96-well plates and treated as described in Results section. On the day of the assay, cells were washed with 100 µl HBSS. An aliquot of 1 mM MitoTracker® Red CM-H₂XRos in DMSO stored at -80 °C was thawed at RT and diluted in HBSS to a final volume of 100 nM. Cells were incubated in a volume of 100 µl per well thereof for 30 min at normal culture conditions (37 °C, 5% CO₂, 90% rH). Subsequent, cells are washed twice with 50 µl PBS and fluorescence signals were measured immediately in 50 µl PBS (excitation: 570 nm (bandwidth: 10 nm); emission: 600 nm (bandwidth: 10 nm); 50x 400 Hz flashes (settle time: 10 ms) gain: 150). Mean background value from cell-free wells incubated dye was subtracted from signals in individual wells before signal of each well was normalized to its protein content [see 5.3.9 for details].

Lipid peroxidation was measured using the fluorescent dye Bodipy 581/591 (4,4-difluoro-5-(4-phenyl-1,3-butadienyl)-4-bora-3a,4a-diaza-s-indacene-3-undecanoic acid). This lipophilic dye accumulates in cellular compartments of high fatty acid content and oxidation results in a shift of fluorescent emission from 590 to 510 nm. The method was performed as instructed by the manufacturer. Briefly, adherent cells were seeded in black 96-well plates and treated as described in Results section. On the day of the assay, cells were washed with 100 µl PBS. Cells were incubated with 100 µM Bodipy dye in a volume of 100 µl per well for 30 min at normal culture conditions (37 °C, 5% CO₂, 90% rH). Subsequently, cells are washed twice with 50 µl PBS and fluorescence signals were measured immediately in 50 µl PBS (excitation: 490 nm (bandwidth: 10 nm); emission: 530 and 600 nm for oxidized or reduced form of the dye, respectively (bandwidth: 10 nm); 50x 400 Hz flashes (settle time: 10 ms) gain: 150). Mean background value from cell-free wells incubated dye was subtracted from signals in individual wells before ratio of ratio of red/green signal of each well was calculated. An increase in red/green ratio represented an increase in lipid peroxidation.

5.3.5 Measurement of Mitochondrial Membrane Potential

Two different dyes were employed to measure mitochondrial membrane potential. JC-1 accumulates within mitochondria and changes its fluorescence on behalf of the potential. In contrast to JC-1, results obtained with TMRM, which accumulates in a membrane potential-dependent manner, may not only represent membrane potential but also total mitochondrial content.

Method using JC-1: Determination of the mitochondrial membrane potential was assayed, using 5,5',6,6'-tetrachloro-1,1',3,3'-tetraethylbenzimidazolylcarbocyanine iodide as instructed by the manufacturer. JC-1 is a fluorescent dye accumulating in mitochondria in a membrane potential-dependent fashion. At high concentrations, JC-1 forms spontaneously aggregates with a strong red fluorescence. Hence, a high membrane potential shifts the emission wavelength of JC-1 from 530 nm (green) in its monomeric form to 590 nm (red) when aggregated. Therefore, a decreased ratio of the red to green signal indicates a depolarization of the mitochondrial membrane. Briefly, adherent cells were seeded in 96-well plates and treated as described in Results section. On the day of the assay, cells were washed with 100 µl/well HBSS. An aliquot of stock solution of the dye (1 mg/ml in DMSO) stored at -80 °C was thawed at RT and diluted 10,000-fold in HBSS. A volume of 100 µl per well of dye solution was added and cells were incubated for 15 min under normal cell culture conditions (37 °C, 5% CO₂, and 90% rH). Cells were washed once with 50 µl PBS and fluorescence signals were measured immediately (JC-1 (green): excitation: 485 nm (bandwidth: 10 nm); emission: 535 nm (bandwidth: 10 nm); 50x 400 Hz flashes (settle time: 0 ms) gain: 150; JC-1 (red): excitation: 550 nm (bandwidth: 10 nm); emission: 600 nm (bandwidth: 10 nm); 50x 400 Hz flashes (settle time: 0 ms) gain: 150). Mean background value from cell-free

wells incubated with dye was subtracted from signals in individual wells before ratio of red to green signals was calculated for each well. Average and standard deviation was calculated from these values and expressed as percentage of DMSO-control. A low value signifies a depolarized membrane potential.

Method using TMRM: The cell-permeable fluorescent tetramethylrhodamine methyl ester (TMRM) accumulates selectively in mitochondria due to a cationic moiety. TMRM diffuses rapidly across the mitochondrial membrane and does not bind to mitochondria. Hence, it can be used for live monitoring of membrane potential. If membrane potential increases—meaning that mitochondrial matrix exhibits a more negative net charge relative to the cytosol—the affinity of TMRM to mitochondria further increases. Briefly, adherent cells were seeded black in 96-well plates and treated as described in the Results section. On the day of the assay, cells were washed with 100 μ l HBSS per well. An aliquot of stock solution of the dye (20 mM in DMSO) stored at -20 °C was thawed at RT and diluted 1,000-fold in HBSS (final volume: 20 μ M). A volume of 100 μ l per well of dye solution was added and cells are incubated for 15 min under normal cell culture conditions (37 °C, 5% CO₂, and 90% rH). Cells were washed once with 50 μ l PBS and resuspended in 50 μ l PBS. Fluorescence signals were measured immediately (excitation: 540 nm (bandwidth: 10 nm); emission: 595 nm (bandwidth: 10 nm); 50x 400 Hz flashes (settle time: 0 ms) gain: 100). Mean background value from cell-free wells incubated with dye was subtracted from signals in individual wells before normalization to protein content [see 5.3.9 for details]. Average and standard deviation was calculated from these values and expressed as percentage of DMSO-control. A low value signifies a depolarized membrane potential.

5.3.6 Measurement of Quinone Reduction (WST-1 Assay)

Water-soluble tetrazolium salts (WST) are converted into the corresponding formazan dye upon reduction by hydroquinones. The use of change in WST-1 (2-(4-iodophenyl)-3-(4-nitrophenyl)-5-(2,4-disulfophenyl)-2H-tetrazolium) absorbance for determination of intracellular reduction of quinones was performed as described by Tan *et al.* [2010]. Briefly, cells were seeded in 96-well plates and cultivated in glucose-free DMEM with 2% FBS and 0.3 g/l glucose on the day before the WST-1 experiment. Inhibitors of quinone-reducing enzymes are preincubated for 1 h in the overnight medium. Shortly before start of the assay, an aliquot of 4.5 mM WST-1 in HBSS stored at -20 °C was thawed in a 37 °C-water bath. After the preincubation time, the medium is replaced by HBSS containing 450 μ M WST-1. Inhibitors are re-administered into the according wells. The reaction is started by the addition of the quinone and conducted under normal culture conditions (37 °C, 5% CO₂, and 90% rH). WST-1 reduction as was followed over a period of 120 min using a multimode plate reader. Mean background value from cell-free wells incubated dye was subtracted from signals in individual wells.

5.3.7 Determination of Extracellular Lactate Levels

Elevated lactate levels in supernatant were described as a hallmark of MELAS cybrids [Davidson *et al.* 2009]. Briefly, MELAS and WT cybrid cells were seeded at a density of 150,000 cells per 3.5-cm diameter cell culture dish in normal growth medium. After 24 hours, the medium was changed to 1 ml challenge medium (DMEM, 2 mg/ml glucose, 10% FBS, 50 μ g/ml uridine, 2.5 mg/ml galactose, 0.11 mg/ml pyruvate, +% Penicillin-Streptomycin) containing either DMSO or compounds. After 48 hours, the medium was removed for lactate measurement and the cells were lysed in 500 μ l lysis solution (4 mM EDTA, 0.2% NP-40, 0.2% Tween-20) for 10 minutes. In a 96-well plate, 90 μ l of reaction buffer (10 mM KH₂PO₄ pH 7.8, 2 mM EDTA, 1 mg/ml BSA, 0.6 mM DCPIP, 0.5 mM PMS, 0.8 mM NAD⁺, 1.5 mM glutamate, 5 U/ml glutamate-pyruvate-transaminase, 12.5 U/ml lactate dehydrogenase) was mixed with 10 μ l medium. After incubation at 30 °C for 30 minutes, absorption at 600 nm was quantified using a multimode plate reader. A lactate standard curve was run in parallel. Finally, the calculated lactate concentration in the medium using the standard was also normalized to protein content of the lysate using BCA assay [see 5.3.9 for details].

5.3.8 Quantification of Live and Dead Cells

To investigate potential protective actions of quinones against several toxic agents, two fluorescent dyes were used. Calcein AM is transported into live cells where esterases remove an acetomethyl group thereby capturing the strongly green fluorescent dye within the cell. The required activity of esterases leads to selective staining of live cells. In contrast, ethidium homodimer is a cell-impermeable red fluorescent that binds selectively to DNA in dead cells whose membrane integrity is compromised, but not in live cells. Briefly, adherent cells were seeded in 96-well plates and cultivated in DMEM 4.5 g/l glucose with 10% FBS. Two days after seeding, medium was carefully transferred into new plates and DMEM without FBS was added to cells. Subsequently, toxic insults such as etoposide (10 μ M for six h) or H₂O₂ (10 μ M for 10 min) were administered. After the incubation period with the toxins, the medium was aspirated and replaced by the previous medium to avoid potential artefacts evoked by growth factors in fresh medium. Idebenone (10 μ M) was administered 24 and one h before, six or 24 h after or co-incubated with stressor treatment, respectively. Subsequently, 48-h post stressor treatment, aliquots stored at -80 °C of calcein AM (4 mM in DMSO) and ethidium homodimer (2 mM in DMSO) were thawed at RT and diluted 150 or 100-fold in PBS, respectively before 5 μ l of this dye solution was added on top of the medium (final concentration: 1.3 μ M calcein AM, 1 μ M ethidium homodimer). After a 5-min incubation at normal culture conditions (37 °C, 5% CO₂, and 90% rH), microscopic images of the cells were acquired using the red and green fluorescence channels (FITC: 50 ms, TRITC: 400 ms; 4 x magnification) and analysed using Image J

software. For the red channel, the following macro script was used to count individual dead cells: `run("Find Edges");` `run("Make Binary");` `run("Analyze Particles...", "size=12-100 pixel circularity=0.00-1.00 show=Outlines include summarize");` `close();`. The result of the macro represented the number of dead cells when applied to pictures acquired using the red channel. A similar script was used for counting live L6 myoblast cells which were larger than dead cells: `run("Enhance Contrast", "saturated=0.8");` `run("Make Binary");` `run("Analyze Particles...", "size=40-500 pixel circularity=0.00-1.00 show=Outlines include summarize");` `close;` To calculate survival, the number of living cells was divided by total cell number, i.e. the sum of live and dead cells.

5.3.9 Protein Determination

Protein levels were quantified using two different assays.

The first assay's mechanism is based on a combination of the peptide bonds-dependent reduction of copper(II) to copper(I) and the colorimetric detection of copper(I) by bicinchoninic acid. The method was performed as instructed by the manufacturer (BCATM Protein Assay Kit). Protein levels were determined for normalization of results obtained in other assays performed on the same cells. Briefly, cells cultured in a 96-well plate were washed once with 200 μ l PBS. Cells were lysed with 50 μ l lysis buffer (4 mM EDTA, 0.2% Triton X-100) for 5 min on a shaker at 300 rpm. In a 96-well plate, 70 μ l of BCA working reagent (50 parts of component "A" mixed with 1 part of component "B") were added. The reaction was started by addition of 10 μ l cell lysate. After 2-h incubation at 37 °C, absorbance at 562 nm was quantified in a multimode plate reader. Protein concentration was calculated using the linear range of a BSA standard (15 – 1000 μ g/ml).

For certain methods such as western blotting it was imperative to process protein extracts as quickly as possible. For this purpose, protein concentrations were also analysed using the DC assay instead of the BCA assay due to significantly reduced turn-around times for the DC assay. In a first step, aromatic amino acids are oxidized by copper(II), which then reacts as copper(I) with the second reagent, Folin. The method was performed as instructed by the manufacturer. Briefly, 2.5 μ l of cell lysate or protein standard was added to a transparent 96-well and 25 μ l of working reagent A' was added on top. A' was a prepared as a mixture of 1 part reagent S and 49 parts of reagent A. Subsequently, a volume of 200 μ l reagent B was added into the wells. After 15-min incubation at room temperature, absorbance at 750 nm was quantified in a multimode plate reader. Protein concentration was calculated using the linear range of a BSA standard (15-1000 μ g/ml).

5.3.10 GAPDH Assay

Glycerolaldehyde phosphate dehydrogenase (GAPDH) assay was used to quantify the silencing of GAPDH expression by siRNA. The assay employs a fluorescent dye which is converted proportionally to the reduction of NAD⁺ to NADH by GAPDH. Providing a surplus of all substrates, the enzyme is the limiting factor of this reaction; thus, change in fluorescence signal indicates the amount of GAPDH protein in a given sample. The method was performed as instructed by the kit's manufacturer. Briefly, HepG2 cells were seeded in 96-well plates and transfected with small interfering RNA (siRNA) by reverse transfection [see 5.4.1]. Two days after, cells were lysed using the provided in the kit. After 20-min incubation at 4 °C, 10 μ l of lysate was transferred into a transparent 96-well plate and 90 μ l of the reaction buffer (88.8 μ l solution A, 0.68 μ l solution B, and 0.47 μ l solution C; all provided in the kit) was added. Fluorescence signals were measured immediately (excitation: 560 nm (bandwidth: 10 nm); emission: 590 nm (bandwidth: 10 nm); 50x 400 Hz flashes (settle time: 0 ms) gain: 100). Concentrations of GAPDH were calculated using a standard of recombinant GAPDH and normalized to protein levels [for details see 5.3.9].

5.3.11 Creatine Kinase Assay

Creatine kinase (CK) is a cytosolic enzyme which is used as a marker for decreased membrane integrity. If membranes become leaky, CK blood concentrations increase. A twenty-fold dilution of blood samples in PBS warmed to 37 °C was added to transparent 96-well plates containing 20 μ l R1 buffer. Freshly prepared R1/R2 mix (ratio 3:1; 80 μ l per well; incubated shortly at 37 °C) was added to samples and the absorbance signal at 340 nm was quantified in 15 kinetic cycles with 60 s interval time at 37 °C. The relative difference between creatine kinase concentration in *mdx* and wt mice was calculated from the average difference in emission signal per minute in 15 kinetic cycles. A standard (serial 1:2 dilution in PBS, ranging from 500- to 32,000-fold dilution of hCPK-MM) was used to compare different assays.

5.3.12 Determination of Blood Levels of Ketone Bodies

β -Hydroxybutyrate (β -HB) is a ketone body which can be used as an energy source instead of glucose. The method was performed as instructed by the manufacturer. Briefly, blood was collected from mice from the vena cava and transferred into ice cold heparin-coated tubes for clearing (10 min, 700 x g, and 4 °C). Supernatant was stored at -80 °C until day of assay. After thawing, 5 μ l serum samples and 45 μ l of β -HB assay buffer were added in duplicates into the designated wells of a transparent 96-well plate. A reaction mix was prepared by assembling 4.6 ml β -HB assay buffer, 200 μ l β -HB enzyme mix, and 200 μ l β -HB substrate mix. Reaction was started by adding 50 μ l reaction mix to each well. After 30-min incubation at RT and protected from light, absorbance at

450 nm was quantified in a multimode plate reader. β -HB serum concentration was calculated using the linear range of a standard (0, 4, 8, 12, 16, 20, 50 mM).

5.4 Gene Knock-Down

5.4.1 Small interfering Ribonucleic Acid-Mediated Gene Knock-Down

Short double-stranded ribonucleic acid (RNA) polymers, so-called small interfering RNA (siRNA), can be designed to selectively bind to a certain messenger RNA (mRNA) and can therefore be employed to selectively silence the expression of a given gene. The method was performed as instructed by the manufacturer. Briefly, a volume of 0.5 μ l siPORT NeoFX was diluted in 9.5 μ l Opti-MEM I medium in a sterile conical tube and incubated for 10 min at RT. In the meantime, 1.5 μ l of 2 μ M siRNA was diluted in 8.5 μ l Opti-MEM I medium. Beside siRNA against NQO1 or ETFDH, non-sense negative siRNA was used as a control. The diluted siRNA was mixed with the dilution containing siPORT NeoFX. After 10-min incubation at RT, 20 μ l siRNA/siPORT NeoFX complexes were dispensed into empty wells of a culture plate. HepG2 cells were washed, trypsinized, cleared, and harvested in normal growth medium at a concentration of 10^5 cells/ml [for methods in culturing cells, see 5.2]. After transferring 80 μ l of cells onto siRNA/siPORT NeoFX complexes, plates were gently mixed by shaking. After 24-h incubation under normal culture conditions (37 °C, 5% CO₂, and 90% rH), medium was replaced by normal growth medium and cells were allowed to grow for additional 24 h. Subsequently, cells were analyzed using WST-1 assay [see 5.3.6 for details], ATP assay [see 5.3.1 for details], and qPCR [see subchapters 5.5.1 – 5.5.3 for details].

5.4.2 Lentiviral Gene Knock-Down of NQO1

In contrast to siRNA, small hairpin RNA (shRNA) is single-stranded and therefore bears the advantage to be easily built up *in vitro* when transduced into cells using a lentiviral plasmid. In order to knock down NQO1 expression levels, NQO1 shRNA lentiviral particles were transduced into two different cell lines. Briefly, HEK and HepG2 cells were seeded in 12-well plates at a concentration of 30,000 cells per well in normal growth medium for 24 h. Medium was replaced by 180 μ l growth medium and 20 μ l stock solution containing 4,000–1,000,000 infectious units (IFU) of lentivirus encoding shRNA against and incubated for 24 h. Cells were then immediately used to quantify NQO1 mRNA expression using qPCR [see subchapters 5.5.1 – 5.5.3 for details] and for ATP rescue experiments [for details see 5.3.1]. Stable clones were cultivated in presence of 2 μ g/ml of the selector puromycin. Cells infected with lentiviral particles—regardless of the applied concentration—showed instant protection against puromycin in mixed cultures, whereas untransduced control cells died immediately.

5.5 Nucleotide Manipulations

5.5.1 Isolation of Ribonucleic Acid

Expression levels of specific genes can be analyzed using quantitative real-time polymerase chain reaction (qPCR). Since gene expression results in transcript products called messenger RNA (mRNA), RNA has to be isolated from the tissue or from cells first. Using reverse transcription, complementary DNA (cDNA) is produced from RNA [see 5.5.2 for details] which in turn serves as template for RNA synthesis [see 5.5.3 for details]. By measuring the amount of produced RNA, expression levels can be calculated, since the two are exponentially proportional. Briefly, RNA was extracted from cultured cells using the High Pure RNA Isolation kit (Roche, Switzerland) according to the manufacturer's recommendations. Briefly, cells were resuspended in 200 μ l PBS before addition of 400 μ l lysis buffer. After thorough 15-sec vortexing, RNA was bound to High Pure filter (8,000 \times g, 15 sec). Flow through was discarded and DNA was degraded by incubation with 90 μ l DNase I incubation buffer added into filter tube for 15 min at RT. Degraded DNA was washed from filter using 500 μ l wash buffer I (8,000 \times g, 15 sec). Flow through was discarded and filter was washed using 500 μ l wash buffer II (8,000 \times g, 15 sec). After repetition of this step using 200 μ l wash buffer II, filter tube was placed into a sterile 1.5-ml tube and RNA was eluted using 50 μ l H₂O. Isolated RNA was stored at -80 °C until day of cDNA synthesis [see 5.5.2 for details].

5.5.2 Synthesis of Complementary Desoxyribonucleic Acid

Synthesis of first-strand cDNA was conducted using High Fidelity Transcriptor cDNA Synthesis kit (Roche, Switzerland) and random hexamer primers in a total volume of 20 ml containing 5 mg RNA. Briefly, an amount of 2 ng total RNA was denatured at 65 °C for 10 min and cooled on ice, before 60 μ M random hexamer primers were added in a total volume of 11.4 μ l per sample. Reaction mix (Transcriptor High Fidelity Reverse Transcriptase Reaction Buffer (8 mM MgCl₂), 20 U/ μ l Protector RNase inhibitor, 1 mM deoxynucleotide each, 5 mM DTT, and 10 U Transcriptor High Fidelity Transcriptase) was added and incubated for 10 min at 55 °C. The resulting cDNA was ready to use for qPCR without further procession or purification steps [see 5.5.3 for details].

5.5.3 Quantitative Real-Time Polymerase Chain Reaction

Real-time PCR was performed with LightCycler® 480 SYBR green 1 Master Mix (Roche, Switzerland) in a LightCycler® 480 mastercycler and results were analyzed with the corresponding software (version 1.5.0.39). Protocol parameters used: 5 minutes at 95 °C followed by 40 cycles of 10 seconds at 95 °C for denaturing, 10 seconds at 56 °C for annealing, and 10 seconds at 72 °C for extension. GAPDH was used as internal control. Target gene sequences were amplified with the primer pairs listed in 6.5.2.

5.6 Proteins Analysis

5.6.1 Western Blotting

Abundance, quantity or phosphorylation status of a specific protein was determined using western blots. Briefly, cells treated according to the respective regime were harvested in ice-cold PBS (200 x g; 5 min) and lysed in an SDS-containing lysis buffer (50 mM Tris pH 7.4, 0.1% SDS, 150 mM NaCl, 2 mM EDTA, 2 mM EGTA, 25 mM β-glycerolphosphate, 0.2% Triton X-100, 0.3% NP-40, and freshly added 25 mM NaF, 0.1 mM NaVa, 1 μM DTT, 0.1% saturated PMSF) for 15 min on ice. SDS was added in order to permeabilize nuclei. After determination of protein levels using DC assay [see 5.3.9 for details], aliquots containing 20 μg protein were diluted in SDS sample buffer (1 M Tris pH 6.8, 30% acrylamide, 20% SDS, 10% glycerol, 5% β-mercaptoethanol, 0.01% bromophenol) in a 2:1 ratio and stored at -20 °C until day of use. Gel chambers were assembled and filled with separation buffer (1.5 M Tris pH 8.8, 30% acrylamide, 10% SDS, and freshly added 0.1% APS and 1% TEMED). Isopropanol was added on top of gel to smoothen the border. After the hardening of the gel, isopropanol was removed and cleft was rinsed with water and dried with a filter paper. Stacking buffer (1 M Tris pH 6.8, 30% acrylamide, 10% SDS, and freshly added 0.1% APS and 1% TEMED) was poured on top and comb was positioned. After the hardening of stacking gel, the comb was gently removed and gaps were thoroughly rinsed with water. Gels were placed into electrophoresis rack and tank was filled with running buffer (25 mM Tris, 192 mM glycine, 10 % SDS). Protein samples were denaturated for three min at 95 °C and then loaded into slots. Electrophoresis was performed at a constant current (25 mA/gel) until gel has run full distance (approximately two hours). Gel was carefully removed from glass and stacking gel was removed. A Whatman paper membrane was placed onto gel and enclosed in each two filter papers on both sides in transfer buffer (25 mM Tris, 192 mM glycine, 20 % SDS, 20% methanol). Gel and membrane were clamped into the running apparatus with the gel facing the anode. Western blot was run at a constant voltage (100 V) for one hour and tank was cooled with ice. Subsequently, membrane was washed in water and stained shortly with penceau to control if protein was on membrane. Membrane is washed in TBST (50 mM TrisHCl pH 7.4, 150 mM NaCl, 0.1% Tween 20). After incubation for one hour in blocking buffer (5% milk powder in TBST), membranes were subjected to primary antibodies in cold blocking buffer overnight at 4 °C. Membranes were washed several times with TBST before secondary antibodies were added in blocking buffer for one hour. After washing with TBST, intensity of IR signal from secondary antibodies were measured in an Odyssey reader.

5.6.2 Histological Staining of Oxidative Stress Markers

Histological stainings were mostly performed in 8-well μ-slides but also conducted in transparent 96-well plates. Cells were seeded at desired density and in the required medium, and treated for the designated duration. For staining of mitochondria, 50 nM MitoTracker® Green FM was added one h prior to fixation. Cells were either fixated in ice-cold methanol for 10 min at RT or in 4% paraformaldehyde (PFA) in PBST (0.25% Triton X-100 in PBS) for 10 min at RT. After several thorough washing steps using PBS, background noise was diminished by incubation of cells in blocking buffer (5% FBS in PBST) for one h at RT. First antibodies were diluted in blocking buffer according to manufacturer's instructions (Nrf-2: 1:1000, γH₂AX: 1:2,500; Akt-1: 1:1000; phospho-Akt: 1:200). Cells were incubated with first antibody at 4 °C overnight. After several washing steps using PBST; secondary antibodies (1:2000 in blocking buffer) were incubated for one h at RT. Four subsequent washing steps using PBS were performed with the second step including 1 μM DAPI. Cells were analyzed using fluorescent microscopy and pictures were taken.

5.7 *Ex vivo* Experiments

5.7.1 Isolation of Hepatocytes

Primary hepatocytes were isolated from 6-week old female NMRI mice as described [Boutin *et al.* 2005]. Briefly, animals were sacrificed by CO₂ inhalation and immediately perfused with 50 ml perfusion buffer (10 mM HEPES pH 7.4, 140 mM NaCl, 5 mM KCl, 2.5 mM Na₂HPO₄, 6 mM glucose and 0.2 mM EGTA; 37 °C). The liver was removed and minced in pre-warmed collagenase buffer (10 mM HEPES pH 7.4, 140 mM NaCl, 5 mM KCl, 2.5 mM Na₂HPO₄, 6 mM glucose, 0.2 mM CaCl₂, 1.3 mM MgSO₄ and 0.05% collagenase D). After incubation for 30 min at 37 °C, hepatocytes were dissociated using a 5-ml syringe. The homogenous solution was filtered through gauze and the viability of cells was assessed using trypan blue staining. Typical viability of isolated hepatocytes was about 90%.

5.7.2 Isolation of Murine Blood and Tissues

Muscle tissues and cerebella from mice were isolated for the determination of ATP levels *in vivo*. Blood samples were taken from either the tail vein of living mice (β -hydroxybutyrate determination of 21-day treated mice) or from the *vena cava* from euthanized animals (creatine kinase determination in *mdx* and WT mice, β -hydroxybutyrate determination of 21-day treated mice). Briefly, animals were sacrificed by CO₂ inhalation and immediately dissected. Cerebella, *m. soleus*, *gastrocnemius lateralis*, diaphragm, and heart tissue were snap-frozen in liquid nitrogen and stored at -20 °C until analyzed.

5.8 *In vivo* Experiments

5.8.1 Animal Husbandry

All animal experiments were approved by the governmental authorities (Kantonales Veterinäramt Basel-Land, Switzerland; permit number BL404) and were in accordance with international guidelines. Animals were kept under standard laboratory conditions (12 h light per day, 22 °C, 40–60% humidity) with food and water available *ad libitum*, if not otherwise stated. Mice were obtained from RCC/Harlan (RCC, Füllinsdorf, Switzerland) or Janvier SAS (Le Genest Saint Isle, France). The strain C57Bl/6 J_{Rj} The black mice show a high spontaneous locomotor activity and are used as genetic background for many mutations. Since it is the inbred strain mostly used in labs, it has been chosen for microarray and food intake experiments in order to obtain comparability to other or later studies. In the strain C57Bl/10, Bulfield *et al.* [1984] described a spontaneous mutation in the dystrophin (*mdx*) gene. Mice homozygous for this mutation were called C57Bl/10 *mdx* and showed signs resembling DMD in humans [Bulfield *et al.* 1984]. Albino RjHan:NMRI mice are used in many fields of pharmaceutical and toxicological research. Upon arrival, mice were allowed to acclimatize for one week before experiments started.

Administration of compounds was performed as advised by the Institute of Laboratory Animal Science of the University of Zurich. Oral drug administration was executed using gavages for *per os* (*p.o.*) application or drug was mixed into the food using carboxymethyl cellulose (CMC) as vehicle if not otherwise stated. Therefore, the appropriate amount of idebenone was dissolved in 0.5% CMC and mixed with rodent chow (the different brands and types used are stated in the according subchapters of Methods; CMC without idebenone for mock treatment) and saccharin or sucrose for taste preference. Weighed portions of food mash were administered to single-caged animals at the start of the dark cycle while supplementary food *ad libitum* was allowed or restricted according to the particular experiment. Other routes of drug or compound administration, such as *interperitoneal* (*i.p.*) or *subcutaneous* (*s.c.*) administration, were not used for the experiments of this thesis.

5.8.2 Glucose Tolerance Test

The glucose tolerance test (GTT) determines the velocity of glucose clearance in blood. In the series of GTT performed, mice differed in strain, age, and sex. Mice were fasted overnight for 16 h and randomized after basal blood glucose levels as determined using a glucometer. For this purpose, the tail was slightly slit using a razor blade. A drop of blood was sufficient for the glucometer to quantify the blood glucose level. After randomization, mice were administered with 2000 mg/kg glucose, 200 or 400 mg/kg idebenone, 300 mg/kg metformin [Foretz *et al.* 2010] or a mixture of 2000 mg/kg glucose and 200 mg/kg idebenone *per os* using a gavage. Olive Oil or 0.5% carboxymethyl cellulose (CMC) were used as vehicle. Blood glucose levels were measured after predetermined time intervals. The average of the percental change from basal values for individual animals was calculated.

5.8.3 Genotyping

To confirm the genetical background of wild-type (WT) and mutant mice bearing a dysfunctional dystrophin gene (C57Bl/10 and C57Bl/10 *mdx*, respectively), the animals were genotyped in regard to the dystrophin gene. Briefly, biopsies were obtained from 2-3 mm-long tips of the tail. DNA from biopsies was extracted by incubation in 250 μ l PCR buffer with nonionic detergents (PBND)-buffer (10 mM Tris-HCl pH 8.3, 50 mM KCl, 2.5 mM MgCl₂, 0.1 mg/ml gelatin, 0.45% v/v Nonidet P40 (NP40), and 0.45% v/v Tween 20) supplemented with 133 μ g/ml proteinase K at 55 °C overnight. Samples are then heated to 95 °C for 10 min to inactivate ProK. Cleared samples (10 min; 18,000 x *g*; RT) are directly used for PCR or store at -20 °C. Melting curves of amplified gene sequences are analyzed using a LightCycler® 480. A sample volume of 1 μ l is added to 19 μ l of PCR buffer (1.3 μ l 3 μ M DyAnchor; 1.3 μ l 3 μ M DySensor, 1 μ l of each 10 μ M of primers Dy-S and Dy-A, and 10 μ l LightCycler® 480 Probes Master in H₂O) onto an according 96-well plate, which is sealed with an adhesive foil. Gene sequence is amplified by PCR (pre-incubation at 95 °C for 5 min followed by 40 cycles of amplification (10 s, 95 °C, ramp rate: 4.4 °C/s; 30 s, 52 °C, ramp rate: 2.2 °C/s; 10 s, 72 °C, ramp rate: 4.4 °C/s) and subsequent melting curve analysis (5 s, 95 °C, ramp rate: 4.4 °C/s; 1 min, 40 °C, ramp rate: 2.2 °C). The melting curves and peaks of the samples are compared to three known genotype standards (WT, homo- and heterozygous *mdx*).

5.8.4 Food Intake Experiments

Male mice of different strains (C57Bl/6 J_{Rk}, C57Bl/10 *mdx*, and RjHan:NMRI) were used for investigating the effects of idebenone on whole-body metabolism. Animals were acclimatized for one week before start of treatment and kept under standard laboratory conditions (12 h light per day, 22±2 °C, 40–60% humidity). The age at start of the experiments differed from seven to 14 weeks and duration of experiments ranged from three to four weeks. Animals had unrestricted access to water and food was available *ad libitum* if not otherwise stated. Idebenone (200 or 400 mg/kg) was administered daily using *p.o.* administration via food. Briefly, the appropriate amount of idebenone was dissolved in 0.5% CMC and mixed with rodent chow (either Teklad 2018s (autoclaved or not) or KLIBAG NAFAG 3436; CMC without idebenone for mock treatment) and 5% (w/w) saccharin for taste preference (in some experiments explicitly mentioned in the Results section, sugar was used for taste preference). Portions of food mash amounting to approximately 60–75% of normal daily food intake were administered to single-caged animals at the start of the dark cycle. Animals had access to homemade running wheels for voluntary locomotor activity if not otherwise stated. Body weight was measured in intervals of two to five days and cumulative change in body weight was calculated. Simultaneously, food intake supplementary to food mash portions was calculated from the difference of food dispenser weight and displayed as averaged cumulative food intake. In addition, relative food intake was calculated as the cumulative change in food intake relative to change in body weight.

5.9 Determination of Changes in Gene Expression Using Microarray

5.9.1 Treatment of Mice

Male C57Bl/6 mice (8 weeks when delivered, acclimatized for 1 week before start of treatment) were kept under standard laboratory conditions (12 h light per day, 22±2 °C, 40–60% humidity) with food and water available *ad libitum*. At the age of nine weeks, idebenone (200 mg/kg) was administered *p.o.* for a period of three weeks. Briefly, the appropriate amount of idebenone was dissolved in 0.5% CMC and mixed with standard rodent chow (Teklad 2018s, autoclaved; CMC without idebenone for mock treatment) and 5% (w/w) saccharin for taste preference. Portions of 8 g food mash were administered to single-caged animals at the start of the dark cycle while allowing access to supplementary food *ad libitum*. After the treatment period, animals were sacrificed and the left heart ventricle was immediately excised and lysed in 1 ml trizol reagent to stabilize total RNA. Homogenates were snap-frozen in liquid nitrogen and stored at -80 °C until further processing.

5.9.2 RNA Isolation and MicroArray

Total RNA was purified from deep-frozen tissue homogenates (trizol) following the standard protocol as described by the manufacturer (PureLink™ RNA Mini kit). Briefly, 50 µl 4-bromoanisole were added to homogenates. After centrifugation (2,000 × g, 5 min, 4 °C), an equal amount of 70% ethanol was added to supernatant and RNA was bound in columns (12,000 × g, 15 sec, RT). RNA was washed using twice 350 µl wash buffer I (each 12,000 × g, 20 sec, RT), separated by a 15-min incubation for DNase treatment. Subsequently, RNA was washed twice using 500 µl wash buffer II, respectively, and eluted in 50 µl H₂O (12,000 × g, 1 min, RT). An average of 4,145 ± 1,271 ng RNA was yielded. After removal of ribosomal RNA using the RiboMinus™ kit and subsequent quality control by the Agilent 2100 Bioanalyzer (mean integrity RNA number value was 8.4 ± 0.4), first-strand cDNA was synthesized from 1.8 µg RNA via reverse transcription using SuperScript II polymerase. Briefly, 4 µl RNA and 1 µl 500 ng/µl T7-(N)₆ primers were annealed at 70 °C for 5 min. Subsequently, a volume of 5 µl SuperScript II polymerase solution (5 U/µl enzyme, 20 U/µl RNase inhibitor, 1 mM dNTP mix, 200 mM DTT, 1× 1st strand buffer) was added and reaction was performed (25 °C for 10 min, 42 °C for 60 min, 70 °C for 10 min).

Subsequently, double-stranded cDNA was synthesized using DNA polymerase 1. Following overnight *in vitro* transcription (37 °C, 16 h), single-stranded cDNA was synthesized from cRNA by reverse transcription using SuperScript II, random primers and dUTP and thereafter cleaned from RNA templates. cDNA was fragmented using UDG and APE1 and labeled with a biotinylated ribonucleotide analog. Samples were hybridized to the Affymetrix GeneChip® Mouse Exon 1.0 ST Arrays (Affymetrix, Santa Clara, CA, USA) covering over one million exon clusters. Hybridization, washing and staining were performed according to instructions of Affymetrix. All steps following tissue homogenization were executed in cooperation with the Life Sciences Training (LST) facilities of the University of Basel.

5.9.3 Statistical Analyses

In microarray experiments, the expression of thousands of genes is measured across different conditions. Therefore, it becomes impossible to make a visual inspection of the relationship between genes or conditions in a multi-dimensional matrix. One way to make sense of the data load is to reduce its dimensionality. Principal component analysis (PCA) is a method that reduces data dimensionality by performing covariance analysis between possibly correlated factors and thus, it summarizes the data. The iterative integration of correlated variables finally condenses into three uncorrelated components of a three-dimensional space which permits visual interpretation of treatment effects. The closer the single representatives of a particular treatment lie together and hence, the smaller the ellipsoid comprising them, the more distinct its effect on gene expression by

this treatment; whereas a wide gap between two ellipsoids of different treatments represents a clear difference in their gene expression pattern. For PCA, as well as for the determination of changes in individual gene expression, two programs were used: Partek gene analysis software (Partek Incorporated, Buchs, Switzerland) and Agilent Genespring GX 10 (Agilent Technologies, Santa Clara, CA, USA). Differences in expression levels of individual genes were expressed as fold change in signal and p -values were computed by unpaired, two-tailed and uncorrected t -test. Different methods were used for discovery of biological pathways which are regulated by idebenone on a gene expression level. Functional analysis includes only gene scores which reach significant difference in expression levels and was performed using DAVID (Database for Annotation, Visualization and Integrated Discovery) [Huang *et al.* 2008, Dennis *et al.* 2003]. DAVID is able to extract biological meaning associated with large gene list. It adopts a strategy to systematically map a large number of genes in a list to the associated biological annotation, i.e. gene ontology (GO) terms, and then statistically highlight the most enriched biological annotations. When the relevant biological differences are modest compared to the noise, as experienced in this experiment, effects of the treatment might not be searched in individual gene expression but in orchestrated modifications of a coherent set of genes. Gene score resampling (GSR) provides a p -value for each gene set and does not require a threshold for gene selection. This means that genes which do not meet a statistical significance for selection can contribute to the score. This analysis was performed using the software ermineJ [Lee *et al.* 2005]. Another method addressing the same problems but utilising a different algorithm was performed using Ariadne Pathway Studio 6 (Ariadne Genomics, Rockville, MD, USA). The so-called gene set enrichment analysis (GSEA) compares the expression pattern of a given gene set and tests if it is significantly different from a random expression pattern of this list.

6 Materials

6.1 Animals

6.1.1 Strains

C57Bl/6 JRj		Janvier SAS	Le Genest Saint Isle, France
C57Bl/10		Harlan	Füllinsdorf, Switzerland
C57Bl/10 <i>mdx</i>		Harlan	Füllinsdorf, Switzerland
RjHan:NMRI		Janvier SAS	Le Genest Saint Isle, France

6.1.2 Animal Chow

Teklad Global 18% Protein Rodent Diet, autoclaved	2018S	Harlan	Indianapolis IN, USA
Extreudat	3436	KLIBA NAFAG	Kaiseraugst, Switzerland

6.1.3 Animal Facility Material

Mouse cage (189mm x 297mm x 128mm)	PC7115 HT	Allentown Inc.	Allentown NJ, USA
Mouse wire bar lid rear pocket	WBL7115 RP	Allentown Inc.	Allentown NJ, USA

6.2 Software

DAVID 6.7		NIH	USA
ErmineJ		Columbia University	New York NY, USA
Genespring GX 10		Aligent Technologies	Santa Clara CA, USA
GIMP 2		GIMP Developer Team	
Ingenuity Pathway Analysis®		Ingenuity® Systems	Redwood City CA, USA
i-control™		Tecan Austria GmbH	Grödig, Austria
imageJ	1.43u	NIH	USA
Partek® Genomic Suite™		Partek Inc.	St. Louis MO, USA
Odyssey® Infrared Scanning System 3.0		LI-COR	Bad-Homburg, Germany

6.3 Machines

Autoclave	SX-700E	Tomy Tech USA, Inc.	Fremont CA, USA
Bioanalyzer 2100	G2940CA	Agilent Technologies	Santa Clara CA, USA
Cell Culture Incubator	BBD6220	Heraeus	Hanau, Germany
Dispomix® Drive		Medic Tools	Zug, Switzerland
Electrophoresis power supply	PS305	Gibco BRL	Carlsbad CA, USA
Eppendorf centrifuge 5417R	5417R	Eppendorf	Hamburg, Germany
Eppendorf centrifuge 5804 (swing-out bucket)	5804	Eppendorf	Hamburg, Germany
GeneChip® Fluidics Station 450	00-0079	Affymetrix	Santa Clara CA, USA
GeneChip® Scanner 3000 7G	00-0213	Affymetrix	Santa Clara CA, USA
GeneChip® AutoLoader with External Barcode Reader	00-0129	Affymetrix	Santa Clara CA, USA
Glucometer Contour		Bayer Vital	Leverkusen, Germany
Infinite® M1000 microplate reader		Tecan Austria GmbH	Austria, Grödig, Austria
Inverted Microscope	IX81	Olympus	Volketswil, Switzerland

LightCycler® 480		Roche Diagnostics GmbH	Mannheim, Germany
Microscope X180		Olympus	
MTS 2/4 digital shaker	3208000	IKA®	Staufen, Germany
Odyssey® Imager		LI-COR	Bad-Homburg, Germany
Refrigerated, table-top swinging bucket centrifuge with 11150 rotor and 13550 buckets	6K15	Sigma	Buchs, Switzerland
Ultrospec® 3000 spectrophotometer		Amersham Pharmaceutical Biotech	Little Chalfont, UK
Vortex-Genie 2		Verrière de Carouge Sàrl	Carouge, Switzerland
Workbench with laminar air flow	SFE.150	SKAN	Basel, Switzerland
Thermocycler	T1	Biometra	Goettingen, Germany
Thermomixer		Eppendorf	Hamburg, Germany
Sartorius balance	MS204	Mettler Toledo	Greifensee, Switzerland
Xenophot HLX 6425 halogen lamp FCR 12 V 100W		OSRAM	Munich, Germany
6.3.1 Pipets			
Pipetman P20	F123600	Gilson	Middleton WI, USA
Pipetman P200	F123601	Gilson	Middleton WI
Pipetman P1000	F123602	Gilson	Middleton WI
Eppendorf Reference 0.5-10 µl		Eppendorf	Hamburg, Germany
SwiftPet® Pipetboy	0301	High Tec Lab	Warsaw, Poland
6.3.2 Miscellaneous			
Quick-Chill Box	DS5114-0012	Nalgene	Rochester NY, USA
6.4 Cells and Cell Lines			
6.4.1 Human Primary Cells			
3DMD primary myoblast cells from human tibialis anterior muscle of a 8-year old male donor suffering from DMD	3DMD	AFM-BTR	Evry, France
5DMD primary myoblast cells from human paravertebral muscle of a 12-year old male donor suffering from DMD	5DMD	AFM-BTR	Evry, France
6DMD primary myoblast cells from human striated muscle of a 13-year old male donor suffering from DMD	6DMD	AFM-BTR	Evry, France
7DMD primary myoblast cells from human muscle of a 9-year old male donor suffering from DMD	7DMD	AFM-BTR	Evry, France
9DMD primary myoblast cells from human paravertebral muscle of a 14-year old male donor suffering from DMD	9DMD	AFM-BTR	Evry, France
12DMD primary myoblast cells from human striated muscle of a 16-year old male donor suffering from DMD	12DMD	AFM-BTR	Evry, France
18DMD primary myoblast cells from human tibialis anterior muscle of a 15-year old male donor suffering from DMD	18DMD	AFM-BTR	Evry, France
2TE primary myoblast cells from human paravertebral muscle of a 16-year old healthy female dono	2TE	AFM-BTR	Evry, France

4TE primary myoblast cells from human paravertebral muscle of a 12-year old healthy female donor	4TE	AFM-BTR	Evry, France
5TE primary myoblast cells from human grand dorsal muscle of a 14-year old healthy male donor	5TE	AFM-BTR	Evry, France
6TE primary myoblast cells from human striated muscle of a 9-year old healthy male donor	6TE	AFM-BTR	Evry, France
8TE primary myoblast cells from human paravertebral muscle of a 15-year old healthy female donor	8TE	AFM-BTR	Evry, France
Primary human fibroblasts from a 32-year old healthy male (C2)	GM08402	Corriell Cell Repositories	Camden NJ, USA
Primary human fibroblasts from a 19-year old healthy femal (C3)	GM08402	Corriell Cell Repositories	Camden NJ, USA

6.4.2 Human Cell Lines

BC1 LCL EBV-Immortalized Human Lymphoblastoid Cell Line; from 14 year old male human	GM15851	Corriell Cell Repositories	Camden NJ, USA
Control EBV-Immortalized Human Lymphoblastoid Cell Line; from 33 year old male human	GM17214	Corriell Cell Repositories	Camden NJ, USA
Control EBV-Immortalized Human Lymphoblastoid Cell Line; from 33 year old female human	GM17229	Corriell Cell Repositories	Camden NJ, USA
Control EBV-Immortalized Human Lymphoblastoid Cell Line; from 25 year old female human	GM17040	Corriell Cell Repositories	Camden NJ, USA
HaCaT spontaneously transformed human keratinocyte cell line	330493	CLS	Eppelheim, Germany
HEK293 human embryonic kidney cell line	CRL-1573	ATCC	Molsheim, France
HepG2 human hepatic cell line	330198	CLS	Eppelheim, Germany
Kearns-Sayer Syndrom EBV-Immortalized Human Lymphoblastoid Cell Line; from 10 year old male human	GM06224	Corriell Cell Repositories	Camden NJ, USA
Kearns-Sayer Syndrom mtND4 EBV-Immortalized Human Lymphoblastoid Cell Line; from 10 year old male human	GM04368	Corriell Cell Repositories	Camden NJ, USA
Leber-Like Optic Atrophy mtND1 EBV-Immortalized Human Lymphoblastoid Cell Line; from 40 year old female human	GM11605	Corriell Cell Repositories	Camden NJ, USA
Leber's Optic Atrophy EBV-Immortalized Human Lymphoblastoid Cell Line; from 33 year old male human	GM03857	Corriell Cell Repositories	Camden NJ, USA
Leber's Optic Atrophy EBV-Immortalized Human Lymphoblastoid Cell Line; from 50 year old male human	GM10624	Corriell Cell Repositories	Camden NJ, USA
Leigh Syndrom mtATP6 EBV-Immortalized Human Lymphoblastoid Cell Line; from 2 year old male human	GM13741	Corriell Cell Repositories	Camden NJ, USA
Leigh Syndrom mtATP6 EBV-Immortalized Human Lymphoblastoid Cell Line; from 12 year old male human	GM13740	Corriell Cell Repositories	Camden NJ, USA
LHON mtND4 EBV-Immortalized Human Lymphoblastoid Cell Line; from 30 year old male human	GM10742	Corriell Cell Repositories	Camden NJ, USA
LHON mtND4 EBV-Immortalized Human Lymphoblastoid Cell Line; from 53 year old male human	GM10744	Corriell Cell Repositories	Camden NJ, USA

MELAS A3243G homoplasmic cybrid cells	RN164	Gift from M. Hirano and M. Davidson	Columbia University, New York NY, USA
SH-SY5Y Human Neuroblastoma Cell Line; from bone marrow tumor from a 4 year old female human, passage 36	330154	CLS	Eppenheim, Germany
Wild-type homoplasmic cybrid cells	RN236	Gift from M. Hirano and M. Davidson	Columbia University, New York NY, USA

6.4.3 Rodent Cell Lines

C2C12 mouse myoblastoids	400476	CLS	Eppenheim, Germany
L6 rat myoblastoids	CRL-1458	ATCC	Molsheim, France
RGC-5 retinal ganglion cell line		Gift from XXX	Zurich, Switzerland

6.5 Macromolecules

6.5.1 Recombinant Enzymes

Collagenase D	11 088 858 00	Roche Diagnostics AG	Rotkreuz, Switzerland
DNAse 1	10 104 159 001	Roche Diagnostics AG	Rotkreuz, Switzerland
DNA polymerase 1			
GAPDH	2039G1	Ambion	Austin TX, USA
hCKP-MM; 965 U/ml	238407	Calbiochem	San Diego CA, USA
Luciferase	BIF1350	Apollo Scientific Ltd.	Cheshire, UK
NAD(P)H:quinone oxidoreductase (NQO1)	D1315	Sigma	Buchs, Switzerland
Proteinase K, recombinant, PCR Grade	03 115 887 001	Roche Diagnostics GmbH	Mannheim, Germany
PureLink™ DNase	12185-010	Invitrogen	Carlsbad CA, USA
Quinone oxidoreductase 2 (NQO2)	Q0380	Sigma	Buchs, Switzerland
SuperScript II polymerase		Invitrogen	Carlsbad CA, USA

6.5.2 Oligonucleotides

T7-(N) ₆ primer			
Ccdc12 forward primer; GAA GTG AAA AGG AGG TGG GG		Microsynth AG	Balgach, Switzerland
Ccdc12 reverse primer; CCT CTT CCT CTA GGC GGC		Microsynth AG	Balgach, Switzerland
Cd24a forward primer; TCT CAC TCA CCA CAA GCA CC		Microsynth AG	Balgach, Switzerland
Cd24a reverse primer; GAA ATT AGC CAA GGC CAA CA		Microsynth AG	Balgach, Switzerland
Dnajc17 forward primer; GAA ATT AGC CAA GGC CAA CA		Microsynth AG	Balgach, Switzerland
Dnajc17 reverse primer; GAT GAT TCA GAA AGG GTG		Microsynth AG	Balgach, Switzerland
Dy-A primer; CCT CAA TCT CTT CAA ATT CTG AC		Microsynth AG	Balgach, Switzerland
Dy-S primer; AAC TCA TCA AAT ATG CGT GTT A		Microsynth AG	Balgach, Switzerland
DyAnchor; CTA TCT GAG TGA CAC TGT GAA GGA GAT GGC-PH		Microsynth AG	Balgach, Switzerland
DySensor; GAA AGA GCA ACA AAA TGG CTT C-FL		Microsynth AG	Balgach, Switzerland

Eml5 forward primer; GCA TGC ATT GGA GAA AGG AT	Microsynth AG	Balgach, Switzerland
Eml5 reverse primer; AAA GGA ATC ATC CCA AAG GG	Microsynth AG	Balgach, Switzerland
Fgf18 forward primer; GGA GTG CGT GTT CAT TGA GA	Microsynth AG	Balgach, Switzerland
Fgf18 reverse primer; AGC CCA CAT ACC AAC CAG AG	Microsynth AG	Balgach, Switzerland
GAPDH forward primer; GAA GGT GAA GGT CGG AGT C	Microsynth AG	Balgach, Switzerland
GAPDH reverse primer; GAA GAT GGT GAT GGG ATT TC	Microsynth AG	Balgach, Switzerland
His1h1b forward primer; AAG CCT AAG AAG ACT GCG GG	Microsynth AG	Balgach, Switzerland
His1h1b reverse primer; AAC TTT CTT CAC TCC AGC CG	Microsynth AG	Balgach, Switzerland
Hist1h4h forward primer; TGT GCC TTC CAC TCT GTT GA	Microsynth AG	Balgach, Switzerland
Hist1h4h reverse primer; CTT TGC CAA GAC CTT TAC CG	Microsynth AG	Balgach, Switzerland
Mapksp1 forward primer; TTT CTT TGC ATT GTG AGG AAG A	Microsynth AG	Balgach, Switzerland
Mapksp1 reverse primer; CCG AGA ACA CAG AGA GAG GG	Microsynth AG	Balgach, Switzerland
Med29 forward primer; GGT GGT TCC TGT TGC TGA TT	Microsynth AG	Balgach, Switzerland
Med29 reverse primer; GAG GTC TGT GCT GTC TGC AA	Microsynth AG	Balgach, Switzerland
Nfyc forward primer; CGG AGT AGA GGC CTT TGT GA	Microsynth AG	Balgach, Switzerland
Nfyc reverse primer; CAG AAG GAC TGG AGG CTT TG	Microsynth AG	Balgach, Switzerland
NQO1 forward primer; CACACTCCAGCAGACGCCCG	Microsynth AG	Balgach, Switzerland
NQO1 reverse primer; TGCCCAAGTGATGGCCACAG	Microsynth AG	Balgach, Switzerland
Olf550 forward primer; CTC TTC TGG CTG GGT ACT CG	Microsynth AG	Balgach, Switzerland
Olf550 reverse primer; ATT CCA CAT AGG TGA AGG CG	Microsynth AG	Balgach, Switzerland
Pcdhb15 forward primer; GAG AAG GCA CCC CTC TCT TC	Microsynth AG	Balgach, Switzerland
Pcdhb15 reverse primer; CCT GCA GCT GGA ATC CTT AG	Microsynth AG	Balgach, Switzerland
Ppbp forward primer; GGC GTC AAG AGA ATC GTC AT	Microsynth AG	Balgach, Switzerland
Ppbp reverse primer; AGG AAA ATG GTT TGG CAC AG	Microsynth AG	Balgach, Switzerland
Tdg forward primer; GTG ATG TAG CAG CGT GGG AG	Microsynth AG	Balgach, Switzerland
Tdg reverse primer; GAC TCA CCA CAG GAT CGG G	Microsynth AG	Balgach, Switzerland
Xp07 forward primer; TGC TGG GAC AGA TAA GGG AC	Microsynth AG	Balgach, Switzerland
Xp07 reverse primer;): CTG TCC CCA TGT CTC GTT TT	Microsynth AG	Balgach, Switzerland
Zfp68 forward primer; CAT AGG GAG GAC GCT CCA	Microsynth AG	Balgach, Switzerland
Zfp68 reverse primer; CCA GGT GAA TTC CAC AGC TA	Microsynth AG	Balgach, Switzerland

6.5.3 siRNAs

ETFDH <i>Silencer</i> ® Pre-designed siRNA (ID No 113116); Target Transcript: NM_004453, OMID ID: 231675; GGACAUCCGUGUGUGUCUAtt-3;	AM16708	Ambion	Autstin TX, USA
ETFDH <i>Silencer</i> ® Pre-designed siRNA (ID No 14819); Target Transcript: NM_004453, OMID ID: 231675; GGAGUUAUGGGUUAUUGAUtt;	AM16708	Ambion	Autstin TX, USA
NQO1 <i>Silencer</i> ® Validated siRNA (ID No 9134); Target Transcript: NM_004453, OMID ID: 231675; GGAAUAAAUGAGAGGGAAUtt;	AM51331	Ambion	Autstin TX, USA

6.5.4 Lentiviral Particles

NQO1 shRNA (h) lentiviral particles	sc-37139-V	Santa Cruz	Santa Cruz CA, USA
-------------------------------------	------------	------------	--------------------

6.5.5 Antibodies

anti-8-oxo-dG (2E2), mouse, monoclonal	4354-mc-050	Trevigen	Helgerman CT, USA
anti-Akt-1 (2H10), mouse, monoclonal	2967	Cell Signaling	Danvers MA, USA
Anti-AMPK alpha (F6)	2793	Cell Signaling	Danvers MA, USA
anti-NCAM (H28.123), mouse, monoclonal	MAB310	Millipore	Volketswil, Switzerland
anti-Nrf 2, rabbit, polyclonal	ab31163-500	Abcam	Cambridge, UK
anti-P-histone γ H2AX (S139), rabbit	2577S	Cell Signaling	Danvers MA, USA
anti-P-AMPK-alpha (Thr172), rabbit, monoclonal	7955	Cell Signaling	Danvers MA, USA
anti-phospho-Akt (Ser473) (D9E), rabbit, monoclonal	4060	Cell Signaling	Danvers MA, USA
Cy3-goat-anti-rabbit 2 nd AB		undeclared	
Cy3-donkey-anti-goat 2 nd AB		undeclared	
Cy3-goat-anti-mouse 2 nd AB		undeclared	
FITC-goat-anti-rabbit 2 nd AB		undeclared	
IRDye 680LT Conjugated Goat (polyclonal) Anti-Rabbit IgG (H+L), Highly Cross Absorbed	926-68021	LI-COR	Bad-Homburg, Germany
IRDye 800CW Conjugated Goat (polyclonal) Anti-Mouse IgG (H+L), Highly Cross Absorbed	926-32210	LI-COR	Bad-Homburg, Germany

6.6 Media, Cell Cultures Supplements and Buffers

6.6.1 Cell Culture Media

RPMI 1640, 500 ml	E15-039	Omnilab	Mettmenstetten, Switzerland
DMEM high glucose (4.5 g/l), without L-glutamine, 500 ml	E15-011	Omnilab	Mettmenstetten, Switzerland
DMEM without L-glutamine, without glucose, 500 ml	P11-013	Omnilab	Mettmenstetten, Switzerland
Medium 199 EBS	E15-033	Omnilab	Mettmenstetten, Switzerland
Opti-MEM I	31985-047	Gibco, Invitrogen	Carlsbad CA, USA

6.6.2 Sera

Fetal Bovine Serum "Gold"	A15-151	Omnilab	Mettmenstetten, Switzerland
Fetal Bovine Serum "Hyclone", from European Union	SH30070. 03	Hyclone	Logan UT, USA

6.6.3 Cell Culture Chemicals

EGF	100-15	Prepro Tec	London, UK
FGF	100-18B	Prepro Tec	London, UK
Insulin	I5500	Sigma	Buchs, Switzerland
Penicillin/Streptomycin, L-glutamine (200 mM)	P11-013	Omnilab	Mettmenstetten, Switzerland
Penicillin, Streptomycin	P11-010	Omnilab	Mettmenstetten, Switzerland
Trypsin 10 x, 5 mg/ml in 10 mg/ml EDTA/PBS	L11-003	Omnilab	Mettmenstetten, Switzerland
Uridine	U3003	Sigma	Buchs, Switzerland

6.6.4 Buffers

Phosphate-buffered Saline without Ca ²⁺ or Mg ²⁺ (PBS)	H15-002	Omnilab	Mettmenstetten, Switzerland
Hank's Buffered Saline Solution (HBSS)	H15-007	Omnilab	Mettmenstetten, Switzerland

6.7 Chemicals

6.7.1 Chemicals for Formulation

Carboxymethylcellulose (CMC), sodium salt	21903	Fluka	Buchs, Switzerland
Hydroxypropyl-beta-cyclodextrin (CyDex)	297561000	Acros Organics	Geel, Belgium
Myglyol 812	050 223	Sasol Germany GmbH	Witten, Germany
Olive Oil, extra vergine		Bertolli	Lucca, Italy
D- α -Tocopherol polyethylene glycol 1000 succinate	S7668	Fluka	Buchs, Switzerland

6.7.2 Chemicals

A23187	C7522	Sigma	Buchs, Switzerland
Acetic acid	42425 5000	Acros Organics	Geel, Belgium
Acetic acid glacial	12404 0010	Acros Organics	Geel, Belgium
N-acetyl-L-cysteine (NAC)	A7250	Sigma	Buchs, Switzerland
30% Acrylamide/Bis Solution, 29:1 (3,3% C)	161-0156	Bio-Rad	San Diego CA, USA
Actinomycin D	A9415	Sigma	Buchs, Switzerland
Adenosine-5'-triphosphate sodium salt (ATP)	A2754	Sigma	Buchs, Switzerland
Albumin from bovine serum (BSA), <i>minimum 98% electrophoresis</i>	A7906	Sigma	Buchs, Switzerland
Antimycin A	A8674	Sigma	Buchs, Switzerland
L-(+)-Arabinose, <i>minimum 99%</i>	S3256	Sigma	Buchs, Switzerland
2,2'-Azobis(2-methylpropionamide) dihydrochloride	44,091-4	Sigma	Buchs, Switzerland
BAPTA/AM	196419	Calbiochem®	San Diego CA, USA
Berberine	B3251	Sigma	Buchs, Switzerland
Bromphenol Blue, sodium salt	B5525	Sigma	Buchs, Switzerland

Capsaicin	M2028	Sigma	Buchs, Switzerland
Coenzyme Q ₀	D9150	Sigma	Buchs, Switzerland
Coenzyme Q ₁	C7965	Sigma	Buchs, Switzerland
Coenzyme Q ₂	C8081	Sigma	Buchs, Switzerland
Coenzyme Q ₄	C2470	Sigma	Buchs, Switzerland
Coenzyme Q ₁₀	C9538	Sigma	Buchs, Switzerland
Cytochrome C, 90%, from bovine heart muscle	11208 0050	Arcos Organics	Geel, Belgium
DecylQ	D7911	Sigma	Buchs, Switzerland
3,3'-Diaminobenzidine, 99%	11208 0050	Arcos Organics	Geel, Belgium
Dicoumarol (3,3'-Methylene-bis(4-hydroxycoumarin))	M1390	Sigma	Buchs, Switzerland
Dimethyl sulfoxide (DMSO)	27,685-5	Sigma	Buchs, Switzerland
Diphenyleneiodonium chloride (DPI)	D2926	Sigma	Buchs, Switzerland
Dithiothreitol (DTT)	D9779	Sigma	Buchs, Switzerland
Dodecyl sulfate, sodium salt (SDS), <i>electrophoresis grade, 98%</i>	41953 0010	Acros Organics	Geel, Belgium
ECL Advance™ blocking agent	RPN 418V	GE Healthcare	Little Chalfont Buckinghamshire, UK
Ethylenediaminetetraacetic acid (EDTA)	11843 0010	Acros Organics	Geel, Belgium
Ethylene glycol-bis(2-aminoethylether)- N,N,N',N'-tetraacetic acid (EGTA)	E4378	Sigma	Buchs, Switzerland
Ethanol	02854	Fluka	Buchs, Switzerland
FCCP	C2920	Sigma	Buchs, Switzerland
Ficoll® PM 400	F4375	Sigma	Buchs, Switzerland
Fluor Save™ Reagent	345789	Calbiochem®	San Diego CA, USA
D-(+)-Galactose	G5388	Sigma	Buchs, Switzerland
Gelatin	G1890	Sigma	Buchs, Switzerland
D-(+)-Glucose	G7021	Sigma	Buchs, Switzerland
Glycerol Phosphate, disodium salt hydrate	G6501	Sigma	Buchs, Switzerland
HEPES	441476L	VWR International AG	Dietikon, Switzerland
4-(Hydroxymercuri)benzoic acid sodium salt (HMB)	55540	Sigma	Buchs, Switzerland
Hydrogen chloride	AC0739	Scharlau	Sentmenat, Spain
Hydrogen peroxide, 50% wt solution in water	51,681-3	Sigma	Buchs, Switzerland
Imatinib mesylate	ALX-270- 492	Enzo Life Sciences	Lausen, Switzerland
Iron(II) sulfate, heptahydrate, <i>minimum 99%</i>	F8632	Sigma	Buchs, Switzerland
Isopropanol	1.09634. 1000	Merck	Darmstadt, Germany
β-lapachone	L2037	Sigma	Buchs, Switzerland
D-Luciferin	360202	Regis Technologies, Inc.	Morton Grove IL, USA
Lumigen™ TMA-6 solution A	RPN 2135V1	GE Healthcare	Little Chalfont Buckinghamshire, UK
Lumigen™ TMA-6 solution B	RPN 2135V2	GE Healthcare	Little Chalfont Buckinghamshire, UK
Magnesium chloride	M2670	Sigma	Buchs, Switzerland
3-Mercaptopropionic acid	M5801	Sigma	Buchs, Switzerland
Malonic acid	M1750	Sigma	Buchs, Switzerland

D-Mannitol	6350	Fluka	Buchs, Switzerland
Metformin (1,1-Dimethylbiguanide hydrochloride)	D15095-9	Aldrich	Buchs, Switzerland
Methanol	200-659-6	Biosolve	Valkenswaard, Netherlands
β -Nicotinamide adenine dinucleotide (NADH), reduced dipotassium salt	N4505	Sigma	Buchs, Switzerland
β -Nicotinamide adenine dinucleotide 2'-phosphate (NADPH), reduced tetrasodium salt	N9660	Sigma	Buchs, Switzerland
3-Nitropropionate	N5636	Sigma	Buchs, Switzerland
Nitro blue tetrazolium	N6876	Sigma	Buchs, Switzerland
Nonidet® P 40 substitue	74385	Sigma	Buchs, Switzerland
Oligomycin	O4876	Sigma	Buchs, Switzerland
Paraformaldehyde (PFA)	441244	Fluka	Buchs, Switzerland
Pentachlorophenol (PCP)	P2604	Sigma	Buchs, Switzerland
L- α -phosphatidylcholine	P3556	Sigma	Buchs, Switzerland
Phosphatungstic acid	S3674	Sigma	Buchs, Switzerland
PJ34	P4365	Sigma	Buchs, Switzerland
Potassium hydroxide	1.05033.1000	Merck	Darmstadt, Germany
PageRuler™ Plus Prestained Protein Ladder	5M1811	Fermentas	Basel, Switzerland
PD 98,059	P215	Sigma	Buchs, Switzerland
Phenazine methosulfate	P9625	Sigma	Buchs, Switzerland
Puromycin			
Pyridaben	46047	Sigma	Buchs, Switzerland
Retionic acid (vitamin A acid)	95152	Fluka	Buchs, Switzerland
Rhein	R7269	Sigma	Buchs, Switzerland
Rotenone	R8875	Sigma	Buchs, Switzerland
Salicylic acid			
Sodium orthovanadate	S6508	Sigma	Buchs, Switzerland
Sodium chloride (NaCl)	No 1.06404.1000	Merck	Darmstadt, Germany
Sodium hydroxide (NaOH)	1.06498.1000	Merck	Darmstadt, Germany
Sodium phosphate dibasic (Na ₂ HPO ₄)	7558-79-4	Juro Supply GmbH	Lucerne, Switzerland
Sodium phosphate monobasic (NaH ₂ PO ₄)	10049-21-5	Acros Organics	Geel, Belgium
Sodium salicylate	71945	Fluka	Buchs, Switzerland
Sodium succinate dibasic	14160	Sigma	Buchs, Switzerland
Succinic acid	S3674	Sigma	Buchs, Switzerland
Sucrose	59378	Sigma	Buchs, Switzerland
1-(3-sulfonatopropyl)-3-carbamoyl-1,4-dihydropyrimidine (NRH-derivate)	S0190	Sigma	Buchs, Switzerland
Stigmatellin	85865	Fluka	Buchs, Switzerland
Tempol	ALX-430-081-M500	Enzo Life Sciences	Lausen, Switzerland
Thapsigargin	T9033	Sigma	Buchs, Switzerland
α -Tocopherol (Vitamin E)	T3251	Sigma	Buchs, Switzerland
Tragacanth	No G1128	Sigma	Buchs, Switzerland
Tris-hydroxymethyl (Tris)			
Tris-(hydroxymethyl)-aminomethane, reagent ACS	424575000	Acros Organics	Geel, Belgium

Tris-(hydroxymethyl)-aminomethane hydrochloride (TRIS-HCl)	1028	Gerbu	Gaiberg, Germany
Triton X-100	T8787	Sigma	Buchs, Switzerland
Trizol	15596-026	Invitrogen	Carlsbad CA, USA
Tween 20	93773	Fluka	Buchs, Switzerland
Valproic acid	P4543	Sigma	Buchs, Switzerland
Wortmannin	W1628	Sigma	Buchs, Switzerland

6.7.3 Fluorescent Dyes

Bodipy 581/591 (4,4-difluoro-5-(4-phenyl-1,3-butadienyl)-4-bora-3a,4a-diaza-s-indacene-3-undecanoic acid)	D3861	Invitrogen	Carlsbad CA, USA
Calcein AM	C-1430	Molecular Probes	Eugene OR, USA
CM-H ₂ DCFCA (5-(and-6)-chloromethyl-2',7'-dichlorodihydrofluorescein diacetate, acetyl ester)	C6827	Invitrogen	Carlsbad CA, USA
DAPI (4',6-diamidino-2-phenylindole dihydrochloride)	D9542	Sigma	Buchs, Switzerland
Ethidium homodimer	E1169	Sigma	Buchs, Switzerland
JC-1 (5,5',6,6'-tetrachloro-1,1',3,3'-tetraethylbenzimidazolylcarbocyanine iodide)	T3168	Invitrogen	Carlsbad CA, USA
MitoTracker [®] Green FM	M7514	Invitrogen	Carlsbad CA, USA
MitoTracker [®] Red CM-H ₂ XRos	M7513	Invitrogen	Carlsbad CA, USA
MitoSOX [™] Red	M36008	Invitrogen	Carlsbad CA, USA
TMRM (tetramethylrhodamine methyl ester)	87919	Sigma	Buchs, Switzerland
WST-1 (2-(4-iodophenyl)-3-(4-nitrophenyl)-5-(2,4-disulfophenyl)-2H-tetrazolium, monosodium salt)	W201	Dojindo Laboratories	Kumamoto, Japan

6.8 Kits

BCA [™] Protein Assay kit	23227	Pierce	Rockford IL, USA
CellTiter-Glo [®] Luminescent Cell Viability Assay kit	G7571	Promega	Madison WI, USA
CK-NAC FS kit	13-11631021	DiaSys Diagnostic Systems GmbH	Holzheim, Germany
DC Protein Assay kit	500-0116	BioRad	San Diego CA, USA
GeneChip [®] WT cDNA Synthesis Kit		Invitrogen	Carlsbad CA, USA
High Fidelity Transcriptor cDNA Synthesis Kit	050912 84001	Roche Diagnostics GmbH	Mannheim, Germany
High Pure RNA Isolation kit	11 828 665 001	Roche Diagnostics GmbH	Mannheim, Germany
β-Hydroxybutyrate (β-HB) Assay Kit	L632-100	BioVision, Inc.	Mountain View CA, USA
KDalert [™] GAPDH Assay	AM1639	Ambion	Austin TX, USA
LightCycler [®] 480 Probes Master	047074 94001	Roche Diagnostics GmbH	Mannheim, Germany
LightCycler [®] 480 SYBR Green I Master	047075 16001	Roche Diagnostics GmbH	Mannheim, Germany
MACS Magnetic-Beads Based Cell Sorting kit	130-142-201	Miltenyi Biotech	Bergisch Gladbach, Germany
PureLink [™] RNA Mini kit	12183-018A	Invitrogen	Carlsbad, CA, USA

RealTime Ready Lysis Kit	06366821001	Roche Diagnostics GmbH	Mannheim, Germany
Ribominus™ Transcriptome Isolation kit (human/mouse)	K155002	Invitrogen	Carlsbad, CA, USA
Silencer® siRNA Starter kit	AM1640	Ambion	Austin TX, USA
Transcriptor High Fidelity cDNA Synthesis Kit	01 091 284 001	Roche Diagnostics GmbH	Mannheim, Germany

6.9 Consumables

6.9.1 Cell Culture Flasks

25-cm ² Cell culture flasks; screw cap with filter	9061	TPP	Trasadingen, Switzerland
75-cm ² Cell culture flasks; screw cap with filter	90076	TPP	Trasadingen, Switzerland
150-cm ² Cell culture flasks; screw cap with filter	90151	TPP	Trasadingen, Switzerland

6.9.2 Cell Culture Dishes

3.5-cm Cell culture dish	353001	BD Falcon	Franklin Lakes NJ, USA
10-cm Cell culture dish	353003	BD Falcon	Franklin Lakes NJ, USA
20-cm Cell culture dish	353025	BD Falcon	Franklin Lakes NJ, USA

6.9.3 Microplates

μClear black sterile Greiner Bio-one 96-well plate	655090	Greiner Bio-one	Frickenhausen, Germany
μClear white sterile Greiner Bio-one 96-well plate	655098	Greiner Bio-one	Frickenhausen, Germany
Falcon® Microtest™ tissue culture plate, 96 well, flat bottom with low evaporation lid	353075	Becton Dickinson Labware	Franklin Lakes NJ, USA
96 Flat Bottom Transparent Polystyrol	655101	Greiner Bio-one	Frickenhausen, Germany
LightCycler® 480 Multiwell Plate 96	04 729 692 001	Roche Diagnostics GmbH	Mannheim, Germany
6-well plate, sterile with lid for cell culture	FA-353046	BD Falcon	Franklin Lakes NJ, USA
8-well μ-slide for immunohistochemistry	80826	Ibidi GmbH	Martinsried, Germany
12-well plate, sterile with lid for cell culture	FA-353043	BD Falcon	Franklin Lakes NJ, USA
24-well plate, sterile with lid for cell culture	FA-353047	BD Falcon	Franklin Lakes NJ, USA

6.9.4 Pipet Tips

ART® 10 pipet tips	2139	Molecular BioProducts, Inc.	San Diego CA, USA
ART® 20P pipet tips	2149P	Molecular BioProducts, Inc.	San Diego CA, USA
ART® 200 pipet tips	2069	Molecular BioProducts, Inc.	San Diego CA, USA
ART® 1000 pipet tips	2279	Molecular BioProducts, Inc.	San Diego CA, USA
2-ml Falcon® pipettes	357507	Becton Dickinson Labware	Franklin Lakes NJ, USA
5-ml Falcon® pipettes	357529	Becton Dickinson Labware	Franklin Lakes NJ, USA
10-ml Falcon® pipettes	357530	Becton Dickinson Labware	Franklin Lakes NJ, USA

Materials

25-ml Falcon® pipettes	357525	Becton Dickinson Labware	Franklin Lakes NJ, USA
T-300-C-R 0.5-10 µl Maxymum Recovery clear, racked pipette tips	301-03-251	Axygen Scientific	Union City CA, USA
T-200-C-R 1-200 µl clear, racked pipette tips	301-02-151	Axygen Scientific	Union City CA, USA
T-1000-C-L-R 1-1000 µl Maxymum Recovery clear, racked pipette tips	301-01-501	Axygen Scientific	Union City CA, USA
6.9.5 Tubes			
Cryotubes, 2 ml	5000-0020	Nalgene	Rochester NY, USA
0.5-ml safe-lock tube	0030 121.023	Eppendorf	Hamburg, Germany
1.5-ml safe-lock tube	0030 120.086	Eppendorf	Hamburg, Germany
2-ml safe-lock tube	0030 120.094	Eppendorf	Hamburg, Germany
15-ml Falcon tube	91015	TPP	Trasadingen, Switzerland
50-ml Faclon tube	91050	TPP	Trasadingen, Switzerland
gentleMACS™ M tubes	130-093-458	Miltenyi Biotec GmbH	Bergisch Gladbach, Germany
Microvette 100 Plasma/Lithium-heparin	20.1282	Sarstedt AG	Sevelen, Switzerland
6.9.6 Miscellaneous			
1-ml disposable cuvettes	759015	Brand	Wertheim, Germany
Fast-Read 102® disposable counting chambers	326349	Biosigma	Cona, Italy
GeneChip® Mouse Exon 1.0 ST Arrays	900817	Affimetrix	Santa Clara CA, USA
LightCycler® 480 Sealing Foil	04 729 757 001	Roche Diagnostics GmbH	Mannheim, Germany

7 Acknowledgements

First of all, I would like to thank Prof. Dr. Markus Rüegg and Dr. Thomas Meier for assuming responsibility for my doctoral thesis and giving me the opportunity to perform it at Santhera Pharmaceuticals (Switzerland) Ltd. and the University of Basel. Further thank goes to Dr. Dirk Fischer for accepting to be a co-referent of this thesis.

Furthermore, I would like to thank Santhera Pharmaceuticals, both the company and everyone working there, especially the Applied Research Team and former co-workers in the company's Biology Department. I would like to thank Nuri Güven for his kind and helpful supervision which included not only suggestions for experiments and assistance in methodological uncertainties, but also critical questions towards data and the manuscript of the thesis. In addition, I much appreciated his viable hints and suggestions for my future carrier and approximately one meter New Scientist journals. In addition, my thanks go to Michael Erb for his calm and important input to my work and his famous fondues; Corinne Anklin for taking care of the animals and sharing tasty vegetarian recipes; Dimitry Robay for his assistance in cell culture and measuring NQO₁ levels in all sorts of cells; Fabrice Heitz for his wit and critical questions; Achim Feurer for the chemical expertise and satiric talent; Isabelle Courdier-Fruh for introducing me to cell culture techniques and Noir Désir; Robert Dallmann for input to animal experiments and the company in Darmstadt; Monika Boroff and Martina Hufschmid for their help in some animal experiments and green vodka; Bettina Cardell for her lab organization skills and her northern humor; Gesa Santos for her kindness and starting the tradition of Monday morning Gipfeli. Sepcial thank also goes to Cesare Mondadori for giving me the opportunity of having a traineeship at Santhera and his belief in me. Of course, my thanks include Inken Fleig for providing me with vitamins and friendship.

I also thank my friends and family which always supported me through the tides of life and, especially, in this period. First, I want to thank my parents, Fritz and Susann, who allowed me to pursuit my choices, not only in my studies, but in general life. Without you, I would not be what and where I am. Of course, a big thank you goes to my brother Mario for being not only a good brother, but also a very good friend. I'm especially grateful for all the intense conversation we've had and—I'm sure—will contiue to have. I also thank my aunt Margret Kindler and my beloved uncle and godfather Hans Kindler for their help in getting me introduced to Basel.

My thanks also reach out to my friends and the kind of extended family they are for me. I did, do, and always will appreciate your company, your support, and your kindheartedness. I consider myself very lucky to have you and to be loved by you. In particular, thanks should be received by Marian Kehl for her support during both hard times and very hard times; throughout boredom and doubts. Thank you! Also, I'm very grateful to call Damiano Azzinarri my friend, for his comfort and thoughts are things I do not want to miss. My thanks go to Niels Hagenbuch for our conversations about the nature of science and about which number of philosophy would be the most suitable. Finally, thanks go to Nathalie Bühler for her astonishing and rich thoughts, her incomparable kindness, and her belief in me when I consisted mostly of doubts. The importance of the support from all of you for this work cannot be overrated.

8 Abbreviations

3-NPA	3-nitropropionate
8-oxo-dG	8-hydroxy-2'-deoxyguanosine
A	adenine
A-T	ataxia-telangiectasia
AACOCF ₃	arachidonyl trifluoromethyl ketone
AD	Alzheimer's disease
AD	actinomycin D
<i>ad lib</i>	ad libitum
ADP	adenosine diphosphate
AMP	adenosine monophosphate
AMPA	2-amino-3-(5-methyl-3-oxo-1,2-oxazol-4-yl)propanoic acid
AMPAR	AMPA receptor
AMPK	AMP-activated protein kinase
ANOVA	analysis of variance
Ant	antimycin A
ARE	antioxidant response element
Astaxanthin	3,3'-dihydroxy-4,4'-diketo-β-carotene
ATP	adenosine triphosphate
BAD	Bcl2/Bclx antagonist
BAPTA	BAPTA-AM (1,2-Bis(2-aminophenoxy)ethane-N,N,N',N'-tetraacetic acid tetrakis(acetoxymethyl ester))
Bcl	apoptosis-inducing factor B-cell lymphoma
BDM	Becker muscular dystrophy
Berb	berberine
BSA	bovine serum albumin
BSO	L-buthionine (S,R)-sulfoximine
C	cytosine
C I	complex I
C II	complex II
C III	complex III
C IV	complex IV
Ca ²⁺	calcium ion
Cap	capsaicine
CCD	cumulative cell doubling
cDNA	complementary DNA
cFI	cumulative supplementary food intake
CHX	cyclohexin
CK	creatin kinase
CMC	carboxymethyl cellulose
CM-H ₂ DCFDA	5-(and-6)-chloromethyl-2',7'-dichlorodihydrofluorescein diacetate, acetyl ester
CO ₂	carbon dioxide
CoA	coenzyme A
CoQ	coenzyme Q
CPT	carnitine palmitoyl transferase
Cr	chrome
CR	calorie restriction
cRNA	complementary RNA

CsA	cyclosporin A
ctrl	control
cyt <i>c</i>	cytochrome <i>c</i>
DAPI	4',6-diamidino-2-phenylindole dihydrochloride
dBW	differences in body weight
DCPIP	2,6-dichlorophenolindophenol
DCPIP	2,6-dichlorophenolindophenol
DHAP	dihydroxyacetone
Dic	dicoumarol
DMD	Duchenne muscular dystrophy
DMEM	Dulbecco's modified Eagle's medium
DMSO	dimethyl sulfoxide
DNA	deoxyribonucleic acid
DPI	diphenylene iodonium
DQ	decylQ
DTT	dithiothreitol
Dys	dystrophin
$\Delta\Psi_m$	mitochondrial membrane potential
EBV	Ebstein-Barr virus
EC ₅₀	half maximal effective concentration
EDTA	ethylenediaminetetraacetic acid
EGTA	ethylene glycol tetraacetic acid
EPR	electron paramagnetic resonance
ERK	extracellular signal-regulated kinase
<i>et al.</i>	et altris
ETC	electron transport chain
ETF	electron-transferring flavoprotein
ETFDH	electron-transferring flavoprotein dehydrogenase
FADH ₂	flavin adenine dinucleotide
FBS	fetal bovine serum
FCCP	Carbonyl cyanide 4-(trifluoromethoxy)phenylhydrazone
FCCP	Carbonyl cyanide- <i>p</i> -trifluoromethoxyphenylhydrazone
Fe ³⁺	ferric iron
Fe-S	iron-sulfur
FMN	flavin mononucleotide
FoxO	forkhead
FRDA	Friedreich's ataxia
G	guanine
G ₃ P	glycerol-3-phosphate
G ₃ PDH	glycerol-3-phosphate dehydrogenase
GABA	γ -aminobutyric acid
Gal	galactose
GAPDH	glycerolaldehyde phosphate dehydrogenase
GO	gene ontology
GPX	glutathione peroxidase
GSEA	gene set enrichment analysis
GSH	glutathione
GSR	gene score resampling
GTP	guanine triphosphate
GTS	glutathione S-transferase

h	hour
H ⁺	proton
H ₂ O	water
H ₂ O ₂	hydrogen peroxide
HBM	4-(Hydroxymercuri)benzoic acid sodium salt
HBSS	Hank's buffered saline solution
HD	Huntington's disease
HEK	human embryonic kidney
HEPES	4-(2-hydroxyethyl)-1-piperazineethanesulfonic acid
HmgCoA	3-hydroxy-3-methylglutaryl-coenzyme A synthase 2
HO [•]	hydroxyl radical
i.e.	id est
<i>i.p.</i>	intraperitoneal
IC ₅₀	half maximal inhibitory concentration
Ide	idebenone
IFU	infection unit
Ima	imatinib
IP ₃	phosphatidylinositol-3
IRJ	ischemic reperfusion injury
JC-1	5,5',6,6'-tetrachloro-1,1',3,3'-tetraethylbenzimidazolylcarbocyanine iodide
KAR	kainate receptor
K _m	Michaelis constant
LCL	lymphoblastoid cells
LHON	Leber's hereditary optic neuropathy
Lip	liposome
lys	lysine
μ	micro
m	milli
m	meter
M	molar
MACS	magnetic beads-based cells sorting
MAP	mitogen-activated protein
MELAS	mitochondrial encephalomyopathy, lactic acidosis, and stroke-like episodes
MEM EBS	minimal essential medium Eagle
MERFF	myoclonic epilepsy and ragged-red fibers
Met	metformin
MgCl ₂	magnesium choride
MIDD	maternally-inherited diabetes and deafness
min	minute
MitoMass	mitochondrial mass
Mn	manganese
MPA	3-mercaptopropionic acid
MPTP	1-methyl-4-phenyl-1,2,3,6-tetrahydropyridine
mPTP	mitochondrial permeability transition pore
MRI	magnetic resonance imaging
mRNA	messenger DNA
mtDNA	mitochondrial DNA
MTT	3-(4,5-dimethylthiazol-2-yl)-2,5-diphenyltetrazolium bromide
n	nano
NAC	<i>N</i> -acetyl- <i>L</i> -cystein

NaCl	sodium chloride
NADH	nicotinamide adenine dinucleotide
NADPH	nicotinamide adenine dinucleotide phosphate
NaOH	sodium hydroxide
NGF	nerve growth factor
NK- κ B	nuclear factor κ B
NMDA	<i>N</i> -methyl- <i>D</i> -aspartate
NMDAR	NMAD receptor
nNOS	nitric oxide-synthesizing NADPH oxidoreductase
NQO1	NAD(P)H:quinone oxidoreductase
NQO2	quinone oxidoreductase 2
Nrf2	nuclear factor (erythroid-derived 2)-like 2
NRH	dihydronicotinamide riboside
O ₂	molecular oxygen
O ₂ ^{•-}	superoxide
Oli	oligomycin
OXPPOS	oxidative phosphorylation
<i>p.o.</i>	per os
pAkt	Akt-1 phosphorylated at Thr172
pAMPK	AMPK phosphorylated at Ser473
PARP1	poly(ADP-ribose) polymerase 1
PBMC	peripheral blood mononuclear cell
PBS	phosphate-buffered saline
PCA	principal component analysis
PCP	pentachlorophenol
PD	Parkinson's disease
PFA	paraformaldehyde
PGC-1 α	peroxisome proliferator-activated receptor gamma coactivator 1-alpha
P _i	inorganic phosphate
PKB	protein kinase B
PPAR	peroxisome proliferator-activated receptor
Ppbp	pro-platelet basic protein
PPP	pentose phosphate pathway
Pyr	pyridaben
Q	quinone
qPCR	quantitative real-time polymerase chain reaction
R ²	coefficient of determination
RCI	respiratory control rate
RET	reverse electron transport
rFI	cumulative relative food intake
RGC	retinal ganglion cell
rH	relative humidity
Rhe	rhein
RNA	ribonucleic acid
RNS	radical nitrogen species
ROOH	hydroperoxide
ROS	reactive oxygen species
Rot	rotenone
RPMI	Rosewell Park Memorial Institute medium
RT	room temperature

s	second
<i>s.c.</i>	subcutaneous
SAR	structure activity relationship
SDS	sodium dodecyl sulfate
SEM	standart error of mean
Ser	serine
shRNA	small hairpin RNA
siRNA	small-interfering RNA
SOD	superoxide dismutase
β -HB	β -hydroxybutyrate
stdev	standard deviation
Stig	stigmatellin
SUMO	small ubiquitin-like modifier
T	thymidine
TCA	citric acid cycle
Tdg	thymine DNA glycosylase
Temp	tempol (4-hydroxy-2,2,6,6-tetramethylpiperidin-1-oxyl)
Thap	thapsigargin
Thr	threonine
TMRM	tetramethylrhodamine methyl ester
tRNA	transfer RNA
Trolox	6-hydroxy-2,5,7,8-tetramethylchroman-2-carboxylic acid
U	uracil
v/v	volume per volume
vCaC	voltage-gated calcium channel
v_{max}	maximal reduction velocity
VPA	valproic acid
w/w	weight per weight
WST-1	2-(4-iodophenyl)-3-(4-nitrophenyl)-5-(2,4-disulfophenyl)-2H-tetrazolium
WT	wild-type
Zn	zinc

9 Table of Figures

Figure 1: Schematic Representation of ATP Production by Anaerobic and Aerobic Glycolysis and Oxidative Phosphorylation	14
Figure 2: Schematic Representation of Mitochondrial Respiration.....	16
Figure 3: Two Different Shuttle Systems Transport Electron Equivalents from NADH into the Mitochondria....	17
Figure 4: Fatty Acid Metabolism and β -Oxidation.....	20
Figure 5: Schematic Representation of Different Modes for Mitochondrial ROS Production.....	23
Figure 6: Schematic Representation of Lipid Peroxidation.....	24
Figure 7: Chemical Structures of Selected Quinones and Related Molecules.....	26
Figure 8: Primary Muscle Cells of Healthy Donors and DMD Patients Cannot Be Discriminated by Mitochondrial Mass, Energy Status or ROS Levels.....	32
Figure 9: Correlation between ATP Levels, Cytosolic and Mitochondrial ROS Level, and Mitochondrial Mass in Primary Muscle Cells of Healthy Donors and DMD Patients.....	34
Figure 10: Mitochondrial Morphology in Primary Myoblasts of Healthy Donors and DMD Patients.....	35
Figure 11: Blood CK and Muscle ATP Levels in Six- and 12-Weeks Old Mice.....	37
Figure 12: Quinones Only Moderately Influence Mitochondrial Parameters.....	38
Figure 13: Influence of Quinones on Cellular ATP Status Depending on Glycolysis- or OXPHOS-Mediated Energy Production.....	39
Figure 14: Influence of ETC Inhibitors, Idebenone, or CoQ ₁ on ATP Levels.....	40
Figure 15: Idebenone and CoQ ₁ Rescue ATP Levels in Rotenone-Treated HepG2 Cells.....	41
Figure 16: ATP Rescue in Presence of Different Complex I Inhibitors.....	43
Figure 17: Influence of Calcium on Mitochondrial ATP Production.....	44
Figure 18: ATP Rescue Is Specific to Certain Short-Chain Benzoquinones.....	45
Figure 19: Idebenone Treatment Does Not Alter Phosphorylation of AMPK.....	46
Figure 20: ATP Rescue of Idebenone and CoQ ₁ Is Dependent on NQO ₁ and Complex III.....	47
Figure 21: Idebenone and Related Quinones Are Substrates for NQO ₁ and NQO ₂	49
Figure 22: Idebenone and Related Quinones Are Reduced in a Selection of Cells and Cell Lines.....	50
Figure 23: Influence of Media Sugar Content on ATP Rescue by Idebenone.....	52
Figure 24: Idebenone and CoQ ₁ Reduce ATP Levels in NQO ₁ -Deficient Cell Lines.....	53
Figure 25: Knock-down of NQO ₁ Expression using shRNA.....	54
Figure 26: Specificity of Oxidoreductase Inhibitors towards NQO ₁ and NQO ₂	55
Figure 27: Pentachlorophenol Selectively Inhibits Reduction of Idebenone.....	56
Figure 28: Reduction of Quinone Is Diversely Inhibited by Different Inhibitors, in Different Cells and in Presence of Different Quinones.....	57
Figure 29: Knock-Down of ETFDH Expression Using siRNA.....	58
Figure 30: Inhibition of Idebenone-Mediated ATP Rescue by Pentachlorophenol Is Not Linked to β -Oxidation.....	59
Figure 31: Effect of Quinones on Mitochondrial Membrane Potential and Lactate Production in MELAS Cybrids.....	61
Figure 32: Alteration of Cumulative Cell Doubling by Different Quinones.....	62
Figure 33: Idebenone Decreases Modification of Akt-1.....	63
Figure 34: CoQ ₁ Elicits DNA Damage Regardless of NQO ₁ Content.....	64
Figure 35: Quinones Affect ROS Levels Differently.....	65
Figure 36: Pre-Treatment with Idebenone Increases Survival of Myoblastoids after Hydrogen Peroxide Stress....	66
Figure 37: Survival of Rat Myoblasts after Hydrogen Peroxide Stress.....	67
Figure 38: Idebenone Reduces Hydrogen Peroxide in Solution.....	68
Figure 39: ATP and ROS Levels after Hydrogen Peroxide Stress.....	69
Figure 40: Idebenone-Mediated Survival Is Independent of Transcription, Translation and NQO ₁ Enzymatic Activity.....	70
Figure 41: Quality Control of Micro Array Data.....	72
Figure 42: Idebenone Does Not Affect ATP Levels in Muscle Tissue with High Mitochondrial Density or Serum β -Hydroxybutyrate Levels <i>in Vivo</i>	75
Figure 43: Idebenone Promotes Increased Food Intake but Does Not Affect Body Weight <i>in Vivo</i>	76
Figure 44: Idebenone Transiently Decreases Blood Glucose Levels Via an Insulin-Independent Mechanism.....	79
Figure 45: Correlations of Parameters Quantified for Idebenone Analogs.....	85
Figure 46: Schematic Representation of Electron Transfer in Complex I and Proposed Inhibition Sites.....	89
Figure 47: Chemical Structures of Complex I Inhibitors.....	90
Figure 48: Potential Scenarios and Targets for Idebenone-Mediated ATP Rescue in Complex I-Deficient Cells.....	93
Figure 49: Schematic representation of NQO ₁ -dependent cytosolic-mitochondrial electron shuttling.....	97
Figure 50: Timing Effects of Idebenone Administration and Suggested Development of Gene Expression and Protein Half Lives.....	101
Figure 51: Schematic Representation of Duchenne Muscular Dystrophy (DMD) Pathology and Suggested Mechanisms of Idebenone.....	106

Figure 52: Schematic Representation of Energy-Related Pathology of <i>Mitochondrial Encephalomyopathy, Lactic Acidosis, and Stroke-like Syndrome</i> (MELAS) and a Suggested Mechanism of Idebenone.	107
Figure 53: Relevant Molecular Interactions of Idebenone.	109
Figure 54: Idebenone Promotes Increased Food Intake but Does Not Affect Body Weight <i>in Vivo</i> (Experiment 0305).	163
Figure 55: Idebenone Does Not Affect Food Intake but Prevents Increase in Body Weight <i>in Vivo</i> (Experiment 0319).	164
Figure 56: Idebenone Does Not Affect Food Intake or Body Weight <i>in Vivo</i> (Experiment 0423).	165
Figure 57: Idebenone Does Not Affect Food Intake or Body Weight <i>in Vivo</i> (Experiment 0436).	166
Figure 58: Idebenone Promotes Increased Food Intake but Does Not Affect Body Weight <i>in Vivo</i> (Experiment 0444).	167
Figure 59: Idebenone Promotes Increased Food Intake but Does Not Affect Body Weight <i>in Vivo</i> (Experiment 0459a).	168
Figure 60: Idebenone Promotes Increased Food Intake but Does Not Affect Body Weight <i>in Vivo</i> (Experiment 0459b).	169

10 Table of Tables

Table 1: Correlation Parameters for Energy Status and Oxidative Stress Levels in Primary Muscle Cells of Healthy Donors and DMD Patients.....	34
Table 2: Selection of Complex I Inhibitors.....	42
Table 3: Steady-state kinetic constants of NQO1 and NQO2 with different quinones.....	50
Table 4: List of Genes Differently Expressed by Idebenone Treatment Selected for Fold Change Exceeding Factor 1.3.....	73
Table 5: Confirmation of Micro Array Data using qPCR.....	74
Table 6: Overview on Different <i>in Vivo</i> Metabolism Experiments.....	78
Table 7: Summary of Idebenone and Analogs in Different Assays.....	82
Table 8: Gene Ontology: Biological Functions According to Expression Pattern of Whole Genome.....	161
Table 9: Gene Ontology: Biological Functions According to Expression Pattern of Significantly Differently Expressed Genes.....	162
Table 10: Vitamin Composition of Different Chows Used <i>in Vivo</i>	170
Table 11: A Selection of Publications on Molecular Effects of Idebenone Relevant to this Thesis.....	171

11 References

- Abdel Baky NA, Zaidi ZF, Fatani AJ, Sayed-Ahmed MM, Yaqub H. Nitric oxide pros and cons: The role of L-arginine, a nitric oxide precursor, and idebenone, a coenzyme-Q analogue in ameliorating cerebral hypoxia in rat. *Brain Res Bull.* 2010;83(1-2):49-56.
- Adikesavan AK, Barrios R, Jaiswal AK. In vivo role of NAD(P)H:quinone oxidoreductase 1 in metabolic activation of mitomycin C and bone marrow cytotoxicity. *Cancer Res.* 2007; 67(17):7966-71.
- Alberts B, Johnson A, Lewis J, Raff M, Roberts K, Walter P. *Molecular Biology of the Cell*, 4th Edition. Garland Science. 2002. ISBN 0-8153-4072-9.
- Amano T, Terao S, Imada I. Effects of 6-(10-hydroxydecyl)-2,3-dimethoxy-5-methyl-1,4-benzoquinone (idebenone) and related benzoquinones on porcine pancreas phospholipase A2 activity. *Biol Pharm Bull.* 1995;18(5):779-81.
- Anisimov VN, Berstein LM, Egormin PA, Piskunova TS, Popovich IG, Zabezhinski MA, Tyndyk ML, Bailey CJ, Turner RC. Metformin. *N Engl J Med.* 1996 Feb 29;334(9):574-9.
- Baracca A, Solaini G, Sgarbi G, Lenaz G, Baruzzi A, Schapira AH, Martinuzzi A, Carelli V. Severe impairment of complex I-driven adenosine triphosphate synthesis in leber hereditary optic neuropathy cybrids. *Arch Neurol.* 2005; 62(5):730-6.
- Barbiroli B, Funicello R, Iotti S, Montagna P, Ferlini A, Zaniol P. 31P-NMR spectroscopy of skeletal muscle in Becker dystrophy and DMD/BMD carriers. Altered rate of phosphate transport. *J Neurol Sci.* 1992; 109(2):188-95.
- Barbiroli B. Clinical and brain bioenergetics improvement with idebenone in a patient with Leber's hereditary optic neuropathy: a clinical and 31P-MRS study. *J Neurol Sci.* 1997; 148(1):25-31.
- Barnils N, Mesa E, Muñoz S, Ferrer-Artola A, Arruga J. Response to idebenone and multivitamin therapy in Leber's hereditary optic neuropathy. *Arch Soc Esp Ophthalmol.* 2007; 82(6):377-80. *Abstract.*
- Barohn RJ, Levine EJ, Olson JO, Mendell JR. Gastric hypomotility in Duchenne's muscular dystrophy. *N Engl J Med.* 1988; 319(1):15-8.
- Bello RI, Gómez-Díaz C, Burón MI, Alcáin FJ, Navas P, Villalba JM. Enhanced anti-oxidant protection of liver membranes in long-lived rats fed on a coenzyme Q10-supplemented diet. *Exp Gerontol.* 2005; 40(8-9):694-706.
- Beretta S, Mattavelli L, Sala G, Tremolizzo L, Schapira AH, Martinuzzi A, Carelli V, Ferrarese C. Leber hereditary optic neuropathy mtDNA mutations disrupt glutamate transport in cybrid cell lines. *Brain.* 2004; 127(Pt 10):2183-92.
- Beyer RE, Segura-Aguilar J, Di Bernardo S, Cavazzoni M, Fato R, Fiorentini D, Galli MC, Setti M, Landi L, Lenaz G. The role of DT-diaphorase in the maintenance of the reduced antioxidant form of coenzyme Q in membrane systems. *Proc Natl Acad Sci U S A.* 1996; 93(6):2528-32.
- Bikman BT, Zheng D, Reed MA, Hickner RC, Houmard JA, Dohm GL. Lipid-induced insulin resistance is prevented in lean and obese myotubes by AICAR treatment. *Am J Physiol Regul Integr Comp Physiol.* 2010; 298(6):R1692-9.
- Binder HJ, Herting DC, Hurst V, Finch SC, Spiro HM. Tocopherol deficiency in man. *N Engl J Med.* 1965; 273(24):1289-97.
- Bobyleva V, Paziienza L, Muscatello U, Kneer N, Lardy H. Short-term hypothermia activates hepatic mitochondrial sn-glycerol-3-phosphate dehydrogenase and thermogenic systems. *Arch Biochem Biophys.* 2000; 380(2):367-72.
- Bodmer M, Vankan P, Dreier M, Kutz KW, Drewe J. Pharmacokinetics and metabolism of idebenone in healthy male subjects. *Eur J Clin Pharmacol.* 2009; 65(5):493-501.
- Bonnet C, Augustin S, Ellouze S, Bénit P, Bouaita A, Rustin P, Sahel JA, Corral-Debrinski M. The optimized allotopic expression of ND1 or ND4 genes restores respiratory chain complex I activity in fibroblasts harboring mutations in these genes. *Biochim Biophys Acta.* 2008; 1783(10):1707-17.
- Boquist L. Pancreatic islets subjected to different concentrations of glucose in vitro. A study with special regard to mitochondrial changes. *Virchows Arch B Cell Pathol.* 1977; 23(3):219-26.
- Borras C, Gambini J, Vina J. Mitochondrial oxidant generation is involved in determining why females live longer than males. *Front Biosci.* 2007 Jan 1;12:1008-13.
- Boland BJ, Silbert PL, Groover RV, Wollan PC, Silverstein MD. Skeletal, cardiac, and smooth muscle failure in Duchenne muscular dystrophy. *Pediatr Neurol.* 1996; 14(1):7-12.

- Bolton JL, Sevestre H, Ibe BO, Thompson JA. Formation and reactivity of alternative quinone methides from butylated hydroxytoluene: possible explanation for species-specific pneumotoxicity. *Chem Res Toxicol.* 1990; 3(1):65-70. *Abstract.*
- Braun U, Paju K, Eimre M, Seppet E, Orlova E, Kadaja L, Trumbeckaite S, Gellerich FN, Zierz S, Jockusch H, Seppet EK. Lack of dystrophin is associated with altered integration of the mitochondria and ATPases in slow-twitch muscle cells of MDX mice. *Biochim Biophys Acta.* 2001; 1505(2-3):258-70.
- Brandsema JF, Stephens D, Hartley J, Yoon G. Intermediate-dose idebenone and quality of life in Friedreich ataxia. *Pediatr Neurol.* 2010; 42(5):338-42.
- Brandt U, Kerscher S, Dröse S, Zwicker K, Zickermann V. Proton pumping by NADH:ubiquinone oxidoreductase. A redox driven conformational change mechanism? *FEBS Lett.* 2003; 545(1):9-17.
- Brière JJ, Schlemmer D, Chretien D, Rustin P. Quinone analogues regulate mitochondrial substrate competitive oxidation. *Biochem Biophys Res Commun.* 2004; 316(4):1138-42.
- Brini M. Ca(2+) signalling in mitochondria: mechanism and role in physiology and pathology. *Cell Calcium.* 2003; 34(4-5):399-405.
- Brown MD, Trounce IA, Jun AS, Allen JC, Wallace DC. Functional analysis of lymphoblast and cybrid mitochondria containing the 3460, 11778, or 14484 Leber's hereditary optic neuropathy mitochondrial DNA mutation. *J Biol Chem.* 2000 22; 275(51):39831-6.
- Brunelle JK, Letai A. Control of mitochondrial apoptosis by the Bcl-2 family. *J Cell Sci.* 2009; 122(Pt 4):437-41.
- Brunmair B, Staniek K, Gras F, Scharf N, Althaym A, Clara R, Roden M, Gnaiger E, Nohl H, Waldhäusl W, Fürnsinn C. Thiazolidinediones, like metformin, inhibit respiratory complex I: a common mechanism contributing to their antidiabetic actions? *Diabetes.* 2004; 53(4):1052-9.
- Bulfield G, Siller WG, Wight PA, Moore KJ. X chromosome-linked muscular dystrophy (mdx) in the mouse. *Proc Natl Acad Sci U S A.* 1984; 81(4):1189-92.
- Burelle Y, Khairallah M, Ascah A, Allen BG, Deschepper CF, Petrof BJ, Des Rosiers C. Alterations in mitochondrial function as a harbinger of cardiomyopathy: lessons from the dystrophic heart. *J Mol Cell Cardiol.* 2010; 48(2):310-21.
- Buyse G, Mertens L, Di Salvo G, Matthijs I, Weidemann F, Eyskens B, Goossens W, Goemans N, Sutherland GR, Van Hove JL. Idebenone treatment in Friedreich's ataxia: neurological, cardiac, and biochemical monitoring. *Neurology.* 2003; 60(10):1679-81.
- Buyse GM, Van der Mieren G, Erb M, D'hooge J, Herijgers P, Verbeke E, Jara A, Van Den Bergh A, Mertens L, Courdier-Fruh I, Barzaghi P, Meier T. Long-term blinded placebo-controlled study of SNT-MC17/idebenone in the dystrophin deficient mdx mouse: cardiac protection and improved exercise performance. *Eur Heart J.* 2009; 30(1):116-24.
- Buyse GM, Van der Mieren G, Erb M, D'hooge J, Herijgers P, Verbeke E, Jara A, Van Den Bergh A, Mertens L, Courdier-Fruh I, Barzaghi P, Meier T. Long-term blinded placebo-controlled study of SNT-MC17/idebenone in the dystrophin deficient mdx mouse: cardiac protection and improved exercise performance. *Eur Heart J.* 2009 Jan;30(1):116-24.
- Cabello CM, Bair WB 3rd, Bause AS, Wondrak GT. Antimelanoma activity of the redox dye DCPIP (2,6-dichlorophenolindophenol) is antagonized by NQO1. *Biochem Pharmacol.* 2009; 78(4):344-54.
- Cabello CM, Lamore SD, Bair WB 3rd, Davis AL, Azimian SM, Wondrak GT. DCPIP (2,6-dichlorophenolindophenol) as a genotype-directed redox chemotherapeutic targeting NQO1*2 breast carcinoma. *Free Radic Res.* 2011; 45(3):276-92.
- Camiña F, Novo-Rodríguez MI, Rodríguez-Segade S, Castro-Gago M. Purine and carnitine metabolism in muscle of patients with Duchenne muscular dystrophy. *Clin Chim Acta.* 1995; 243(2):151-64.
- Campbell N, Reece J. *Biology*, 7th Edition. Benjamin Cummings. 2005. ISBN 0-80-537146-X.
- Cardoso SM, Pereira C, Oliveira CR. The protective effect of vitamin E, idebenone and reduced glutathione on free radical mediated injury in rat brain synaptosomes. *Biochem Biophys Res Commun.* 1998; 246(3):703-10.
- Carelli V, Barboni P, Zacchini A, Mancini R, Monari L, Cevoli S, Liguori R, Sensi M, Lugaresi E, Montagna P. Leber's Hereditary Optic Neuropathy (LHON) with 14484/ND6 mutation in a North African patient. *J Neurol Sci.* 1998; 160(2):183-8.
- Chang Y, Lin YW, Wang SJ. Idebenone inhibition of glutamate release from rat cerebral cortex nerve endings by suppression of voltage-dependent calcium influx and protein kinase A. *Naunyn Schmiedebergs Arch Pharmacol.* 2011; [Epub ahead of print] *Abstract.*
- Chapela SP, Burgos HI, Salazar AI, Nievas I, Kriguer N, Stella CA. Biochemical study of idebenone effect on mitochondrial metabolism of yeast. *Cell Biol Int.* 2008; 32(1):146-50.
- Chatterjee A, Dasgupta S, Sidransky D. Mitochondrial subversion in cancer. *Cancer Prev Res (Phila).* 2011; 4(5):638-54.

- Chelikani P, Fita I, Loewen PC. Diversity of structures and properties among catalases. *Cell Mol Life Sci.* 2004; 61(2):192-208.
- Chen YW, Zhao P, Borup R, Hoffman EP. Expression profiling in the muscular dystrophies: identification of novel aspects of molecular pathophysiology. *Cell Biol.* 2000; 151(6):1321-36.
- Chinnery PF, Turnbull DM. Epidemiology and treatment of mitochondrial disorders. *Am J Med Genet.* 2001; 106(1):94-101.
- Clay HB, Sullivan S, Konradi C. Mitochondrial dysfunction and pathology in bipolar disorder and schizophrenia. *Int J Dev Neurosci.* 2011; 29(3):311-24.
- Civenni G, Bezzi P, Trotti D, Volterra A, Racagni G. Inhibitory effect of the neuroprotective agent idebenone on arachidonic acid metabolism in astrocytes. *Eur J Pharmacol.* 1999; 370(2):161-7.
- Colucci MA, Moody CJ, Couch GD. Natural and synthetic quinones and their reduction by the quinone reductase enzyme NQO1: from synthetic organic chemistry to compounds with anticancer potential. *Org Biomol Chem.* 2008; 6(4):637-56.
- Cortelli P, Montagna P, Pierangeli G, Lodi R, Barboni P, Liguori R, Carelli V, Iotti S, Zaniol P, Lugaresi E, Barbiroli B. Clinical and brain bioenergetics improvement with idebenone in a patient with Leber's hereditary optic neuropathy: a clinical and 31P-MRS study. *J Neurol Sci.* 1997; 148(1):25-31.
- Coudé FX, Grimber G, Pelet A, Benoit Y. Action of the antiepileptic drug, valproic acid, on fatty acid oxidation in isolated rat hepatocytes. *Biochem Biophys Res Commun.* 1983; 115(2):730-6.
- Crane FL. Biochemical functions of coenzyme Q10. *J Am Coll Nutr.* 2001; 20(6):591-8.
- Cummings SW, Curtis BB 2nd, Peterson JA, Prough RA. The effect of the tert-butylquinone metabolite of butylated hydroxyanisole on cytochrome P-450 monooxygenase activity. *Xenobiotica.* 1990; 20(9):915-24.
- Danielson SR, Carelli V, Tan G, Martinuzzi A, Schapira AH, Savontaus ML, Cortopassi GA. Isolation of transcriptomal changes attributable to LHON mutations and the cybridization process. *Brain.* 2005; 128(Pt 5):1026-37.
- Danielson SR, Wong A, Carelli V, Martinuzzi A, Schapira AH, Cortopassi GA. Cells bearing mutations causing Leber's hereditary optic neuropathy are sensitized to Fas-induced apoptosis. *J Biol Chem* 2002;277:5810-5815.
- Davidson MM, Walker WF, Hernandez-Rosa E. The m.3243A>G mtDNA mutation is pathogenic in an in vitro model of the human blood brain barrier. *Mitochondrion.* 2009; 9(6):463-70.
- de Moura MB, dos Santos LS, Van Houten B. Mitochondrial dysfunction in neurodegenerative diseases and cancer. *Environ Mol Mutagen.* 2010; 51(5):391-405.
- Deconinck N, Dan B. Pathophysiology of duchenne muscular dystrophy: current hypotheses. *Pediatr Neurol.* 2007; 36(1):1-7.
- Degli Esposti MD, Ngo A, Ghelli A, Benelli B, Carelli V, McLennan H, Linnane AW. The interaction of Q analogs, particularly hydroxydecyl benzoquinone (idebenone), with the respiratory complexes of heart mitochondria. *Arch Biochem Biophys.* 1996a; 330(2):395-400.
- Degli Esposti M, Ngo A, McMullen GL, Ghelli A, Sparla F, Benelli B, Ratta M, Linnane AW. The specificity of mitochondrial complex I for ubiquinones. *Biochem J.* 1996b; 313 (Pt 1):327-34.
- Degli Esposti M. Inhibitors of NADH-ubiquinone reductase: an overview. *Biochim Biophys Acta.* 1998; 1364(2):222-35.
- Dennis G Jr, Sherman BT, Hosack DA, Yang J, Gao W, Lane HC, Lempicki RA. DAVID: Database for Annotation, Visualization, and Integrated Discovery. *Genome Biol.* 2003; 4(5):P3.
- Deschamps D, Fisch C, Fromenty B, Berson A, Degott C, Pessayre D. Inhibition by salicylic acid of the activation and thus oxidation of long chain fatty acids. Possible role in the development of Reye's syndrome. *J Pharmacol Exp Ther.* 1991; 259(2):894-904.
- Di Prospero NA, Baker A, Jeffries N, Fischbeck KH. Neurological effects of high-dose idebenone in patients with Friedreich's ataxia: a randomised, placebo-controlled trial. *Lancet Neurol.* 2007; 6(10):878-86.
- Diaz F, Moraes CT. Mitochondrial biogenesis and turnover. *Cell Calcium.* 2008; 44(1):24-35.
- Disatnik MH, Dhawan J, Yu Y, Beal MF, Whirl MM, Franco AA, Rando TA. Evidence of oxidative stress in mdx mouse muscle: studies of the pre-necrotic state. *J Neurol Sci.* 1998; 161(1):77-84.
- Dragan M, Dixon SJ, Jaworski E, Chan TS, O'Brien PJ, Wilson JX. Coenzyme Q(1) depletes NAD(P)H and impairs recycling of ascorbate in astrocytes. *Brain Res.* 2006; 1078(1):9-18.
- Drahota Z, Rauchova H, Jesina P, Vojtisková A, Houstek J. Glycerophosphate-dependent peroxide production by brown fat mitochondria from newborn rats. *Gen Physiol Biophys.* 2003; 22(1):93-102.
- Dupont-Versteegden EE, Baldwin RA, McCarter RJ, Vonlanthen MG. Does muscular dystrophy affect metabolic rate? A study in mdx mice. *J Neurol Sci.* 1994; 121(2):203-7.
- Ehmsen J, Poon E, Davies K. The dystrophin-associated protein complex. *J Cell Sci.* 2002; 115(Pt 14):2801-3.

- Emery AE. Population frequencies of inherited neuromuscular diseases--a world survey. *Neuromuscul Disord.* 1991; 1(1):19-29.
- Endlicher R, Kriváková P, Rauchová H, Nůsková H, Cervinková Z, Drahotka Z. Peroxidative damage of mitochondrial respiration is substrate-dependent. *Physiol Res.* 2009; 58(5):685-92.
- Fato R, Bergamini C, Leoni S, Strocchi P, Lenaz G. Generation of reactive oxygen species by mitochondrial complex I: implications in neurodegeneration. *Neurochem Res.* 2008; 33(12):2487-501.
- Fato R, Bergamini C, Bortolus M, Maniero AL, Leoni S, Ohnishi T, Lenaz G. Differential effects of mitochondrial Complex I inhibitors on production of reactive oxygen species. *Biochim Biophys Acta.* 2009; 1787(5):384-92.
- Floreani M, Napoli E, Martinuzzi A, Pantano G, De Riva V, Trevisan R, Bisetto E, Valente L, Carelli V, Dabbeni-Sala F. Antioxidant defences in cybrids harboring mtDNA mutations associated with Leber's hereditary optic neuropathy. *FEBS J.* 2005; 272(5):1124-35.
- Ferreira IL, Resende R, Ferreira E, Rego AC, Pereira CF. Multiple defects in energy metabolism in Alzheimer's disease. *Curr Drug Targets.* 2010; 11(10):1193-206.
- Fiorillo C, Ponziani V, Giannini L, Cecchi C, Celli A, Nassi N, Lanzilao L, Caporale R, Nassi P. Protective effects of the PARP-1 inhibitor PJ34 in hypoxic-reoxygenated cardiomyoblasts. *Cell Mol Life Sci.* 2006; 63(24):3061-71.
- Fong PY, Turner PR, Denetclaw WF, Steinhart RA. Increased activity of calcium leak channels in myotubes of Duchenne human and mdx mouse origin. *Science.* 1990; 250(4981):673-6.
- Fontaine E, Bernardi P. Progress on the mitochondrial permeability transition pore: regulation by complex I and ubiquinone analogs. *J Bioenerg Biomembr.* 1999; 31(4):335-45.
- Foretz M, Hébrard S, Leclerc J, Zarrinpashneh E, Soty M. Metformin inhibits hepatic gluconeogenesis in mice independently of the LKB1/AMPK pathway via a decrease in hepatic energy state. *J Clin Invest.* 2010; 120(7):2355-2369.
- Fornuskova D, Brantova O, Tesarova M, Stiburek L, Honzik T, Wenchich L, Tietzeova E, Hansikova H, Zeman J. The impact of mitochondrial tRNA mutations on the amount of ATP synthase differs in the brain compared to other tissues. *Biochim Biophys Acta.* 2008; 1782(5):317-25.
- Freestone PS, Chung KK, Guatteo E, Mercuri NB, Nicholson LF, Lipski J. Acute action of rotenone on nigral dopaminergic neurons--involvement of reactive oxygen species and disruption of Ca²⁺ homeostasis. *Eur J Neurosci.* 2009; 30(10):1849-59.
- Frerman FE. Reaction of electron-transfer flavoprotein ubiquinone oxidoreductase with the mitochondrial respiratory chain. *Biochim Biophys Acta.* 1987; 893(2):161-9.
- Gannoun-Zaki L, Fournier-Bidoz S, Le Cam G, Chambon C, Millasseau P, Léger JJ, Dechesne CA. Down-regulation of mitochondrial mRNAs in the mdx mouse model for Duchenne muscular dystrophy. *FEBS Lett.* 1995; 375(3):268-72.
- Garedeu A, Henderson SO, Moncada S. Activated macrophages utilize glycolytic ATP to maintain mitochondrial membrane potential and prevent apoptotic cell death. *Cell Death Differ.* 2010; 17(10):1540-50.
- Genova ML, Pich MM, Biondi A, Bernacchia A, Falasca A, Bovina C, Formiggini G, Parenti Castelli G, Lenaz G. Mitochondrial production of oxygen radical species and the role of Coenzyme Q as an antioxidant. *Exp Biol Med (Maywood).* 2003; 228(5):506-13.
- Geromel V, Darin N, Chrétien D, Bénil P, DeLonlay P, Rötig A, Munnich A, Rustin P. Coenzyme Q(10) and idebenone in the therapy of respiratory chain diseases: rationale and comparative benefits. *Mol Genet Metab.* 2002; 77(1-2):21-30.
- Geromel V, Parfait B, von Kleist-Retzow JC, Chretien D, Munnich A, Rötig A, Rustin P. The consequences of a mild respiratory chain deficiency on substrate competitive oxidation in human mitochondria. *Biochem Biophys Res Commun.* 1997; 236(3):643-6.
- Ghelli A, Zanna C, Porcelli AM, et al. Leber's hereditary optic neuropathy (LHON) pathogenic mutations induce mitochondrialdependent apoptotic death in transmitochondrial cells incubated with galactose medium. *J Biol Chem.* 2003; 278:4145-4150.
- Ghelli A, Porcelli AM, Zanna C, Martinuzzi A, Carelli V, Rugolo M. Protection against oxidant-induced apoptosis by exogenous glutathione in Leber hereditary optic neuropathy cybrids. *Invest Ophthalmol Vis Sci.* 2008; 49(2):671-6.
- Ghelli A, Porcelli AM, Zanna C, Vidoni S, Mattioli S, Barbieri A, Iommarini L, Pala M, Achilli A, Torrioni A, Rugolo M, Carelli V. The background of mitochondrial DNA haplogroup J increases the sensitivity of Leber's hereditary optic neuropathy cells to 2,5-hexanedione toxicity. *PLoS One.* 2009; 4(11):e7922.
- Gieseler A, Schultze AT, Kupsch K, Haroon MF, Wolf G, Siemen D, Kreutzmann P. Inhibitory modulation of the mitochondrial permeability transition by minocycline. *Biochem Pharmacol.* 2009; 77(5):888-96.
- Gil J, Almeida S, Oliveira CR, Rego AC. Cytosolic and mitochondrial ROS in staurosporine-induced retinal cell apoptosis. *Free Radic Biol Med.* 2003; 35(11):1500-14.

- Gillis JC, Benefield P, McTavish D. Idebenone. A review of its pharmacodynamic and pharmacokinetic properties, and therapeutic use in age-related cognitive disorders. *Drugs Aging*. 1994; 5(2):133-52.
- Grandison RC, Piper MD, Partridge L. Amino-acid imbalance explains extension of lifespan by dietary restriction in *Drosophila*. *Nature*. 2009; 462(7276):1061-4.
- Gross J, Bhattacharya D. Endosymbiont or host: who drove mitochondrial and plastid evolution? *Biol Direct*. 2011; 6:12.
- Guarente L. Mitochondria--a nexus for aging, calorie restriction, and sirtuins? *Cell*. 2008; 132(2):171-6.
- Guha N, Chang JS, Chokkalingam AP, Wiemels JL, Smith MT, Buffler PA. NQO1 polymorphisms and de novo childhood leukemia: a HuGE review and meta-analysis. *Am J Epidemiol*. 2008; 168(11):1221-32.
- Gumprich E, Dahl R, Yerushalmi B, Devereaux MW, Sokol RJ. Nitric oxide ameliorates hydrophobic bile acid-induced apoptosis in isolated rat hepatocytes by non-mitochondrial pathways. *J Biol Chem*. 2002; 277(28):25823-30.
- Gündüz D, Kasseckert SA, Härtel FV, Aslam M, Abdallah Y, Schäfer M, Piper HM, Noll T, Schäfer C. Accumulation of extracellular ATP protects against acute reperfusion injury in rat heart endothelial cells. *Cardiovasc Res*. 2006; 71(4):764-73.
- Gutteridge JM, Halliwell B. The measurement and mechanism of lipid peroxidation in biological systems. *Trends Biochem Sci*. 1990; 15(4):129-35.
- Haas RH. Autism and mitochondrial disease. *Dev Disabil Res Rev*. 2010; 16(2):144-53.
- Haginoya K, Miyabayashi S, Kikuchi M, Kojima A, Yamamoto K, Omura K, Uematsu M, Hino-Fukuyo N, Tanaka S, Tsuchiya S. Efficacy of idebenone for respiratory failure in a patient with Leigh syndrome: a long-term follow-up study. *J Neurol Sci*. 2009; 278(1-2):112-4.
- Haefeli RH, Erb M, Gemperli AC, Robay D, Courdier Fruh I, Anklin C, Dallmann R, Gueven N. NQO1-Dependent Redox Cycling of Idebenone: Effects on Cellular Redox Potential and Energy Levels. *PLoS One*. 2011; 6(3):e17963.
- Haigis MC, Sinclair DA. Mammalian sirtuins: biological insights and disease relevance. *Annu Rev Pathol*. 2010; 5:253-95.
- Han Y, Wang Q, Song P, Zhu Y, Zou MH. Redox regulation of the AMP-activated protein kinase. *PLoS One*. 2010; 5(11):e15420.
- Hanada M, Feng J, Hemmings BA. Structure, regulation and function of PKB/AKT— a major therapeutic target. *Biochim Biophys Acta*. 2004; 1697(1-2):3-16.
- Haroony MF, Fatima A, Schöler S, Gieseler A, Horn TF, Kirches E, Wolf G, Kreuzmann P. Minocycline, a possible neuroprotective agent in Leber's hereditary optic neuropathy (LHON): studies of cybrid cells bearing 11,778 mutation. *Neurobiol Dis*. 2007; 28(3):237-50.
- Hausse AO, Aggoun Y, Bonnet D, Sidi D, Munnich A, Rötig A, Rustin P. Idebenone and reduced cardiac hypertrophy in Friedreich's ataxia. *Heart*. 2002; 87(4):346-9.
- Hayes JD, Chanas SA, Henderson CJ, McMahon M, Sun C, Moffat GJ, Wolf CR, Yamamoto M. The Nrf2 transcription factor contributes both to the basal expression of glutathione S-transferases in mouse liver and to their induction by the chemopreventive synthetic antioxidants, butylated hydroxyanisole and ethoxyquin. *Biochem Soc Trans*. 2000; 28(2):33-41. *Abstract*.
- Higaki Y, Mikami T, Fujii N, Hirshman MF, Koyama K, Seino T, Tanaka K, Goodyear LJ. Oxidative stress stimulates skeletal muscle glucose uptake through a phosphatidylinositol 3-kinase-dependent pathway. *Am J Physiol Endocrinol Metab*. 2008; 294(5):E889-97.
- Hirano M, Ricci E, Koenigsberger MR, Defendini R, Pavlakis SG, DeVivo DC, DiMauro S, Rowland LP. Melas: an original case and clinical criteria for diagnosis. *Neuromuscul Disord*. 1992; 2(2):125-35. *Abstract*.
- Hirano M, Pavlakis SG. Mitochondrial myopathy, encephalopathy, lactic acidosis, and strokelike episodes (MELAS): current concepts. *J Child Neurol*. 1994; 9(1):4-13. *Abstract*.
- Hochachka PW, Mommsen TP. Protons and anaerobiosis. *Science*. 1983; 219(4591):1391-7.
- Hopf FW, Turner PR, Steinhardt RA. Calcium misregulation and the pathogenesis of muscular dystrophy. *Subcell Biochem*. 2007; 45:429-64. *Abstract*.
- Houchi H, Azuma M, Oka M, Morita K. Idebenone inhibits catecholamine secretion through its blocking action on Ca²⁺ channels in cultured adrenal chromaffin cells. *Jpn J Pharmacol*. 1991b; 57(4):553-8.
- Houchi H, Yoshizumi M, Minakuchi K, Azuma M, Morita K, Oka M. Idebenone, an agent improving cerebral metabolism, stimulates [¹⁴C]tyrosine uptake and [¹⁴C]catecholamine formation by cultured bovine adrenal chromaffin cells. *Biochem Pharmacol*. 1991a; 42(4):951-4.
- Huang da W, Sherman BT, Lempicki RA. Systematic and integrative analysis of large gene lists using DAVID bioinformatics resources. *Nat Protoc*. 2009; 4(1):44-57.

- Hudson G, Carelli V, Spruijt L, Gerards M, Mowbray C, Achilli A, Pyle A, Elson J, Howell N, La Morgia C, Valentino ML, Huoponen K, Savontaus ML, Nikoskelainen E, Sadun AA, Salomao SR, Belfort R Jr, Griffiths P, Man PY, de Coo RF, Horvath R, Zeviani M, Smeets HJ, Torroni A, Chinnery PF. Clinical expression of Leber hereditary optic neuropathy is affected by the mitochondrial DNA-haplogroup background. *Am J Hum Genet.* 2007; 81(2):228-33.
- Hunter MI, Mohamed JB. Plasma antioxidants and lipid peroxidation products in Duchenne muscular dystrophy. *Clin Chim Acta.* 1986; 155(2):123-31.
- Hutchinson DS, Csikasz RI, Yamamoto DL, Shabalina IG, Wikström P, Wilcke M, Bengtsson T. Diphenylene iodonium stimulates glucose uptake in skeletal muscle cells through mitochondrial complex I inhibition and activation of AMP-activated protein kinase. *Cell Signal.* 2007; 19(7):1610-20.
- Hwang JH, Kim DW, Jo EJ, Kim YK, Jo YS, Park JH, Yoo SK, Park MK, Kwak TH, Kho YL, Han J, Choi HS, Lee SH, Kim JM, Lee I, Kyung T, Jang C, Chung J, Kweon GR, Shong M. Pharmacological stimulation of NADH oxidation ameliorates obesity and related phenotypes in mice. *Diabetes.* 2009; 58(4):965-74.
- Ikejiri Y, Mori E, Ishii K, Nishimoto K, Yasuda M, Sasaki M. Idebenone improves cerebral mitochondrial oxidative metabolism in a patient with MELAS. *Neurology.* 1996; 47(2):583-5.
- Imada I, Fujita T, Sugiyama Y, Okamoto K, Kobayashi Y. Effects of idebenone and related compounds on respiratory activities of brain mitochondria, and on lipid peroxidation of their membranes. *Arch Gerontol Geriatr.* 1989; 8(3):323-41.
- Inzucchi SE, Maggs DG, Spollett GR, Page SL, Rife FS, Walton V, Shulman GI. Efficacy and metabolic effects of metformin and troglitazone in type II diabetes mellitus. *N Engl J Med.* 1998; 338(13):867-72.
- Itoh K, Chiba T, Takahashi S, Ishii T, Igarashi K, Katoh Y, Oyake T, Hayashi N, Satoh K, Hatayama I, Yamamoto M, Nabeshima Y. An Nrf2/small Maf heterodimer mediates the induction of phase II detoxifying enzyme genes through antioxidant response elements. *Biochem Biophys Res Commun.* 1997; 236(2):313-22.
- James AM, Wei YH, Pang CY, Murphy MP. Altered mitochondrial function in fibroblasts containing MELAS or MERRF mitochondrial DNA mutations. *Biochem J.* 1996; 318 (Pt 2):401-7.
- James AM, Cochemé HM, Smith RA, Murphy MP. Interactions of mitochondria-targeted and untargeted ubiquinones with the mitochondrial respiratory chain and reactive oxygen species. Implications for the use of exogenous ubiquinones as therapies and experimental tools. *J Biol Chem.* 2005; 280(22):21295-312.
- Jaiswal AK. Characterization and partial purification of microsomal NAD(P)H:quinone oxidoreductases. *Arch Biochem Biophys.* 2000; 375(1):62-8.
- Jauslin ML, Wirth T, Meier T, Schoumacher F. A cellular model for Friedreich Ataxia reveals small-molecule glutathione peroxidase mimetics as novel treatment strategy. *Hum Mol Genet.* 2002; 11(24):3055-63.
- Jauslin ML, Meier T, Smith RA, Murphy MP. Mitochondria-targeted antioxidants protect Friedreich Ataxia fibroblasts from endogenous oxidative stress more effectively than untargeted antioxidants. *FASEB J.* 2003; 17(13):1972-4.
- Jauslin ML, Vertuani S, Durini E, Buzzoni L, Ciliberti N, Verdecchia S, Palozza P, Meier T, Manfredini S. Protective effects of Fe-Aox29, a novel antioxidant derived from a molecular combination of Idebenone and vitamin E, in immortalized fibroblasts and fibroblasts from patients with Friedreich Ataxia. *Mol Cell Biochem.* 2007; 302(1-2):79-85.
- Jou SH, Chiu NY, Liu CS. Mitochondrial dysfunction and psychiatric disorders. *Chang Gung Med J.* 2009; 32(4):370-9.
- Kalayci M, Unal MM, Gul S, Acikgoz S, Kandemir N, Hanci V, Edebalı N, Acikgoz B. The effect of Coenzyme Q10 on ischemia and neuronal damage in an experimental traumatic brain injury model in rats. *BMC Neurosci.* 2011; 12(1):75.
- Kakahana M, Yamazaki N, Nagaoka A. Effects of idebenone on the levels of acetylcholine, choline, free fatty acids, and energy metabolites in the brains of rats with cerebral ischemia. *Arch Gerontol Geriatr.* 1989; 8(3):247-56.
- Kandel ES, Hay N. The regulation and activities of the multifunctional serine/threonine kinase Akt/PKB. *Exp Cell Res.* 1999; 253(1):210-29.
- Kaneko S, Sugimura M, Inoue T, Satoh M. Effects of several cerebroprotective drugs on NMDA channel function: evaluation using *Xenopus* oocytes and [³H]MK-801 binding. *Eur J Pharmacol.* 1991; 207(2):119-28.
- Kar AM, Nag D, Shukla R. Trigeminal neuropathy secondary to lymphoma. *J Indian Med Assoc.* 1979; 73(12):221.
- Kaufmann P, Shungu DC, Sano MC, Jhung S, Engelstad K, Mitsis E, Mao X, Shanske S, Hirano M, DiMauro S, De Vivo DC. Cerebral lactic acidosis correlates with neurological impairment in MELAS. *Neurology.* 2004; 62(8):1297-302.
- Kean EA. Inhibitory action of rhein on the reduced nicotinamide adenine dinucleotidedehydrogenase complex of mitochondrial particles and on other dehydrogenases. *Biochem Pharmacol.* 1970; 19(7):2201-2. *Abstract.*

- Kelly KR, Abbott MJ, Turcotte LP. Short-term AMP-regulated protein kinase activation enhances insulin-sensitive fatty acid uptake and increases the effects of insulin on fatty acid oxidation in L6 muscle cells. *Exp Biol Med (Maywood)*. 2010; 235(4):514-21.
- Kemp GJ, Taylor DJ, Dunn JF, Frostick SP, Radda GK. Cellular energetics of dystrophic muscle. *J Neurol Sci*. 1993; 116(2):201-6.
- King MS, Sharpley MS, Hirst J. Reduction of hydrophilic ubiquinones by the flavin in mitochondrial NADH:ubiquinone oxidoreductase (Complex I) and production of reactive oxygen species. *Biochemistry*. 2009; 48(9):2053-62.
- Kinnally KW, Peixoto PM, Ryu SY, Dejean LM. Is mPTP the gatekeeper for necrosis, apoptosis, or both? *Biochim Biophys Acta*. 2011; 1813(4):616-22.
- Kirby DM, McFarland R, Ohtake A, Dunning C, Ryan MT, Wilson C, Ketteridge D, Turnbull DM, Thorburn DR, Taylor RW. Mutations of the mitochondrial ND1 gene as a cause of MELAS. *J Med Genet*. 2004; 41(10):784-9.
- Kiyota Y, Hamajo K, Miyamoto M, Nagaoka A. Effect of idebenone (CV-2619) on memory impairment observed in passive avoidance task in rats with cerebral embolization. *Jpn J Pharmacol*. 1985; 37(3):300-2.
- Klaassen CD, Reisman SA. Nrf2 the rescue: effects of the antioxidative/electrophilic response on the liver. *Toxicol Appl Pharmacol*. 2010; 244(1):57-65.
- Klivenyi P, Karg E, Rozsa C, Horvath R, Komoly S, Nemeth I, Turi S, Vecsei L. alpha-Tocopherol/lipid ratio in blood is decreased in patients with Leber's hereditary optic neuropathy and asymptomatic carriers of the 11778 mtDNA mutation. *J Neurol Neurosurg Psychiatry*. 2001; 70(3):359-62.
- Korsten A, de Coo IF, Spruijt L, de Wit LE, Smeets HJ, Sluiter W. Patients with Leber hereditary optic neuropathy fail to compensate impaired oxidative phosphorylation. *Biochim Biophys Acta*. 2010; 1797(2):197-203.
- Koenig X, Dysek S, Kimbacher S, Mike AK, Cervenka R, Lukacs P, Nagl K, Dang XB, Todt H, Bittner RE, Hilber K. Voltage-gated ion channel dysfunction precedes cardiomyopathy development in the dystrophic heart. *PLoS One*. 2011; 6(5):e20300.
- Kruger NJ, von Schaewen A. The oxidative pentose phosphate pathway: structure and organisation. *Curr Opin Plant Biol*. 2003; 6(3):236-46.
- Kutz K, Drewe J, Vankan P. Pharmacokinetic properties and metabolism of idebenone. *J Neurol*. 2009; 256 Suppl 1:31-5.
- Kuznetsov AV, Winkler K, Wiedemann FR, von Bossanyi P, Dietzmann K, Kunz WS. Impaired mitochondrial oxidative phosphorylation in skeletal muscle of the dystrophin-deficient mdx mouse. *Mol Cell Biochem*. 1998; 183(1-2):87-96.
- Lam YT, Stocker R, Dawes IW. The lipophilic antioxidants alpha-tocopherol and coenzyme Q10 reduce the replicative lifespan of *Saccharomyces cerevisiae*. *Free Radic Biol Med*. 2010; 49(2):237-44.
- Lawlor MA, Alessi DR. PKB/Akt: a key mediator of cell proliferation, survival and insulin responses? *J Cell Sci*. 2001; 114(Pt 16):2903-10.
- Lekoubou A, Kouamé-Assouan AE, Cho TH, Luauté J, Nighoghossian N, Derex L. Effect of long-term oral treatment with L-arginine and idebenone on the prevention of stroke-like episodes in an adult MELAS patient. *Rev Neurol (Paris)*. 2011; [Epub ahead of print] Abstract.
- Lee HK, Braynen W, Keshav K, Pavlidis P. ErmineJ: tool for functional analysis of gene expression data sets. *BMC Bioinformatics*. 2005; 6:269.
- Lee HJ, Lee HJ, Lee EO, Ko SG, Bae HS, Kim CH, Ahn KS, Lu J, Kim SH. Mitochondria-cytochrome C-caspase-9 cascade mediates isorhamnetin-induced apoptosis. *Cancer Lett*. 2008; 270(2):342-53.
- Lenaz G, Bovina C, D'Aurelio M, Fato R, Formiggini G, Genova ML, Giuliano G, Merlo Pich M, Paolucci U, Parenti Castelli G, Ventura B. Role of mitochondria in oxidative stress and aging. *Ann N Y Acad Sci*. 2002; 959:199-213.
- Lenaz G, Fato R, Formiggini G, Genova ML. The role of Coenzyme Q in mitochondrial electron transport. *Mitochondrion*. 2007; 7 Suppl:S8-33.
- Lenaz G, Fato R, Genova ML, Bergamini C, Bianchi C, Biondi A. Mitochondrial Complex I: structural and functional aspects. *Biochim Biophys Acta*. 2006; 1757(9-10):1406-20.
- Levin LA. Mechanisms of retinal ganglion specific-cell death in Leber hereditary optic neuropathy. *Trans Am Ophthalmol Soc*. 2007; 105:379-91.
- Lin SJ, Ford E, Haigis M, Liszt G, Guarente L. Calorie restriction extends yeast life span by lowering the level of NADH. *Genes Dev*. 2004; 18(1):12-6.
- Lindinger MI, Kowalchuk JM, Heigenhauser GJ. Applying physicochemical principles to skeletal muscle acid-base status. *Am J Physiol Regul Integr Comp Physiol*. 2005; 289(3):R891-4.
- Linnane AW, Kios M, Vitetta L. Coenzyme Q(10)--its role as a prooxidant in the formation of superoxide anion/hydrogen peroxide and the regulation of the metabolome. *Mitochondrion*. 2007; 7 Suppl:S51-61.

- Lodi R, Carelli V, Cortelli P, Iotti S, Valentino ML, Barboni P, Pallotti F, Montagna P, Barbiroli B. Phosphorus MR spectroscopy shows a tissue specific in vivo distribution of biochemical expression of the G3460A mutation in Leber's hereditary optic neuropathy. *J Neurol Neurosurg Psychiatry*. 2002; 72(6):805-7.
- Long DJ 2nd, Jaiswal AK. Mouse NRH:quinone oxidoreductase (NQO2): cloning of cDNA and gene- and tissue-specific expression. *Gene*. 2000; 252(1-2):107-17.
- Longo N, Amat di San Filippo C, Pasquali M. Disorders of carnitine transport and the carnitine cycle. *Am J Med Genet C Semin Med Genet*. 2006; 142C(2):77-85.
- López LC, Quinzii CM, Area E, Naini A, Rahman S, Schuelke M, Salviati L, Dimauro S, Hirano M. Treatment of CoQ(10) deficient fibroblasts with ubiquinone, CoQ analogs, and vitamin C: time- and compound-dependent effects. *PLoS One*. 2010; 5(7):e11897.
- Lustyik G, O'Leary JJ. Effects of idebenone on mitogen-induced proliferation of human lymphocytes. *Arch Gerontol Geriatr*. 1990; 11(3):307-17.
- Lynch DR, Perlman SL, Meier T. A phase 3, double-blind, placebo-controlled trial of idebenone in friedreich ataxia. *Arch Neurol*. 2010; 67(8):941-7.
- Mackey DA, Oostra RJ, Rosenberg T, Nikoskelainen E, Bronte-Stewart J, Poulton J, Harding AE, Govan G, Bolhuis PA, Norby S. Primary pathogenic mtDNA mutations in multigeneration pedigrees with Leber hereditary optic neuropathy. *Am J Hum Genet*. 1996; 59(2):481-5.
- Mahoney LB, Denny CA, Seyfried TN. Caloric restriction in C57BL/6J mice mimics therapeutic fasting in humans. *Lipids Health Dis*. 2006; 5:13.
- Malfatti E, Bugiani M, Invernizzi F, de Souza CF, Farina L, Carrara F, Lamantea E, Antozzi C, Confalonieri P, Sanseverino MT, Giugliani R, Uziel G, Zeviani M. Novel mutations of ND genes in complex I deficiency associated with mitochondrial encephalopathy. *Brain*. 2007; 130(Pt 7):1894-904.
- Marcuello A, Martínez-Redondo D, Dahmani Y, Casajús JA, Ruiz-Pesini E, Montoya J, López-Pérez MJ, Díez-Sánchez C. Human mitochondrial variants influence on oxygen consumption. *Mitochondrion*. 2009; 9(1):27-30.
- Marella M, Seo BB, Thomas BB, Matsuno-Yagi A, Yagi T. Successful amelioration of mitochondrial optic neuropathy using the yeast NDI1 gene in a rat animal model. *PLoS One*. 2010; 5(7):e11472.
- Marroquin LD, Hynes J, Dykens JA, Jamieson JD, Will Y. Circumventing the Crabtree effect: replacing media glucose with galactose increases susceptibility of HepG2 cells to mitochondrial toxicants. *Toxicol Sci*. 2007; 97(2):539-47.
- Mashima Y, Hiida Y, Oguchi Y. Remission of Leber's hereditary optic neuropathy with idebenone. *Lancet*. 1992; 340(8815):368-9.
- Mashima Y, Kigasawa K, Wakakura M, Oguchi Y. Do idebenone and vitamin therapy shorten the time to achieve visual recovery in Leber hereditary optic neuropathy? *J Neuroophthalmol*. 2000; 20(3):166-70.
- Mathupala SP, Ko YH, Pedersen PL. The pivotal roles of mitochondria in cancer: Warburg and beyond and encouraging prospects for effective therapies. *Biochimica et Biophysica Acta*. 2010; 1797(6-7):1225-1230.
- Mayer LD, Hope MJ, Cullis PR, Janoff AS. Solute distributions and trapping efficiencies observed in freeze-thawed multilamellar vesicles. *Biochim Biophys Acta* 1985; 817: 193-196.
- McArdle A, Edwards RH, Jackson MJ. How does dystrophin deficiency lead to muscle degeneration?--evidence from the mdx mouse. *Neuromuscul Disord*. 1995; 5(6):445-56.
- McGarry JD, Foster DW. Regulation of hepatic fatty acid oxidation and ketone body production. *Annu Rev Biochem*. 1980; 49:395-420.
- McGuire JJ, Anderson DJ, Bennett BM. Inhibition of the biotransformation and pharmacological actions of glyceryl trinitrate by the flavoprotein inhibitor, diphenylethylideneiodonium sulfate. *J Pharmacol Exp Ther*. 1994; 271(2):708-14.
- McKenzie M, Liolitsa D, Akinshina N, Campanella M, Sisodiya S, Hargreaves I, Nirmalanathan N, Sweeney MG, Abou-Sleiman PM, Wood NW, Hanna MG, Duchon MR. Mitochondrial ND5 gene variation associated with encephalomyopathy and mitochondrial ATP consumption. *J Biol Chem*. 2007; 282(51):36845-52.
- Melov S, Schneider JA, Day BJ, Hinerfeld D, Coskun P, Mirra SS, Crapo JD, Wallace DC. A novel neurological phenotype in mice lacking mitochondrial manganese superoxide dismutase. *Nat Genet*. 1998; 18(2):159-63.
- Merker MP, Audi SH, Bongard RD, Lindemer BJ, Krenz GS. Influence of pulmonary arterial endothelial cells on quinone redox status: effect of hyperoxia-induced NAD(P)H:quinone oxidoreductase 1. *Am J Physiol Lung Cell Mol Physiol*. 2006; 290(3):L607-19.
- Miura Y, Endo T. Survival responses to oxidative stress and aging. *Geriatr Gerontol Int*. 2010; 10 Suppl 1:S1-9.
- Miyamoto M, Coyle JT. Idebenone attenuates neuronal degeneration induced by intrastriatal injection of excitotoxins. *Exp Neurol*. 1990; 108(1):38-45.
- Mochel F, Haller RG. Energy deficit in Huntington disease: why it matters. *J Clin Invest*. 2011; 121(2):493-9.

- Monks TJ, Hanzlik RP, Cohen GM, Ross D, Graham DG. Quinone chemistry and toxicity. *Toxicol Appl Pharmacol.* 1992; 112(1):2-16.
- Mordente A, Martorana GE, Minotti G, Giardina B. Antioxidant properties of 2,3-dimethoxy-5-methyl-6-(10-hydroxydecyl)-1,4-benzoquinone (idebenone). *Chem Res Toxicol.* 1998; 11(1):54-63.
- Moreira PI, Zhu X, Wang X, Lee HG, Nunomura A, Petersen RB, Perry G, Smith MA. Mitochondria: a therapeutic target in neurodegeneration. *Biochim Biophys Acta.* 2010; 1802(1):212-20.
- Moreira PI, Oliveira CR. Mitochondria as potential targets in antidiabetic therapy. *Handb Exp Pharmacol.* 2011; (203):331-56.
- Mühlenhoff U, Richhardt N, Ristow M, Kispal G, Lill R. The yeast frataxin homolog Yfh1p plays a specific role in the maturation of cellular Fe/S proteins. *Hum Mol Genet.* 2002; 11(17):2025-36.
- Murakami M, Zs-Nagy I. Superoxide radical scavenging activity of idebenone in vitro studied by ESR spin trapping method and direct ESR measurement at liquid nitrogen temperature. *Arch Gerontol Geriatr.* 1990; 11(3):199-214.
- Murphy MP. How mitochondria produce reactive oxygen species. *Biochem J.* 2009; 417(1):1-13.
- Nagai Y, Narumi S, Nagaoka A, Nagawa Y. In vivo electrochemical detection of 5-hydroxyindoles in the dorsal hippocampus of anesthetized rats treated with idebenone (CV-2619). *Jpn J Pharmacol.* 1985; 37(2):222-5.
- Nagai Y, Yoshida K, Narumi S, Tanayama S, Nagaoka A. Brain distribution of idebenone and its effect on local cerebral glucose utilization in rats. *Arch Gerontol Geriatr.* 1989; 8(3):257-72.
- Nagaoka A, Shino A, Kakihana M, Iwatsuka H. Inhibitory effect of idebenone (CV-2619), a novel compound, on vascular lesions in hypertensive rats. *Jpn J Pharmacol.* 1984; 36(3):291-9.
- Nagaoka A, Suno M, Shibota M, Kakihana M. Effects of idebenone on neurological deficits, local cerebral blood flow, and energy metabolism in rats with experimental cerebral ischemia. *Arch Gerontol Geriatr.* 1989; 8(3):193-202.
- Napolitano A, Salvetti S, Vista M, Lombardi V, Siciliano G, Giraldi C. Long-term treatment with idebenone and riboflavin in a patient with MELAS. *Neurol Sci.* 2000; 21(5 Suppl):S981-2.
- Narumi S, Nagai Y, Kakihana M, Yamazaki N, Nagaoka A, Nagawa Y. Effects of idebenone (CV-2619) on metabolism of monoamines, especially serotonin, in the brain of normal rats and rats with cerebral ischemia. *Jpn J Pharmacol.* 1985b; 37(3):235-44.
- Narumi S, Nagaoka A, Nagawa Y. Effects of idebenone (CV-2619) on endogenous monoamine release and cyclic AMP formation in diencephalon slices from rats. *Jpn J Pharmacol.* 1985a; 37(2):218-21.
- Nishimoto T, Matsumoto A, Kihara T, Akaike A, Sugimoto H. Protective effect of H₂O₂ against subsequent H₂O₂-induced cytotoxicity involves activation of the PI3K-Akt signaling pathway. *Cell Mol Biol (Noisy-le-grand).* 2010; 56 Suppl:OL1447-52. *Abstract.*
- Newman ZL, Sirianni N, Mawhinney C, Lee MS, Leppla SH, Moayeri M, Johansen LM. Auranofin protects against anthrax lethal toxin-induced activation of the Nlrp1b inflammasome. *Antimicrob Agents Chemother.* 2011; 55(3):1028-35.
- Nitta A, Hasegawa T, Nabeshima T. Oral administration of idebenone, a stimulator of NGF synthesis, recovers reduced NGF content in aged rat brain. *Neurosci Lett.* 1993; 163(2):219-22.
- O'Brien PJ. Molecular mechanisms of quinone cytotoxicity. *Chem Biol Interact.* 1991; 80(1):1-41.
- Ohnishi T, Salerno JC. Conformation-driven and semiquinone-gated proton-pump mechanism in the NADH-ubiquinone oxidoreductase (complex I). *FEBS Lett.* 2005; 579(21):4555-61.
- Okamoto K, Watanabe M, Morimoto H, Imada I. Synthesis, metabolism, and in vitro biological activities of 6-(10-hydroxydecyl)-2,3-dimethoxy-5-methyl-1,4-benzoquinone (CV-2619)-related compounds. *Chem Pharm Bull (Tokyo).* 1988; 36(1):178-89.
- Oliveira BF, Nogueira-Machado JA, Chaves MM. The role of oxidative stress in the aging process. *ScientificWorldJournal.* 2010; 10:1121-8.
- Paulsen MT, Ljungman M. The natural toxin juglone causes degradation of p53 and induces rapid H₂AX phosphorylation and cell death in human fibroblasts. *Toxicol Appl Pharmacol.* 2005; 209(1):1-9.
- Paolino D, Iannone M, Cardile V, Renis M, Puglisi G, Rotiroti D, Fresta M. Tolerability and improved protective action of idebenone-loaded pegylated liposomes on ethanol-induced injury in primary cortical astrocytes. *J Pharm Sci.* 2004; 93(7):1815-27.
- Park J, Lee J, Choi C. Mitochondrial Network Determines Intracellular ROS Dynamics and Sensitivity to Oxidative Stress through Switching Inter-Mitochondrial Messengers. *PLoS One.* 2011; 6(8):e23211.
- Pavlakakis SG, Phillips PC, DiMauro S, De Vivo DC, Rowland LP. Mitochondrial myopathy, encephalopathy, lactic acidosis, and strokelike episodes: a distinctive clinical syndrome. *Ann Neurol.* 1984; 16(4):481-8.

- Peri V, Ajdukovic B, Holland P, Tuana BS. Dystrophin predominantly localizes to the transverse tubule/Z-line regions of single ventricular myocytes and exhibits distinct associations with the membrane. *Mol Cell Biochem.* 1994; 130(1):57-65. *Abstract.*
- Perriello G, Misericordia P, Volpi E, Santucci A, Santucci C, Ferrannini E, Ventura MM, Santeusano F, Brunetti P, Bolli GB. Acute antihyperglycemic mechanisms of metformin in NIDDM. Evidence for suppression of lipid oxidation and hepatic glucose production. *Diabetes.* 1994; 43(7):920-8. *Abstract.*
- Pineda M, Arpa J, Montero R, Aracil A, Domínguez F, Galván M, Mas A, Martorell L, Sierra C, Brandi N, García-Arumí E, Rissech M, Velasco D, Costa JA, Artuch R. Idebenone treatment in paediatric and adult patients with Friedreich ataxia: long-term follow-up. *Eur J Paediatr Neurol.* 2008; 12(6):470-5.
- Pink JJ, Planchon SM, Tagliarino C, Varnes ME, Siegel D, Boothman DA. NAD(P)H:Quinone oxidoreductase activity is the principal determinant of beta-lapachone cytotoxicity. *J Biol Chem.* 200; 275(8):5416-24.
- Pommer R, Schoeler S, Mawrin C, Szibor R, Kirches E. The G11778A LHON mutation does not enhance ethambutol cytotoxicity in a cybrid model. *Clin Neuropathol.* 2008; 27(6):414-23.
- Popinigis J, Antosiewicz J, Kaczor JJ, Rauchová H, Lenaz G. Oxidation of glycerol-3-phosphate in porcine and bovine adrenal cortex mitochondria. *Acta Biochim Pol.* 2004; 51(4):1075-80.
- Qi X, Lewin AS, Hauswirth WW, Guy J. Optic neuropathy induced by reductions in mitochondrial superoxide dismutase. *Invest Ophthalmol Vis Sci.* 2003; 44(3):1088-96.
- Ragusa RJ, Chow CK, Porter JD. Oxidative stress as a potential pathogenic mechanism in an animal model of Duchenne muscular dystrophy. *Neuromuscul Disord.* 1997; 7(6-7):379-86.
- Rambold AS, Kostecky B, Elia N, Lippincott-Schwartz J. Tubular network formation protects mitochondria from autophagosomal degradation during nutrient starvation. *Proc Natl Acad Sci U S A.* 2011; 108(25):10190-5.
- Rando TA, Disatnik MH, Yu Y, Franco A. Muscle cells from mdx mice have an increased susceptibility to oxidative stress. *Neuromuscul Disord.* 1998; 8(1):14-21.
- Rauchová H, Drahotka Z, Bergamini C, Fato R, Lenaz G. Modification of respiratory-chain enzyme activities in brown adipose tissue mitochondria by idebenone (hydroxydecyl-ubiquinone). *J Bioenerg Biomembr.* 2008; 40(2):85-93.
- Rauchová H, Drahotka Z, Rauch P, Fato R, Lenaz G. Coenzyme Q releases the inhibitory effect of free fatty acids on mitochondrial glycerophosphate dehydrogenase. *Acta Biochim Pol.* 2003; 50(2):405-13.
- Rauchová H, Vrbacký M, Bergamini C, Fato R, Lenaz G, Houstek J, Drahotka Z. Inhibition of glycerophosphate-dependent H₂O₂ generation in brown fat mitochondria by idebenone. *Biochem Biophys Res Commun.* 2006; 339(1):362-6.
- Reers M, Smith TW, Chen LB. J-aggregate formation of a carbocyanine as a quantitative fluorescent indicator of membrane potential. *Biochemistry.* 1991; 30(18):4480-6.
- Rego AC, Santos MS, Oliveira CR. Influence of the antioxidants vitamin E and idebenone on retinal cell injury mediated by chemical ischemia, hypoglycemia, or oxidative stress. *Free Radic Biol Med.* 1999; 26(11-12):1405-17.
- Reimers CD, Schlotter B, Eicke BM, Witt TN. Calf enlargement in neuromuscular diseases: a quantitative ultrasound study in 350 patients and review of the literature. *J Neurol Sci.* 1996; 143(1-2):46-56.
- Rezin GT, Amboni G, Zugno AI, Quevedo J, Streck EL. Mitochondrial dysfunction and psychiatric disorders. *Neurochem Res.* 2009; 34(6):1021-9.
- Richard D, Picard F. Brown fat biology and thermogenesis. *Front Biosci.* 2011; 16:1233-60.
- Riedel E. *Anorganische Chemie.* Berlin; New York: de Gruyter 2002. ISBN 3-11-01739-1.
- Ristow M, Zarse K. How increased oxidative stress promotes longevity and metabolic health: The concept of mitochondrial hormesis (mitohormesis). *Exp Gerontol.* 2010; 45(6):410-8.
- Roberts RA, Ghiasvand F, Parker D. Biochemistry of exercise-induced metabolic acidosis. *Am J Physiol Regul Integr Comp Physiol.* 2004; 287(3):R502-16.
- Romanello V, Guadagnin E, Gomes L, Roder I, Sandri C, Petersen Y, Milan G, Masiero E, Del Piccolo P, Foretz M, Scorrano L, Rudolf R, Sandri M. Mitochondrial fission and remodelling contributes to muscle atrophy. *EMBO J.* 2010; 29(10):1774-85.
- Romano AD, Serviddio G, de Mattheis A, Bellanti F, Vendemiale G. Oxidative stress and aging. *J Nephrol.* 2010; 23 Suppl 15:S29-36.
- Rötig A, de Lonlay P, Chretien D, Foury F, Koenig M, Sidi D, Munnich A, Rustin P. Aconitase and mitochondrial iron-sulphur protein deficiency in Friedreich ataxia. *Nat Genet.* 1997; 17(2):215-7.
- Rustin P, von Kleist-Retzow JC, Chantrel-Groussard K, Sidi D, Munnich A, Rötig A. Effect of idebenone on cardiomyopathy in Friedreich's ataxia: a preliminary study. *Lancet.* 1999; 354(9177):477-9.
- Saadati HG, Hsu HY, Heller KB, Sadun AA. A histopathologic and morphometric differentiation of nerves in optic nerve hypoplasia and Leber hereditary optic neuropathy. *Arch Ophthalmol.* 1998; 116(7):911-6.

- Sadoulet-Puccio HM, Kunkel LM. Dystrophin and its isoforms. *Brain Pathol.* 1996; 6(1):25-35.
- Sadun AA, Morgia CL, Carelli V. Leber's Hereditary Optic Neuropathy. *Curr Treat Options Neurol.* 2011; 13(1):109-17.
- Sala G, Trombin F, Beretta S, Tremolizzo L, Presutto P, Montopoli M, Fantin M, Martinuzzi A, Carelli V, Ferrarese C. Antioxidants partially restore glutamate transport defect in leber hereditary optic neuropathy cybrids. *J Neurosci Res.* 2008; 86(15):3331-7.
- Sano M, Ishii K, Momose Y, Uchigata M, Senda M. Cerebral metabolism of oxygen and glucose in a patient with MELAS syndrome. *Acta Neurol Scand.* 1995; 92(6):497-502. *Abstract.*
- Sarnat HB, Marin-García J. Pathology of mitochondrial encephalomyopathies. *Can J Neurol Sci.* 2005; 32(2):152-66.
- Sasman F, Antonicka H, Shoubridge EA. The A3243G tRNA^{Leu}(UUR) MELAS mutation causes amino acid misincorporation and a combined respiratory chain assembly defect partially suppressed by overexpression of EFTu and EFG2. *Hum Mol Genet.* 2008; 17(23):3697-707.
- Schafer FQ, Buettner GR. Redox environment of the cell as viewed through the redox state of the glutathione disulfide/glutathione couple. *Free Radic Biol Med.* 2001; 30(11):1191-212.
- Schmeltz I, Tosk J, Jacobs G, Hoffmann D. Redox potential and quinone content of cigarette smoke. *Anal Chem.* 1977; 49(13):1924-9.
- Scholte HR, Luyt-Houwen IE, Busch HF, Jennekens FG. Muscle mitochondria from patients with Duchenne muscular dystrophy have a normal beta oxidation, but an impaired oxidative phosphorylation. *Neurology.* 1985; 35(9):1396-7.
- Schon EA. Mitochondrial genetics and disease. *Trends Biochem Sci.* 2000; 25(11):555-60.
- Schuler F, Casida JE. The insecticide target in the PSST subunit of complex I. *Pest Manag Sci.* 2001; 57(10):932-40.
- Schulz JB, Di Prospero NA, Fischbeck K. Clinical experience with high-dose idebenone in Friedreich ataxia. *J Neurol.* 2009; 256 Suppl 1:42-5.
- Schütz E, Wieland E, Heine L, Hensel A, Schmiedl A, Armstrong VW, Richter J, Schuff-Werner P, Günther E, Oellerich M. Acceleration of hepatocellular energy by idebenone during early reperfusion after cold preservation ameliorates heat shock protein 70 gene expression in a pig liver model. *Transplantation.* 1997; 64(6):901-7.
- Seo JH, Hwang JM, Park SS. Antituberculosis medication as a possible epigenetic factor of Leber's hereditary optic neuropathy. *Clin Experiment Ophthalmol.* 2010; 38(4):363-6.
- Serbinova E, Kagan V, Han D, Packer L. Free radical recycling and intramembrane mobility in the antioxidant properties of alpha-tocopherol and alpha-tocotrienol. *Free Radic Biol Med.* 1991; 10(5):263-75.
- Seznez H, Simon D, Monassier L, Criqui-Filipe P, Gansmuller A, Rustin P, Koenig M, Puccio H. Idebenone delays the onset of cardiac functional alteration without correction of Fe-S enzymes deficit in a mouse model for Friedreich ataxia. *Hum Mol Genet.* 2004; 13(10):1017-24.
- Shargorodsky M, Debby O, Matas Z, Zimlichman R. Effect of long-term treatment with antioxidants (vitamin C, vitamin E, coenzyme Q10 and selenium) on arterial compliance, humoral factors and inflammatory markers in patients with multiple cardiovascular risk factors. *Nutr Metab (Lond).* 2010; 7:55.
- Sies H. Glutathione and its role in cellular functions. *Free Radic Biol Med.* 1999; 27(9-10):916-21.
- Šimkovič M, Frerman FE. Alternative quinone substrates and inhibitors of human electron-transfer flavoprotein-ubiquinone oxidoreductase. *Biochem J.* 2004; 378(Pt 2):633-40.
- Skinner C, Lin SJ. Effects of calorie restriction on life span of microorganisms. *Appl Microbiol Biotechnol.* 2010; 88(4):817-28.
- Smeitink JA, Sengers RC, Trijbels FJ, van den Heuvel LP. Nuclear genes and oxidative phosphorylation disorders: a review. *Eur J Pediatr.* 2000; 159 Suppl 3:S27-31.
- Smith CV, Jones DP, Guenther TM, Lash LH, Lauterburg BH. Compartmentation of glutathione: implications for the study of toxicity and disease. *Toxicol Appl Pharmacol.* 1996; 140(1):1-12.
- Smith DL Jr, Nagy TR, Allison DB. Calorie restriction: what recent results suggest for the future of ageing research. *Eur J Clin Invest.* 2010a; 40(5):440-50.
- Smith DL Jr, Elam CF Jr, Mattison JA, Lane MA, Roth GS, Ingram DK, Allison DB. Metformin supplementation and life span in Fischer-344 rats. *J Gerontol A Biol Sci Med Sci.* 2010b; 65(5):468-74.
- Sokol RJ, Dahl R, Devereaux MW, Yerushalmi B, Kobak GE, Gumprich E. Human hepatic mitochondria generate reactive oxygen species and undergo the permeability transition in response to hydrophobic bile acids. *J Pediatr Gastroenterol Nutr.* 2005; 41(2):235-43.
- Sortino MA, Battaglia A, Pampana F, Carfagna N, Post C, Canonico PL. Neuroprotective effects of nicergoline in immortalized neurons. *Eur J Pharmacol.* 1999; 368(2-3):285-90.

- Sperl W, Skladal D, Gnaiger E, Wyss M, Mayr U, Hager J, Gellerich FN. High resolution respirometry of permeabilized skeletal muscle fibers in the diagnosis of neuromuscular disorders. *Mol Cell Biochem.* 1997; 174(1-2):71-8.
- Sproule DM, Kaufmann P. Mitochondrial encephalopathy, lactic acidosis, and strokelike episodes: basic concepts, clinical phenotype, and therapeutic management of MELAS syndrome. *Ann N Y Acad Sci.* 2008; 1142:133-58.
- St-Pierre J, Buckingham JA, Roebuck SJ, Brand MD. Topology of superoxide production from different sites in the mitochondrial electron transport chain. *J Biol Chem.* 2002; 277(47):44784-90.
- Starkov AA, Fiskum G, Chinopoulos C, Lorenzo BJ, Browne SE, Patel MS, Beal MF. Mitochondrial alpha-ketoglutarate dehydrogenase complex generates reactive oxygen species. *J Neurosci.* 2004; 24(36):7779-88.
- Stavropoulou C, Zachaki S, Alexoudi A, Chatzi I, Georgakakos VN, Terzoudi GI, Pantelias GE, Karageorgiou CE, Sambani C. The C(609)T inborn polymorphism in NAD(P)H:quinone oxidoreductase 1 is associated with susceptibility to multiple sclerosis and affects the risk of development of the primary progressive form of the disease. *Free Radic Biol Med.* 2011; 51(3):713-8.
- Straub V, Rafael JA, Chamberlain JS, Campbell KP. Animal models for muscular dystrophy show different patterns of sarcolemmal disruption. *J Cell Biol.* 1997; 139(2):375-85.
- Suen DF, Norris KL, Youle RJ. Mitochondrial dynamics and apoptosis. *Genes Dev.* 2008; 22(12):1577-90.
- Sugiyama Y, Fujita T, Matsumoto M, Okamoto K, Imada I. Effects of idebenone (CV-2619) and its metabolites on respiratory activity and lipid peroxidation in brain mitochondria from rats and dogs. *J Pharmacobiodyn.* 1985; 8(12):1006-17.
- Sugiyama Y, Fujita T. Stimulation of the respiratory and phosphorylating activities in rat brain mitochondria by idebenone (CV-2619), a new agent improving cerebral metabolism. *FEBS Lett.* 1985; 184(1):48-51.
- Suno M, Nagaoka A. Inhibition of lipid peroxidation by idebenone in brain mitochondria in the presence of succinate. *Arch Gerontol Geriatr.* 1989a; 8(3):291-7.
- Suno M, Nagaoka A. Inhibition of brain mitochondrial swelling by idebenone. *Arch Gerontol Geriatr.* 1989b; 8(3):299-305.
- Suno M, Nagaoka A. Inhibition of lipid peroxidation by a novel compound (CV-2619) in brain mitochondria and mode of action of the inhibition. *Biochem Biophys Res Commun.* 1984c; 125(3):1046-52.
- Suno M, Shibota M, Nagaoka A. Effects of idebenone on lipid peroxidation and hemolysis in erythrocytes of stroke-prone spontaneously hypertensive rats. *Arch Gerontol Geriatr.* 1989; 8(3):307-11.
- Suno M, Terashita Z, Nagaoka A. Inhibition of platelet aggregation by idebenone and the mechanism of the inhibition. *Arch Gerontol Geriatr.* 1989d; 8(3):313-21.
- Suzuki A, Yoshida M, Yamamoto H, Ozawa E. Glycoprotein-binding site of dystrophin is confined to the cysteine-rich domain and the first half of the carboxy-terminal domain. *FEBS Lett.* 1992; 308(2):154-60.
- Sykiotis GP, Bohmann D. Stress-activated cap'n'collar transcription factors in aging and human disease. *Sci Signal.* 2011; 3(112):re3.
- Szondy Z, Mastroberardino PG, Váradi J, Farrace MG, Nagy N, Bak I, Viti I, Wieckowski MR, Melino G, Rizzuto R, Tószaki A, Fesus L, Piacentini M. Tissue transglutaminase (TG2) protects cardiomyocytes against ischemia/reperfusion injury by regulating ATP synthesis. *Cell Death Differ.* 2006; 13(10):1827-9.
- Tai KK, Pham L, Truong DD. Idebenone Induces Apoptotic Cell Death in the Human Dopaminergic Neuroblastoma SHSY-5Y Cells. *Neurotox Res.* 2011; [Epub ahead of print]. *Abstract.*
- Takeuchi R, Murase K, Furukawa Y, Furukawa S, Hayashi K. Stimulation of nerve growth factor synthesis/secretion by 1,4-benzoquinone and its derivatives in cultured mouse astroglial cells. *FEBS Lett.* 1990; 261(1):63-6.
- Takuma K, Yoshida T, Lee E, Mori K, Kishi T, Baba A, Matsuda T. CV-2619 protects cultured astrocytes against reperfusion injury via nerve growth factor production. *Eur J Pharmacol.* 2000; 406(3):333-9.
- Tam EW, Feigenbaum A, Addis JB, Blaser S, Mackay N, Al-Dosary M, Taylor RW, Ackerley C, Cameron JM, Robinson BH. A novel mitochondrial DNA mutation in COX1 leads to strokes, seizures, and lactic acidosis. *Neuropediatrics.* 2008; 39(6):328-34.
- Tanaka S, Tsuchiya S. Efficacy of idebenone for respiratory failure in a patient with Leigh syndrome: a long-term follow-up study. *J Neurol Sci.* 2009; 278(1-2):112-4.
- Tang JC, Yang H, Song XY, Song XH, Yan SL, Shao JQ, Zhang TL, Zhang JN. Inhibition of cytochrome P450 enzymes by rhein in rat liver microsomes. *Phytother Res.* 2009; 23(2):159-64.
- Testai FD, Gorelick PB. Inherited metabolic disorders and stroke part 1: Fabry disease and mitochondrial myopathy, encephalopathy, lactic acidosis, and strokelike episodes. *Arch Neurol.* 2010; 67(1):19-24.
- Tidball JG, Wehling-Henricks M. The role of free radicals in the pathophysiology of muscular dystrophy. *J Appl Physiol.* 2007; 102(4):1677-86.

- Tieu K, Perier C, Caspersen C, Teismann P, Wu DC, Yan SD, Naini A, Vila M, Jackson-Lewis V, Ramasamy R, Przedborski S. D-beta-hydroxybutyrate rescues mitochondrial respiration and mitigates features of Parkinson disease. *J Clin Invest*. 2003; 112(6):892-901.
- Tillement L, Lecanu L, Papadopoulos V. Alzheimer's disease: effects of β -amyloid on mitochondria. *Mitochondrion*. 2011; 11(1):13-21.
- Tonon C, Lodi R. Idebenone in Friedreich's ataxia. *Expert Opin Pharmacother*. 2008; 9(13):2327-37.
- Tonska K, Kodron A, Bartnik E. Genotype-phenotype correlations in Leber hereditary optic neuropathy. *Biochim Biophys Acta* 2010; 1797:1119-23.
- Torii H, Yoshida K, Kobayashi T, Tsukamoto T, Tanayama S. Disposition of idebenone (CV-2619), a new cerebral metabolism improving agent, in rats and dogs. *J Pharmacobiodyn*. 1985; 8(6):457-67.
- Touboul D, Brunelle A, Halgand F, De La Porte S, Lapr evote O. Lipid imaging by gold cluster time-of-flight secondary ion mass spectrometry: application to Duchenne muscular dystrophy. *J Lipid Res*. 2005; 46(7):1388-95.
- Tran UC, Clarke CF. Endogenous synthesis of coenzyme Q in eukaryotes. *Mitochondrion*. 2007; 7 Suppl:S62-71.
- Treberg JR, Brand MD. A model of the proton translocation mechanism of complex I. *J Biol Chem*. 2011; 286(20):17579-84.
- Tretter L, Takacs K, K ov er K, Adam-Vizi V. Stimulation of H₂O₂ generation by calcium in brain mitochondria respiring on alpha-glycerophosphate. *J Neurosci Res*. 2007; 85(15):3471-9.
- Tsao K, Aitken PA, Johns DR. Smoking as an aetiological factor in a pedigree with Leber's hereditary optic neuropathy. *Br J Ophthalmol*. 1999; 83(5):577-81.
- Tsuruo Y, Ishimura K, Tamura M, Kagawa S, Morita K. Biochemical and histochemical studies of the effects of cerebral metabolism-improving drugs on NADPH diaphorase activity in mouse brain. *Jpn J Pharmacol*. 1994; 65(3):285-8.
- Turner PR, Fong PY, Denetclaw WF, Steinhardt RA. Increased calcium influx in dystrophic muscle. *J Cell Biol*. 1991; 115(6):1701-12.
- Turner N, Li JY, Gosby A, To SW, Cheng Z, Miyoshi H, Taketo MM, Cooney GJ, Kraegen EW, James DE, Hu LH, Li J, Ye JM. Berberine and its more biologically available derivative, dihydroberberine, inhibit mitochondrial respiratory complex I: a mechanism for the action of berberine to activate AMP-activated protein kinase and improve insulin action. *Diabetes* 2008; 57(5):1414-8.
- Twig G, Hyde B, Shirihai OS. Mitochondrial fusion, fission and autophagy as a quality control axis: the bioenergetic view. *Biochim Biophys Acta*. 2008; 1777(9):1092-7.
- van Hellenberg Hubar JL, Gabre els FJ, Ruitenbeek W, Sengers RC, Renier WO, Thijssen HO, ter Laak HJ. MELAS syndrome. Report of two patients, and comparison with data of 24 patients derived from the literature. *Neuropediatrics*. 1991; 22(1):10-4.
- Vander Heiden MG, Cantley LC, Thompson CB. Understanding the Warburg effect: the metabolic requirements of cell proliferation. *Science*. 2009; 324(5930):1029-33.
- Vainzof M, Ayub-Guerrieri D, Onofre PC, Martins PC, Lopes VF, Zilberztajn D, Maia LS, Sell K, Yamamoto LU. Animal models for genetic neuromuscular diseases. *J Mol Neurosci*. 2008; 34(3):241-8.
- Villalba JM, Parrado C, Santos-Gonzalez M, Alca in FJ. Therapeutic use of coenzyme Q₁₀ and coenzyme Q₁₀-related compounds and formulations. *Expert Opin Investig Drugs*. 2010; 19(4):535-54.
- Villalta SA, Nguyen HX, Deng B, Gotoh T, Tidball JG. Shifts in macrophage phenotypes and macrophage competition for arginine metabolism affect the severity of muscle pathology in muscular dystrophy. *Hum Mol Genet*. 2009; 18(3):482-96.
- Vi na J, Lloret A, Vall es SL, Borr as C, Bad a MC, Pallard o FV, Sastre J, Alonso MD. Effect of gender on mitochondrial toxicity of Alzheimer's A β peptide. *Antioxid Redox Signal*. 2007; 9(10):1677-90.
- Wang XJ, Xu JX. Possible involvement of Ca²⁺ signaling in rotenone-induced apoptosis in human neuroblastoma SH-SY5Y cells. *Neurosci Lett*. 2005; 376(2):127-32.
- Wang Y, Mohsen AW, Mihalik SJ, Goetzman ES, Vockley J. Evidence for physical association of mitochondrial fatty acid oxidation and oxidative phosphorylation complexes. *J Biol Chem*. 2010; 285(39):29834-41.
- Wallace DC. Mitochondrial diseases in man and mouse. *Science*. 1999; 283(5407):1482-8.
- Washizu T, Takahashi M, Azakami D, Ikeda M, Arai T. Activities of enzymes in the malate-aspartate shuttle in the peripheral leukocytes of dogs and cats. *Vet Res Commun*. 2001; 25(8):623-9.
- Waterhouse C, Keilson J. Cori cycle activity in man. *J Clin Invest*. 1969; 48(12):2359-66.
- Watzke N, Diekert K, Obrdlk P. Electrophysiology of respiratory chain complexes and the ADP-ATP exchanger in native mitochondrial membranes. *Biochemistry*. 2010; 49(48):10308-18.
- Weisiger RA, Fridovich I. Superoxide dismutase. Organelle specificity. *J Biol Chem*. 1973; 248(10):3582-92.

- Wempe MF, Lightner JW, Zoeller EL, Rice PJ. Investigating idebenone and idebenone linoleate metabolism: in vitro pig ear and mouse melanocyte studies. *J Cosmet Dermatol*. 2009; 8(1):63-73.
- Wen Y, Li W, Poteet EC, Xie L, Tan C, Yan LJ, Ju X, Liu R, Qian H, Marvin MA, Goldberg MS, She H, Mao Z, Simpkins JW, Yang SH. Alternative mitochondrial electron transfer as a novel strategy for neuroprotection. *J Biol Chem*. 2011; 286(18):16504-15.
- Whitehead NP, Yeung EW, Allen DG. Muscle damage in mdx (dystrophic) mice: role of calcium and reactive oxygen species. *Clin Exp Pharmacol Physiol*. 2006; 33(7):657-62.
- Wieland E, Oellerich M, Braun F, Schtüz E. c-fos and c-jun mRNA expression in a pig liver model of ischemia/reperfusion: effect of extended cold storage and the antioxidant idebenone. *Clin Biochem*. 2000; 33(4):285-90.
- Williams IA, Allen DG. Intracellular calcium handling in ventricular myocytes from mdx mice. *Am J Physiol Heart Circ Physiol*. 2007; 292(2):H846-55.
- Winger JA, Hantschel O, Superti-Furga G, Kuriyan J. The structure of the leukemia drug imatinib bound to human quinone reductase 2 (NQO2). *BMC Struct Biol*. 2009; 9:7.
- Wong A, Cavelier L, Collins-Schramm HE, Seldin MF, McGrogan M, Savontaus ML, Cortopassi GA. Differentiation-specific effects of LHON mutations introduced into neuronal NT2 cells. *Hum Mol Genet*. 2002; 11(4):431-8.
- Wong LJ. Pathogenic mitochondrial DNA mutations in protein-coding genes. *Muscle Nerve* 2007; 36(3):279-93.
- Wu K, Knox R, Sun XZ, Joseph P, Jaiswal AK, Zhang D, Deng PS, Chen S. Catalytic properties of NAD(P)H:quinone oxidoreductase-2 (NQO2), a dihydronicotinamide riboside dependent oxidoreductase. *Arch Biochem Biophys*. 1997; 347(2):221-8.
- Xie W, Wan OW, Chung KK. New insights into the role of mitochondrial dysfunction and protein aggregation in Parkinson's disease. *Biochim Biophys Acta*. 2010; 1802(11):935-41.
- Yamada K, Nitta A, Hasegawa T, Fuji K, Hiramatsu M, Kameyama T, Furukawa Y, Hayashi K, Nabeshima T. Orally active NGF synthesis stimulators: potential therapeutic agents in Alzheimer's disease. *Behav Brain Res*. 1997; 83(1-2):117-22.
- Yamazaki N, Take Y, Nagaoka A, Nagawa Y. Beneficial effect of idebenone (CV-2619) on cerebral ischemia-induced amnesia in rats. *Jpn J Pharmacol*. 1984; 36(3):349-56.
- Yen MY, Lee HC, Liu JH, Wei YH. Compensatory elevation of complex II activity in Leber's hereditary optic neuropathy. *Br J Ophthalmol*. 1996; 80(1):78-81.
- Yen MY, Kao SH, Wang AG, Wei YH. Increased 8-hydroxy-2'-deoxyguanosine in leukocyte DNA in Leber's hereditary optic neuropathy. *Invest Ophthalmol Vis Sci*. 2004; 45(6):1688-91.
- Yerushalmi B, Dahl R, Devereaux MW, Gumprich E, Sokol RJ. Bile acid-induced rat hepatocyte apoptosis is inhibited by antioxidants and blockers of the mitochondrial permeability transition. *Hepatology*. 2001; 33(3):616-26.
- Ying W. NAD⁺/NADH and NADP⁺/NADPH in cellular functions and cell death: regulation and biological consequences. *Antioxid Redox Signal*. 2008; 10(2):179-206. *Abstract*.
- Yurova MV, Kovalenko IG, Poroshina TE, Semenchenko AV. Metformin slows down aging and extends life span of female SHR mice. *Cell Cycle*. 2008; 7(17):2769-73.
- Zanna C, Ghelli A, Porcelli AM, Carelli V, Martinuzzi A, Rugolo M. Apoptotic cell death of cybrid cells bearing Leber's hereditary optic neuropathy mutations is caspase independent. *Ann N Y Acad Sci*. 2003; 1010:213-7.
- Zanna C, Ghelli A, Porcelli AM, Martinuzzi A, Carelli V, Rugolo M. Caspase-independent death of Leber's hereditary optic neuropathy cybrids is driven by energetic failure and mediated by AIF and Endonuclease G. *Apoptosis*. 2005; 10(5):997-1007.
- Zhai H, Cordoba-Diaz M, Wa C, Hui X, Maibach HI. Determination of the antioxidative capacity of an antioxidant complex and idebenone: an in vitro rapid and sensitive method. *J Cosmet Dermatol*. 2008; 7(2):96-100.
- Zhou GQ, Xie HQ, Zhang SZ, Yang ZM. Current understanding of dystrophin-related muscular dystrophy and therapeutic challenges ahead. *Chin Med J (Engl)*. 2006; 119(16):1381-91.
- Zhou C, Li XC, Fang WH, Yang XL, Hu LL, Zhou S, Zhou JF. Inhibition of CYP450 1A and 3A by berberine in crucian carp *Carassius auratus gibelio*. *Comp Biochem Physiol C Toxicol Pharmacol*. 2011; [Epub ahead of print] *Abstract*.
- Zs-Nagy I. Chemistry, toxicology, pharmacology and pharmacokinetics of idebenone: a review. *Arch Gerontol Geriatr*. 1990; 11(3):177-86.

12 Appendices

12.1 Appendix I: Tables of Gene Ontology from Micro Array Data

Table 8: Gene Ontology: Biological Functions According to Expression Pattern of Whole Genome.
Expression Data of whole genome was analyzed for gene ontology of biological function using ermineJ software.

Biological Function	GO Number	p-value
Calcium ion homeostasis	GO:0055074	5.27E-04
negative regulation of immune system process	GO:0002683	3.47E-04
myeloid cell differentiation	GO:0030099	2.37E-04
metal ion homeostasis	GO:0055065	1.82E-04
membrane lipid biosynthetic process	GO:0046467	1.80E-04
microtubule-based movement	GO:0007018	1.68E-04
chromosome segregation	GO:0007059	5.21E-04
cytoskeleton-dependent intracellular transport	GO:0030705	5.08E-04
DNA packaging	GO:0006323	1.68E-03
transforming growth factor beta receptor signaling pathway	GO:0007179	2.28E-03
regulation of DNA binding	GO:0051101	5.21E-03
sphingolipid metabolic process	GO:0006665	6.02E-03
regulation of leukocyte mediated immunity	GO:0002703	6.79E-03
lymphocyte differentiation	GO:0030098	7.20E-03
transmembrane receptor protein serine/threonine kinase signaling	GO:0007178	7.39E-03
DNA damage response, signal transduction	GO:0042770	8.25E-03
regulation of cytokine production	GO:0001817	9.67E-03
glycoprotein metabolic process	GO:0009100	9.47E-03
DNA-dependent DNA replication	GO:0006261	1.04E-02
regulation of protein kinase cascade	GO:0010627	1.44E-02
extracellular matrix organization	GO:0030198	1.42E-02
protein amino acid glycosylation	GO:0006486	1.71E-02
phospholipid biosynthetic process	GO:0008654	1.92E-02
DNA recombination	GO:0006310	2.57E-02
ribonucleoside triphosphate metabolic process	GO:0009199	2.96E-02
regulation of MAPKKK cascade	GO:0043408	3.57E-02
response to hormone stimulus	GO:0009725	3.50E-02
sterol metabolic process	GO:0016125	3.69E-02
integrin-mediated signaling pathway	GO:0007229	3.80E-02
anti-apoptosis	GO:0006916	4.34E-02
cell cycle checkpoint	GO:0000075	4.25E-02
acyl-CoA metabolic process	GO:0006637	4.21E-02
regulation of cell adhesion	GO:0030155	4.37E-02
electron transport chain	GO:0022900	4.36E-02
antigen processing and presentation	GO:0019882	4.43E-02
transmembrane transport	GO:0055085	4.71E-02
negative regulation of T cell proliferation	GO:0042130	4.91E-02
regulation of cytoskeleton organization	GO:0051493	4.91E-02

Table 9: Gene Ontology: Biological Functions According to Expression Pattern of Significantly Differently Expressed Genes.

Expression Data of genes expressed differently with a significance of at least 0.05 as calculated using GeneSpring GX 10 software was analyzed for gene ontology of biological function using DAVID software.

Biological Function	GO Number	p-value
sphingolipid metabolic process	GO:0006665	0.001139
membrane lipid metabolic process	GO:0006643	0.001376
M phase of mitotic cell cycle	GO:0000087	0.005133
positive regulation of leukocyte migration	GO:0002687	0.006496
cell division	GO:0051301	0.00731
mitosis	GO:0007067	0.011559
nuclear division	GO:0000280	0.011559
mitotic cell cycle	GO:0000278	0.012205
organelle fission	GO:0048285	0.0149
regulation of leukocyte migration	GO:0002685	0.017264
M phase	GO:0000279	0.017488
vesicle-mediated transport	GO:0016192	0.021238
establishment of protein localization	GO:0045184	0.023734
cellular protein localization	GO:0034613	0.025921
DNA replication initiation	GO:0006270	0.026804
cellular macromolecule localization	GO:0070727	0.027546
intracellular protein transport	GO:0006886	0.030189
cellular calcium ion homeostasis	GO:0006874	0.032183
regulation of apoptosis	GO:0042981	0.034256
protein transport	GO:0015031	0.036048
regulation of programmed cell death	GO:0043067	0.038445
calcium ion homeostasis	GO:0055074	0.038529
protein localization	GO:0008104	0.039355
regulation of cell death	GO:0010941	0.04067
cellular metal ion homeostasis	GO:0006875	0.047511

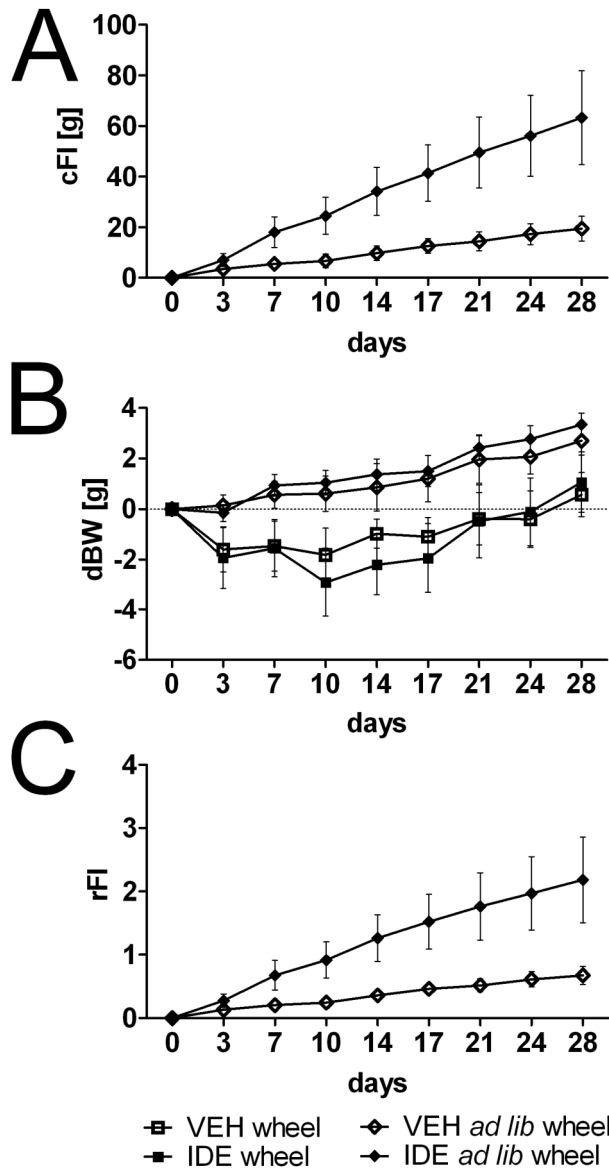
12.2 Appendix II: Figures of Additional *in Vivo* Experiments

Figure 54: Idebenone Promotes Increased Food Intake but Does Not Affect Body Weight *in Vivo* (Experiment 0305).

Male C57Bl/10 *mdx* mice (age seven weeks at start of experiment; $n = 8$) were treated with 400 mg/kg idebenone (IDE; filled) or vehicle (VEH; empty) *p.o.* in food for four weeks. Animals had either no supplementary food on top of food mash for idebenone administration (squares) or access to food *ad libitum* (*ad lib*; diamonds) which was weighted to calculate (A) their cumulative supplementary food intake (cFI). Body weight was also measured to calculate (B) differences in body weight (dBW) and (C) the relative cumulative food intake (rFI) which was defined as difference in food intake divided by body weight. All animals had access to a wheel all the time for voluntary locomotion.

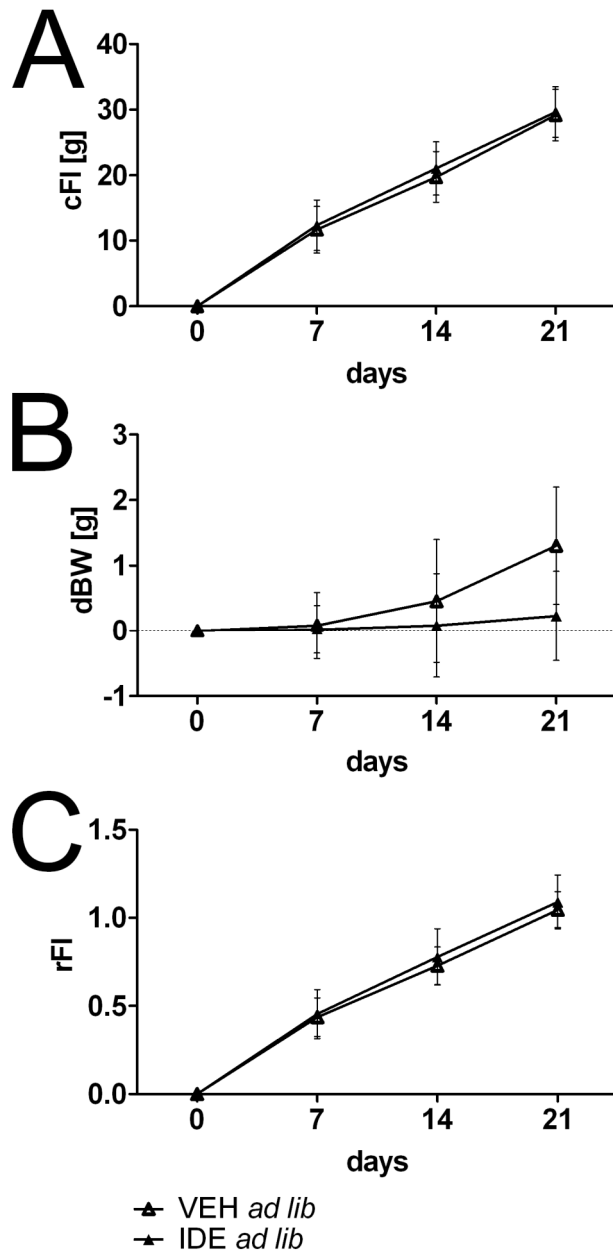


Figure 55: Idebenone Does Not Affect Food Intake but Prevents Increase in Body Weight *in Vivo* (Experiment 0319).

Male C57Bl/6 mice (age nine weeks at start of experiment; $n = 5$) were treated with 200 mg/kg idebenone (IDE; filled) or vehicle (VEH; empty) *p.o.* in food for four weeks. Animals had access to food *ad libitum* (*ad lib*) which was weighted to calculate (A) their cumulative supplementary food intake (cFI). Body weight was also measured to calculate (B) differences in body weight (dBW) and (C) the relative cumulative food intake (rFI) which was defined as difference in food intake divided by body weight.

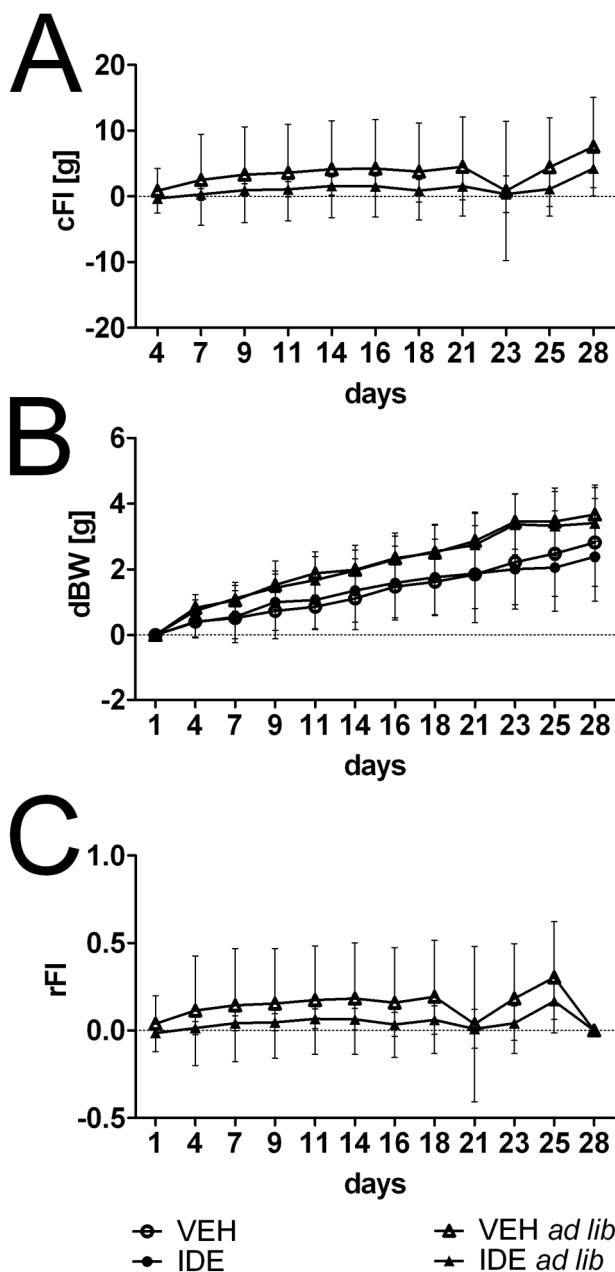


Figure 56: Idebenone Does Not Affect Food Intake or Body Weight *in Vivo* (Experiment 0423).

Male C57Bl/6 mice (age eight weeks at start of experiment; $n = 10$) were treated with 200 mg/kg idebenone (IDE; filled) or vehicle (VEH; empty) *p.o.* in food for three weeks. Animals had either no supplementary food on top of food mash for idebenone administration (circles) or access to food *ad libitum* (*ad lib*; triangles) which was weighted to calculate (A) their cumulative supplementary food intake (cFI). Body weight was also measured to calculate (B) differences in body weight (dBW) and (C) the relative cumulative food intake (rFI) which was defined as difference in food intake divided by body weight.

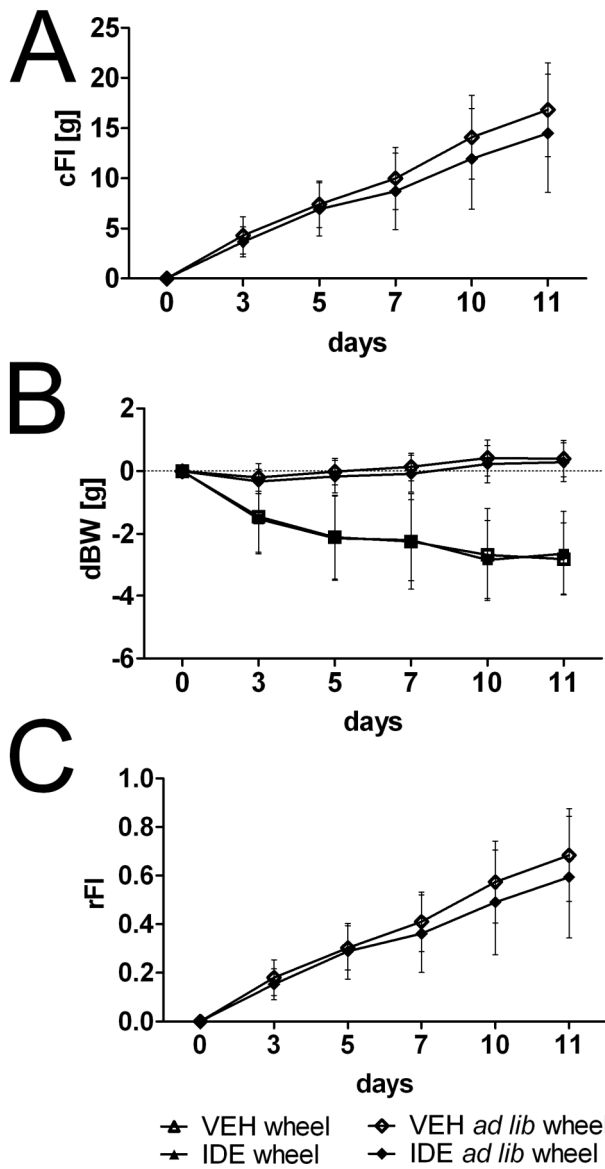


Figure 57: Idebenone Does Not Affect Food Intake or Body Weight *in Vivo* (Experiment 0436).

Male C57Bl/10 *mdx* mice (age eight weeks at start of experiment; n = 10) were treated with 400 mg/kg idebenone (IDE; filled) or vehicle (VEH; empty) *p.o.* in food for four weeks. Animals had access to food *ad libitum* (*ad lib*) which was weighted to calculate (A) their cumulative supplementary food intake (cFI). Body weight was also measured to calculate (B) differences in body weight (dBW) and (C) the relative cumulative food intake (rFI) which was defined as difference in food intake divided by body weight. All animals had access to a wheel all the time for voluntary locomotion.

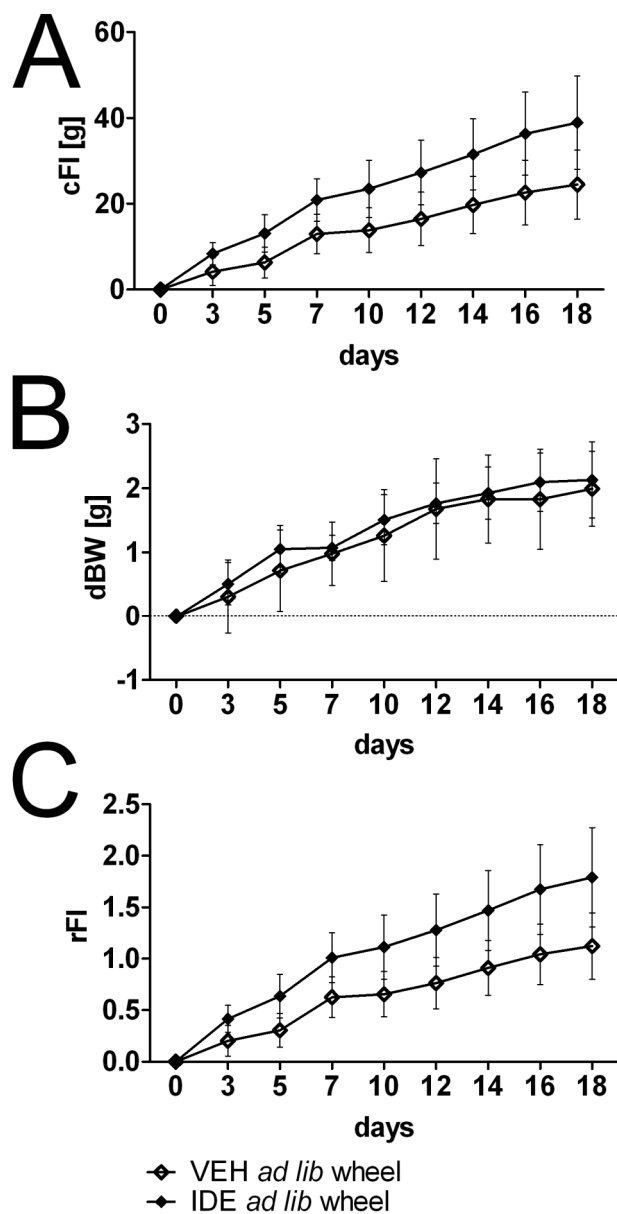


Figure 58: Idebenone Promotes Increased Food Intake but Does Not Affect Body Weight *in Vivo* (Experiment 0444).

Male C57Bl/6 mice (age six weeks at start of experiment; $n = 10$) were treated with 400 mg/kg idebenone (IDE; filled) or vehicle (VEH; empty) *p.o.* in food for four weeks. Animals had access to food *ad libitum* (*ad lib*) which was weighted to calculate (A) their cumulative supplementary food intake (cFI). Body weight was also measured to calculate (B) differences in body weight (dBW) and (C) the relative cumulative food intake (rFI) which was defined as difference in food intake divided by body weight. All animals had access to a wheel all the time for voluntary locomotion.

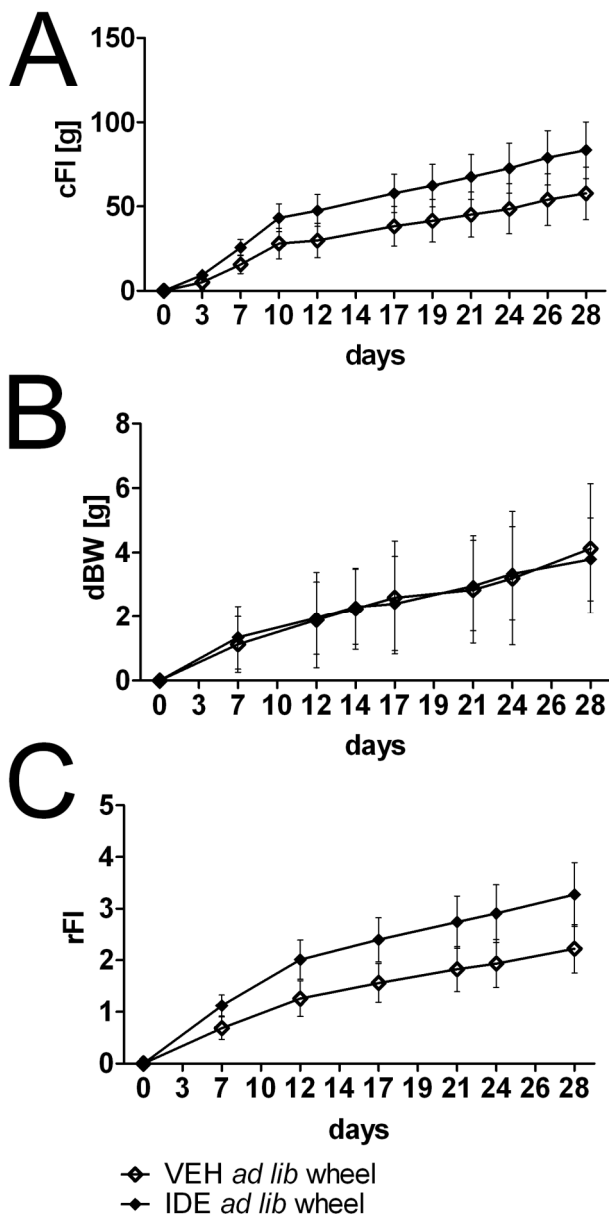


Figure 59: Idebenone Promotes Increased Food Intake but Does Not Affect Body Weight *in Vivo* (Experiment 0459a).

Male C57Bl/6 mice (age six weeks at start of experiment; $n = 6$) were treated with 400 mg/kg idebenone (IDE; filled) or vehicle (VEH; empty) *p.o.* in food for four weeks. Animals had access to food *ad libitum* (*ad lib*) which was weighted to calculate (A) their cumulative supplementary food intake (cFI). Body weight was also measured to calculate differences in (B) body weight (dBW) and (C) the relative cumulative food intake (rFI) which was defined as difference in food intake divided by body weight. All animals had access to a wheel all the time for voluntary locomotion.

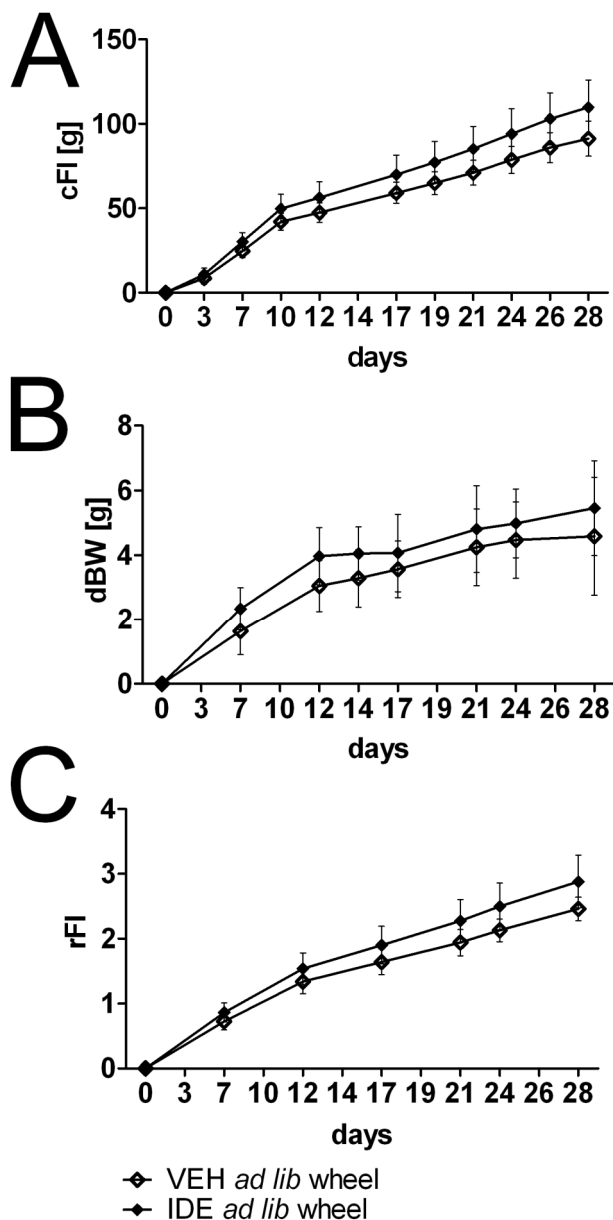


Figure 6c: Idebenone Promotes Increased Food Intake but Does Not Affect Body Weight *in Vivo* (Experiment 0459b).

Male RjHan:NMRI mice (age six weeks at start of experiment; $n = 6$) were treated with 400 mg/kg idebenone (IDE; filled) or vehicle (VEH; empty) *p.o.* in food for four weeks. Animals had access to food *ad libitum* (*ad lib*) which was weighted to calculate (A) their cumulative supplementary food intake (cFI). Body weight was also measured to calculate (B) differences in body weight (dBW) and (C) the relative cumulative food intake (rFI) which was defined as difference in food intake divided by body weight. All animals had access to a wheel all the time for voluntary locomotion.

12.3 Appendix III: Vitamin Composition of Different Chows Used *in Vivo***Table 10: Vitamin Composition of Different Chows Used *in Vivo*.**

Teklad 2018S was used in all *in vivo* experiments described in this work with the exception of experiment 0423 in which KLIBAG NAFAG 3436 was used.

	KLIBAG NAFAG 3436	Teklad 2018S
Vitamin A	14,000 IU/kg	30,700 IU/kg
Vitamin D3	1,000 IU/kg	2,050 IU/kg
Vitamin E	110 mg/kg	126 mg/kg
Vitamin K3	2 mg/kg	102 mg/kg
Vitamin B1	30 mg/kg	117.6 mg/kg
Vitamin B2	20 mg/kg	27.2 mg/kg
Vitamin B6	14 mg/kg	26.8 mg/kg
Vitamin B12	0.05 mg/kg	0.15 mg/kg
Nicotinic acid	70 mg/kg	87.3 mg/kg
Pantothenic acid	33 mg/kg	141.6 mg/kg
Folic acid	2 mg/kg	8.41 mg/kg
Biotin	0.22 mg/kg	0.82 mg/kg
Choline	2,000 mg/kg	1,120 mg/kg
Vitamin C	40 mg/kg	0 mg/kg

12.4 Appendix IV: Relevant Publications Describing Molecular Effects by Idebenone

Table 11: A Selection of Publications on Molecular Effects of Idebenone Relevant to this Thesis.

Effect	Authors	Finding	Test system	C _{effective} , EC ₅₀ , or IC ₅₀
Antioxidant	Abdel Baky <i>et al.</i> (2010)	Idebenone rescues partially from hemic hypoxia in rats (decreases lipid peroxidation, and increases GSH and SOD levels)	Hemic hypoxia	100 mg/kg
	Amano <i>et al.</i> (1995)	Idebenone stabilizes membranes and inhibits phospholipase A ₂ activity	Porcine pancreas cells	32 µM
	Cardoso <i>et al.</i> (1998)	Idebenone prevents ROS formation in the cytosol and mitochondria and inhibits lipid peroxidation	Ascorbate/iron-induced ROS	50 µM
	Geromel <i>et al.</i> (2002)	Idebenone is a pro-oxidant.	Review	-
	Gil <i>et al.</i> (2003)	Idebenone reduces ROS levels and intracellular Ca ²⁺ concentration and thus, caspase-3 activity, and rescues cells from staurosporine-induced cell death.	Staurosporin-induced apoptosis in retinal cells	1 µM
	Gumpricht <i>et al.</i> (2002)	Idebenone reduces apoptosis.	Bile acid-treated, freshly isolated rat hepatocytes	100 µM
	Jauslin <i>et al.</i> (2002)	Idebenone protects against BSO toxicity.	FRDA lymphoblastoid cells	0.5 µM
	Jauslin <i>et al.</i> (2003)	Idebenone protects against BSO toxicity.	FRDA lymphoblastoid cells	0.43 µM
	Jauslin <i>et al.</i> (2007)	Combination of idebenone and vitamin E protects against BSO toxicity.	FRDA lymphoblastoid cells	0.41 µM
	Mordente <i>et al.</i> (1998)	Idebenone is a radical scavenger and inhibits lipid peroxidation.	Cell free assays and isolated rat liver microsomes	> 2 µM
	Rustin <i>et al.</i> (1999)	Idebenone has an antioxidative effect in human heart homogenates.	Human FRDA heart homogenates	60 µM
	Sortino <i>et al.</i> (1999)	Idebenone ameliorates viability.	GSH-depleted cells	1 µM

	Suno and Nagaoka (1989a)	Idebenone protects against lipid peroxidation and this effect is enhanced in presence of succinate.	Iron/ADP-induced ROS	84 μ M
	Suno and Nagaoka (1989b)	Idebenone inhibits mitochondrial swelling and lipid peroxidation.	Isolated brain mitochondria	37-50 μ M
	Suno <i>et al.</i> (1989)	Idebenone inhibits lipid peroxidation stabilizes membranes.	Erythrocytes	30 mg/kg
	Suno and Nagaoka (1989)	Idebenone inhibits platelet aggregation, prostaglandin synthesis, and thromboxane B ₂ production.	Platelets	>125 μ M
	Rauchová <i>et al.</i> (2006)	Idebenone inhibits H ₂ O ₂ generated by either glycerophosphate dehydrogenase and FeCN.	Isolated brown adipose mitochondria	50 nM
	Rauchová <i>et al.</i> (2011)	Idebenone increases glycerolphosphate dehydrogenase activity.	Isolated liver mitochondria	14 μ M
	Rego <i>et al.</i> (1999)	Idebenone protects against oxidative stress.	Ischemia and hypoglycemia renal model	10 μ M
	Wieland <i>et al.</i> (2000)	Idebenone attenuates lipid peroxidation and decreases c-jun and c-fos expression.	Perfused pig livers	280 mg/kg
	Zhani <i>et al.</i> (2008)	Idebenone is an antioxidant.	Superoxide quenching	30 mM
	Sokol <i>et al.</i> (2005)	Idebenone reduces ROS production and mitochondrial swelling.	Bile acid-treated mitochondria	100 μ M
	Yerushalmi <i>et al.</i> (2001)	Idebenone rescues apoptosis.	Bile-acid treated, isolated rat hepatocytes	100 μ M
Pro-oxidant	Geromel <i>et al.</i> (2002)	Review		-
	Genova <i>et al.</i> (2003)	Idebenone is a pro-oxidant via complex I interaction.	Bovine mitochondria	2 μ mol/mg protein
	Lenaz <i>et al.</i> (2002)	Idebenone is a pro-oxidant via complex I interaction.	Bovine mitochondria	2 μ mol/mg protein
Survival	Gumpricht <i>et al.</i> (2002)	Idebenone reduces apoptosis.	Bile acid-treated, freshly isolated rat hepatocytes	100 μ M

	Jauslin <i>et al.</i> (2002)	Idebenone protects against BSO toxicity.	FRDA lymphoblastoid cells	0.5 μ M
	Jauslin <i>et al.</i> (2003)	Idebenone protects against BSO toxicity.	FRDA lymphoblastoid cells	0.43 μ M
	Jauslin <i>et al.</i> (2007)	Combination of idebenone and vitamin E protects against BSO toxicity.	FRDA lymphoblastoid cells	0.41 μ M
	Sortino <i>et al.</i> (1999)	Idebenone ameliorates viability.	GSH-depleted cells	1 μ M
	Yerushalmi <i>et al.</i> (2001)	Idebenone rescues apoptosis.	Bile-acid treated, isolated rat hepatocytes	100 μ M
Mitochondrial Interactions	Chapela <i>et al.</i> (2008)	Idebenone increases mitochondrial membrane potential and ameliorates growth rates.	Yeast under low oxygen conditions	44-88 μ M
	Degli Esposti (1996a)	Idebenone inhibits complex I and complex I-dependent reduction of idebenone is 63% rotenone-sensitive.	Isolated beef mitochondria	40 μ M
	Degli Esposti (1998)	Idebenone inhibits complex I.	Review	-
	García-Giménez <i>et al.</i> (2011)	Idebenone inhibits mitogenesis.	FRDA cells	5 μ M
	Imada <i>et al.</i> (1989)	Idebenone restores succinate oxidase and NADH oxidase. In normal canine mitochondria, idebenone inhibits NADH oxidase.	CoQ ₁₀ -depleted and normal canine mitochondria	1-10 μ M
	Kakihana <i>et al.</i> (1998)	Idebenone increases lactate levels and decreases ATP and acetylcholine levels.	Rat brains with cerebral ischemia	10 mg/kg
	King <i>et al.</i> (2009)	Idebenone binds at NADH-binding site of complex I and competes for Q binding site due to slow reaction.	Recombinant enzyme complex	100 μ M
	Lenaz <i>et al.</i> (2002)	Idebenone is a pro-oxidant via complex I interaction.	Bovine mitochondria	2 μ mol/mg protein
	Lenaz <i>et al.</i> (2007)	Idebenone inhibits complex I.	Review	-

	Nagaoka <i>et al.</i> (1989)	Idebenone inhibits increase in lactate and decrease in ATP and ameliorates neurological deficits related to cerebral ischemia.	Ischemia in rats	10-100 mg/kg
	Rauchová <i>et al.</i> (2008)	Idebenone stimulates glycerolphosphate dehydrogenase and inhibits complex I.	Isolated brown adipose mitochondria	13 µM
	Watzke (2010)	Idebenone inhibits complex I.	Isolated mitochondria	4 µM
	Sugiyama and Fujita (1985)	Idebenone reduces state 3 respiration with NADH-linked substrates.	<i>Ex vivo</i> treatment of isolated mitochondria	250 nM-100 µM
	Sugiyama <i>et al.</i> (1985)	Idebenone increases state 3 respiration, decreases state 4 respiration and increases respiration control rate (RCI; state 3/state4 resp.) with glutamate as substrate. With succinate, only RCI is increased significantly.	<i>In vivo</i> treatment of isolated mitochondria	100-300 mg/kg
	Yu and Yu (1982)	Idebenone shows only 80% of succinate:Q reductase activity and only 20% of succinate:cytochrome c activity compared to CoQ ₂ .	Isolated enzymes	20 µM
Ca²⁺ Homeostasis	Chang <i>et al.</i> (2011)	Idebenone blocks Ca _v 2.2 and Ca _v 2.1 calcium channels and suppresses protein kinase A signaling cascade.	Rat cerebral nerve endings	50 µM
	Gil <i>et al.</i> (2003)	Idebenone reduces ROS levels and intracellular Ca ²⁺ concentration and thus, caspase-3 activity, and rescues cells from staurosporine-induced cell death.	Staurosporin-induced apoptosis in retinal cells	1 µM
	Houchi <i>et al.</i> (1991)	Idebenone blocks calcium channels.	Adrenal chromafin cells	1-100 µM

	Kaneko <i>et al.</i> (1990)	Idebenone inhibits voltage-gated calcium channels.	Xenopus oocytes	10-100 μ M
	Newman <i>et al.</i> (2011)	Idebenone inhibits voltage-gated potassium channels (Kv1.5 and Kv2.1)	High throughput assay	50 μ M
Neurological Biochemistry	Gillis <i>et al.</i> (1994)	Pharmacokinetics: 300-400 μ g/l peak plasma after 1-2 h and 30-50 mg in adults. Mild to moderate improvement of mild form of dementia.	Humans	30-50 mg/patient
	Kakihana <i>et al.</i> (1998)	Idebenone increases lactate levels and decreases ATP and acetylcholine levels.	Rat brains with cerebral ischemia	10 mg/kg
	Kaneko <i>et al.</i> (1991)	Idebenone augments currents of KARs or AMPARs in presence of their agonists. No influence on NMDARs.	Xenopus oocytes	> 10 μ M
	Nagaoka <i>et al.</i> (1989)	Idebenone inhibits increase in lactate and decrease in ATP and ameliorates neurological deficits related to cerebral ischemia	Ischemia in rats	10-100 mg/kg
	Nitta <i>et al.</i> (1993)	Idebenone increases NGF levels in hippocampus, frontal and parietal cortices of aged rats.	Aged rats	10-20 mg/kg
	Miyamoto <i>et al.</i> (1990)	Idebenone rescued survival of cholinergic and GABAergic cells in presence of AMPAR or KAR agonists, but not NMDAR agonist.	Excitotoxicity in striatum	3-10 mg/kg
	Takeuchi <i>et al.</i> (1990)	Idebenone increases NGF production.	Astrocytes	10-18 μ M
	Takuma <i>et al.</i> (2000)	Idebenone protects astrocytes not by reducing ROS levels, but by increased NGF production.	Reperfusion injury in astrocytes	10 nM - 10 μ M

	Yamada <i>et al.</i> (1997)	Idebenone ameliorates behavioural tests (water maze, passive avoidance, habituation test), increases acetylcholine activity.	Review	-
Enzyme Interaction	Civenni <i>et al.</i> (1999)	Idebenone inhibits cyclooxygenase and lipoxygenase.	Astroglia and platelets	1-20 μ M
	Tsuruo <i>et al.</i> (1994)	Idebenone is a substrate for a nitric oxygen synthesizing NADPH diaphorase in the brain.	Brain homogenates	3-10 μ M
	Schütz <i>et al.</i> (1997)	Idebenone metabolism during reperfusion after cold preservation.	Reperfusion in pig liver	280 mg/kg
	Suno and Nagaoka (1989)	Idebenone inhibits platelet aggregation, prostaglandin synthesis, and thromboxane B ₂ production.	Platelets	>125 μ M
Toxicity	Lustyik <i>et al.</i> (1990)	Idebenone is cytotoxic at concentrations higher than 75 μ M.	Human lymphoblastoid cells	> 75 μ M
	Tai <i>et al.</i> (2011)	Idebenone induces apoptosis.	Human neuroblastoid cells	> 25 μ M
	Wempe <i>et al.</i> (2009)	Idebenone might lead to toxicity.	Pig ears	1-10 μ M

13 Curriculum Vitae

Roman Hans Haefeli

Personalities

Date of birth: 1st March 1983
Nationality: Swiss
Marital status: Unmarried

Languages

German, English, French, Italian

Education

Ph.D. in Neurobiology <i>University of Basel, Biozentrum Santhera Pharmaceuticals (Switzerland) Ltd., Dept. of Biology</i>	9/2008 – 9/2011
Diploma in Natural Sciences <i>Swiss Federal Institute of Technology (ETH) Zurich</i>	10/2002 – 4/2007
Matura in Latin (Type B) <i>Kantonsschule Zürcher Oberland (KZO), Wetzikon, Switzerland</i>	8/1997 – 2/2002

Working Experience

Doctoral Student <i>University of Basel, Biozentrum Santhera Pharmaceuticals (Switzerland) Ltd. Thesis: Molecular Effects of Idebenone. PD Dr. Thomas Meier and Prof. Dr. Markus Rüegg.</i>	9/2008 – 9/2011
Traineeship <i>Santhera Pharmaceuticals (Switzerland) Ltd.</i>	2/2008 – 8/2008
Diploma Student <i>Swiss Federal Institute of Technology (ETH) Zurich, Institute of Behavioural Neuroscience Diploma Thesis: <i>In vitro</i> characterization of fluorescently tagged rat brain-derived neurotrophic factor. Dr. Jean-Charles Patema.</i>	2/2006 – 8/2006

